

**Characterization of multiple regulatory networks and responses to environmental  
signals in *Pseudomonas syringae* during its association with plants**

by

**Xilan Yu**

A dissertation submitted to the graduate faculty  
in partial fulfillment of the requirements for the degree of

DOCTOR OF PHILOSOPHY

Major: Genetics

Program of Study Committee:  
Gwyn A. Beattie, Major Professor  
Daniel S. Nettleton  
Lyric C. Bartholomay  
Larry J. Halverson  
Chris F. Minion

Iowa State University  
Ames, Iowa  
2013

Copyright © Xilan Yu, 2013. All rights reserved.

## TABLE OF CONTENTS

<b>ABSTRACT.....</b>	<b>iv</b>
 <b>CHAPTER 1. GENERAL INTRODUCTION .....</b>	<b>1</b>
Introduction.....	1
Dissertation Organization .....	3
Literature Review.....	4
Leaf colonization of <i>Pseudomonas syringae</i> .....	4
Water stress tolerance of <i>P. syringae</i> during leaf colonization .....	4
Pathogenicity and virulence of <i>P. syringae</i> .....	10
Regulatory systems of fitness and virulence in <i>P. syringae</i> .....	14
Introduction to thesis and the collaboration underlying the work .....	20
References.....	23
 <b>CHAPTER 2. TRANSCRIPTIONAL RESPONSES OF <i>PSEUDOMONAS SYRINGAE</i> TO GROWTH IN EPIPHYTIC VERSUS APOPLASTIC LEAF SITES.....</b>	<b>31</b>
Abstract.....	31
Introduction.....	32
Results and Discussion .....	34
Conclusions.....	52
Methods.....	54
Acknowledgements.....	62
References.....	62
Tables.....	67
Figures.....	68
 <b>CHAPTER 3. <i>PSEUDOMONAS SYRINGAE</i> STRAINS DIFFER IN THE CONTRIBUTION OF THEIR TREHALOSE BIOSYNTHETIC PATHWAYS TO TREHALOSE ACCUMULATION.....</b>	<b>73</b>
Abstract.....	73
Introduction.....	74
Results.....	78
Discussion.....	81
Materials and Methods.....	86
Acknowledgements.....	87
References.....	88
Tables.....	90
Figures.....	91

## **CHAPTER 4. TRANSCRIPTIONAL ANALYSIS OF THE GLOBAL REGULATORY NETWORKS ACTIVE IN *PSEUDOMONAS SYRINGAE* DURING LEAF**

<b>COLONIZATION .....</b>	<b>96</b>
Abstract .....	96
Introduction.....	97
Results and Discussion .....	102
Conclusions.....	124
Materials and Methods.....	127
References.....	132
Tables.....	138
Figures.....	159

## **CHAPTER 5. GENERAL CONSLUSIONS ..... 167**

General Discussions.....	167
Recommendations for Future Research .....	169

## **ACKNOWLEDGMENTS ..... 171**

## **APPENDIX..... 172**

## ABSTRACT

*Pseudomonas syringae* is a model bacterial plant pathogen that is adapted for growth and survival on leaf surfaces and in the leaf interior of its host plants. *P. syringae* likely experiences distinct environmental conditions in different phases of its interaction with plants. In this study, we used global transcriptome profiling of *P. syringae* pv. *syringae* B728a to analyze genes and traits that were responsive to growth and survival on the leaf surface versus in the leaf apoplast. We found that the epiphytic environment specifically favors active relocation via flagellar motility, swarming motility, chemosensing, and chemotaxis, whereas the apoplastic environment favors traits contributing to virulence including the synthesis of two phytotoxins and syringolin A as well as the degradation of an alternative amino acid that suppresses virulence. Through comparing the transcriptomes of *in planta* cells to those of cells exposed to various stresses in culture media, we found that water limitation is a major stress that limits B728a growth and survival in these leaf habitats. *P. syringae* can adapt to water stress by the production of a potent compatible solute, trehalose. Distinct *P. syringae* strains vary in their ability to tolerate water stress, possibly due, in part, to differences in the production or regulation of trehalose. To investigate this possibility, we compared the relative contribution of the trehalose biosynthetic pathways to trehalose synthesis in two closely related *P. syringae* strains B728a and DC3000 and characterized an apparent interdependency between these pathways. Our data showed that, of the two trehalose biosynthesis pathways, only one was required for trehalose production in B728a whereas both were needed in DC3000, and moreover that differences in trehalose production may help explain differences in their water stress tolerance. Lastly, to understand the

contribution of distinct regulators to fitness and pathogenicity of *P. syringae*, we performed a transcriptome analysis of B728a and mutants lacking each of nine regulators, including quorum-sensing regulators (AhlR and AefR), global regulators (GacS, SalA and RetS), and alternative sigma factors (RpoN, AlgU, RpoS, and HrpL), with cells recovered from the surface and interior of bean leaves as well as exposed to various environmental stresses. Our data showed that AhlR and AefR had negligible roles during B728a leaf colonization, whereas GacS and SalA had major roles. GacS/SalA formed a large regulatory network with both plant signal-dependent and plant signal-independent branches. RetS functioned almost exclusively to repress secondary metabolite genes when B728a cells were not in the leaf environment. Among the alternative sigma factors, RpoN influenced the majority of the genome whereas AlgU influenced a large number and RpoS a small number of genes, with plant signals strongly attenuating RpoN activation of the AlgU-regulated genes. Lastly, HrpL influenced very few genes *in planta*, due primarily to suppression by GacS and SalA. Collectively, our results highlight the role of these regulators during *P. syringae* colonization of leaves and the central importance of signals in the leaf environment on their regulation.

## CHAPTER 1. GENERAL INTRODUCTION

### Introduction

Many bacterial foliar pathogens including the agriculturally important plant pathogen *Pseudomonas syringae* have complex interactions with their host plants. These interactions include multiplication and survival on leaf surfaces, modification of the environment to favor growth, invasion of plant leaves, multiplication in the intercellular spaces, and evasion of plant defense responses, often with the subsequent induction of disease lesions. As one of the most extensively studied *P. syringae* strains, *P. syringae* pv. *syringae* B728a exhibits a pronounced epiphytic stage followed by an apoplastic stage; that is, it establishes populations on leaf surfaces and then in the leaf interior. *P. syringae* likely encounters distinct environmental conditions in these distinct stages of their interactions with plants. We performed global transcriptome profiling of B728a and analysed gene expression to understand the environmental conditions that B728a experiences and the cellular traits that it uses to grow and survive during these stages of its lifecycle. One important finding is that water limitation is a major stress influencing *P. syringae* growth and survival both on and in plant leaves. *P. syringae* can adapt to water stress during leaf colonization, in part, by accumulating compatible solutes. The disaccharide trehalose is a particularly potent compatible solute that contributes to water stress tolerance in *P. syringae*. We characterized trehalose production in B728a and also in DC3000, a *P. syringae* strain that is less tolerant to water stress than B728a and a poor epiphytic colonist. We specifically investigated the relative contribution of distinct trehalose biosynthetic pathways to trehalose production and water

stress tolerance in these two strains. Lastly, a large number of regulators that coordinate the expression of *P. syringae* fitness and virulence traits are known, but their importance to the epiphytic and apoplastic stages of the *P. syringae* lifecycle are not. In order to develop a comprehensive understanding of the interactions among these regulators, distinct host environments, and *P. syringae* traits contributing to colonization and virulence, we performed global transcriptome profiling of nine B728a mutants that lacked global regulators that we predicted to play key roles during *P. syringae* -plant interactions.

## **Dissertation Organization**

This dissertation is divided into five chapters. The first chapter provides a review of the literature on the water stress tolerance and pathogenicity of *Pseudomonas syringae* during leaf colonization, as well as the key regulatory systems that are predicted to coordinate fitness and virulence traits. The second chapter presents studies on the transcriptional responses of *P. syringae* to growth on leaf surfaces versus in the leaf apoplast to reveal how this species adapts to environmental conditions within these distinct leaf habitats. The third chapter characterizes the trehalose biosynthetic pathways present in two closely related *P. syringae* strains and their relative contribution to trehalose accumulation and water stress tolerance of the strains. The fourth chapter presents a transcriptome analysis of *P. syringae* and nine regulatory mutants lacking global regulators, which aims at generating a comprehensive understanding of the coordinated expression of fitness and virulence traits within the host environments of this species. The fifth chapter contains my general conclusions and possible future work.



## Literature Review

### Leaf colonization by *Pseudomonas syringae*

*Pseudomonas syringae* is a gram-negative bacterial plant pathogen that causes diseases on a broad range of plant species and is subdivided into about 50 pathovars based on host specificity (Sawada et al., 1999). As a foliar pathogen, *P. syringae* is well-adapted for colonizing leaf surfaces and the leaf apoplast, where it is likely exposed to stressful conditions. *P. syringae* cells modify the plant environment to favor surface growth and survival, and establish and maintain large epiphytic populations that serve as inocula for subsequent infection. As a pathogen, *P. syringae* invades plant leaves through natural openings such as open stomata, hydathodes or wounds, and multiplies in the intercellular spaces. In the apoplast, *P. syringae* initiates the onset of disease on susceptible plants and elicits a localized necrosis, or hypersensitive response, on resistant and non-host plants. Eventually, the apoplastic cells can egress to the surface through lesions and open stomata and spread to healthy plant tissue.

### Water stress tolerance of *P. syringae* during leaf colonization

During its colonization of leaf surfaces, *P. syringae* must confront various environmental stresses, including limited nutrient availability, and large and rapid fluctuations in water availability, temperature, and solar UV radiation. Mounting evidence has shown that low water availability may be the most hostile environmental condition faced by *P. syringae* during leaf colonization (Chang et al., 2007b; Freeman and Beattie, 2009a; Hirano and Upper, 1990; Yu et

al., 2013a). Like most bacteria, *P. syringae* have numerous traits that enable them to withstand water limitation, including both desiccation and osmotic stress, with the latter resulting from the concentration of dissolved solutes as water evaporates from the leaf surface. The multiple strategies that may be used by *P. syringae* to counteract this abiotic stress are described below.

### **Aggregate formation**

To cope with desiccation, *P. syringae* cells can form large aggregates that are generally encapsulated within extracellular polymeric substances (EPS). These help maintain a highly hydrated surface layer surrounding the cells and prevent desiccation (Beattie and Lindow, 1999; Chang et al., 2007b; Monier and Lindow, 2003a). Highly aggregated *P. syringae* cells exhibited superior survival over solitary cells on bean leaf surfaces that were periodically exposed to desiccation stress (Monier and Lindow, 2003a). Alginate is an important component of EPS that is widespread among pseudomonads (Fialho et al., 1990) and can hold several times its weight of water (Sutherland, 2001). In *P. syringae*, the synthesis of alginate is stimulated by desiccation and osmotic stress (Keith and Bender, 1999; Singh et al., 1992), and contributes to environmental stress tolerance and epiphytic fitness on leaf surfaces (Keith and Bender, 1999; Yu et al., 1999b).

### **Compatible solute synthesis**

Additionally, *P. syringae* can protect themselves against osmotic stress by the *de novo* synthesis of compatible solutes. These are compounds that can be accumulated to high cytosolic concentrations and function to counteract high osmolarity without disrupting normal cellular

processes. Compatible solutes usually have neutral charges and can help maintain the structure and function of molecules inside cells in the presence of high osmolarity (Freeman et al., 2010; Kurz et al., 2010a). The compatible solutes synthesized *de novo* in *P. syringae* include trehalose, N-acetylglutaminylglutamine amide (NAGGN), and L-glutamate.

*Trehalose.* Trehalose is an  $\alpha,\alpha$ -1,1-linked disaccharide and is produced to help bacteria endure stresses such as low water availability (desiccation or high osmolarity), cold, heat and oxidative stress (Arguelles, 2000). In addition to functioning as a stress-protectant, trehalose can also function as a precursor to carbon/energy storage molecules (Chandra et al., 2011). Trehalose accumulates as a compatible solute at high osmolarities in many bacteria and is synthesized by a range of biosynthetic pathways. In *P. syringae*, there are two pathways that have been identified or predicted to synthesize trehalose, the TreXYZ and TreS pathways (Freeman et al., 2010; Kurz et al., 2010a). The TreXYX pathway functions to convert glycogen or linear  $\alpha$ -glucans to trehalose (Maruta et al., 1996a, b; Maruta et al., 2000), whereas the TreS pathway converts maltose to trehalose (Kalscheuer et al., 2010; Nishimoto et al., 1996). In *P. syringae* pv. tomato strain DC3000, loss of both biosynthetic pathways eliminated trehalose accumulation and significantly reduced DC3000 osmotolerance in culture and fitness on leaves (Freeman et al., 2010), thus demonstrating the importance of trehalose to the ecology of *P. syringae*. The role of trehalose in the ecology of *P. syringae* pv. syringae strain B728a, which exhibits significantly greater osmotolerance and epiphytic fitness than DC3000, has yet to be examined.

*NAGGN*. The dipeptide NAGGN was first found to act as a compatible solute in *Sinorhizobium meliloti* (Smith and Smith, 1989) based on its accumulation when cells were grown under osmotic stress. Biochemical and genetic studies with *S. meliloti* have demonstrated that NAGGN is synthesized from glutamine in a nonribosomal peptide synthesis pathway (Sagot et al., 2010). Specifically, NAGGN in *S. meliloti* is first catalyzed by an N-acetylglutaminylglutamine synthetase (Ngg), which carries out the N-acetylation of one glutamine and the formation of a peptide bond with a second glutamine, with the product receiving an amide nitrogen of yet a third glutamine via the amidotransferase AsnO.

NAGGN has also been found to function as a compatible solute in pseudomonads. In *P. aeruginosa*, the orthologs of *ngg* and *asnO* were induced by osmotic stress (Aspedon et al., 2006). In *P. syringae*, NAGGN was predicted to be synthesized using a different pathway, and the gene cluster for NAGGN biosynthesis was identified (Kurz et al., 2010a). The biosynthetic pathway for NAGGN in *P. syringae* was predicted to involve two enzymes for the first step, an acetyltransferase (P syr\_3748, GgnB) and an amidotransferase (P syr\_3747, GgnA), which each use glutamine as a precursor, and then fusion of these products via an aminopeptidase (P syr\_3749, GgnC). The genes for NAGGN biosynthesis form a putative operon that is highly conserved in pseudomonads, including *P. fluorescens*, *P. entomophila*, *P. putida*, *P. stutzeri*, *P. mendocina*, and *P. aeruginosa*. The functionality of these genes in NAGGN biosynthesis was confirmed based on that inactivating P syr\_3747 eliminated NAGGN accumulation in *P. syringae* B728a (Kurz et al., 2010a). Interestingly, NAGGN may contribute differentially to the

osmotolerance of distinct *P. syringae* strains. In B728a, loss of NAGGN synthesis loci led to significantly reduced growth of cells under high osmotic stress (Kurz et al., 2010a), whereas in DC3000, deletion of *ggnAB* caused only a modest reduction in growth under high osmotic stress (Freeman and Beattie, unpublished data). These results suggest that B728a may derive greater benefit from NAGGN than DC3000.

*L-glutamate*. L-glutamate has been identified as a compatible solute in *P. syringae*. <sup>13</sup>C-NMR data indicates that it accumulates to lower levels than trehalose and NAGGN in response to high osmotic stress (Freeman et al., 2010; Li et al., 2013a). However, compared with trehalose and NAGGN, glutamine plays very minor roles in bacterial osmotolerance, based on that L-glutamate cannot compensate for the loss of both trehalose and NAGGN biosynthetic loci in B728a under high osmotic stress (Li et al., 2013a). Thus far, the metabolic processes that result in the accumulation of L-glutamate in response to osmotic stress are not known.

### **Quaternary ammonium compounds (QACs)**

In addition to *de novo* synthesis of compatible solutes, *P. syringae* can rapidly take up osmoprotective compounds from plants or environment in an energy-saving manner. Osmoprotectants are defined as compounds that, when provided exogenously, enhance the growth of cells under hyperosmotic conditions; thus, they include compounds that function as, or are converted to, compatible solutes following uptake. Compounds that were found to function as osmoprotectants for *P. syringae* include the quaternary ammonium compounds (QACs), glycine betaine, choline, phosphocholine, and carnitine (Chen and Beattie, 2007). QACs contain

a fully methyl-substituted nitrogen. Among these compounds, glycine betaine functions directly as an effective compatible solute, whereas other QACs serve as osmoprotectants via conversion to glycine betaine (Chen and Beattie, 2007). *P. syringae* has evolved multiple transporters to utilize the plant-derived QACs; these include OpuC, CbcXWV, and BetT (Chen and Beattie, 2008a; Chen and Beattie, 2007; Chen et al., 2010). As an ATP-binding cassette (ABC) family transporter, OpuC is the primary transporter for glycine betaine and one of the multiple transporters for choline under high osmolarity (Chen and Beattie, 2007). The CbcXWV transporter is an ABC transporter that functions primarily in QAC uptake for catabolism; it is a homolog of the *E. coli* ProU transporter and does not appear to be regulated by high osmolarity (Chen et al., 2010). Lastly, BetT is a secondary transporter in the betaine-choline-carnitine transporter (BCCT) family. BetT activity is induced in response to high osmolarity, and it rapidly transports choline when present in high concentrations and mediates significant uptake under low osmolarity, suggesting its dual roles in both osmotolerance and catabolism (Chen and Beattie, 2008a).

Glycine betaine is produced by a limited number of plant species, usually in response to water limitation or high salinity, whereas choline and phosphocholine are widely available in plants (Storey and Jones, 1975). The use of choline-specific reporter assays has suggested that *P. syringae* accesses a rich choline environment on plant tissues, including on leaves; moreover, the loss of choline transporters led to a significant reduction in its epiphytic fitness (Chen, 2013). A reservoir of QACs in plants is the membrane lipid phosphatidylcholine (PC), which comprises

approximately 60% of the total membrane lipids in eukaryotes. This reservoir may provide QACs in the form of phosphocholine and choline due to the action of phospholipases in the plant or even in *P. syringae*, as supported by phospholipase activity in *P. aeruginosa* (Wargo et al., 2008). Uptake of these QACs can then result in their conversion to glycine betaine for use as a compatible solute or energy source (Li et al., 2013a).

There is also a dynamic interconnection between *de novo* synthesized compatible solutes and QACs. Recently, glycine betaine accumulation inside cells was shown to inhibit the synthesis and accumulation of trehalose, NAGGN, and glutamate (Li et al., 2013a). In particular, when grown under hyperosmolarity, *P. syringae* cells initially accumulated glycine betaine as a compatible solute, but later catabolized it to de-repress the synthesis of endogenous compatible solutes. Moreover, recent studies have shown that phosphocholine is a particularly potent osmoprotectant based on its ability to induce the synthesis of trehalose under high osmotic stress (Li and Beattie, unpublished data). Collectively, these data indicate that *P. syringae* may use a variety of strategies to tolerate water stress during leaf colonization.

### **Pathogenicity and virulence of *P. syringae***

*P. syringae* pathovars that cause foliar diseases enter plants through natural openings such as open stomata, hydathodes and wounds. After entry into the apoplast, they grow and cause the onset of disease symptoms on susceptible plants but elicit a hypersensitive response on resistant

and non-host plants. Eventually, the apoplastic cells egress from the intracellular part of the leaf to the surface through lesions and open stomata; they can then spread to healthy plant tissues.

### **The type III secretion system and effector proteins**

Like many bacterial pathogens, *P. syringae* has developed the ability to suppress plant defenses and promote disease by injecting effector proteins directly into plant cells via the type III secretion system (T3SS) (DebRoy et al., 2004; Galan and Collmer, 1999; Hauck et al., 2003). Following contact with a host cell, *P. syringae* forms a T3SS complex, which is a needle-like syringe structure that penetrates the plant cell wall to translocate protein effectors directly across the host cell membrane and into the cytoplasm (Marlovits et al., 2004). The structural components of the T3SS are encoded by *h*ypersensitive *r*esponse and *p*athogenicity (*hrp*) genes and *h*ypersensitive *r*esponse and *c*onserved (*hrc*) genes in gene clusters. These are often flanked by type III effector genes and other virulence genes, which collectively comprise pathogenicity islands (Alfano et al., 2000).

The effectors are encoded by *hop* (*h*rp-dependent *o*uter *p*rotein) or *avr* (avirulence) genes. About 60 distinct effector families have been identified in *P. syringae* genomes by a number of computational and functional approaches (Baltrus et al., 2011; O'Brien et al., 2011). Effector repertoires vary in size among *P. syringae* strains, from three for a nonpathogenic strain of *P. syringae* pv. *syringae* to 38 for a *P. syringae* pv. *avellanea* strain with an unpublished sequence. Only 12 effectors are common among the first three fully sequenced *P. syringae* strains: *P. syringae* pv. *tomato* DC3000, *P. syringae* pv. *syringae* B728a, and *P. syringae* pv. *phaseolicola*



1448A (Cunnac et al., 2009). Most effectors contribute to pathogenesis by interfering with and/or suppressing plant defenses, including basal defenses (DebRoy et al., 2004; Hauck et al., 2003) and the hypersensitive response (Abramovitch et al., 2003; Jamir et al., 2004). For example, effectors have been found that interfere with plant hormone signaling (Chen et al., 2007; de Torres-Zabala et al., 2007) and the proteasome system (Nomura et al., 2006).

The T3SS and effector genes in *P. syringae* are induced by plant-derived signals and environmental conditions (Rahme et al., 1992), which include certain carbon sources in the culture medium (Huynh et al., 1989a) and specific temperature for bacterial growth (van Dijk et al., 1999). Interestingly, these genes can be negatively regulated by plant cutin-related signals (Xiao et al., 2004), suggesting *P. syringae* may repress T3SS-related genes during epiphytic growth on leaf surfaces. It seems that T3SS and some specific effectors could influence the epiphytic survival and growth of *P. syringae* (Lee et al., 2012a).

### **Phytotoxins and related compounds**

In addition to protein effectors, the repertoire of virulence traits in *P. syringae* includes phytotoxins. *P. syringae* can produce phytotoxins that contribute significantly to virulence, and the toxins that have been characterized in *P. syringae* strains include coronatine, syringolin A, syringomycin, syringopeptin, mangotoxin, tabtoxin, and phaseolotoxin. Coronatine produced by DC3000 not only mimics the plant hormone signal jasmonate to activate the jasmonic acid signaling pathway and suppress salicylic acid-mediated defense (Brooks et al., 2005; Zhao et al., 2003), but also reopens the stomata after *P. syringae*-induced stomatal closure (Melotto et al.,

2006). A compound with a similar function in stomatal opening was identified in *P. syringae* pv. *syringae* strains: syringolin A (SylA). SylA is the most abundant variant of a family of structurally-related cyclic lipopeptides (Waspi et al., 1999). SylA functions as a virulence factor by counteracting stomatal closure by irreversibly inhibiting the plant proteasome (Groll et al., 2008; Schellenberg et al., 2010b). Recently, SylA was shown to facilitate colonization from wound infection sites by suppressing salicylic acid signaling in plant immune responses as well as promoting bacterial motility (Misas-Villamil et al., 2013).

Syngomycin (Syr) and syringopeptin (Syp) are produced by *P. syringae* pv. *syringae* strains. These phytotoxins are representatives of two distinct classes of cyclic lipodepsipeptides. By forming transmembrane pores that result in cytotoxic cation influxes, Syr and Syp cause cytolysis and induce necrosis in cultured plant cells (Hutchison and Gross, 1997; Hutchison et al., 1995; Iacobellis et al., 1992); the extent to which this cytolysis occurs *in planta*, however, is not known, but these compounds are widely predicted to enhance nutrient leakage within plant tissues. As lipopeptides, Syr and Syp also exhibit potent biosurfactant activity and thus lower the interfacial tension of water (Hutchison and Gross, 1997; Hutchison et al., 1995).

Some *P. syringae* pathovars produce another group of phytotoxins that are composed of oligopeptides; these function by inhibiting the biosynthetic enzymes for some amino acids. Mangotoxin produced by certain *P. syringae* pv. *syringae* strains, is a small oligopeptide that inhibits ornithine acetyl transferase for ornithine and arginine biosynthesis (Arrebola et al., 2003), and was recently shown to contribute to the virulence and also the epiphytic fitness of a

strain (Arrebola et al., 2009). Tabtoxin, originally described from *P. syringae* pv. *tabaci*, is a dipeptide whose hydrolysis product irreversibly inhibits glutamine synthetase and therefore blocks glutamine synthesis. This blockage causes the toxic accumulation of ammonia, which induces chlorosis in plant tissues (Thomas et al., 1983). Phaseolotoxin is mainly produced by *P. syringae* pv. *phaseolicola* strains. It is a tripeptide whose hydrolysis product irreversibly inhibits ornithine carbamoyl transferase, causing an accumulation of ornithine and a deficiency of arginine, which also leads to chlorosis (Mitchell and Bielecki, 1977).

## **Regulatory systems of fitness and virulence in *P. syringae***

### **The two-component system GacS/GacA**

The global activator genes *gacS* and *gacA* encode a global signal transduction system composed of a membrane-bound histidine kinase (GacS) that senses environmental signals and a corresponding transmembrane response regulator (GacA) that mediates a cellular response, generally through differential regulation of target gene expression. The GacS/GacA two-component system was first discovered in *P. syringae* B728a based on the dramatic loss of virulence when *gacS* was inactivated (Willis et al., 1990). Although GacS was first named LemA based on the loss of lesion manifestation, GacA was later discovered as a regulator of antibiotic production in *P. fluorescens* and was named GacA for its ability to function in global antibiotic and cyanide control (Laville et al., 1992). Since these discoveries, the GacS/GacA two-component system has been studied extensively in fluorescent pseudomonads (Heeb and

Haas, 2001) and shows global regulatory effects on gene expression in these organisms, including in *P. syringae* (Chatterjee et al., 2003; Marutani et al., 2008).

In *P. syringae* pv. *syringae* B728a, GacS/GacA is involved not only in necrotic lesion formation on bean, but also the production of the phytotoxin syringomycin (Hrabak and Willis, 1993), the secondary metabolite syringolin (Reimann et al., 1995; Waspi et al., 1998a), the polysaccharide alginate and a protease (Hrabak and Willis, 1993). GacS/GacA is also involved in the production of the phytotoxins syringopeptin in *P. syringae* B301D (Wang et al., 2006) and coronatine in *P. syringae* DC3000 (Chatterjee et al., 2003). GacS/GacA is also involved in regulating swarming behavior in both B728a (Kinscherf and Willis, 1999) and DC3000 (Chatterjee et al., 2003), which may be a phenotype influencing bacterial colonization of the leaf surface as well as leaf interior (Misas-Villamil et al., 2013). A regulator that functions downstream of GacS/GacA, SalA, was first identified in *P. syringae* B728a as an activator of both syringomycin production and lesion formation (Kitten et al., 1998). It has since been shown to be a component of the GacS/GacA regulatory system in other *P. syringae* strains, including *P. syringae* pv. *syringae* B301D (Wang et al., 2006) and *P. syringae* pv. *tomato* DC3000 (Chatterjee et al., 2003). SalA positively regulates genes for the production of syringomycin and syringopeptin (Kitten et al., 1998; Lu et al., 2005).

### **Alternative sigma factors**

In bacteria, sigma factors are proteins that bind to the core RNA polymerase and help direct the holoenzyme to recognize specific promoters in the transcription initiation process. Typically, one primary sigma factor controls the expression of most genes and ensures essential cellular activities, while a variety of alternative sigma factors compete with the primary sigma factor for binding to the RNA polymerase; this controls the expression of specific genes in response to

distinct environmental conditions (Gruber and Gross, 2003). *P. syringae* pv. *syringae* B728a possesses a total of 15 sigma factors, 10 of which are extracytoplasmic function (ECF) sigma factors, which are sequestered at the membrane by the cognate transmembrane anti-sigma factors to rapidly respond to extracytoplasmic stresses (Helmann, 2002). These ECF sigma factors, including AlgU, HrpL, SigX, PvdS, AcsS and five FecI-type ECF sigma factors, have been identified in the completely sequenced genomes of three *P. syringae* pathovars (Oguiza et al., 2005). Here, we will discuss only the sigma factors that are predicted to be most involved in the regulation of fitness and virulence in *P. syringae*; these include the two ECF sigma factors AlgU and HrpL and the two alternative sigma factors RpoN and RpoS.

In *P. syringae*, AlgU (also known as AlgT) which is closely related to RpoE in other gram-negative bacteria, controls the production of the exopolysaccharide alginate as well as contributes to tolerance to several environmental stresses, including osmotic stress and oxidative stress (Keith and Bender, 1999). The contribution of AlgU to *P. syringae* fitness *in planta* (Schenk et al., 2008; Yu et al., 1999b) is likely due, in part, to its positive activation of alginate production, since alginate has been shown to enhance bacterial tolerance to water stress (Chang et al., 2007b) and *P. syringae* on leaves appear to be exposed to water stress (Yu et al., 2013a). AlgU may also regulate other genes in *P. syringae* cells on leaves that contribute to stress tolerance and successful leaf colonization, although the AlgU regulon has not yet been characterized in *P. syringae* or any pseudomonad.

The regulation of AlgU activity is complex, but probably shares many common features between *P. aeruginosa* and *P. syringae*. In *P. aeruginosa*, AlgU activity is tightly controlled by the anti-sigma factors MucA and MucB, encoded by the genes located downstream of *algU*. The

*mucA* gene encodes a transmembrane protein that directly sequesters AlgU to the inner membrane, and *mucB* encodes a periplasmic protein that interacts with MucA and stabilizes the MucA-AlgU complex to ensure tight control. Extracytoplasmic stresses initiate the destabilization of the MucB-MucA-AlgU complex, such as by the detection of misfolded proteins, resulting in the degradation or cleavage of MucA and release of AlgU into the cytosol. Once AlgU becomes active, the transcription of AlgU-regulated genes is initiated.

Another ECF factor, HrpL, is required for the expression of genes for the type III secretion system and effector proteins in *P. syringae*. These HrpL-regulated genes have been widely studied in *P. syringae* strains from pathovars syringae, tomato, phaseolicola and tabaci (Lindeberg et al., 2006; Studholme et al., 2009b). The expression of *hrpL* requires HrpR and HrpS proteins that belong to the NtrC class of two-component regulatory systems (Xiao et al., 1994). HrpR and HrpS form a heterodimer and bind to the *hrpL* promoter through interactions with the alternative sigma factor RpoN (Hendrickson et al., 2000a; Hutcheson et al., 2001). RpoN-dependent *hrpL* expression and HrpL regulation of pathogenicity and virulence in *P. syringae* present a hierarchical regulatory network among alternative sigma factors. HrpL activates the transcription of the *hrp* and *hrc* genes and effector genes by facilitating RNA polymerase holoenzyme binding to the promoter regions that contain the consensus sequence GGAACC-N<sub>16</sub>-CCACNNA, also known as the hrp box (Fouts et al., 2002).

In addition to the *hrpL*, *hrp* and *hrc* genes, the alternative sigma factor RpoN is also required for the expression of biosynthetic genes for the phytotoxin coronatine in *P. syringae* pvs. glycinea (Alarcon-Chaidez et al., 2003) and maculicola (Hendrickson et al., 2000b), and thus

contribute to virulence and *in planta* growth in *P. syringae*. RpoN-regulated genes also include genes for type VI secretion system in *P. syringae* (Bernard et al., 2011). Although RpoN was first identified as a sigma factor that is active during nitrogen starvation, and continues to be widely recognized for its contribution to the use of alternative nitrogen sources, including in *P. syringae* (Alarcon-Chaidez et al., 2003) and *P. aeruginosa* (Totten et al., 1990), RpoN has been thoroughly studied in *P. aeruginosa* and has been closely linked to its virulence. The involvement of RpoN-dependent regulation in virulence in pathogenic pseudomonads is additional to its physiological role in nitrogen metabolism. The RpoN-regulated genes in this species include synthesis genes for pili (Ishimoto and Lory, 1989), flagella (Totten et al., 1990), alginate (Boucher et al., 2000), and quorum-sensing autoinducers (Heurlier et al., 2003; Thompson et al., 2003), with the latter two identified as important virulence factors.

In contrast to RpoN, the alternative sigma factor RpoS is a stationary phase sigma factor that is widely recognized for its role in stress tolerance in bacteria, including in pseudomonads such as *P. fluorescens* (Stockwell and Loper, 2005). Whereas RpoS contributes to stress tolerance and fitness on roots in *P. fluorescens* (Stockwell and Loper, 2005), its contribution to the fitness of this species on leaves was surprisingly minor (Stockwell et al., 2009) or negligible (Hagen et al., 2009). Thus, although RpoS in *P. syringae* contributes to protection from near-UV irradiation (Miller et al., 2001) and may be required for tolerance to an array of stresses based on its role in other pseudomonads (Stockwell and Loper, 2005; Whistler et al., 1998), the extent to which it serves as a regulator in *P. syringae* cells *in planta* is not yet known.

## Quorum sensing signaling system

In bacteria, quorum sensing is another global signal transduction system. It involves the production of small diffusible signal molecules that reflect the population density in diffusion-limited environments, thus allowing coordinated gene regulation in response to cell density (Fuqua et al., 1994). The most common signal molecule is acylated homoserine lactone (AHL), which is synthesized by an AHL synthase (a LuxI homolog) and interacts with an AHL-responsive transcriptional activator (a LuxR homolog) to regulate the expression of target genes (Fuqua et al., 2001; Whitehead et al., 2001).

The *P. syringae* strain B728a was found to have a LuxI homolog, AhlI, that is responsible for the production of the AHL 3-oxo-hexanoyl-homoserine lactone (C6-HSL) (Quinones et al., 2004). Similarly, the LuxR homolog AhlR binds with C6-HSL and activates transcription of *ahII* via a positive feedback loop. The transcription of *ahII* is positively regulated by GacA (Quinones et al., 2004), as was previously shown for the *ahII* and *ahIR* homologs in DC3000 (Chatterjee et al., 2003), and by another quorum-sensing regulator, AefR (AHL and epiphytic fitness regulator). AefR operates downstream of AhlR-mediated activation of *ahII* transcription and operates independently of GacS regulation (Quinones et al., 2004). The genes regulated by AhlI/AhlR and GacS have not yet been identified in *P. syringae*.

Quorum sensing is important for the expression of virulence factors by many plant-pathogenic bacteria. Identifying the ecological role of quorum sensing in the ecology of *P. syringae* during its association with plants has not been as straightforward as with other plant



pathogens, in part due to the only subtle effects resulting from the loss of *ahII* and *ahlR*. The only extensive study on quorum sensing in *P. syringae* was performed with a B728a mutant lacking *ahII* and *ahlR* (Quinones et al., 2005). This mutant was not strongly altered in virulence; however, like an *aeiR* mutant, it showed subtle changes in lesion formation that paralleled a change in swarming motility in culture (Quinones et al., 2005). Similarly, both mutants showed changes in survival and aggregate formation on leaves that paralleled changes in alginate production in culture. The two mutants, however, appeared to differ in their production of extracellular enzymes involved in tissue maceration (Quinones et al., 2005).

## **Introduction to thesis and the collaboration underlying the work**

The complexity of the regulatory circuits influencing the expression of genes relevant to *P. syringae*-plant interactions, including the multiple hierarchies such as the HrpR/HrpS-RpoN-HrpL and GacS/GacA-SalA-AeiR-AhII/AhIR regulatory cascades, indicates the need for a comprehensive study of these regulatory circuits to better understand the contribution of each to *P. syringae* ecology and biology during both the epiphytic and apoplastic stages of its lifecycle. Given the key role of environmental factors in influencing these regulatory cascades, a critical requirement for such a study is that mutants lacking these regulators are compared side-by-side under the same environmental conditions so that meaningful conclusions can be made. A major goal of this thesis was to perform this comprehensive study.

An ORF-based microarray analysis of *P. syringae* pv. *syringae* strain B728a and nine regulator deletion mutants subjected to seven treatment conditions was performed as a collaboration between the research groups of Drs. Gwyn Beattie (Iowa State University), Steven Lindow (University of California, Berkley), Dennis Gross (Texas A&M University), and Dan Nettleton (Iowa State University). Graduate students and postdoctoral researchers who contributed to this project were I, Russell A. Scott (University of California, Berkley), Jessica W. Greenwald (Texas A&M University), Dr. Angela Records (Texas A&M University), and Steven P. Lund (Iowa State University).

The laboratory-based research was divided among the Beattie, Gross, and Lindow laboratories, with the coordinated design of the microarray and the gene expression analyses performed in consultation with Dr. Nettleton. I performed all of the experiments to identify the optimal basal medium, which served as the central point of comparison for all of the studies, and the optimal conditions for the environmental stress treatments that were performed *in vitro*. I took the lead in developing methods for recovering bacterial RNA from the cells recovered *in planta*, with input and consultation across the Beattie, Gross and Lindow laboratories. The construction of the deletion mutants, optimization of the number of cells of each mutant that had to be inoculated *in planta* for sufficient RNA recovery, and the exposure of the mutants and the wild type strains to the treatments, with subsequent RNA extraction, were performed in distinct laboratories based on the selected mutants: the Lindow laboratory did this for two quorum sensing regulatory mutants, the Gross laboratory did this for three global regulatory mutants, and

I did this in the Beattie laboratory for the four alternative sigma factor mutants. The hybridization to the microarray was done by Roche Nimblegen and I collated all of the data into one large dataset. Statistical analyses of this dataset were performed in collaboration with the Nettleton laboratory, with the Beattie laboratory serving as the project coordinator to facilitate data sharing, analysis, and interpretation throughout the process.

Graduate students in each of the Gross and Lindow laboratories performed an initial evaluation of the biological significance of the data with respect to their mutants, and then performed follow-up experimental studies that were focused on narrow aspects of the studies as part of their dissertations. Thus, the dissertations of the other graduate students on the project included aspects of the statistical approach (Steve Lund), evaluation of the role of SalA in achromabactin regulation (Jessica Greenwald), evaluation of the role of RetS and GacS in regulation of the type VI secretion genes (Angela Records), and the mechanistic basis of the lack of quorum regulation in B728a (Russell Scott). I evaluated and interpreted the data to address the big picture questions of how B728a responded differently to the epiphytic versus apoplastic environments (Chapter 2) and how the multiple regulatory networks were integrated, primarily *in planta* (Chapter 4). Chapter 2 was published as a co-authored work in the *Proceedings of the National Academy of Sciences, U.S.A.*, and Chapter 4 will be a co-authored manuscript that will be submitted to *mBio*. Lastly, Chapter 3 describes experimental studies, which, in part, followed up on the finding of a critical role of water stress in B728a during leaf colonization.

## References

- Abramovitch, R.B., Kim, Y.J., Chen, S.R., Dickman, M.B., and Martin, G.B. (2003). *Pseudomonas* type III effector AvrPtoB induces plant disease susceptibility by inhibition of host programmed cell death. *Embo J* 22, 60-69.
- Alarcon-Chaidez, F.J., Keith, L., Zhao, Y.F., and Bender, C.L. (2003). RpoN (sigma(54)) is required for plasmid-encoded coronatine biosynthesis in *Pseudomonas syringae*. *Plasmid* 49, 106-117.
- Alfano, J.R., Charkowski, A.O., Deng, W.L., Badel, J.L., Petnicki-Ocwieja, T., van Dijk, K., and Collmer, A. (2000). The *Pseudomonas syringae* Hrp pathogenicity island has a tripartite mosaic structure composed of a cluster of type III secretion genes bounded by exchangeable effector and conserved effector loci that contribute to parasitic fitness and pathogenicity in plants. *Proc Natl Acad Sci U S A* 97, 4856-4861.
- Arguelles, J.C. (2000). Physiological roles of trehalose in bacteria and yeasts: a comparative analysis. *Arch Microbiol* 174, 217-224.
- Arrebola, E., Cazorla, F.M., Codina, J.C., Gutierrez-Barranquero, J.A., Perez-Garcia, A., and de Vicente, A. (2009). Contribution of mangotoxin to the virulence and epiphytic fitness of *Pseudomonas syringae* pv. *syringae*. *Int Microbiol* 12, 87-95.
- Arrebola, E., Cazorla, F.M., Duran, V.E., Rivera, E., Olea, F., Codina, J.C., Perez-Garcia, A., and de Vicente, A. (2003). Mangotoxin: a novel antimetabolite toxin produced by *Pseudomonas syringae* inhibiting ornithine/arginine biosynthesis. *Physiol Mol Plant Pathol* 63, 117-127.
- Aspedon, A., Palmer, K., and Whiteley, M. (2006). Microarray analysis of the osmotic stress response in *Pseudomonas aeruginosa*. *J Bacteriol* 188, 2721-2725.
- Baltrus, D.A., Nishimura, M.T., Romanchuk, A., Chang, J.H., Mukhtar, M.S., Cherkis, K., Roach, J., Grant, S.R., Jones, C.D., and Dangl, J.L. (2011). Dynamic evolution of pathogenicity revealed by sequencing and comparative genomics of 19 *Pseudomonas syringae* isolates. *PLoS Pathog* 7, e1002132.
- Beattie, G.A., and Lindow, S.E. (1999). Bacterial colonization of leaves: a spectrum of strategies. *Phytopathology* 89, 353-359.
- Bernard, C.S., Brunet, Y.R., Gavioli, M., Lloubes, R., and Cascales, E. (2011). Regulation of type VI secretion gene clusters by sigma(54) and cognate enhancer binding proteins. *J Bacteriol* 193, 2158-2167.
- Boucher, J.C., Schurr, M.J., and Deretic, V. (2000). Dual regulation of mucoidy in *Pseudomonas aeruginosa* and sigma factor antagonism. *Mol Microbiol* 36, 341-351.
- Brooks, D.M., Bender, C.L., and Kunkel, B.N. (2005). The *Pseudomonas syringae* phytotoxin coronatine promotes virulence by overcoming salicylic acid-dependent defences in *Arabidopsis thaliana*. *Mol Plant Pathol* 6, 629-639.
- Chandra, G., Chater, K.F., and Bornemann, S. (2011). Unexpected and widespread connections between bacterial glycogen and trehalose metabolism. *Microbiol* 157, 1565-1572.

- Chang, W.S., van de Mortel, M., Nielsen, L., de Guzman, G.N., Li, X.H., and Halverson, L.J. (2007). Alginate production by *Pseudomonas putida* creates a hydrated microenvironment and contributes to biofilm architecture and stress tolerance under water-limiting conditions. *J Bacteriol* *189*, 8290-8299.
- Chatterjee, A., Cui, Y.Y., Yang, H.L., Collmer, A., Alfano, J.R., and Chatterjee, A.K. (2003). GacA, the response regulator of a two-component system, acts as a master regulator in *Pseudomonas syringae* pv. tomato DC3000 by controlling regulatory RNA, transcriptional activators, and alternate sigma factors. *Mol Plant Microbe Interact* *16*, 1106-1117.
- Chen, C., and Beattie, G.A. (2008). *Pseudomonas syringae* BetT is a low-affinity choline transporter that is responsible for superior osmoprotection by choline over glycine betaine. *J Bacteriol* *190*, 2717-2725.
- Chen, C.L., and Beattie, G.A. (2007). Characterization of the osmoprotectant transporter OpuC from *Pseudomonas syringae* and demonstration that cystathionine-beta-synthase domains are required for its osmoregulatory function. *J Bacteriol* *189*, 6901-6912.
- Chen, C.L., Li, S.S., McKeever, D.R., and Beattie, G.A. (2013). The widespread plant-colonizing bacterial species *Pseudomonas syringae* detect and exploit an extracellular pool of choline in hosts. *Plant J* doi: 10.1111/tpj.12262.
- Chen, C.L., Malek, A.A., Wargo, M.J., Hogan, D.A., and Beattie, G.A. (2010). The ATP-binding cassette transporter Cbc (choline/betaine/carnitine) recruits multiple substrate-binding proteins with strong specificity for distinct quaternary ammonium compounds. *Mol Microbiol* *75*, 29-45.
- Chen, Z.Y., Agnew, J.L., Cohen, J.D., He, P., Shan, L.B., Sheen, J., and Kunkel, B.N. (2007). *Pseudomonas syringae* type III effector AvrRpt2 alters *Arabidopsis thaliana* auxin physiology. *Proc Natl Acad Sci U S A* *104*, 20131-20136.
- Cunnac, S., Lindeberg, M., and Collmer, A. (2009). *Pseudomonas syringae* type III secretion system effectors: repertoires in search of functions. *Curr Opin Microbiol* *12*, 53-60.
- de Torres-Zabala, M., Truman, W., Bennett, M.H., Lafforgue, G., Mansfield, J.W., Egea, P.R., Bogre, L., and Grant, M. (2007). *Pseudomonas syringae* pv. *tomato* hijacks the *Arabidopsis* abscisic acid signalling pathway to cause disease. *Embo J* *26*, 1434-1443.
- DebRoy, S., Thilmony, R., Kwack, Y.B., Nomura, K., and He, S.Y. (2004). A family of conserved bacterial effectors inhibits salicylic acid-mediated basal immunity and promotes disease necrosis in plants. *Proc Natl Acad Sci U S A* *101*, 9927-9932.
- Fialho, A.M., Zielinski, N.A., Fett, W.F., Chakrabarty, A.M., and Berry, A. (1990). Distribution of alginate gene sequences in the *Pseudomonas* rRNA homology group I-*Azomonas*-*Azotobacter* lineage of superfamily B procaryotes. *Appl Environ Microbiol* *56*, 436-443.
- Fouts, D.E., Abramovitch, R.B., Alfano, J.R., Baldo, A.M., Buell, C.R., Cartinhour, S., Chatterjee, A.K., D'Ascenzo, M., Gwinn, M.L., Lazarowitz, S.G., *et al.* (2002). Genomewide identification of *Pseudomonas syringae* pv. *tomato* DC3000 promoters controlled by the HrpL alternative sigma factor. *Proc Natl Acad Sci U S A* *99*, 2275-2280.

- Freeman, B.C., and Beattie, G.A. (2009). Bacterial growth restriction during host resistance to *Pseudomonas syringae* is associated with leaf water loss and localized cessation of vascular activity in *Arabidopsis thaliana*. *Mol Plant Microbe Interact* 22, 857-867.
- Freeman, B.C., Chen, C.L., and Beattie, G.A. (2010). Identification of the trehalose biosynthetic loci of *Pseudomonas syringae* and their contribution to fitness in the phyllosphere. *Environ Microbiol* 12, 1486-1497.
- Fuqua, C., Parsek, M.R., and Greenberg, E.P. (2001). Regulation of gene expression by cell-to-cell communication: acyl-homoserine lactone quorum sensing. *Annu Rev Genet* 35, 439-468.
- Fuqua, W.C., Winans, S.C., and Greenberg, E.P. (1994). Quorum sensing in bacteria: the LuxR-LuxI family of cell density-responsive transcriptional regulators. *J Bacteriol* 176, 269-275.
- Galan, J.E., and Collmer, A. (1999). Type III secretion machines: bacterial devices for protein delivery into host cells. *Science* 284, 1322-1328.
- Groll, M., Schellenberg, B., Bachmann, A.S., Archer, C.R., Huber, R., Powell, T.K., Lindow, S., Kaiser, M., and Dudler, R. (2008). A plant pathogen virulence factor inhibits the eukaryotic proteasome by a novel mechanism. *Nature* 452, 755-758.
- Gruber, T.M., and Gross, C.A. (2003). Multiple sigma subunits and the partitioning of bacterial transcription space. *Annu Rev Microbiol* 57, 441-466.
- Hagen, M.J., Stockwell, V.O., Whistler, C.A., Johnson, K.B., and Loper, J.E. (2009). Stress tolerance and environmental fitness of *Pseudomonas fluorescens* A506, which has a mutation in RpoS. *Phytopathology* 99, 679-688.
- Hauck, P., Thilmony, R., and He, S.Y. (2003). A *Pseudomonas syringae* type III effector suppresses cell wall-based extracellular defense in susceptible *Arabidopsis* plants. *Proc Natl Acad Sci U S A* 100, 8577-8582.
- Heeb, S., and Haas, D. (2001). Regulatory roles of the GacS/GacA two-component system in plant-associated and other gram-negative bacteria. *Mol Plant Microbe Interact* 14, 1351-1363.
- Helmann, J.D. (2002). The extracytoplasmic function (ECF) sigma factors. *Adv Microb Physiol* 46, 47-110.
- Hendrickson, E.L., Guevera, P., and Ausubel, F.M. (2000a). The alternative sigma factor RpoN is required for *hrp* activity in *Pseudomonas syringae* pv. *maculicola* and acts at the level of *hrpL* transcription. *J Bacteriol* 182, 3508-3516.
- Hendrickson, E.L., Guevera, P., Penaloza-Vazquez, A., Shao, J., Bender, C., and Ausubel, F.M. (2000b). Virulence of the phytopathogen *Pseudomonas syringae* pv. *maculicola* is *rpoN* dependent. *J Bacteriol* 182, 3498-3507.
- Heurlier, K., Denervaud, V., Pessi, G., Reimmann, C., and Haas, D. (2003). Negative control of quorum sensing by RpoN (sigma(54)) in *Pseudomonas aeruginosa* PAO1. *J Bacteriol* 185, 2227-2235.
- Hirano, S.S., and Upper, C.D. (1990). Population biology and epidemiology of *Pseudomonas syringae*. *Annu Rev Phytopathol* 28, 155-177.

- Hrabak, E.M., and Willis, D.K. (1993). Involvement of the *lemA* gene in production of syringomycin and protease by *Pseudomonas syringae* pv. *syringae*. *Mol Plant Microbe Interact* 6, 368-375.
- Hutcheson, S.W., Bretz, J., Sussan, T., Jin, S.M., and Pak, K. (2001). Enhancer-binding proteins HrpR and HrpS interact to regulate *hrp*-encoded type III protein secretion in *Pseudomonas syringae* strains. *J Bacteriol* 183, 5589-5598.
- Hutchison, M.L., and Gross, D.C. (1997). Lipopeptide phytotoxins produced by *Pseudomonas syringae* pv. *syringae*: comparison of the biosurfactant and ion channel-forming activities of syringopeptin and syringomycin. *Mol Plant Microbe Interact* 10, 347-354.
- Hutchison, M.L., Tester, M.A., and Gross, D.C. (1995). Role of biosurfactant and ion channel-forming activities of syringomycin in transmembrane ion flux: a model for the mechanism of action in the plant-pathogen interaction. *Mol Plant Microbe Interact* 8, 610-620.
- Huynh, T.V., Dahlbeck, D., and Staskawicz, B.J. (1989). Bacterial blight of soybean: regulation of a pathogen gene determining host cultivar specificity. *Science* 245, 1374-1377.
- Iacobellis, N.S., Lavermicocca, P., Grgurina, I., Simmaco, M., and Ballio, A. (1992). Phytotoxic properties of *Pseudomonas syringae* pv. *syringae* toxins. *Physiol Mol Plant Pathol* 40, 107-116.
- Ishimoto, K.S., and Lory, S. (1989). Formation of pilin in *Pseudomonas aeruginosa* requires the alternative sigma factor (RpoN) of RNA polymerase. *Proc Natl Acad Sci U S A* 86, 1954-1957.
- Jamir, Y., Guo, M., Oh, H.S., Petnicki-Ocwieja, T., Chen, S.R., Tang, X.Y., Dickman, M.B., Collmer, A., and Alfano, J.R. (2004). Identification of *Pseudomonas syringae* type III effectors that can suppress programmed cell death in plants and yeast. *Plant J* 37, 554-565.
- Kalscheuer, R., Syson, K., Veeraraghavan, U., Weinrick, B., Biermann, K.E., Liu, Z., Sacchettini, J.C., Besra, G., Bornemann, S., and Jacobs, W.R. (2010). Self-poisoning of *Mycobacterium tuberculosis* by targeting GlgE in an alpha-glucan pathway. *Nat Chem Biol* 6, 376-384.
- Keith, L.M.W., and Bender, C.L. (1999). AlgT (sigma(22)) controls alginate production and tolerance to environmental stress in *Pseudomonas syringae*. *J Bacteriol* 181, 7176-7184.
- Kinscherf, T.G., and Willis, D.K. (1999). Swarming by *Pseudomonas syringae* B728a requires *gacS* (*lemA*) and *gacA* but not the acyl-homoserine lactone biosynthetic gene *ahII*. *J Bacteriol* 181, 4133-4136.
- Kitten, T., Kinscherf, T.G., McEvoy, J.L., and Willis, D.K. (1998). A newly identified regulator is required for virulence and toxin production in *Pseudomonas syringae*. *Mol Microbiol* 28, 917-929.
- Kurz, M., Burch, A.Y., Seip, B., Lindow, S.E., and Gross, H. (2010). Genome-driven investigation of compatible solute biosynthesis pathways of *Pseudomonas syringae* pv. *syringae* and their contribution to water stress tolerance. *Appl Environ Microbiol* 76, 5452-5462.

- Laville, J., Voisard, C., Keel, C., Maurhofer, M., Defago, G., and Haas, D. (1992). Global control in *Pseudomonas fluorescens* mediating antibiotic synthesis and suppression of black root rot of tobacco. *Proc Natl Acad Sci U S A* 89, 1562-1566.
- Lee, J., Teitzel, G.M., Munkvold, K., del Pozo, O., Martin, G.B., Michelmore, R.W., and Greenberg, J.T. (2012). Type III secretion and effectors shape the survival and growth pattern of *Pseudomonas syringae* on leaf surfaces. *Plant Physiol* 158, 1803-1818.
- Li, S., Yu, X., and Beattie, G.A. (2013). Glycine betaine catabolism contributes to *Pseudomonas syringae* tolerance to hyperosmotic stress by relieving betaine-mediated suppression of compatible solute synthesis. *J Bacteriol* 195, 2415-2423.
- Lindeberg, M., Cartinhour, S., Myers, C.R., Schechter, L.M., Schneider, D.J., and Collmer, A. (2006). Closing the circle on the discovery of genes encoding Hrp regulon members and type III secretion system effectors in the genomes of three model *Pseudomonas syringae* strains. *Mol Plant Microbe Interact* 19, 1151-1158.
- Lu, S.E., Wang, N., Wang, J.L., Chen, Z.J., and Gross, D.C. (2005). Oligonucleotide microarray analysis of the salA regulon controlling phytotoxin production by *Pseudomonas syringae* pv. *syringae*. *Mol Plant Microbe Interact* 18, 324-333.
- Marlovits, T.C., Kubori, T., Sukhan, A., Thomas, D.R., Galan, J.E., and Unger, V.M. (2004). Structural insights into the assembly of the type III secretion needle complex. *Science* 306, 1040-1042.
- Maruta, K., Hattori, K., Nakada, T., Kubota, M., Sugimoto, T., and Kurimoto, M. (1996a). Cloning and sequencing of trehalose biosynthesis genes from *Arthrobacter* sp Q36. *Biochim Biophys Acta* 1289, 10-13.
- Maruta, K., Hattori, K., Nakada, T., Kubota, M., Sugimoto, T., and Kurimoto, M. (1996b). Cloning and sequencing of trehalose biosynthesis genes from *Rhizobium* sp M-11. *Biosci Biotechnol Biochem* 60, 717-720.
- Maruta, K., Kubota, M., Fukuda, S., and Kurimoto, M. (2000). Cloning and nucleotide sequence of a gene encoding a glycogen debranching enzyme in the trehalose operon from *Arthrobacter* sp Q36. *Biochim Biophys Acta* 1476, 377-381.
- Marutani, M., Taguchi, F., Ogawa, Y., Hossain, M.M., Inagaki, Y., Toyoda, K., Shiraishi, T., and Ichinose, Y. (2008). Gac two-component system in *Pseudomonas syringae* pv. *tabaci* is required for virulence but not for hypersensitive reaction. *Mol Genet Genomics* 279, 313-322.
- Melotto, M., Underwood, W., Koczan, J., Nomura, K., and He, S.Y. (2006). Plant stomata function in innate immunity against bacterial invasion. *Cell* 126, 969-980.
- Miller, C.D., Mortensen, W.S., Braga, G.U.L., and Anderson, A.J. (2001). The *rpoS* gene in *Pseudomonas syringae* is important in surviving exposure to the near-UV in sunlight. *Curr Microbiol* 43, 374-377.
- Misas-Villamil, J.C., Kolodziejek, I., Crabill, E., Kaschani, F., Niessen, S., Shindo, T., Kaiser, M., Alfano, J.R., and van der Hoorn, R.A. (2013). *Pseudomonas syringae* pv. *syringae* uses



- proteasome inhibitor syringolin A to colonize from wound infection sites. *PLoS Pathog* 9, e1003281.
- Mitchell, R.E., and Bielecki, R.L. (1977). Involvement of phaseolotoxin in halo blight of beans: transport and conversion to functional toxin. *Plant Physiol* 60, 723-729.
- Monier, J.M., and Lindow, S.E. (2003). Differential survival of solitary and aggregated bacterial cells promotes aggregate formation on leaf surfaces. *Proc Natl Acad Sci U S A* 100, 15977-15982.
- Nishimoto, T., Nakano, M., Nakada, T., Chaen, H., Fukuda, S., Sugimoto, T., Kurimoto, M., and Tsujisaka, Y. (1996). Purification and properties of a novel enzyme, trehalose synthase, from *Pimelobacter* sp R48. *Biosci Biotechnol Biochem* 60, 640-644.
- Nomura, K., DebRoy, S., Lee, Y.H., Pumplin, N., Jones, J., and He, S.Y. (2006). A bacterial virulence protein suppresses host innate immunity to cause plant disease. *Science* 313, 220-223.
- O'Brien, H.E., Thakur, S., and Guttman, D.S. (2011). Evolution of plant pathogenesis in *Pseudomonas syringae*: a genomics perspective. *Annu Rev Phytopathol* 49, 269-289.
- Oguiza, J.A., Kiil, K., and Ussery, D.W. (2005). Extracytoplasmic function sigma factors in *Pseudomonas syringae*. *Trends Microbiol* 13, 565-568.
- Quinones, B., Dulla, G., and Lindow, S.E. (2005). Quorum sensing regulates exopolysaccharide production, motility, and virulence in *Pseudomonas syringae*. *Mol Plant Microbe Interact* 18, 682-693.
- Quinones, B., Pujol, C.J., and Lindow, S.E. (2004). Regulation of AHL production and its contribution to epiphytic fitness in *Pseudomonas syringae*. *Mol Plant Microbe Interact* 17, 521-531.
- Rahme, L.G., Mindrinos, M.N., and Panopoulos, N.J. (1992). Plant and environmental sensory signals control the expression of *hrp* genes in *Pseudomonas syringae* pv. phaseolicola. *J Bacteriol* 174, 3499-3507.
- Reimann, C., Hofmann, C., Mauch, F., and Dudler, R. (1995). Characterization of a rice gene induced by *Pseudomonas syringae* pv. *syringae*: requirement for the bacterial *lemA* gene function. *Physiol Mol Plant Pathol* 46, 71-81.
- Sagot, B., Gaysinski, M., Mehiri, M., Guignon, J.M., Le Rudulier, D., and Alloing, G. (2010). Osmotically induced synthesis of the dipeptide N-acetylglutaminylglutamine amide is mediated by a new pathway conserved among bacteria. *Proc Natl Acad Sci U S A* 107, 12652-12657.
- Sawada, H., Suzuki, F., Matsuda, I., and Saitou, N. (1999). Phylogenetic analysis of *Pseudomonas syringae* pathovars suggests the horizontal gene transfer of *argK* and the evolutionary stability of *hrp* gene cluster. *J Mol Evol* 49, 627-644.
- Schellenberg, B., Ramel, C., and Dudler, R. (2010). *Pseudomonas syringae* virulence factor syringolin A counteracts stomatal immunity by proteasome inhibition. *Mol Plant Microbe Interact* 23, 1287-1293.

- Schenk, A., Weingart, H., and Ullrich, M.S. (2008). The alternative sigma factor AlgT, but not alginate synthesis, promotes *in planta* multiplication of *Pseudomonas syringae* pv. *glycinea*. *Microbiology* 154, 413-421.
- Singh, S., Koehler, B., and Fett, W.F. (1992). Effect of osmolarity and dehydration on alginate production by fluorescent *Pseudomonads*. *Curr Microbiol* 25, 335-339.
- Smith, L.T., and Smith, G.M. (1989). An osmoregulated dipeptide in stressed *Rhizobium meliloti*. *J Bacteriol* 171, 4714-4717.
- Stockwell, V.O., Hockett, K., and Loper, J.E. (2009). Role of RpoS in stress tolerance and environmental fitness of the phyllosphere bacterium *Pseudomonas fluorescens* strain 122. *Phytopathology* 99, 689-695.
- Stockwell, V.O., and Loper, J.E. (2005). The sigma factor RpoS is required for stress tolerance and environmental fitness of *Pseudomonas fluorescens* Pf-5. *Microbiology* 151, 3001-3009.
- Storey, R., and Jones, R.G.W. (1975). Betaine and choline levels in plants and their relationship to NaCl stress. *Plant Sci Lett* 4, 161-168.
- Studholme, D.J., Ibanez, S.G., MacLean, D., Dangl, J.L., Chang, J.H., and Rathjen, J.P. (2009). A draft genome sequence and functional screen reveals the repertoire of type III secreted proteins of *Pseudomonas syringae* pathovar *tabaci* 11528. *BMC Genomics* 10, 395.
- Sutherland, I.W. (2001). Microbial polysaccharides from Gram-negative bacteria. *Int Dairy J* 11, 663-674.
- Thomas, M.D., Langstonunkefer, P.J., Uchytel, T.F., and Durbin, R.D. (1983). Inhibition of glutamine-synthetase from pea by tabtoxinine-beta-lactam. *Plant Physiol* 71, 912-915.
- Thompson, L.S., Webb, J.S., Rice, S.A., and Kjelleberg, S. (2003). The alternative sigma factor RpoN regulates the quorum sensing gene *rhII* in *Pseudomonas aeruginosa*. *FEMS Microbiol Lett* 220, 187-195.
- Totten, P.A., Lara, J.C., and Lory, S. (1990). The *rpoN* gene product of *Pseudomonas aeruginosa* is required for expression of diverse genes, including the flagellin gene. *J Bacteriol* 172, 389-396.
- van Dijk, K., Fouts, D.E., Rehm, A.H., Hill, A.R., Collmer, A., and Alfano, J.R. (1999). The Avr (effector) proteins HrmA (HopPsyA) and AvrPto are secreted in culture from *Pseudomonas syringae* pathovars via the Hrp (type III) protein secretion system in a temperature- and pH-sensitive manner. *J Bacteriol* 181, 4790-4797.
- Wang, N., Lu, S.E., Wang, J.L., Chen, Z.J., and Gross, D.C. (2006). The expression of genes encoding lipodepsipeptide phytotoxins by *Pseudomonas syringae* pv. *syringae* is coordinated in response to plant signal molecules. *Mol Plant Microbe Interact* 19, 257-269.
- Wargo, M.J., Szwergold, B.S., and Hogan, D.A. (2008). Identification of two gene clusters and a transcriptional regulator required for *Pseudomonas aeruginosa* glycine betaine catabolism. *J Bacteriol* 190, 2690-2699.

- Waspi, U., Blanc, D., Winkler, T., Ruedi, P., and Dudler, R. (1998). Syringolin, a novel peptide elicitor from *Pseudomonas syringae* pv. *syringae* that induces resistance to *Pyricularia oryzae* in rice. *Mol Plant Microbe Interact* 11, 727-733.
- Waspi, U., Hassa, P., Staempfli, A.A., Molleyres, L.P., Winkler, T., and Dudler, R. (1999). Identification and structure of a family of syringolin variants: Unusual cyclic peptides from *Pseudomonas syringae* pv. *syringae* that elicit defense responses in rice. *Microbiol Res* 154, 89-93.
- Whistler, C.A., Corbell, N.A., Sarniguet, A., Ream, W., and Loper, J.E. (1998). The two-component regulators GacS and GacA influence accumulation of the stationary-phase sigma factor sigma(S) and the stress response in *Pseudomonas fluorescens* Pf-5. *J Bacteriol* 180, 6635-6641.
- Whitehead, N.A., Barnard, A.M.L., Slater, H., Simpson, N.J.L., and Salmond, G.P.C. (2001). Quorum-sensing in gram-negative bacteria. *FEMS Microbiol Rev* 25, 365-404.
- Willis, D.K., Hrabak, E.M., Rich, J.J., Barta, T.M., Lindow, S.E., and Panopoulos, N.J. (1990). Isolation and characterization of a *Pseudomonas syringae* pv. *syringae* mutant deficient in lesion formation on bean. *Mol Plant Microbe Interact* 3, 149-156.
- Xiao, F.M., Goodwin, S.M., Xiao, Y.M., Sun, Z.Y., Baker, D., Tang, X.Y., Jenks, M.A., and Zhou, J.M. (2004). *Arabidopsis* CYP86A2 represses *Pseudomonas syringae* type III genes and is required for cuticle development. *Embo J* 23, 2903-2913.
- Xiao, Y.X., Heu, S.G., Yi, J.S., Lu, Y., and Hutcheson, S.W. (1994). Identification of a putative alternate sigma factor and characterization of a multicomponent regulatory cascade controlling the expression of *Pseudomonas syringae* pv. *syringae* pss61 *hrp* and *hrmA* genes. *J Bacteriol* 176, 1025-1036.
- Yu, J., Penaloza-Vazquez, A., Chakrabarty, A.M., and Bender, C.L. (1999). Involvement of the exopolysaccharide alginate in the virulence and epiphytic fitness of *Pseudomonas syringae* pv. *syringae*. *Mol Microbiol* 33, 712-720.
- Yu, X., Lund, S.P., Scott, R.A., Greenwald, J.W., Records, A.H., Nettleton, D., Lindow, S.E., Gross, D.C., and Beattie, G.A. (2013). Transcriptional responses of *Pseudomonas syringae* to growth in epiphytic versus apoplastic leaf sites. *Proc Natl Acad Sci U S A* 110, E425-434.
- Zhao, Y.F., Thilmony, R., Bender, C.L., Schaller, A., He, S.Y., and Howe, G.A. (2003). Virulence systems of *Pseudomonas syringae* pv. *tomato* promote bacterial speck disease in tomato by targeting the jasmonate signaling pathway. *Plant J* 36, 485-499.

## CHAPTER 2. TRANSCRIPTIONAL RESPONSES OF *PSEUDOMONAS SYRINGAE* TO GROWTH IN EPIPHYTIC VERSUS APOPLASTIC LEAF SITES

A paper published in *Proc Natl Acad Sci U S A* (2013) 110, E425-E434

Xilan Yu<sup>1</sup>, Steven P. Lund<sup>2</sup>, Russell Scott<sup>3</sup>, Jessica W. Greenwald<sup>4</sup>, Angela H. Records<sup>4</sup>, Dan Nettleton<sup>2</sup>, Steven E. Lindow<sup>3</sup>, Dennis C. Gross<sup>4</sup> and Gwyn A. Beattie<sup>1\*</sup>

<sup>1</sup>Department of Plant Pathology and Microbiology, Iowa State University

<sup>2</sup>Department of Statistics, Iowa State University

<sup>3</sup>Department of Plant and Microbial Biology, University of California-Berkeley

<sup>4</sup>Department of Plant Pathology and Microbiology, Texas A&M University

### Abstract

Some strains of the foliar pathogen *Pseudomonas syringae* are adapted for growth and survival on leaf surfaces and in the leaf interior. Global transcriptome profiling was used to evaluate if these two habitats offer distinct environments for bacteria and thus present distinct driving forces for adaptation. The transcript profiles of *Pseudomonas syringae* pv. *syringae* B728a support a model in which leaf surface, or epiphytic, sites specifically favor flagellar motility, swarming motility based on HAA surfactant production, chemosensing and chemotaxis, indicating active relocation primarily on the leaf surface. Epiphytic sites also promote high transcript levels for phenylalanine degradation, which may help counteract phenylpropanoid-based defenses prior to leaf entry. In contrast, intercellular, or apoplastic, sites favor the high-level expression of genes for  $\gamma$ -amino butyric acid (GABA) metabolism, for which

degradation would attenuate GABA repression of virulence, and synthesis of phytotoxins, two novel secondary metabolites, and syringolin A, which supports roles for these compounds in virulence, including a role for syringolin A in suppressing defense responses beyond stomatal closure. A comparison of the transcriptomes from the *in planta* cells to those of cells exposed to osmotic stress, oxidative stress, and iron and nitrogen starvation indicated that the environments in both leaf habitats were particularly limited in water availability, with water limitation being more severe in the apoplast than on the leaf surface under the conditions tested. These findings contribute to a coherent model of the adaptations of this widespread bacterial phytopathogen to distinct habitats within its host.

## Introduction

Plant leaves are colonized by an abundance of microorganisms. Among these is *Pseudomonas syringae*, which is a model bacterial foliar pathogen with a wide host range and vast geographic distribution. *P. syringae* strains vary in their ability to establish and maintain epiphytic, or leaf surface, populations prior to infection. One of the most well-studied *P. syringae* strains, *P. syringae* pv. *syringae* B728a, has a particularly pronounced epiphytic phase when growing on leaves of the host plant bean (*Phaseolus vulgaris* L.), but can also establish populations in the intercellular spaces, or apoplast, that may or may not be associated with visible symptoms of bacterial brown spot. For some foliar bacterial pathogens like B728a, populations can reach  $10^7$  cells per gram of fresh tissue in epiphytic sites and  $10^{10}$  cells per gram

in apoplastic sites. We predict that the driving forces for *P. syringae* adaptations for growth and survival in epiphytic sites are distinct from those in the apoplast, and that these forces are mainly shaped by the external environment for the former and by plant defense responses for the latter. In particular, leaf surface bacteria likely encounter fluctuations in water availability, temperature and solar radiation as well as frequent nutrient limitation due to a heterogeneous distribution of nutrients (Monier and Lindow, 2003b). In contrast, bacteria in the apoplast likely experience slight acidity and oxidative stress resulting from the plant's defenses.

To better understand the interactions of bacterial phytopathogens with leaves, most work has focused on specific factors contributing to virulence or fitness (Hirano et al., 1999; Scholz-Schroeder et al., 2001; Yu et al., 1999) and specific environmental conditions influencing survival (Joyner and Lindow, 2000; Leveau and Lindow, 2001), although *in vivo* expression technologies have been used to identify many *P. syringae* genes that are induced in or on leaves (Boch et al., 2002; Marco et al., 2005). These studies have rarely attempted to integrate knowledge of the environmental conditions in leaf habitats with the *P. syringae* adaptations used to survive or exploit those habitats. In this study we used global transcriptome profiling to understand the various environmental conditions that *P. syringae* cells encounter during their association with plants. We analyzed genes and traits in B728a that were responsive to growth on the leaf surface, in the leaf apoplast, and under four environmental conditions predicted to be characteristic of these habitats. Our findings suggest that B728a cells experience vastly different environments when growing on the surface versus the interior of leaves and identify distinct

traits that are likely used for persistence and growth in these environments. Collectively, these results demonstrate both epiphytic and apoplastic stages in the B728a lifecycle.

## Results and discussion

### ***P. syringae* encounters distinct environmental stresses *in planta*.**

We collected RNA from B728a cells that were exposed to seven treatments, each with two biological replicates in each of three laboratories. The treatments included exposing cells to a basal medium, sodium chloride to confer an osmotic stress, hydrogen peroxide to confer an oxidative stress, iron limitation, nitrogen limitation, and epiphytic and apoplastic growth (see Materials and Methods and Figs S1-S6). The RNA was labeled and hybridized to an ORF-based microarray by Roche-NimbleGen. A comparison of the treatments based on a hierarchical clustering of the transcript abundances showed that N limitation had the largest effect on the transcriptomes (Fig 1). N limitation affected a majority of the B728a genes and thus likely imposed a large metabolic shift, as supported by the lack of growth during N limitation (Fig S4). The transcriptomes of the *in planta* treatments highly diverged from the other treatments, with clear differences between epiphytic and apoplastic cells (Fig 1). Among the remaining treatments, osmotic stress had the largest effect, whereas oxidative stress and iron limitation had relatively small effects. These results may reflect a broader array of genes required for cellular adaptation to osmotic than oxidative stress and low iron, and/or stress attenuation due to

peroxide detoxification. Collectively, this hierarchical clustering indicates that each treatment had a detectably distinct impact on the cells.

We evaluated the extent to which the transcriptomes *in planta* reflected exposure to each environmental stress by correlation analysis of the combined dataset, i.e., the pooled data from the three laboratories. When transcript levels relative to the basal medium were plotted for the *in vitro* and *in planta* treatments, the transcripts that were increased in the epiphytic and apoplastic sites most strongly correlated with those increased in the osmotic stress and N limitation treatments (Fig 2). These plots also show the general direction and magnitude of the changes in transcript abundance, with the N limitation treatment causing large decreases as well as increases in transcript abundance and the other stresses primarily causing only increases. This is consistent with N limitation inducing a metabolic downshift and the other stresses inducing specific adaptations. Prior reports documented that B728a cells decrease in size following inoculation (Monier and Lindow, 2003b), suggestive of a metabolic downshift in most cells. However, the predominance of increases rather than decreases in the transcript levels in the epiphytic and apoplastic cells relative to the basal medium (Fig 2) suggests that, at least by 48 to 72 h after inoculation, the majority of cells were not in a physiological state of starvation like that of the N-limited cells.

We also evaluated the extent to which the transcriptomes *in planta* reflected exposure to each stress by using multiple regression analysis. For the transcriptomes identified in each laboratory and the combined dataset, we regressed the transcript levels of all of the genes in the epiphytic



transcriptome on those of the *in vitro* stresses and basal medium while constraining the coefficients to be non-negative and to sum to one (Table 1); we did the same for the apoplastic transcriptome data. The resulting coefficients suggested a large contribution of osmotic stress and N limitation to the transcriptome of cells in epiphytic and apoplastic sites. Moreover, within each dataset, the osmotic stress transcriptome was more strongly correlated to the apoplastic than epiphytic transcriptome, suggesting that *P. syringae* experienced a more severe water limitation in the leaf interior than on the leaf surface. Surprisingly, the *in planta* transcriptomes were most poorly correlated with the oxidative stress transcriptome. This again could be due to the relatively small impact of oxidative stress on the transcriptome of *P. syringae*, to an unexpected attenuation of the applied stress, or to a distinct response of the cells to oxidative stress *in planta* than *in vitro*.

### ***P. syringae* encounters distinct environments in epiphytic versus apoplastic sites.**

For the combined dataset, the transcript levels of 65% of the B728a genes were altered by growth in epiphytic sites as compared to in the basal medium, and 22% of these were altered in epiphytic but not apoplastic sites (Fig 3). Similarly 50% of the B728a genes were altered in apoplastic sites, with 8% altered specifically in the apoplast. A large impact of the *in planta* treatments on gene expression, and a distinct response to epiphytic versus apoplastic sites, was similarly evidenced in the individual datasets generated in each lab.

To identify the B728a adaptations specific to each environment, we identified the functional categories in which the representation of differentially expressed genes was greater than that in

all of the B728a genes (Fig 4, Tables S1-S2); genes were designated as differentially expressed based on a  $P$ -value  $< 0.05$  and a  $q$ -value  $< 0.01$ . Genes in the chemosensing and chemotaxis category were unique in being over-represented among induced genes in epiphytic cells and among repressed genes in apoplastic cells (Figs 4A, B). Genes in the sulfur metabolism and transport category were over-represented among induced genes in epiphytic but not apoplastic cells. In contrast, genes in the phage and IS elements and mechanosensitive ion channels categories were over-represented among induced genes in apoplastic but not epiphytic cells. Many other categories showed quantitative differences between epiphytic and apoplastic cells based on the percentage of differentially expressed genes (Figs 4A, B). For categories with particularly large differences, or for individual gene sets within these categories, we calculated the mean fold-changes in transcript abundance across all of the genes in the category or gene set (Fig 5) and will discuss many of these below. The categories with over-represented genes that were induced in cells exposed to osmotic stress and iron and N limitation generally reflected the functions known for bacterial responses to these stresses (Fig 4C).

***P. syringae* traits strongly favored on the leaf surface include motility and specific amino acid metabolism pathways.**

*Flagellar synthesis and motility.* The mean induction level of genes in this category was  $>4.5$ -fold more for cells in epiphytic than apoplastic sites (Fig 5 and Table S3). Flagellar motility contributes to *P. syringae* invasion of bean leaves (Panopoulous and Schroth, 1974) and to *Salmonella enterica* invasion through stomata into submerged leaves (Kroupitski et al., 2009). It also contributes to B728a fitness on bean leaf surfaces, in part, by promoting movement to sites

protected from environmental stresses (Haefele and Lindow, 1987). The strong preferential expression of flagellar motility genes on leaf surfaces suggests more active relocation for nutrients on the surface than in the interior, as well as possibly movement to stomata for entry into the interior.

Swarming motility by B728a requires surfactant production (Burch et al., 2012). The *rhlA* gene that is involved in synthesizing the surfactant 3-(3-hydroxyalkanoyloxy) alkanolic acid (HAA) (Burch et al., 2012) was also induced more in epiphytic cells (9.1-fold) than in apoplastic cells (6.7-fold). Although the *rhlA* transcripts were more abundant than 97% of the other B728a genes in the basal medium, this gene was induced 50-fold by N limitation. Based on the known role of HAA in swarming motility, this induction pattern is consistent with HAA and swarming motility contributing to cellular motility to acquire nutrients on leaf surfaces.

*Chemosensing and chemotaxis.* Genes in this category were generally induced in epiphytic cells but repressed in apoplastic cells (Fig 5 and Table S3). This finding suggests that active, directed movement to nutrients is not needed in the apoplast. The role of chemotaxis in *P. syringae* fitness and pathogenesis has not been evaluated. *P. syringae* exhibits chemotaxis to host extracts (Cuppels, 1988), to likely breakdown products from plant phosphatidylcholine (C. Chen and G.A. Beattie, unpublished data), and to the plant hormone ethylene (Kim et al., 2007), although the gene for the putative ethylene methyl-accepting chemotaxis protein, Psyr\_2682, was not induced *in planta*. The need for chemosensing and chemotaxis on leaves is supported by the heterogeneous distribution of nutrients on leaves, as assessed using a fructose bioreporter

(Leveau and Lindow, 2001), and the preferential formation of *P. syringae* aggregates near glandular trichomes (Monier and Lindow, 2004), suggesting a benefit from attraction to the compounds at these sites.

*Phenylalanine metabolism.* Although amino acid metabolism and transport genes generally were decreased in expression *in planta* (Fig 4B), phenylalanine catabolism genes were induced an average of 12.2-fold in epiphytic cells and 5.9-fold in apoplastic cells (Fig 5). These genes encode orthologs to *P. putida* enzymes that degrade phenylalanine to tyrosine via PhhAB and tyrosine to homogentisate, acetoacetate and fumarate via Hpd, HmgABC and a two-subunit acetoacetyl-CoA transferase DhcAB (Arias-Barrau et al., 2004). Although B728a lacks an HmgC ortholog, genes for the other seven enzymes were induced in both *in planta* sites. The induction of *phhAB* by phenylalanine (Fig S7) suggests that sufficient phenylalanine is present to induce a high level of expression on leaf surfaces and a moderate level in the apoplast. Phenylalanine in plants serves as a substrate for the synthesis of phenylpropanoid compounds, which are important in plant defense. Moreover, phenylalanine and tyrosine levels increase in *Arabidopsis* plants following infection with *P. syringae* strain DC3000, based on metabolomic analyses (Ward et al., 2010), and suppression of genes for some key phenylpropanoid biosynthetic enzymes was associated with *P. syringae* type III effector proteins (Truman et al., 2006). These observations support a model in which *P. syringae* infection elicits phenylalanine synthesis as a step toward phenylpropanoid synthesis, and *P. syringae* delivery of effector proteins suppresses this plant defense response. Our results are surprising in their support for increased catabolism of

these amino acids by B728a, particularly on leaf surfaces, suggesting that B728a activates these plant defenses prior to infection of the apoplast and counteracts this defense response through active aromatic amino acid degradation on the leaf surface.

*Tryptophan and IAA metabolism.* Transcripts for the *trpAB* operon also showed large increases in the cells recovered from plants. In *P. putida*, *trpAB* is induced by TrpI in response to indole 3-glycerol phosphate (InGP) whereas *trpEGDC* is repressed by TrpI in response to tryptophan (Molina-Henares et al., 2009). Transcripts of *trpEFGDC* in B728a decreased approximately 2-fold in both *in planta* sites (Table S3), suggesting the presence of tryptophan both on and in the leaves. In contrast, the approximately 4.2-fold induction of *trpAB* in epiphytic cells, and 1.6-fold induction in apoplastic cells, suggests the presence of InGP. A likely source of InGP on leaves is from TrpA-mediated conversion of indole to InGP, and this may be converted to tryptophan via TrpAB (Molina-Henares et al., 2009). A likely source of the indole is from the plant, as suggested by the recent demonstration that *P. syringae* infection of *Arabidopsis* plants resulted in an increase in *Arabidopsis* transcripts involved in the synthesis of indole derivatives (Ward et al., 2010).

B728a has the genetic capacity to convert tryptophan to indole-3-acetamide (IAM) and then to indole-3-acetic acid (IAA) using the IaaM and IaaH proteins, respectively (Mazzola and White, 1994). We observed a 5- to 7-fold induction of *iaaM-1* *in planta*, but almost no *iaaH-1* or *iaaH-2* expression, suggesting that IAM but not IAA was likely produced *in planta*. The fate of IAM, if produced, is not clear. B728a also appears to have the genetic capacity to convert

indole-3-acetaldoxime, which is produced in *Arabidopsis* following *P. syringae* infection (Ward et al., 2010), to IAA. This pathway involves a putative aldoxime dehydratase (Psyr\_0006) that dehydrates indole-3-acetaldoxime to indole-3-acetonitrile and a nitrilase (Psyr\_0007) that has been shown to convert indole-3-acetonitrile to IAA (Howden et al., 2009). Transcript levels for these two genes, however, were extremely low in basal medium and were not altered *in planta*, suggesting that IAA was not likely produced by this pathway. Although IAA production by another *P. syringae* strain influences its interaction with bean plants (Mazzola and White, 1994), our results do not provide evidence for IAA production by B728a on leaves.

***P. syringae* traits strongly favored in the apoplast include GABA uptake and catabolism and the production of various secondary metabolites.**

*GABA metabolism and transport.* Genes involved in the metabolism and transport of the non-protein amino acid  $\gamma$ -amino butyric acid (GABA) were induced an average of 4.1-fold in apoplastic sites and 2.2-fold in epiphytic sites (Fig 5). These genes include *gabP*, which encodes a GABA permease for uptake, and three paralogs for *gabT* and *gabD*, which encode enzymes that sequentially convert GABA to succinate (Park et al., 2010). With the exception of *gabD-2*, all of these genes were induced *in planta* and were induced more in the apoplast than on the leaf surface. They were also induced by N limitation (Table S3), consistent with the use of GABA as a C and N source (Rico and Preston, 2008). Similar to in B728a, *gabP* in *P. syringae* pv. *phaseolicola* was induced by apoplastic fluid from bean leaves (Hernandez-Morales et al., 2009).

This induction likely reflects the availability of plant-derived GABA. The presence of plant-derived GABA in bean is suggested by the high levels of GABA found in the apoplastic fluid of healthy, uninfected tomato leaves (Rico and Preston, 2008), and the 3-fold increase in GABA levels in *Arabidopsis* leaves following *P. syringae* infection (Ward et al., 2010).

Interestingly, GABA may play a regulatory role in addition to its nutritional role based on the fact that high GABA concentrations (>1 mM) inhibited *P. syringae* growth *in planta*, strongly reduced expression of the *hrpL* and *avrPto* virulence genes, and induced the *Arabidopsis* defense gene *PRI* (Park et al., 2010). The greater induction of genes for GABA catabolism in the apoplast than in epiphytic sites may be associated with a greater need to prevent

GABA-mediated repression of virulence genes during its apoplastic, or pathogenic, phase.

Several of the GABA genes, including *gabT* and *gabD*, were induced by osmotic stress; this is consistent with the speculation that GabT has a role in polyamine homeostasis and thus in osmoregulation (Park et al., 2010).

*Production of secondary metabolites.* Many genes for secondary metabolites that are synthesized by nonribosomal peptide synthetases (NRPSs) or NRPSs fused with polyketide synthetases (PKSs) were induced more in the apoplast than on leaf surfaces. For example, genes involved in the synthesis and transport of the phytotoxins syringomycin and syringopeptin were induced an average of 11.4- and 4.9-fold in apoplastic and epiphytic sites, respectively (Fig 5). This is consistent with a previous report that the syringomycin *syrE* gene was induced in B728a during its association with bean leaves (Marco et al., 2005). Transcript levels of most syringomycin and

syringopeptin genes were not affected by the *in vitro* treatments, consistent with the need for plant-derived compounds for induction (Mo and Gross, 1991). Transcripts for the syringomycin synthesis genes were increased more than those of the syringopeptin genes *in planta*. The relative contribution of these phytotoxins to virulence on bean leaves is not known, but for strain B301D on immature cherry fruit, syringopeptin was found to contribute more to virulence than syringomycin (Scholz-Schroeder et al., 2001).

The *sylABCDE* genes involved in the synthesis and transport of syringolin A, a compound produced by a mixed NRPS/PKS, were induced 5.8- and 1.6-fold in cells in the apoplast and on the leaf surface, respectively (Fig 5). Syringolin A was first identified as a peptide elicitor of resistance to a fungal pathogen in rice (Waspi et al., 1998b), but later was recognized as a virulence factor of B728a on bean. Syringolin A was recently shown to contribute to B728a virulence on bean by counteracting an initial step in basal plant immunity, stomatal closure (Schellenberg et al., 2010a). Syringolin A does this by irreversibly inhibiting the eukaryotic proteasome, which may prevent turnover of the key defense protein *NPRI* (Schellenberg et al., 2010a). Although open stomata should primarily benefit cells on the leaf surface, greater induction of the *syl* genes in the apoplast than on the leaf surface suggests additional functions for syringolin A, including suppression of additional host defenses following movement into the apoplast and promoting egression back onto the leaf surface after colonization of the apoplast.

A third set of genes encoding NRPSs are the genes involved in syringafactin synthesis. The syringafactin synthesis (*syfAB*) and regulatory (*syfR*) genes were induced in the apoplast



(3.9-fold) and slightly less in epiphytic sites (Fig 5). Siringafactin is a linear lipopeptide surfactant that contributes to *P. syringae* swarming motility (Berti et al., 2007). The induction of this surfactant on the surface of an agar medium occurs at the transcriptional level (Burch et al., 2011), which supports the possibility that increased transcript levels *in planta* correlates with increased syringafactin production. The *syfAB* transcript levels in the basal medium and the induction levels *in planta* were much lower than those for the HAA surfactant-encoding *rhlA* gene, which when combined with the higher *syfAB* induction in apoplastic than epiphytic sites, and higher *rhlA* induction in epiphytic than apoplastic sites, suggests that these two surfactants may have distinctive roles during B728a interactions with leaves.

Two uncharacterized secondary metabolites showed elevated transcripts *in planta*, an operon encoding several PKSs, Psyr\_4311-Psyr\_4315, and the NRPS-encoding gene, Psyr\_3722 (Table S3). These genes, and all of the other NRPS- and PKS-encoding genes that were induced *in planta*, were induced more in the apoplast than on the leaf surface. This finding suggests a greater role for these secondary metabolites during the pathogenic than epiphytic phase of B728a's association with leaves. Transcript levels of genes for three other NRPSs, as encoded by Psyr\_1792-1795, Psyr\_4662 and Psyr\_5009-5012, were not altered in the *in planta* treatments, although Psyr\_5009-5012 showed induction by iron and N limitation.

***P. syringae* experienced distinct nutritional and abiotic environments on leaf surfaces versus in the leaf interior.**

*Water limitation.* Three of the functional categories that were over-represented based on gene induction *in planta* were also induced by osmotic stress (Fig 4A, C). These categories included polysaccharide synthesis and regulation, compatible solute synthesis, and quaternary ammonium compound (QAC) metabolism and transport. Transcripts of genes involved in the synthesis and regulation of alginate, a polysaccharide associated with enhanced tolerance to water limitation (Chang et al., 2007a), were increased an average of 2-fold by the *in planta* treatments (Fig 5) and 3.8-fold by osmotic stress (Table S3). Biosynthetic genes for the two major compatible solutes of B728a, *N*-acetylglutaminyglutamine amide (NAGGN) and trehalose, showed an even more pronounced induction *in planta* than the alginate genes, with an average of 13.2- and 8.2-fold induction in the apoplast for the NAGGN and trehalose genes, respectively (Fig 5), as well as a strong response to osmotic stress, with an average of 42.5- and 10.9-fold induction, respectively (Table S3). The NAGGN and trehalose synthesis genes and the genes encoding transporters for osmoprotective QAC compounds were induced more in the apoplast than on leaf surfaces (Fig 5, Table S3). Assuming these genes show a proportional response to water limitation, as is known for some of them (S. Li and G. Beattie, unpublished data, Kurz et al., 2010b), greater induction in the apoplast suggests that B728a was even more limited for water in the leaf interior than on the leaf surface under the growth conditions used. Water limitation in the apoplast may result from low water content, such as from rapid evapotranspiration, and/or a high concentration of solutes, such as from nutrient leakage and secretion in the mesophyll.

*Iron limitation.* We did not find evidence that B728a cells were limited for iron *in planta*. Three of the four functional categories that were over-represented in the transcriptomes of the

iron-limited cells were not over-represented in either of the *in planta* transcriptomes (Fig 4A, C). Genes for the siderophore pyoverdine were induced 5-fold more by iron limitation than those for the siderophore achromobactin, but none of these were induced *in planta*. Citrate can also function as a siderophore in *P. syringae* DC3000 (Jones and Wildermuth, 2011), but putative genes for citrate-mediated iron uptake were not induced by iron limitation. Siderophore-mediated ferric iron uptake occurs via TonB-dependent outer membrane receptors, with subsequent reduction and transport into the cell. Of the six TonB-ExbB-ExbD operons in B728a, only one, Psyr\_0203-Psyr\_0205, was induced by iron limitation, and this was not induced *in planta*. Genes for iron storage proteins in the Dps, ferritin and bacterioferritin families were, on average, repressed 2-fold by iron limitation but induced 2-fold *in planta*. Lastly, three *fecIR*-like operons that encode regulators activating iron starvation responses were induced by iron limitation, as expected, but were not induced *in planta*. Collectively, these results indicate that iron is available to B728a cells both on leaf surfaces and in the apoplast. This conclusion is consistent with the finding that few B728a cells were iron-limited on bean leaves (Joyner and Lindow, 2000) and that DC3000 growth in the apoplast was not affected by loss of siderophore production (Jones and Wildermuth, 2011).

*Oxidative stress.* Genes for antioxidant enzymes were over-represented in the transcriptome of cells exposed to oxidative stress but were not over-represented in the *in planta* transcriptomes (Table S1). Distinct antioxidant enzymes were expressed *in vitro* than *in planta*. Of 17 antioxidant enzymes, genes for five were induced by oxidative stress: *ahpF*, *ahpC*, *ohr*, *katA* and *sodA*. Genes for a distinct set of six were induced *in planta*: *cpoF*, which is predicted to encode a chloroperoxidase involved in the reduction of hydrogen peroxide, the catalase-encoding *katE*,

*katG* and *katN* genes, and the superoxide dismutase-encoding *sodA* and *sodC* genes. All but one of these were induced more in the apoplast than on the leaf surface, as illustrated by the 49-, 31- and 15-fold induction of *cpoF*, *katE* and *katN* in the apoplast, respectively, but only 11-, 12- and 8-fold induction in epiphytic sites. These results suggest that B728a was exposed to some oxidative stress in plants and to more oxidative stress in the apoplast than on the leaf surface, which is consistent with a role for oxidative stress in plant defense, but also that B728a invokes distinct protective enzymes against oxidative stress in a host plant than in culture.

*Nutritional metabolism.* We investigated whether B728a was N limited *in planta*. N limitation *in vitro* decreased the transcript levels of 33% of the B728a genes, demonstrating that the N limitation treatment caused a major metabolic downshift and thus conferred a severe limitation for N. An over-representation analysis showed that N limitation favored the induction of genes in the N metabolism category (Fig 4C), including many that are known or predicted to be induced by N limitation (Table S3). An over-representation analysis also indicated that the N limitation treatment and growth *in planta* affected genes in many of the same functional categories (Figs 4B, D). To evaluate whether this similarity suggested N limitation *in planta*, we examined the expression of a collection of genes assembled as indicators for N versus C limitation based on previous studies with *Sinorhizobium meliloti* and *Bacillus licheniformis* (Krol and Becker, 2011; Voigt et al., 2007) (Table S4). We found only equivocal evidence for N limitation in or on leaves, based on that only 33% of the N limitation indicator genes were induced in epiphytic sites, and only 11% were induced in the apoplast; moreover, only a quarter of the N metabolism

genes that were induced by the N limitation treatment were induced in epiphytic sites, and only 13% were induced in the apoplast. The strongest evidence against at least severe N limitation on and in leaves was the finding that of the 15 N metabolism genes that were induced the most by N limitation *in vitro* (Table S3), none were induced in the apoplast and only three were weakly induced in epiphytic sites. Thus, as we concluded above, the majority of B728a cells were not in a physiological state of starvation like that of the N-limited cells.

About half of the sulfur metabolism and transport genes were induced more in epiphytic sites than in apoplastic sites (Figs 4A, 5). These genes included many involved in sulfonate uptake and metabolism, sulfate transport, sulfite oxidation and thiosulfate reduction (Table S1). A previous study identified the B728a sulfonate metabolism *ssuE* gene as plant inducible (Marco et al., 2005), as we did here, but also identified the sulfur-related genes *cysE* and *betC* as plant inducible, which we did not. In general, sulfur nutrition in the phyllosphere is poorly understood.

Phosphate metabolism and transport genes were not over-represented among the differentially expressed genes *in planta*; however, the genes that were expressed suggest active phosphate scavenging. An alkaline phosphatase and an ortholog of a protein involved in alkaline phosphatase secretion in *P. aeruginosa*, Psyr\_3150, were both induced *in planta*, as was the PhoB/PhoR two-component regulator of phosphate assimilation and a phosphate transporter (Table S3). All of these genes showed greater levels of induction in epiphytic sites than in the apoplast, with the transporter showing the largest difference, an 18.5-fold increase in epiphytic sites as compared to only 3.5-fold in the apoplast. The explanation for greater phosphate

scavenging on the leaf surface than in the apoplast is not clear, but could reflect differences in chemistry or competition from the small epiphytic microbial communities that were likely present.

As expected, carbohydrate and organic acid metabolism and transport genes were over-represented among the genes induced *in planta*, with half of these genes induced in both epiphytic and apoplastic cells (Fig 4A). Among the carbohydrates, a gene for a transporter of fucose, a plant cell wall component, was induced only on the leaf surface (Table S5), and transporter genes for the five-carbon sugars ribose, arabinose and xylose were induced in both environments, with those for xylose metabolism induced over 20-fold. In contrast, genes for the transport and metabolism of sucrose, inositol, and an unidentified disaccharide were induced far more in the apoplast than on the leaf surface. Among the organic acids, transporter genes for acetate, citrate, malate and an unidentified dicarboxylate were induced more in epiphytic than apoplastic cells, whereas transporter genes for glycolate, malonate and an unidentified tricarboxylate were induced more in the apoplast (Table S5). The presence of fructose, mannitol and succinate in the basal medium precluded the detection of genes activated by their presence *in planta*.

Metabolism and transport genes for a few amino acids were induced *in planta*. These included transporters for glutamate/aspartate, glutamine, methionine, and histidine, and with the exception of the histidine transporter, these were induced to similar levels in the epiphytic and apoplastic sites. The *liuDCBAE* genes, which are predicted to catalyze the second half of the

leucine catabolic pathway, were induced an average of 5-fold *in planta* (Table S3). Moreover, genes supporting histidine catabolism via urocanate were induced, and like the histidine transporter, were induced more in epiphytic than apoplastic sites (Table S3). Histidine is among the least abundant amino acids in leachates from bean leaves (Morgan and Tukey, 1964) and in apoplastic fluids from tomato leaves (Rico and Preston, 2008), suggesting that induction of these genes may reflect a novel role for histidine, consistent with the recent demonstration that histidine or urocanate has a key role in biofilm formation (Cabral et al., 2011).

The expression of several additional metabolic genes provides insights into the nutritional environment of leaves for *P. syringae*. First, only 15% of the genes involved in nucleotide metabolism were induced, but half of these were predicted to promote degradation of the purine base xanthine and were induced on leaves and even more in the leaf apoplast (Table S3). This degradation may be associated with reducing the capacity for bean to generate superoxide as a component of defense (Montalbini, 1992). Second, genes for the potassium transporter KdpFABC were induced an average of 3.6-fold on leaf surfaces but were not induced in the apoplast. The conserved regulation of this transporter, namely induction by an osmotic upshift and by severe potassium starvation, suggests more osmotic fluctuations in epiphytic than apoplastic sites, as *kdpFABC* expression decreases once cells reach homeostasis in the presence of osmotic stress, or a deficit of potassium in surface sites, although the driving force for such a deficit is not clear. Third, the *betLAB* genes that enable conversion of choline to the osmoprotective compound glycine betaine were induced, and were induced more in the apoplast

(8.1-fold) than in epiphytic sites (3.3-fold), supporting previous evidence that choline is abundant on leaves (Chen and Beattie, 2008b) and that water stress may be greater in the apoplast. Thirteen genes that contribute to glycine betaine catabolism in B728a (S. Li and G.A. Beattie, unpublished data) were also induced *in planta* (Table S3), suggesting that these QAC compounds serve as a source of nutrition as well as osmoprotection. Last, a polyamine transporter gene was induced 13.4- and 8.7-fold in epiphytic and apoplastic sites, respectively (Table S3), suggesting that polyamines such as spermidine or putrescine, which are known to be abundant in plants, are used by *P. syringae* during leaf colonization.

Although the type III secretion system (T3SS) and its secreted factors are critical to *P. syringae* virulence (Truman et al., 2006), the T3SS genes were expressed at low levels in the basal medium and *in planta* (Table S3). Almost 90% of these genes were induced by the low N treatment, consistent with the role of RpoN in expression of *hrpL*. Their lack of detectable expression *in planta* may be due to induction in only a subset of the cells, as was recently shown for *avrPto* in B728a in epiphytic and apoplastic sites (Lee et al., 2012b), or to induction that was only transient after infection and no longer detectable by 48 to 72 after inoculation.

***P. syringae* phage genes were induced *in planta* and particularly in the apoplast.**

A surprising finding was that phage-related genes in B728a were over-represented among the differentially expressed genes in cells from apoplastic but not epiphytic sites (Fig 4A). B728a has two clusters of putative prophage or phage genes, the 90-gene region Psyr\_2762 to



Psyr\_2854 and the 7-gene region Psyr\_4586 to Psyr\_4592, and another 28 that are insertion elements, transposases, phage integrases or other phage-related genes. None of the genes in the 7-gene region were induced *in planta*, whereas 60 of the 90 genes in the other region were induced in apoplastic cells, at an average of 3.2-fold, and 35 were induced in epiphytic cells, at an average of 2-fold. A similar bias toward the apoplast was shown in the remaining 28 genes, with six showing increased expression in the apoplast as compared to only two on leaf surfaces. Consistent with our findings, a recent characterization of the infectivity of phage isolated from the leaf surface versus from the leaf interior demonstrated greater infectivity of phage from the leaf interior (Koskella et al., 2011).

## Conclusions

Global transcriptome profiling of *P. syringae* B728a cells recovered from the leaf surface and leaf interior indicate that these two habitats offer distinct environments for the bacteria and thus likely present distinct driving forces for *P. syringae* adaptation. This conclusion is congruent with the finding that these habitats select for distinct bacterial and phage communities (Koskella et al., 2011). Overall, the transcript profiles of B728a support a model in which the epiphytic environment favors motility, chemosensing and chemotaxis, including HAA surfactant-mediated swarming and offers a nutritional environment that requires scavenging of phosphate but not iron, active uptake of exogenous sulfur compounds, and utilization of plant-derived indole as a source of tryptophan. Although the microhabitats on a leaf are heterogeneous in their

environmental conditions and these studies captured only the average transcript levels across cells, the transcript profiles indicate that the leaf environment is water limited in general. Furthermore, they suggest that the cells in epiphytic sites experienced greater fluctuations but less severe shortages in water availability than the cells in the apoplast under the conditions tested. The epiphytic environment also favored phenylalanine degradation, which may be a mechanism to counteract phenylpropanoid-based plant defense responses even prior to infection of the apoplast.

Transcript profiles in the apoplast support a model in which B728a cells experience at least low levels of oxidative stress, with a potentially distinct response to this stress *in planta* than in culture. Moreover, the cells experience surprisingly high levels of water stress, which could be related to plant defense, as shown for a resistance response (Freeman and Beattie, 2009b), or as an effect of rapid evapotranspiration or high solute concentrations in interior sites. The apoplastic environment favors the degradation of the alternative amino acid GABA, which may contribute to virulence by attenuating GABA repression of virulence (Park et al., 2010), and also favors the synthesis of secondary metabolites, including two phytotoxins, several as-yet uncharacterized secondary metabolites, and syringolin A. Syringolin A production in the apoplast suggests an expanded function to include suppression of host defenses beyond stomatal closure and possibly eventual enhancement of stomatal opening for egression back to the surface. Lastly, the apoplastic environment preferentially activates phage-related genes within the B728a chromosome; this has interesting implications for the activation and activity of phages and their

associated role in gene transfer, community dynamics and possibly even pathogen control in the leaf habitat.

## Methods

### Bacterial strain and growth media

The complete genome sequence is available for *P. syringae* pv. *syringae* strain B728a (Feil et al., 2005), a foliar pathogen originally isolated from a bean leaf (*Phaseolus vulgaris* L.) in Wisconsin (Loper and Lindow, 1987a). B728a was grown in King's B medium (King et al., 1954) containing 50 µg/ml of rifampin or in modified Hrp MM-mannitol medium (Huynh et al., 1989b), designated HMM medium, which contained 0.2% D-fructose, 0.2% D-mannitol, 0.2% succinate, 10 mM L-glutamine, 10 µM FeCl<sub>3</sub>, 10 µM N-(β-ketocaproyl)-L-homoserine lactone (AHL), 50 mM potassium phosphate buffer, 7.6 mM (NH<sub>4</sub>)<sub>2</sub>SO<sub>4</sub>, 1.7 mM MgCl<sub>2</sub>, and 1.7 mM NaCl. This study was part of a broader study evaluating nine B728a mutants; the inclusion of the glutamine, FeCl<sub>3</sub>, and AHL in this medium was to meet the needs of these mutants. All chemicals were purchased from Sigma-Aldrich (St. Louis, MO). Bacteria were grown at 25°C.

### Exposure of bacteria to environmental stress conditions *in vitro* for RNA extraction.

B728a cells were grown on solid King's B medium, transferred to liquid HMM medium and subcultured twice in this medium. When the cells reached late-log phase ( $5 \times 10^8$  CFU/ml), they were collected by centrifugation at 5,000xg for 10 min. The cell pellets were resuspended in HMM

medium lacking L-glutamine,  $\text{FeCl}_3$ , AHL and  $(\text{NH}_4)_2\text{SO}_4$ , designated HMM-FeN medium. The cells were washed in HMM-FeN and resuspended in HMM-FeN to a final density of  $2.5 \times 10^9$  CFU/ml. Aliquots were transferred to 5 test tubes and diluted to  $2.5 \times 10^8$  CFU/ml with either 1) HMM medium, 2) HMM medium with NaCl to a final concentration of 0.23 M, 3) HMM medium with  $\text{H}_2\text{O}_2$  to a final concentration of 0.5 mM, 4) HMM medium lacking  $\text{FeCl}_3$  but with N,N'-di(2-hydroxybenzyl)ethylenediamine- N,N'-diacetic acid monohydrochloride hydrate (HBED) (Strem Chemicals Inc., Newburyport, MA) to a final concentration of 100  $\mu\text{M}$ , or 5) HMM medium lacking L-glutamine,  $(\text{NH}_4)_2\text{SO}_4$  and AHL; these were designated as the basal medium, osmotic stress, oxidative stress, iron limitation and nitrogen limitation treatments, respectively. Cells were incubated with shaking at  $25^\circ\text{C}$  and were diluted with an RNA stabilizing agent (RNAprotect Bacteria Reagent, Qiagen Inc., Valencia, CA) after 15 min for tubes 1-3 and after 2 h for tubes 4 and 5. This procedure was performed simultaneously with two replicate cultures derived from independent colonies, and the treated cells from the two cultures were combined after dilution with the RNA stabilizing agent. These were harvested by centrifugation at  $5,000 \times g$  for 10 min, the supernatant was removed, and the cell pellets were stored at  $-20^\circ\text{C}$ . This procedure was repeated in its entirety at a separate time, and the RNA isolated from each of the two cell pellets, as described below, was pooled. This pooled RNA, which was derived from 4 independent cultures, served as a single biological replicate for a treatment. Two biological replicates for each treatment were generated in this way at each of three separate laboratories, one

at each Iowa State University, University of California-Berkeley and Texas A&M University, designated as laboratories A, B, and C.

### **Growth of bacteria *in planta* for RNA extraction.**

Beans (*P. vulgaris* cultivar Bush Blue Lake 274) were grown in potting medium until the primary leaves were fully expanded, with an average of 5 germinated plants per 4-inch pot. The inoculum cells were grown as described above for the *in vitro* treatments, and after the initial collection by centrifugation, the cells were suspended in water containing 0.01% Silwet L-77 (Lehle Seeds, Round Rock, TX) to a density of  $1 \times 10^6$  CFU/ml. To establish epiphytic populations, bacteria were introduced by spraying onto the leaves to run-off on both adaxial and abaxial surfaces, immediately enclosing the plants in a mist chamber with 95% relative humidity, and incubating for 24 h. The chamber was partially opened until evaporation of the visible water on the leaves; the chamber was then re-sealed and the plants were incubated without active humidification for another 48 h. The incubations were at 25°C with ambient but not supplemental lighting. A total of 400 to 600 primary leaves were collected, immediately submerged in 2 L of an acidic phenol RNA stabilizing solution (10 ml water-saturated phenol (pH<7.0), 190 ml ethanol, 1.8 L water) (Khodursky et al., 2003), sonicated for 10 min, and then physically removed from the solution. The bacterial cells in the suspension were harvested by centrifugation at 5,000xg for 10 min and the cell pellets were suspended in residual supernatant and filtered through a 5- $\mu$ m filter (Millex-SV syringe filter unit, Millipore Corporation, Billerica, MA). The cells in the filtrate were

harvested by centrifugation at 5,000xg for 5 min, the supernatant was discarded, and the pellets were placed at -20°C. The cells collected from the 400 to 600 leaves on a single day served as a biological replicate, and the procedure was repeated to provide two biological replicates. Due to the availability of facilities, all of the epiphytic treatments were conducted at the University of California-Berkeley laboratory, with cultures provided from each of the other laboratories and the cell pellets returned to those laboratories for RNA extraction and analysis.

To establish apoplastic populations, bacteria were introduced by vacuum infiltration into leaves that were submerged in the inoculum. The plants and bacteria were grown, and the inoculum prepared, as described above. Infiltrated plants were incubated for 48 h under plant growth lights with a 12-h photoperiod. A total of 40 to 80 leaves were collected and immediately submerged in an acidic phenol RNA stabilizing solution, described above. The leaves were cut into squares ( $\sim 3 \times 3 \text{ mm}^2$ ) while submerged, and the plant tissues and liquid were sonicated for 10 min. The solution was filtered through Whatman filter paper #1, with repeated filter changes. The filtrate was centrifuged at 7,000xg for 10 min and the pellet was suspended in residual supernatant. The suspension was filtered through a 5- $\mu\text{m}$  filter with repeated filter changes. The bacterial cells were harvested by centrifugation at 7,000xg for 10 min, the supernatant was discarded, and the pellets were flash frozen and placed at -20°C. The cells collected from the 40 to 80 leaves on a single day served as a biological replicate, and two biological replicates were generated at each of the three laboratories.

### **RNA extraction, microarray design and hybridization.**

RNA was purified using a Qiagen RNeasy mini kit and DNA was removed using the on-column DNase I digestion with subsequent DNase I removal. RNA integrity was evaluated using an Agilent 2100 bioanalyzer. RNA samples were sent to Roche NimbleGen Inc. (Reykjavík, Iceland) for conversion into cDNA, labeling with U-CYA-3 fluorophore, and hybridization to a B728a ORF-based microarray.

The B728a microarray was designed using the complete genome sequence for B728a (RefSeqNC\_007005.1) and 75 predicted small, noncoding RNA (sRNA) genes. The latter included 13 sRNAs that were known or similar to known sRNAs, 46 putative sRNAs that were predicted by Small RNA Identification Protocol using High throughput Technologies (SIPHT) (Livny et al., 2008), and 16 putative sRNAs that were identified in a previous screen for plant-inducible genes (M.L. Marco and S.E. Lindow, unpublished data). Each gene was represented by 14 60-mer nucleotide probes, with a few exceptions, namely 11 ORFs and 4 sRNAs that were represented by fewer probes due to their short size or low complexity. Two ORFs, Psyr\_2216 and Psyr\_3732, and 13 sRNA genes were omitted from the array due to their extreme shortness or low complexity, while another 16 ORFs and 1 sRNA showed sequence similarity to other probe sets that was too high to enable them to be represented by the remaining probes. A total of 5,132 features were represented on the final microarray, including 5,071 ORFs and 61 putative sRNAs. Each slide contained 4 replicate arrays. Although the data are not included in this report, the microarray experiment was performed with an additional nine B728a mutant strains that were

each subjected to the five *in vitro* and two *in planta* treatments in a full factorial design; thus, the treatments were arranged on the slides to maximize the pairing of treatment comparisons of interest. The data for all 10 strains were included in the analysis, described below, although only the results for the wild-type B728a are presented in this report. The expression data from this report have been deposited in the National Center for Biotechnology Information's Gene Expression Omnibus (GEO) according to the MIAME guidelines and are accessible through GEO (accession no. GSE42544).

### **Microarray data analysis.**

The fluorescence intensity for each probe was measured and subjected to robust multiarray averaging (RMA), which included adjustment for the background intensity,  $\log_2$  transformation, quantile normalization and median polishing (Irizarry et al., 2003). A robust estimated mean value was determined for each feature on the array. A linear model analysis of the resulting data was conducted for each feature. Each linear model included fixed effects for replications, treatments, strains, and treatment-by-strain interactions, as well as a fixed intercept parameter and one random error effect for each observation. Limma analysis (Smyth, 2004) was applied to share information across genes when estimating error variances. This was done separately for distinct groups of treatments that had similar absolute median residuals. The resulting variance estimates were used to calculate Welch *t*-statistics and corresponding *P*-values among all pairwise treatment comparisons of interest. For each comparison of interest, *q*-values were estimated from



the corresponding distribution of  $P$ -values, as described previously (Nettleton et al., 2006).

Features exhibiting a  $P$ -value  $< 0.05$  and a  $q$ -value  $< 0.01$ , i.e., an estimated False Discovery Rate less than 1%, were identified as differentially expressed.

A meta-analysis was performed on the datasets from the three laboratories using the following approach. The set of three two-sided  $P$ -values corresponding to a single gene that were derived from the three laboratory datasets were considered to result from a common hypothesis test across the three laboratories. For each two-sided  $P$ -value, the corresponding quantile ( $\alpha = 0.5p$ ) from a standard normal distribution was found, and the positive or negative quantile sign was matched to the sign of the  $t$ -statistic from which the original  $P$ -value was calculated. The average of the three quantiles was further compared to a standard normal distribution with mean 0 and variance 1/3 in order to obtain a single two-sided  $P$ -value based on the combined information across the three laboratory datasets. The  $q$ -values were estimated from the distribution of corresponding  $P$ -values, as described above, and features in the meta-analysis exhibiting a  $P$ -value  $< 0.05$  and a  $q$ -value  $< 0.01$  were identified as differentially expressed.

Within a dataset from a laboratory, the linear model analysis yielded an estimated fold-change value between a treatment and the basal medium for each feature on the microarray. For the combined dataset from the three laboratories, the estimated fold-change values were computed by exponentiating the average of the estimated log-transformed fold-change values for the three laboratory datasets using the inverse of the estimated variances as weights. The geometric mean of

the fold-change values across genes were calculated based on exponentiating the arithmetic mean of the log-transformed fold-change values.

### **Hierarchical clustering.**

A dendrogram was generated using the fluorescent intensities for each of the biological replicates from the three laboratory datasets. The data for each gene was subjected to an ANOVA across the seven treatments. The observed intensities from the 500 genes that exhibited the lowest *P*-values in an F-test for the combined effect of all treatments from this ANOVA were used to perform hierarchical clustering among all the samples. The observed intensities for each gene were divided by the gene's estimated standard deviation, so that each gene would contribute roughly equally to the distance metric during clustering. The hierarchical clustering was performed by the "hclust" function in R using Manhattan distance in a "bottom up" approach.

### **Assignment and analysis of gene representation in functional categories.**

The B728a genes were assigned to 63 functional categories (Table S2). These assignments were based on the genome annotation, KEGG pathway assignments, and known or predicted functions based on the literature. Each gene was assigned to a single functional category or to no category if it could be placed into multiple categories or its function was unknown. For each functional category, we formed a 2x2 contingency table reporting the number of differentially expressed and non-differentially expressed genes included in the given category and, separately,

those for genes not included in the given category. We then performed a Fisher's exact test to evaluate overrepresentation of the differentially expressed genes. We performed this analysis separately for the differentially induced genes and the differentially repressed genes.  $q$ -values were generated from the resulting  $P$ -values, as described above.

## Acknowledgements

We thank David Morgan and Jia Wang for help with the bacterial recovery from leaf surfaces. This project was supported by the National Research Initiative of the USDA-CSREES grant No. 2008-35600-18786.

## References

- Arias-Barrau, E., Olivera, E.R., Luengo, J.M., Fernandez, C., Galan, B., Garcia, J.L., Diaz, E., and Minambres, B. (2004). The homogentisate pathway: A central catabolic pathway involved in the degradation of L-phenylalanine, L-tyrosine, and 3-hydroxyphenylacetate in *Pseudomonas putida*. *J Bacteriol* 186, 5062-5077.
- Berti, A.D., Greve, N.J., Christensen, Q.H., and Thomas, M.G. (2007). Identification of a biosynthetic gene cluster and the six associated lipopeptides involved in swarming motility of *Pseudomonas syringae* pv. tomato DC3000. *J Bacteriol* 189, 6312-6323.
- Boch, J., Joardar, V., Gao, L., Robertson, T.L., Lim, M., and Kunkel, B.N. (2002). Identification of *Pseudomonas syringae* pv. tomato genes induced during infection of *Arabidopsis thaliana*. *Mol Microbiol* 44, 73-88.
- Burch, A.Y., Browne, P.J., Dunlap, C.A., Price, N.P., and Lindow, S.E. (2011). Comparison of biosurfactant detection methods reveals hydrophobic surfactants and contact-regulated production. *Environ Microbiol* 13, 2681-2691.
- Burch, A.Y., Shimada, B.K., Mullin, S.W.A., Dunlap, C.A., Bowman, M.J., and Lindow, S.E. (2012). *Pseudomonas syringae* coordinates production of a motility-enabling surfactant with flagellar assembly. *J Bacteriol* 194, 1287-1298.
- Cabral, M.P., Soares, N.C., Aranda, J., Parreira, J.R., Rumbo, C., Poza, M., Valle, J., Calamia, V., Lasa, I., and Bou, G. (2011). Proteomic and functional analyses reveal a unique lifestyle for

- Acinetobacter baumannii* biofilms and a key role for histidine metabolism. *J Proteom Res* 10, 3399-3417.
- Chang, W.S., van de Mortel, M., Nielsen, L., de Guzman, G.N., Li, X.H., and Halverson, L.J. (2007). Alginate production by *Pseudomonas putida* creates a hydrated microenvironment and contributes to biofilm architecture and stress tolerance under water-limiting conditions. *J Bacteriol* 189, 8290-8299.
- Chen, C., and Beattie, G.A. (2008). *Pseudomonas syringae* BetT is a low-affinity choline transporter that is responsible for superior osmoprotection by choline over glycine betaine. *J Bacteriol* 190, 2717-2725.
- Cuppels, D.A. (1988). Chemotaxis by *Pseudomonas syringae* pv. tomato. *Appl Environ Microbiol* 54, 629-632.
- Feil, H., Feil, W.S., Chain, P., Larimer, F., DiBartolo, G., Copeland, A., Lykidis, A., Trong, S., Nolan, M., Goltsman, E., *et al.* (2005). Comparison of the complete genome sequences of *Pseudomonas syringae* pv. syringae B728a and pv. tomato DC3000. *Proc Natl Acad Sci U S A* 102, 11064-11069.
- Freeman, B.C., and Beattie, G.A. (2009). Bacterial growth restriction during host resistance to *Pseudomonas syringae* is associated with leaf water loss and localized cessation of vascular activity in *Arabidopsis thaliana*. *Mol Plant Microbe In* 22, 857-867.
- Haefele, D.M., and Lindow, S.E. (1987). Flagellar motility confers epiphytic fitness advantages upon *Pseudomonas syringae*. *Appl Environ Microbiol* 53, 2528-2533.
- Hernandez-Morales, A., De la Torre-Zavala, S., Ibarra-Laclette, E., Hernandez-Flores, J.L., Jofre-Garfias, A.E., Martinez-Antonio, A., and Alvarez-Morales, A. (2009). Transcriptional profile of *Pseudomonas syringae* pv. phaseolicola NPS3121 in response to tissue extracts from a susceptible *Phaseolus vulgaris* L. cultivar. *Bmc Microbiol* 9, 257.
- Hirano, S.S., Charkowski, A.O., Collmer, A., Willis, D.K., and Upper, C.D. (1999). Role of the Hrp type III protein secretion system in growth of *Pseudomonas syringae* pv. syringae B728a on host plants in the field. *Proc Natl Acad Sci USA* 96, 9851-9856.
- Howden, A.J., Rico, A., Mentlak, T., Miguët, L., and Preston, G.M. (2009). *Pseudomonas syringae* pv. syringae B728a hydrolyses indole-3-acetonitrile to the plant hormone indole-3-acetic acid. *Mol Plant Pathol* 10, 857-865.
- Huynh, T.V., Dahlbeck, D., and Staskawicz, B.J. (1989). Bacterial blight of soybean: regulation of a pathogen gene determining host cultivar specificity. *Science* 245, 1374-1377.
- Irizarry, R.A., Hobbs, B., Collin, F., Beazer-Barclay, Y.D., Antonellis, K.J., Scherf, U., and Speed, T.P. (2003). Exploration, normalization, and summaries of high density oligonucleotide array probe level data. *Biostatistics* 4, 249-264.
- Jones, A.M., and Wildermuth, M.C. (2011). The phytopathogen *Pseudomonas syringae* pv. tomato DC3000 has three high-affinity iron-scavenging systems functional under iron limitation conditions but dispensable for pathogenesis. *J Bacteriol* 193, 2767-2775.

- Joyner, D.C., and Lindow, S.E. (2000). Heterogeneity of iron bioavailability on plants assessed with a whole-cell GFP-based bacterial biosensor. *Microbiol-Uk* 146, 2435-2445.
- Khodursky, A.B., Bernstein, J.A., Peter, B.J., Rhodius, V., Wendisch, V.F., and Zimmer, D.P. (2003). *Escherichia coli* spotted double-strand DNA microarrays: RNA extraction, labeling, hybridization, quality control, and data management. *Methods Mol Biol* 224, 61-78.
- Kim, H.E., Shitashiro, M., Kuroda, A., Takiguchi, N., and Kato, J. (2007). Ethylene chemotaxis in *Pseudomonas aeruginosa* and other *Pseudomonas* species. *Microb Environ* 22, 186-189.
- King, E.O., Ward, M.K., and Raney, D.E. (1954). Two simple media for the demonstration of pyocyanin and fluorescein. *J Lab Clin Med* 44, 301-307.
- Koskella, B.K.B., Thompson, J.N., Preston, G.M., and Buckling, A. (2011). Local biotic environment shapes the spatial scale of bacteriophage adaptation to bacteria. *Am Nat* 177, 440-451.
- Krol, E., and Becker, A. (2011). ppGpp in *Sinorhizobium meliloti*: Biosynthesis in response to sudden nutritional downshifts and modulation of the transcriptome. *Mol Microbiol* 81, 1233-1254.
- Kroupitski, Y., Golberg, D., Belausov, E., Pinto, R., Swartzberg, D., Granot, D., and Sela, S. (2009). Internalization of *Salmonella enterica* in leaves is induced by light and involves chemotaxis and penetration through open stomata. *Appl Environ Microbiol* 75, 6076-6086.
- Kurz, M., Burch, A.Y., Seip, B., Lindow, S.E., and Gross, H. (2010). Genome-driven investigation of compatible solute biosynthesis pathways of *Pseudomonas syringae* pv. *syringae* and their contribution to water stress tolerance. *Appl Environ Microbiol* 76, 5452-5462.
- Lee, J., Teitzel, G.M., Munkvold, K., del Pozo, O., Martin, G.B., Micheltore, R.W., and Greenberg, J.T. (2012). Type III secretion and effectors shape the survival and growth pattern of *Pseudomonas syringae* on leaf surfaces. *Plant Physiol* 158, 1803-1818.
- Leveau, J.H.J., and Lindow, S.E. (2001). Appetite of an epiphyte: Quantitative monitoring of bacterial sugar consumption in the phyllosphere. *Proc Natl Acad Sci USA* 98, 3446-3453.
- Livny, J., Teonadi, H., Livny, M., and Waldor, M.K. (2008). High-throughput, kingdom-wide prediction and annotation of bacterial non-coding RNAs. *PLoS One* 3, e3197.
- Loper, J.E., and Lindow, S.E. (1987). Lack of evidence for *in situ* fluorescent pigment production by *Pseudomonas syringae* pv. *syringae* on bean leaf surfaces. *Phytopathology* 77, 1449-1454.
- Marco, M.L., Legac, J., and Lindow, S.E. (2005). *Pseudomonas syringae* genes induced during colonization of leaf surfaces. *Environ Microbiol* 7, 1379-1391.
- Mazzola, M., and White, F.F. (1994). A Mutation in the indole-3-acetic acid biosynthesis pathway of *Pseudomonas syringae* pv. *syringae* affects growth in *Phaseolus vulgaris* and syringomycin production. *J Bacteriol* 176, 1374-1382.
- Mo, Y.Y., and Gross, D.C. (1991). Plant signal molecules activate the *syrB* gene, which is required for syringomycin production by *Pseudomonas syringae* pv. *syringae*. *J Bacteriol* 173, 5784-5792.

- Molina-Henares, M.A., Garcia-Salamanca, A., Molina-Henares, A.J., de la Torre, J., Herrera, M.C., Ramos, J.L., and Duque, E. (2009). Functional analysis of aromatic biosynthetic pathways in *Pseudomonas putida* KT2440. *Microb Biotechnol* 2, 91-100.
- Monier, J.M., and Lindow, S.E. (2003). *Pseudomonas syringae* responds to the environment on leaves by cell size reduction. *Phytopathology* 93, 1209-1216.
- Monier, J.M., and Lindow, S.E. (2004). Frequency, size, and localization of bacterial aggregates on bean leaf surfaces. *Appl Environ Microbiol* 70, 346-355.
- Montalbini, P. (1992). Changes in xanthine oxidase activity in bean leaves induced by *Uromyces phaseoli* infection. *J Phytopathol* 134, 63-74.
- Morgan, J.V., and Tukey, H.B. (1964). Characterization of leachate from plant foliage. *Plant Physiol* 39, 590-593.
- Nettleton, D., Hwang, J.T.G., Caldo, R.A., and Wise, R.P. (2006). Estimating the number of true null hypotheses from a histogram of *p* values. *J Agr Biol Envir St* 11, 337-356.
- Panopoulos, N.J., and Schroth, M.N. (1974). Role of flagellar motility in invasion of bean leaves by *Pseudomonas phaseolicola*. *Phytopathology* 64, 1389-1397.
- Park, D.H., Mirabella, R., Bronstein, P.A., Preston, G.M., Haring, M.A., Lim, C.K., Collmer, A., and Schuurink, R.C. (2010). Mutations in  $\gamma$ -aminobutyric acid (GABA) transaminase genes in plants or *Pseudomonas syringae* reduce bacterial virulence. *Plant J* 64, 318-330.
- Rico, A., and Preston, G.M. (2008). *Pseudomonas syringae* pv. tomato DC3000 uses constitutive and apoplast-induced nutrient assimilation pathways to catabolize nutrients that are abundant in the tomato apoplast. *Mol Plant Microbe In* 21, 269-282.
- Schellenberg, B., Ramel, C., and Dudler, R. (2010). *Pseudomonas syringae* virulence factor syringolin A counteracts stomatal immunity by proteasome inhibition. *Mol Plant Microbe In* 23, 1287-1293.
- Scholz-Schroeder, B.K., Hutchison, M.L., Grgurina, I., and Gross, D.C. (2001). The contribution of syringopeptin and syringomycin to virulence of *Pseudomonas syringae* pv. *syringae* strain B301D on the basis of *sypA* and *syrB1* biosynthesis mutant analysis. *Mol Plant Microbe In* 14, 336-348.
- Smyth, G.K. (2004). Linear models and empirical bayes methods for assessing differential expression in microarray experiments. *Stat Appl Genet Mol Biol* 3, Art 3.
- Truman, W., de Zabala, M.T., and Grant, M. (2006). Type III effectors orchestrate a complex interplay between transcriptional networks to modify basal defence responses during pathogenesis and resistance. *Plant J* 46, 14-33.
- Voigt, B., Hoi, L.T., Jurgen, B., Albrecht, D., Ehrenreich, A., Veith, B., Evers, S., Maurer, K.H., Hecker, M., and Schweder, T. (2007). The glucose and nitrogen starvation response of *Bacillus licheniformis*. *Proteomics* 7, 413-423.
- Ward, J.L., Forcat, S., Beckmann, M., Bennett, M., Miller, S.J., Baker, J.M., Hawkins, N.D., Vermeer, C.P., Lu, C.A., Lin, W.C., *et al.* (2010). The metabolic transition during disease

following infection of *Arabidopsis thaliana* by *Pseudomonas syringae* pv. tomato. Plant J 63, 443-457.

- Waspi, U., Blanc, D., Winkler, T., Ruedi, P., and Dudler, R. (1998). Syringolin, a novel peptide elicitor from *Pseudomonas syringae* pv. syringae that induces resistance to *Pyricularia oryzae* in rice. Mol Plant Microbe In 11, 727-733.
- Yu, J., Penaloza-Vazquez, A., Chakrabarty, A.M., and Bender, C.L. (1999). Involvement of the exopolysaccharide alginate in the virulence and epiphytic fitness of *Pseudomonas syringae* pv. syringae. Mol Microbiol 33, 712-720.

Table 1. Correlation coefficients from a multiple regression analysis of the transcriptome in epiphytic or apoplastic sites on the transcriptomes of cells exposed to the basal medium and to each of the four environmental stresses *in vitro*.

	Epiphytic sites <sup>1</sup>				Apoplastic sites <sup>1</sup>			
	Lab-A	Lab-B	Lab-C	Combined dataset	Lab -A	Lab -B	Lab -C	Combined dataset
Osmotic stress	0.40	0.47	0.25	0.42	0.50	0.75	0.42	0.64
N limitation	0.34	0.32	0.33	0.36	0.46	0.22	0.41	0.28
Oxidative stress	0	0.02	0.26	0	0	0	0	0
Fe limitation	0.26	0.15	0.10	0.18	0.04	0.04	0.16	0.07

<sup>1</sup>Multiple regression analysis was performed with the constraints that the coefficients were non-negative and had to sum to one. The transcriptome data were in the form of the transcript abundances weighted with variances using a least-squares approach. Regression analyses were performed separately for the data from each laboratory and from the combined dataset.



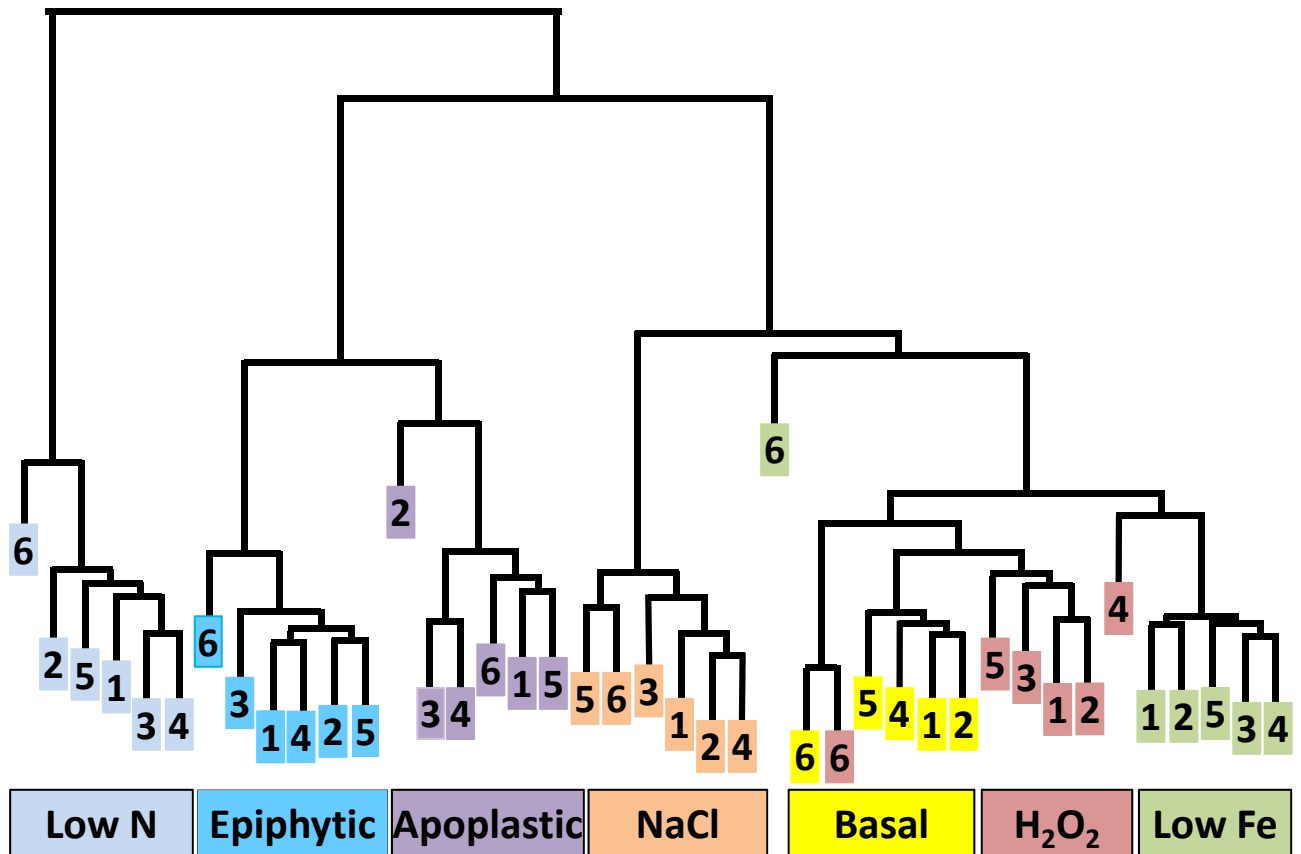


Fig 1. Each environmental treatment induced a distinct stimulon. The hierarchical clustering was based on 500 genes with the lowest *P*-values in an F-test for the combined effect of all seven treatments among all the samples. Numbers 1-2, 3-4, and 5-6 refer to the two replicate samples from laboratories A, B, and C, respectively. The color indicates the treatments, which include: Low N, nitrogen limitation; Epiphytic, epiphytic sites; Apoplastic, apoplastic sites; NaCl, osmotic stress; Basal, basal medium; H<sub>2</sub>O<sub>2</sub>, oxidative stress; and Low Fe, iron limitation.

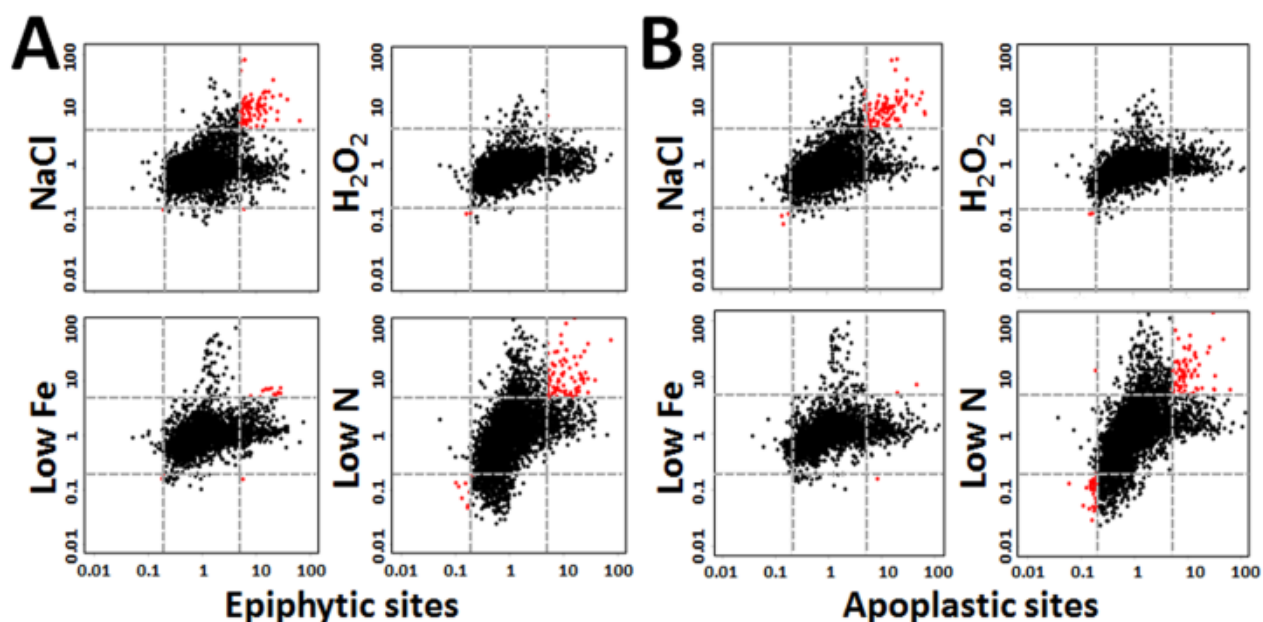


Fig 2. Correlation between the *P. syringae* transcriptomes of cells exposed to environmental stresses *in vitro* and those recovered from (A) epiphytic sites or (B) apoplastic sites. The log(fold-change) values of the transcript levels of all of the genes in the *in vitro* stress treatments relative to in the basal medium (y-axes) were plotted against those of the *in planta* treatments relative to in the basal medium (x-axes). The dotted grey lines indicate 5-fold changes in transcript levels, with red dots indicating genes that were altered  $\geq 5$ -fold in both plotted treatments.

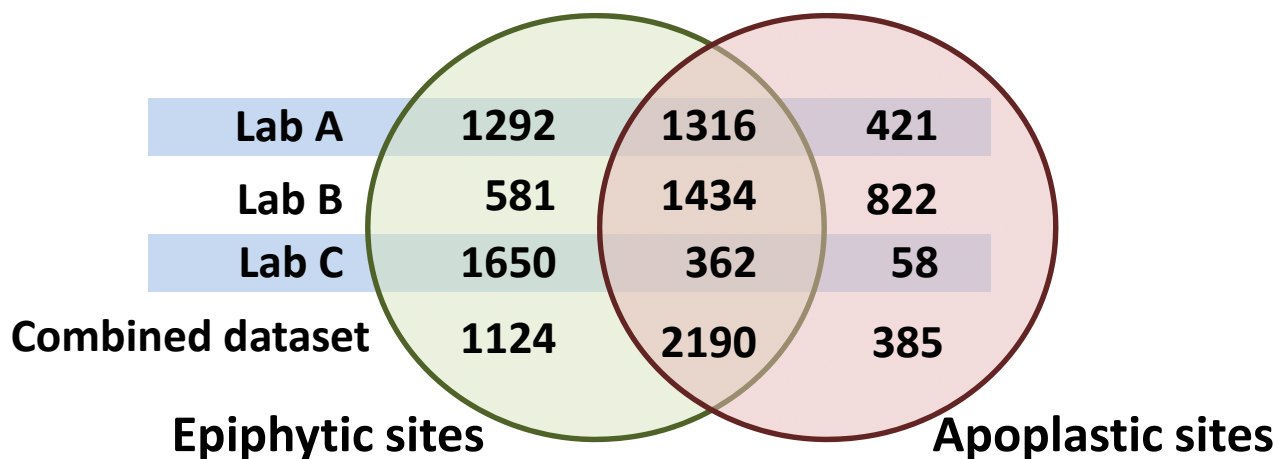


Fig 3. Comparison of the numbers of genes showing significant differences in transcript abundance in epiphytic and apoplastic sites. The Venn diagram indicates the number of genes showing differences in transcript abundance ( $P$ -value  $< 0.05$  and  $q$ -value  $< 0.01$ ) in cells isolated from each leaf habitat. The total number of putative genes in the datasets was 5,132. The results are shown in separate rows for datasets originating from each of the three laboratories as well as from a meta-analysis of the combined datasets.

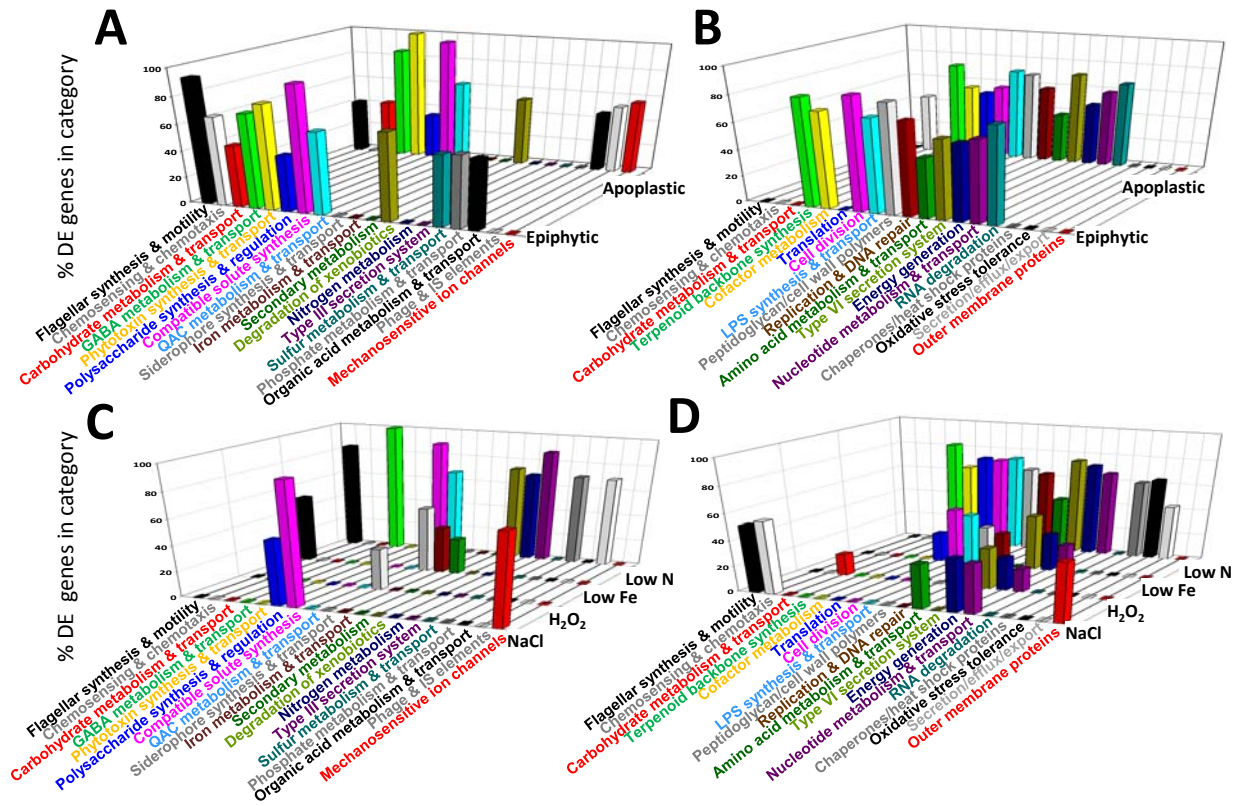


Fig 4. Percentage of genes in functional categories that were over-represented among the differentially expressed (DE) genes in each treatment. The *x*-axis indicates the functional categories that were significantly over-represented in one or more sets of DE genes ( $q$ -value < 0.05), with the DE genes identified based on a  $q$ -value < 0.01. The *y*-axis labels indicate the treatments that were compared to the basal medium. The *z*-axis indicates the percentage of genes within the category specified on the *x*-axis that was DE between the treatment indicated on the *y*-axis and the basal medium. This analysis was applied separately to genes with increased transcript abundance (A, C) and those with decreased transcript abundance (B, D) when compared to cells in the basal medium. For clarity, the *in planta* treatments (A, B) are shown separately from the *in vitro* treatments (C, D). The results for all of the functional categories are shown in Table S1.

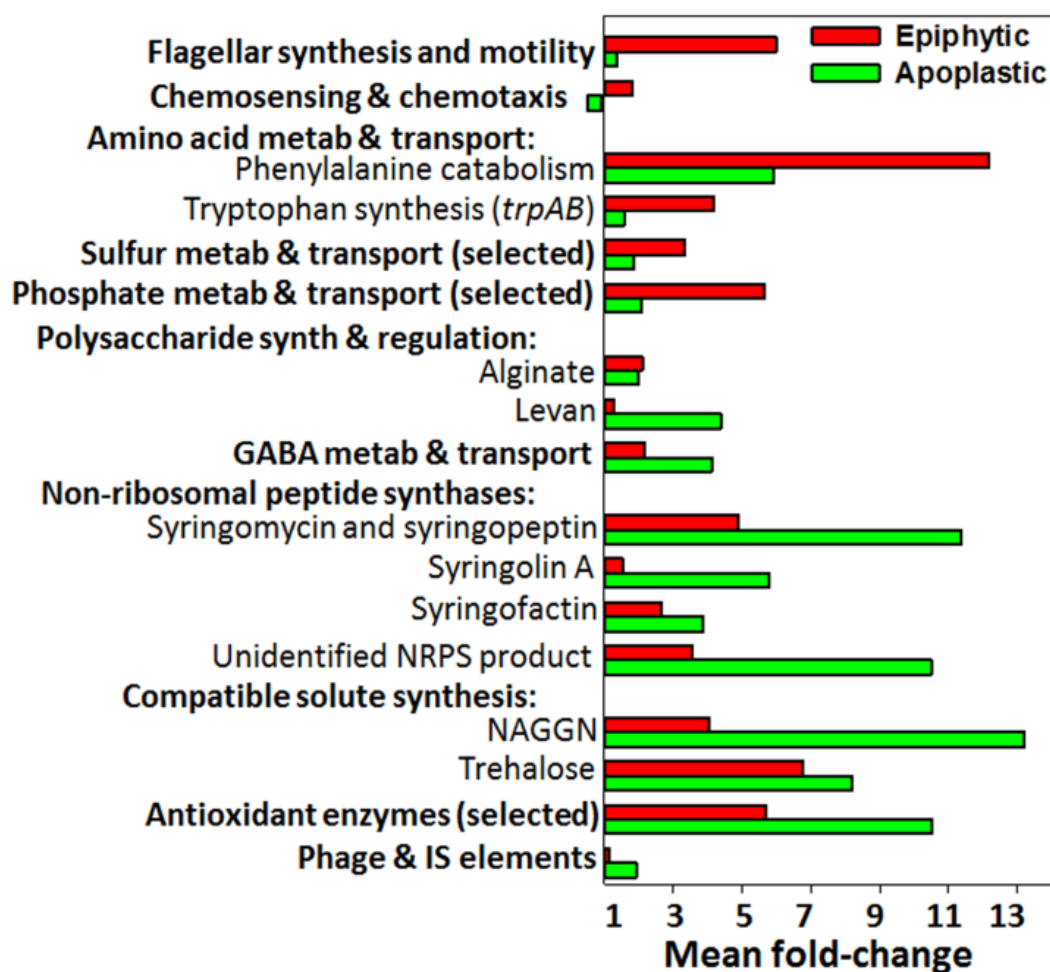


Fig 5. The geometric mean of the fold-change in transcript levels of all of the genes in selected functional categories or selected genes associated with individual traits. The fold-change values were relative to transcript levels in the basal medium. The geometric means were calculated by exponentiating the arithmetic average of all of the estimated log fold-changes in each category. The unidentified non-ribosomal peptide synthase (NRPS) was encoded by Psyr\_4311-4315.

# CHAPTER 3. *PSEUDOMONAS SYRINGAE* STRAINS DIFFER IN THE CONTRIBUTION OF THEIR TREHALOSE BIOSYNTHETIC PATHWAYS TO TREHALOSE ACCUMULATION

Xilan Yu and Gwyn A. Beattie

Department of Plant Pathology & Microbiology,

Iowa State University; Ames, IA, 50010, USA

## Abstract

The foliar pathogen *Pseudomonas syringae* is exposed to fluctuations in water availability, and thus water stress, during colonization of leaves. *P. syringae* strains vary in their ability to tolerate water stress, and this may be associated with differences in the production or regulation of the compatible solute trehalose. *P. syringae* pv. tomato strain DC3000 has two trehalose biosynthesis pathways, both of which are required for trehalose production and contribute to osmotolerance. Here, we found that *P. syringae* pv. syringae strain B728a utilizes primarily a single pathway, the conversion of  $\alpha$ -glucan to trehalose by TreXYZ, to synthesize trehalose. Deletion of the *treXYZ* locus significantly reduced growth under hyperosmotic conditions, whereas loss of the TreS pathway, which involves converting maltose to trehalose, only slightly reduced growth. Measurements of the trehalose accumulation under hyperosmotic conditions showed a striking difference between the strains. Whereas deletion of the *treXYZ* locus mutants reduced trehalose

levels by >85% in both strains, deletion of the *treS* locus reduced trehalose levels by 94% in DC3000 but only 10% in B728a. Thus, B728a did not exhibit the interdependency between the *treXYZ* and *treS* loci for trehalose production as was observed in DC3000. To explore the mechanism of this interdependency, we evaluated the impact of maltose amendment on the osmotolerance of the DC3000 *treXYZ* mutant; addition of exogenous maltose failed to rescue the reduced growth of the *treXYZ* mutant under osmotic stress, suggesting that the dependence of the *treS* mutant of DC3000 on a functional *treXYZ* locus was not due to the TreXYZ pathway providing maltose, although we cannot rule out a failure to transport maltose. Collectively, we demonstrated differences among *P. syringae* strains in the contribution of distinct pathways to trehalose biosynthesis and accumulation, suggesting a possible mechanistic basis for differences in osmotolerance.

## Introduction

*Pseudomonas syringae* is a foliar pathogen as well as a common resident on leaves. Due to the highly exposed nature of aerial plant surfaces, *P. syringae* must confront large and rapid fluctuations in water availability during leaf colonization (Axtell and Beattie, 2002; Beattie, 2011; Monier and Lindow, 2005). Our previous transcriptome studies have shown that water limitation is a major stress limiting *P. syringae* survival and growth on plant leaves (Chapter 2). To alleviate the detrimental effects of water limitation, *P. syringae* accumulates soluble compounds, designated compatible solutes or osmolytes, by *de novo* synthesis or uptake from the environment. These

compatible solutes are small organic molecules, including polyols, peptides, and amino acids and their derivatives (Kurz et al., 2010), that can be accumulated to a high concentration without being toxic to cells. *P. syringae* can accumulate several endogenous osmolytes by *de novo* synthesis, namely the disaccharide trehalose, the dipeptide N-acetylglutaminylglutamine amide (NAGGN) and L-glutamate under water-limiting conditions (Freeman et al., 2010; Kurz et al., 2010).

Among these *de novo* synthesized compatible solutes, trehalose plays an important role in enabling the maximal osmotolerance by *P. syringae* (Kurz et al., 2010). Trehalose is an  $\alpha,\alpha$ -1,1-linked disaccharide and is produced to help bacteria tolerate stresses, such as low water availability (high osmolarity or desiccation), cold, heat and oxidative stress (Arguelles, 2000). In bacteria, trehalose is often synthesized by three common biosynthetic pathways, TreXYZ, TreS, and OtsA/OtsB (Freeman et al., 2010; Kurz et al., 2010). Trehalose can be synthesized from glycogen (a large  $\alpha$ -glucan) through the sequential actions of (i) glycogen phosphorylase (TreX), which is a debranching enzyme that acts on glycogen, (ii) maltooligosyltrehalose synthase (TreY), which converts linear  $\alpha$ -glucans into maltooligosyltrehalose, and (iii) maltooligosyltrehalose trehalohydrolase (TreZ), which converts maltooligosyltrehalose into trehalose and maltose or maltotriose (Maruta et al., 1996a, b; Maruta et al., 2000) (Fig. 1). Trehalose can also be derived from maltose by trehalose synthase (TreS) and this reaction is reversible (Kalscheuer et al., 2010; Nishimoto et al., 1996) (Fig. 1). Thus, maltose is common to both the TreXYZ and TreS pathways. In addition, *E. coli* has been reported to synthesize trehalose via the sequential actions of OtsA, a trehalose-6-phosphate synthase that converts glucose-6-phosphate to



trehalose-6-phosphate, and OtsB, a trehalose-6-phosphate phosphatase that hydrolyzes trehalose-6-phosphate to release trehalose (Gibson et al., 2002). *P. syringae* has genes for the TreXYZ and TreS pathways (Freeman et al., 2010; Kurz et al., 2010) but surprisingly is lacking genes for the OtsA/OtsB pathway, despite their presence in *P. savastanoi* and *P. stutzeri* A1501 (Kurz et al., 2010).

The trehalose biosynthetic pathways have been characterized in *P. syringae* pv. tomato strain DC3000 (Freeman et al., 2010). Both TreXYZ and TreS significantly contribute to trehalose synthesis and accumulation in DC3000, and deletion of either pathway leads to significantly reduced DC3000 osmotolerance both in culture and on plant leaves (Freeman et al., 2010). Interestingly, although there are two putative *treS* genes in DC3000, one gene, PSPTO\_2761, was found to be induced and required for trehalose synthesis under osmotic stress, whereas the other gene, PSPTO\_2952, was not (Freeman et al., 2010). In *P. syringae* pv syringae strain B728a, trehalose also accumulated in response to osmotic stress and the genes for the TreXYZ and TreS pathways were predicted (Kurz et al., 2010). These include Psyr\_2997, Psyr\_2995, and Psyr\_2993, which are predicted to encode TreX, TreY and TreZ, respectively, as well as Psyr\_2490 and Psyr\_2736, which are both predicted to encode TreS, which catalyzes the reversible conversion between trehalose and maltose (Fig. 1). B728a is much more tolerant to osmotic stress than DC3000, and this higher tolerance may be associated with differences in the regulation or production of trehalose.

In addition to acting as a stress protectant, trehalose can also function as a precursor to carbon and energy storage molecules (Chandra et al., 2011). Specifically, trehalose can function as a precursor for  $\alpha$ -glucan synthesis by the newly identified GlgE pathway, which was discovered in mycobacteria (Elbein et al., 2010; Kalscheuer et al., 2010) and enables the synthesis of an  $\alpha$ -glucan such as glycogen via the sequential actions of TreS, Pep2, GlgE and GlgB (Fig. 1). Through comparative genomic analyses, all four GlgE pathway genes were found in all of the *Pseudomonas* spp. with complete genome sequences, except that *treS* and *pep2* are fused and annotated as just *treS*, with the genes forming a conserved three-gene putative operon, *treS-glgE-glgB*, in DC3000 (Freeman et al., 2010) and B728a (Fig. 2). Thus, TreS is likely to be involved in the interplay of trehalose and glycogen metabolism by deciding the fate of maltose and trehalose, whereas TreXYZ is specifically associated with trehalose biosynthesis.

The *treXYZ* and *treS* loci in DC3000 are both required for trehalose synthesis under hyperosmotic conditions (Freeman et al., 2010), suggesting the presence of a regulatory or biochemical interconnectedness of these two pathways. Given the greater osmotolerance of B728a over DC3000 and the critical role of trehalose accumulation in *P. syringae* osmotolerance, we investigated whether the strains differed in the relative contribution of these two pathways to trehalose synthesis and whether B728a exhibits the same interdependency of its trehalose biosynthetic pathways as observed in DC3000. Moreover, we took the first steps toward understanding the mechanistic basis for the interdependency of these two pathways in DC3000.

## Results

### **The relative contribution of the TreXYZ and TreS pathways to osmotolerance differs between DC3000 and B728a**

To understand the trehalose biosynthetic pathways in B728a, we evaluated the transcript levels of the putative trehalose biosynthetic genes in cells after a 15 min exposure to hyperosmotic upshock in an ORF-based microarray (Chapter 2). As shown in Fig. 2A, the transcript levels of *treX*, *treY*, *treZ*, and *treS* were induced 10- to 16-fold, which are significantly higher than the 1.4- and 2.4-fold induction in DC3000 (Freeman et al., 2010). These data support the role of trehalose production as an osmoadaptation mechanism in *P. syringae*.

To confirm the function of the trehalose biosynthetic genes in B728a, we deleted the Psyr\_2489-2491 and Psyr\_2992-3001 regions containing the putative *treS* and *treXYZ* loci separately, generating the single deletion mutants B $\Delta$ *tre1* and B $\Delta$ *tre2*, respectively (Fig. 2B). We also generated the double mutant B $\Delta$ *tre1* $\Delta$ *tre2* (Fig. 2B). The growth of these mutants was examined in MinAS medium with or without 0.3 M NaCl amendment. As expected, B728a exhibited delayed growth in the presence of osmotic stress (Fig. 3). The mutants B $\Delta$ *tre1*, B $\Delta$ *tre2*, and B $\Delta$ *tre1* $\Delta$ *tre2* grew similarly to the wild type in the absence of osmotic stress (Fig. 3A); however, the mutants B $\Delta$ *tre2* and B $\Delta$ *tre1* $\Delta$ *tre2* exhibited delayed growth and grew to lower cell densities than the wild type in the NaCl-amended medium (Fig. 3B). Surprisingly, B $\Delta$ *tre1* displayed only slightly reduced growth compared with the wild type, whereas strains containing the  $\Delta$ *tre2* deletion were greatly reduced (Fig. 3B). These data indicate that in B728a, the

TreXYZ pathway plays a dominant role in trehalose synthesis, whereas the TreS pathway played no role or only a minor role. This contrasts sharply with the finding of severe reductions in the growth of both the  $\Delta tre1$  and  $\Delta tre2$  mutants of DC3000 and the conclusion that the loss of either pathway from DC3000 reduced growth under osmotic stress (Freeman et al., 2010).

### **The relative contribution of the TreXYZ and TreS to trehalose synthesis differs between DC3000 and B728a**

To determine if the reduced growth of the mutants was correlated with a compromised ability to synthesize trehalose, we quantified the intracellular trehalose levels in the  $B\Delta tre1$ ,  $B\Delta tre2$ , and  $B\Delta tre1\Delta tre2$  mutants as well as in B728a after growing cells in hyperosmotic conditions (MinAS medium amended with either 0.3 M NaCl or 0.5 M NaCl) for 20 h. Our data showed that  $B\Delta tre1$  produced 10% less trehalose than the wild type when grown at high osmotic stress (0.5 M NaCl) ( $P < 0.1$ ) (Fig. 4A) but did not produce less in cells grown at a moderate osmotic stress (0.3 M NaCl) (Fig. 4B); this is consistent with the slightly reduced growth of  $B\Delta tre1$  under high osmolarity (Fig. 3B). However, the mutants  $B\Delta tre2$  and  $B\Delta tre1\Delta tre2$  showed significantly reduced trehalose production (>98%) compared with the wild type under moderate and high osmotic stress ( $P < 0.05$ ) (Fig. 4A and B), consistent with their severely reduced growth under osmotic stress (Fig. 3B). These data confirmed the strongly dominant role of TreXYZ over the TreS pathways for trehalose production in B728a.

We also quantified the trehalose production of DC3000 and its mutant derivatives *DC $\Delta$ tre1*, *DC $\Delta$ tre2*, and *DC $\Delta$ tre1 $\Delta$ tre1* (Table 1) when cells were grown in MinAS medium with 0.3 M NaCl for 20h. Due to the greater osmosensitivity of DC3000 when compared to B728a, a NaCl concentration of 0.3M is as stressful for DC3000 as 0.5M is for B728a (Chen and Beattie, unpublished data). As expected, loss of either the TreXYZ pathway, the TreS pathway, or both pathways significantly reduced trehalose biosynthesis (>85%) (Fig. 4C), which was consistent with the previous demonstration of reduced trehalose production in these mutants as determined using  $^{13}\text{C}$ -nuclear magnetic resonance spectroscopy ( $^{13}\text{C}$ -NMR) and thin layer chromatography (Freeman et al., 2010) and also with the reduced growth of these DC3000 mutants in hyperosmotic media (Fig. 5C). The lower level of trehalose production in DC3000 ( $0.31 \pm 0.01$ ) than in B728a ( $0.49 \pm 0.01$ ) at 0.3 M NaCl reflects the lower level of induction of all of the trehalose genes in DC3000 as compared to B728a (Fig. 2), and could explain the lower osmotolerance of DC3000 than B728a. The difference between *B $\Delta$ tre1* and *DC $\Delta$ tre1* in trehalose production highlights a major difference between the strains in the importance of the TreS pathway for trehalose synthesis.

### **Exogenous maltose does not activate trehalose production via the TreS pathway in DC3000 nor enhance it in B728a**

As the maltose produced by the TreXYZ pathway could provide the substrate for TreS to synthesize trehalose (Fig. 1), we hypothesized that in the absence of exogenous maltose, the

TreS pathway utilizes maltose released by the TreXYZ pathway during its degradation of maltodextrins, and that this would explain part of the interdependency of these pathways in DC3000. To evaluate this possibility, we examined whether adding exogenous maltose could rescue the reduced bacterial growth of the  $DC\Delta tre1$  mutant, which lacked the *glgE-treS-glgB* operon, under high osmolarity. The growth of DC3000 and its mutants  $DC\Delta tre1$ ,  $DC\Delta tre2$ , and  $DC\Delta tre1\Delta tre2$  was examined in MinAS medium amended with 0.3 M NaCl in the presence or absence of 0.2% maltose. Similar to the reduced growth of the  $DC\Delta tre2$  mutant in the absence of maltose (Fig. 5C) as observed previously (Freeman et al., 2010), the  $DC\Delta tre2$  mutant exhibited reduced growth in the presence of maltose (Fig. 5D). Thus, the availability of exogenous maltose to the cells did not enable independent TreXYZ pathway function in the  $DC\Delta tre2$  mutant. Similarly, when B728a and its mutants  $B\Delta tre1$ ,  $B\Delta tre2$ , and  $B\Delta tre1\Delta tre2$  were grown with and without exogenous maltose, the reduced growth of  $B\Delta tre2$  was not altered by the availability of exogenous maltose (Fig. 6D).

## Discussion

B728a is better adapted for the colonization of plant leaf surfaces (Lindeberg et al., 2012) and exhibits better osmotolerance than DC3000 (Chen and Beattie, unpublished data). However, little is known about the factors that underlie these differences. As trehalose is an important determinant in bacterial osmotolerance, strain differences in trehalose synthesis and accumulation could contribute to these differences. In this study we demonstrated that the strains

differed in their relative dependence on the two trehalose biosynthetic pathways for osmoadaptation. In DC3000, the TreXYZ and TreS pathways were both required for trehalose synthesis, and deletion of either pathway strongly reduced trehalose production and osmotolerance. In contrast, the TreXYZ pathway in B728a had a dominant role in trehalose synthesis for osmoadaptation whereas the TreS pathway had only a minor, secondary role. Deletion of the B728a *treXYZ* loci significantly reduced or eliminated trehalose production, leading to reduced bacterial growth under hyperosmotic conditions, whereas deletion of the *treS* locus only marginally reduced trehalose production and bacterial growth under the same conditions (Fig. 3 and Fig. 4).

At least two mechanisms could explain why loss of the *treI* locus decreased the osmotolerance of DC3000 but not B728a. First, B728a expressed the *treXYZ* genes at a higher level, as reflected in the higher relative transcript levels under osmotic stress (Fig. 2A), and thus may have produced more TreXYZ enzymes and synthesized more trehalose, and the greater trehalose levels ensured greater osmotolerance in the absence of the TreS pathway. Alternatively, NAGGN synthesis may have compensated for the loss of the TreS pathway in B728a but not in DC3000. In DC3000, NAGGN had a relatively small role in osmotolerance based on the fact that trehalose synthesis mostly compensated for the loss of NAGGN synthesis under osmotic stress conditions (Freeman and Beattie, unpublished data). In contrast, NAGGN had a relatively large role in osmotolerance based on the relatively large reduction in growth of a B728a mutant deficient in NAGGN production under osmotic stress conditions (Kurz et al., 2010). Lastly, both

mechanisms may be active, with a combination of high levels of trehalose and NAGGN conferring the nearly wild-type level of tolerance of  $B\Delta tre1$  to osmotic stress.

Although there are two *treS* homologs in B728a, the second predicted *treS* homolog, Psyr\_2736, did not contribute to trehalose synthesis based on the loss of trehalose production in the  $B\Delta tre1\Delta tre2$  mutant, which maintained Psyr\_2736. The lack of trehalose production in the  $DC\Delta tre1\Delta tre2$  mutant indicated a similar lack of activity of the second *treS* locus in DC3000 (Freeman et al., 2010). Interestingly, the second *treS* locus in B728a was induced more than 8-fold by osmotic stress (Chapter 2), although it was not induced by osmotic stress in DC3000 (Freeman et al., 2010).

In the absence of an exogenous source of maltose, the maltose produced by the TreXYZ pathway could serve as a required substrate for TreS in the synthesis of trehalose in DC3000 (Fig. 1); this could explain part of the interdependency of these pathways in this strain. To test this hypothesis, we grew the strains in media amended with maltose. The presence of exogenous maltose, however, did not compensate for the reduced growth of strains lacking the TreXYZ pathway,  $DC\Delta tre2$  and  $B\Delta tre2$ , under hyperosmotic conditions (Fig. 5D and Fig. 6D). Although this result suggests that TreS-mediated trehalose production does not depend on maltose generated from the TreXYZ pathway, we cannot exclude the possibility that *P. syringae* does not transport maltose. A lack of transport may be reflected in the inability of either strain to grow on maltose when it was provided as a sole carbon source (Chen and Beattie, 2007) although this could also be due to the absence of a functional maltase for catabolism. Further studies to



experimentally test this possibility should include examining the effects of exogenous maltose on osmotolerance and trehalose synthesis in *P. syringae* cells expressing a maltose transporter from *E. coli*. Alternatively, if the cells are able to take up maltose but the maltose is immediately directed to glucan synthesis via the GlgE pathway instead of being converted to trehalose by TreS (Fig. 1), then a  $\Delta glgE$  mutant may accumulate more trehalose in the presence of exogenous maltose.

Trehalose production was lost in the DC $\Delta treI$  mutant based on direct trehalose quantification (Fig. 4) and also  $^{13}\text{C}$ -NMR and thin layer chromatography data (Freeman et al., 2010). This finding suggests that the TreXYZ pathway depends on a functional *glgE-treS-glgB* locus (Freeman et al., 2010). GlgE, encoded by the *glgE* gene upstream of *treS*, can generate reducing ends that are a required feature of substrates for TreY and TreZ (Kim et al., 2000); thus, GlgE may have a dominant role in generating the linear maltooligosaccharide precursors used by TreY in *P. syringae* (Fig. 1). This is supported by the absence of *glgC* in *P. syringae*, which along with *glgA*, encode the primary pathway for glycogen synthesis in most bacteria (Fig. 1) (Chandra et al., 2011). The absence of this pathway in *P. syringae* suggests that *glgE* and *glgB* together encode the primary glycogen biosynthetic pathway, and thus the linear  $\alpha$ -glucans serve as a primary branch point toward glycogen versus trehalose. Directing the linear  $\alpha$ -glucans toward trehalose is consistent with the lack of evidence for glycogen accumulation in *P. syringae*, including under conditions in which trehalose is accumulated (Freeman et al., 2010). To investigate if the TreXYZ pathway in DC3000 depends on a functional *glgE-treS-glgB* locus

because of a requirement for GlgE to generate precursors for the TreYZ pathway, the effect of overexpression of *glgE* in DC $\Delta$ *treI* on trehalose accumulation could be evaluated. The lack of dependence of B728a on the *glgE* locus for TreYZ-mediated trehalose production indicates that B728a has a sufficient linear maltooligosaccharide pool in the absence of GlgE activity to make trehalose; many factors could affect this pool size, including the relative activities of GlgB and TreX.

The mechanisms underlying the greater osmotolerance of B728a over DC3000 remain unclear. The genes involved in trehalose synthesis are more highly induced in B728a than in DC3000 in response to the same NaCl treatment (Fig. 2), which might reflect a higher sensitivity and responsiveness to osmotic stress of the relevant transcriptional regulators in B728a. For example, the sigma factor AlgU, which was implicated by transcriptome analysis in positive regulation of the trehalose biosynthesis genes in B728a (see Chapter 4), may be released from sequestration by its anti-sigma factor in the membrane more easily in B728a than DC3000 under the same osmotic stress conditions, and this may contribute to higher levels of trehalose in B728a. Moreover, the interdependence of the two trehalose biosynthetic pathways in DC3000 may reflect a limitation to the overall capacity of DC3000 for trehalose production, as supported by the lower levels of trehalose produced by DC3000 versus B728a in response to the same level of osmotic stress (Figs. 4B and C). This would be expected if DC3000 relies solely on a GlgE-mediated pathway for generating precursors for trehalose synthesis whereas B728 has access to both the GlgE and an additional pathway for such precursors. Overall, our data support

the possibility that differences in trehalose synthesis or regulation contribute to the differences in osmotolerance of two well-studied *P. syringae* strains.

## **Materials and methods**

### **Bacterial strains and growth conditions**

The bacterial strains and plasmids used in this study are described in Table 1. Bacteria were grown at 25°C in King's B medium before inoculating into MinAS medium (Miller, 1972), which contained 10 mM of succinate as a carbon source. NaCl was added to the stated final concentrations of 0.3 M or 0.5 M. Cells were grown at 25°C with shaking at 240 rpm. Antibiotics were added to the growth media as needed at the following concentrations ( $\mu\text{g ml}^{-1}$ ): kanamycin, 50; rifampin, 100; tetracycline, 20; and spectinomycin, 60.

### **Construction of B728a deletion mutants**

Unmarked deletion mutants of B728a were generated as described previously (Li et al., 2013). Briefly, two approximately 1-kb fragments flanking the target locus were amplified from B728a genomic DNA using the primer pairs listed in Table 2. A kanamycin cassette containing flanking FRT sites was PCR-amplified from pKD13 (Datsenko and Wanner, 2000) with FRT-F: 5'-ATTGTGTAGGCTGGAGCTGCTTC-3' and FRT-R: 5'-CCATGGTCCATATGAATATCCTCC-3'. These three fragments were ligated together by splice-overlap-extension (SOE) PCR to produce a single 3.5-kb fusion product, which was cloned into *Sma*I-digested pTOK2T and transformed into NEB10 $\beta$ . The plasmid was then

introduced into B728a cells by a tri-parental mating. The deletion mutants were identified as Rif<sup>r</sup> Km<sup>r</sup> Tet<sup>s</sup> and confirmed by PCR. The *kan* cassette was excised by introducing pFlp2Ω, sucrose (20%) counter-selection, and was confirmed by PCR and DNA sequencing.

### **Trehalose quantification assays**

The B728a cells were grown in MinAS medium containing 0.3 or 0.5 M NaCl for 20 h. Cells were harvested by centrifugation at 5,000xg for 10 min and washed once in MinAS medium with 0.3 or 0.5 M NaCl. Cells were then lysed using three alternating freeze–thaw cycles in liquid nitrogen and 60°C water and resuspended in 0.8 ml dH<sub>2</sub>O. 20-50 µl samples were used for trehalose quantitation using trehalose kit according to manufacturer’s protocol (Megazyme, Ireland) and were normalized to total protein as measured using the Pierce BCA protein assay kit (Thermo Fisher Scientific Inc., Rockford, IL).

### **Evaluation of bacterial growth in culture**

Cell growth was monitored in microtiter plates based on measurements at both 630 nm and 450 nm to compensate for the optical interference of water condensation within the wells.

## **Acknowledgments**

We would like to thank Dr. Shanshan Li for help with trehalose quantitation assay and critical reading of this manuscript. This project was supported by the National Research

Initiative Competitive Grants Program Grant 2008-35600-18766 from the US Department of Agriculture National Institute of Food and Agriculture.

## References

- Arguelles, J.C. (2000). Physiological roles of trehalose in bacteria and yeasts: a comparative analysis. *Arch Microbiol* 174, 217-224.
- Axtell, C.A., and Beattie, G.A. (2002). Construction and characterization of a *proU-gfp* transcriptional fusion that measures water availability in a microbial habitat. *Appl Environ Microb* 68, 4604-4612.
- Beattie, G.A. (2011). Water relations in the interaction of foliar bacterial pathogens with plants. *Annu Rev Phytopathol* 49, 533-555.
- Chandra, G., Chater, K.F., and Bornemann, S. (2011). Unexpected and widespread connections between bacterial glycogen and trehalose metabolism. *Microbiol* 157, 1565-1572.
- Chen, C.L., and Beattie, G.A. (2007). Characterization of the osmoprotectant transporter OpuC from *Pseudomonas syringae* and demonstration that cystathionine-beta-synthase domains are required for its osmoregulatory function. *J Bacteriol* 189, 6901-6912.
- Datsenko, K.A., and Wanner, B.L. (2000). One-step inactivation of chromosomal genes in *Escherichia coli* K-12 using PCR products. *Proc Natl Acad Sci U S A* 97, 6640-6645.
- Ditta, G., Stanfield, S., Corbin, D., and Helinski, D.R. (1980). Broad host range DNA cloning system for Gram-negative bacteria - Construction of a gene bank of *Rhizobium meliloti*. *Proc Natl Acad Sci U S A* 77, 7347-7351.
- Elbein, A.D., Pastuszak, I., Tackett, A.J., Wilson, T., and Pan, Y.T. (2010). Last step in the conversion of trehalose to glycogen a mycobacterial enzyme that transfers maltose from maltose 1-phosphate to glycogen. *J Biol Chem* 285, 9803-9812.
- Frederix, M., and Downie, A.J. (2011). Quorum sensing: regulating the regulators. *Adv Microb Physiol* 58, 23-80.
- Freeman, B.C., Chen, C.L., and Beattie, G.A. (2010). Identification of the trehalose biosynthetic loci of *Pseudomonas syringae* and their contribution to fitness in the phyllosphere. *Environ Microbiol* 12, 1486-1497.
- Gibson, R.P., Lloyd, R.M., Charnock, S.J., and Davies, G.J. (2002). Characterization of *Escherichia coli* OtsA, a trehalose-6-phosphate synthase from glycosyltransferase family 20. *Acta Crystallogr D Biol Crystallogr* 58, 349-351.
- Hoang, T.T., Karkhoff-Schweizer, R.R., Kutchma, A.J., and Schweizer, H.P. (1998). A broad-host-range F<sub>1</sub>p-*FRT* recombination system for site-specific excision of chromosomally-located DNA sequences: application for isolation of unmarked *Pseudomonas aeruginosa* mutants. *Gene* 212, 77-86.

- Kalscheuer, R., Syson, K., Veeraraghavan, U., Weinrick, B., Biermann, K.E., Liu, Z., Sacchettini, J.C., Besra, G., Bornemann, S., and Jacobs, W.R. (2010). Self-poisoning of *Mycobacterium tuberculosis* by targeting GlgE in an alpha-glucan pathway. *Nat Chem Biol* 6, 376-384.
- Kim, Y.H., Kwon, T.K., Park, S., Seo, H.S., Cheong, J.J., Kim, C.H., Kim, J.K., Lee, J.S., and Choi, Y.D. (2000). Trehalose synthesis by sequential reactions of recombinant maltooligosyltrehalose synthase and maltooligosyltrehalose trehalohydrolase from *Brevibacterium helvolum*. *Appl Environ Microb* 66, 4620-4624.
- Kurz, M., Burch, A.Y., Seip, B., Lindow, S.E., and Gross, H. (2010). Genome-driven investigation of compatible solute biosynthesis pathways of *Pseudomonas syringae* pv. *syringae* and their contribution to water stress tolerance. *Appl Environ Microb* 76, 5452-5462.
- Li, S., Yu, X., and Beattie, G.A. (2013). Glycine betaine catabolism contributes to *Pseudomonas syringae* tolerance to hyperosmotic stress by relieving betaine-mediated suppression of compatible solute synthesis. *J Bacteriol* 195, 2415-2423.
- Lindeberg, M., Cunnac, S., and Collmer, A. (2012). *Pseudomonas syringae* type III effector repertoires: last words in endless arguments. *Trends Microbiol* 20, 199-208.
- Loper, J.E., and Lindow, S.E. (1987). Lack of evidence for *in situ* fluorescent pigment production by *Pseudomonas syringae* pv. *syringae* on bean leaf surfaces. *Phytopathology* 77, 1449-1454.
- Maruta, K., Hattori, K., Nakada, T., Kubota, M., Sugimoto, T., and Kurimoto, M. (1996a). Cloning and sequencing of trehalose biosynthesis genes from *Arthrobacter* sp Q36. *Biochim Biophys Acta* 1289, 10-13.
- Maruta, K., Hattori, K., Nakada, T., Kubota, M., Sugimoto, T., and Kurimoto, M. (1996b). Cloning and sequencing of trehalose biosynthesis genes from *Rhizobium* sp M-11. *Biosci Biotechnol Biochem* 60, 717-720.
- Maruta, K., Kubota, M., Fukuda, S., and Kurimoto, M. (2000). Cloning and nucleotide sequence of a gene encoding a glycogen debranching enzyme in the trehalose operon from *Arthrobacter* sp Q36. *Biochim Biophys Acta* 1476, 377-381.
- Miller, J.H. (1972). Experiments in molecular genetics. Cold Spring Harbor Laboratory, Cold Spring Harbor, NY.
- Monier, J.M., and Lindow, S.E. (2005). Aggregates of resident bacteria facilitate survival of immigrant bacteria on leaf surfaces. *Microb Ecol* 49, 343-352.
- Moore, R.A., Starratt, A.N., Ma, S.W., Morris, V.L., and Cuppels, D.A. (1989). Identification of a chromosomal region required for biosynthesis of the phytotoxin coronatine by *Pseudomonas syringae* pv. *tomato*. *Can J Microbiol* 35, 910-917.
- Nishimoto, T., Nakano, M., Nakada, T., Chaen, H., Fukuda, S., Sugimoto, T., Kurimoto, M., and Tsujisaka, Y. (1996). Purification and properties of a novel enzyme, trehalose synthase, from *Pimelobacter* sp R48. *Biosci Biotechnol Biochem* 60, 640-644.

Table 1. Strains and plasmids used in this study

Strains or plasmids	Description or relevant genotype	Source
<i>P. syringae</i>		
B728a	Wild type; Rif <sup>r</sup>	(Loper and Lindow, 1987)
B $\Delta$ <i>tre1</i>	B728a $\Delta$ Psyr_2489-Psyr_2491; Rif <sup>r</sup>	This work
B $\Delta$ <i>tre2</i>	B728a $\Delta$ Psyr_2992-Psyr_3001; Rif <sup>r</sup>	This work
B $\Delta$ <i>tre1</i> $\Delta$ <i>tre2</i>	B728a $\Delta$ Psyr_2489-Psyr_2491 $\Delta$ Psyr_2992-Psyr_3001; Rif <sup>r</sup>	This work
DC3000	Wild type; Rif <sup>r</sup>	(Moore et al., 1989)
DC $\Delta$ <i>tre1</i>	DC3000 $\Delta$ PSPTO2760- $\Delta$ PSPTO2762; Rif <sup>r</sup>	(Freeman et al., 2010)
DC $\Delta$ <i>tre2</i>	DC3000 $\Delta$ PSPTO3125- $\Delta$ PSPTO3134; Rif <sup>r</sup>	(Freeman et al., 2010)
DC $\Delta$ <i>tre1</i> $\Delta$ <i>tre2</i>	DC3000 $\Delta$ PSPTO2760- $\Delta$ PSPTO2762 $\Delta$ PSPTO3125- $\Delta$ PSPTO3134; Rif <sup>r</sup>	(Freeman et al., 2010)
Plasmid		
pTOK2T	pTOK2 with restored <i>lacZ</i> activity; Tet <sup>r</sup>	
pKD13	Template for <i>kan</i> cassette flanked by FLP recombination target sites; Ap <sup>r</sup> Km <sup>r</sup>	
pFlp2 $\Omega$	Encodes Flp recombinase, suicide vector in <i>P. syringae</i> derived from pFlp2 (Hoang et al., 1998); Ap <sup>r</sup> Spc <sup>r</sup>	C. Chen and G.A. Beattie, unpublished data
pRK2013	RP4 transfer functions for mobilization; Km <sup>r</sup>	(Ditta et al., 1980)

Table 2. Primers used for the generation of deletion mutants in B728a.

Mutant	Target genes for deletion <sup>a</sup>	Flanking genes <sup>a</sup>	Primer sequences for amplifying flanking genes (5' $\rightarrow$ 3') <sup>b</sup>
B $\Delta$ <i>tre1</i>	2489-2491	2488	F1: AAGCGATTCTCTGGTTGCTGTC R1: <u>AGCCTACACAATCGCTCAAGACGTCGAGCATCACTCCTCACG</u>
		2492	F2: <u>ATATCCGGGTAGGCGCAATCACTATCCTCAAACCGAAGAAAGACT</u> R2: TGAACCTGTTCTGAGCCGAC
B $\Delta$ <i>tre2</i>	2992-3001	2991	F1: GCGACTCGGCTCTCTACAGT R1: <u>GCCTACACAATCGCTCAAGACGTCGGCGCTAATCATCAATTTT</u>
		3002	F2: <u>ATATCCGGGTAGGCGCAATCACTCTGAGTTCGCTGAATGCCTG</u> R2: TTCCTGCTCGATAGCCTTGT

<sup>a</sup> Gene numbers correspond to Psyr numbers.

<sup>b</sup> Underlined nucleotide bases indicate regions that complement 5' and 3' ends of the FRT-kanamycin cassette from pKD13.

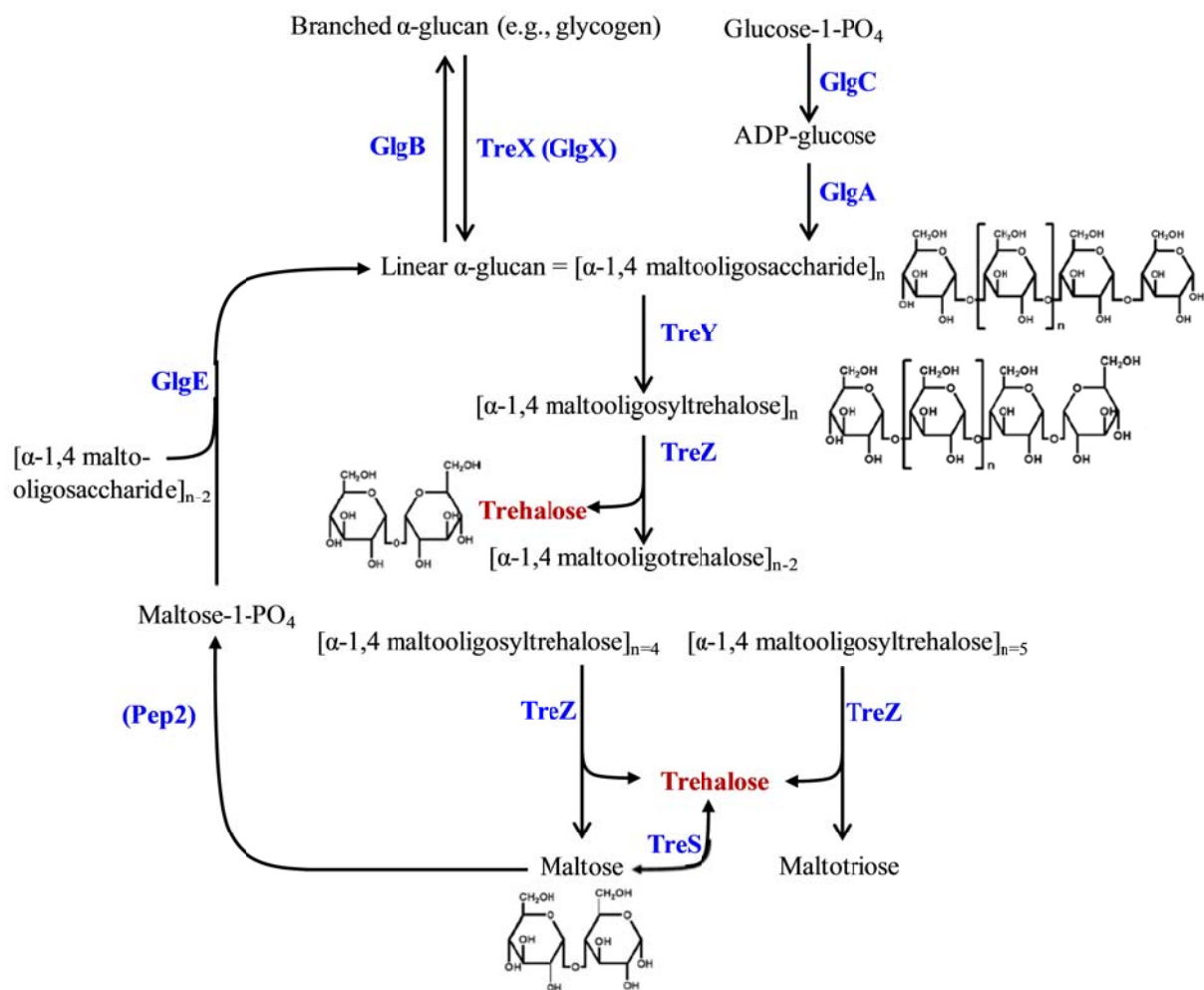


Fig.1. Proposed trehalose biosynthetic pathways in *P. syringae*. TreX (GlgX), debranching enzyme; GlgB, branching enzyme; TreY, maltooligosyltrehalose synthase; TreZ, maltooligosyltrehalose trehalohydrolase; TreS, trehalose synthase; GlgC, nucleotide diphosphoglucose pyrophosphorylase; GlgE, maltosyl-transferase; Pep2, maltokinase. TreX may aid the function of TreY and TreZ. Pep2 is present as a fusion protein with TreS.



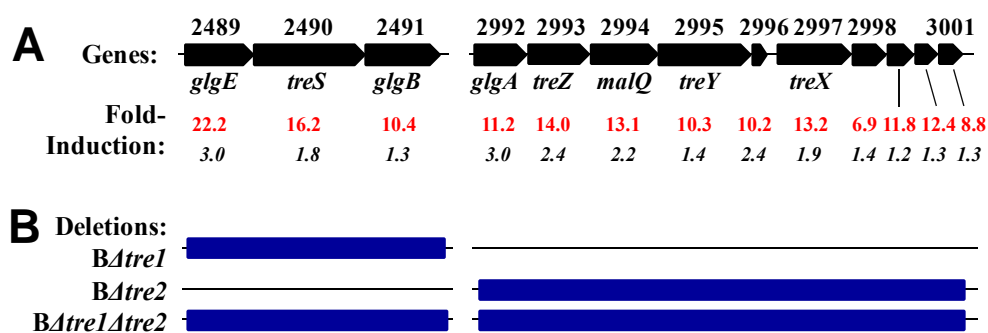


Fig.2. The trehalose biosynthetic loci in B728a. (A) The organization of trehalose biosynthetic genes. The fold-induction levels of the trehalose synthesis genes after 15 min exposure to 0.22 M NaCl are shown for in B728a; the numbers are Psyr\_numbers. B728a (red) and DC3000 (black) as evaluated using global gene expression analysis, with all of the genes shown exhibiting significant induction ( $P < 0.05$  and  $q\text{-value} < 0.01$ ). The data for DC3000 were adapted from (Freeman et al., 2010). (B) The deleted loci in the indicated B728a mutants, *BΔtre1*, *BΔtre2*, and *BΔtre1Δtre2* are represented as blue boxes. Similar deletions were made in the *DCΔtre1*, *DCΔtre2*, and *DCΔtre1Δtre2* mutants (Freeman et al., 2010).

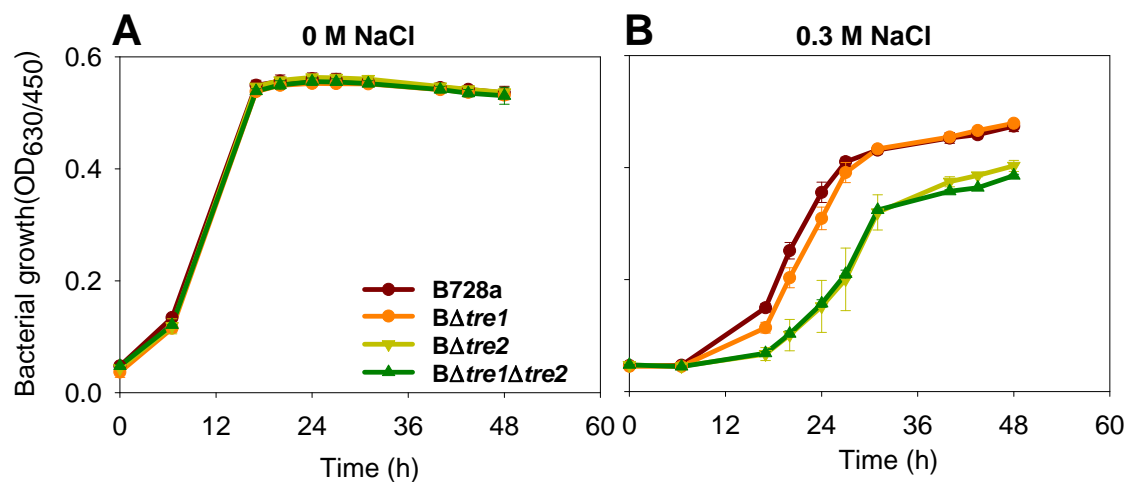


Fig.3. Growth of B728a and its mutant derivatives in (A) unamended MinAS medium and (B) MinAS medium amended with 0.3 M NaCl. Values represent mean  $\pm$  standard error of the mean (SEM) ( $n=3$ ).

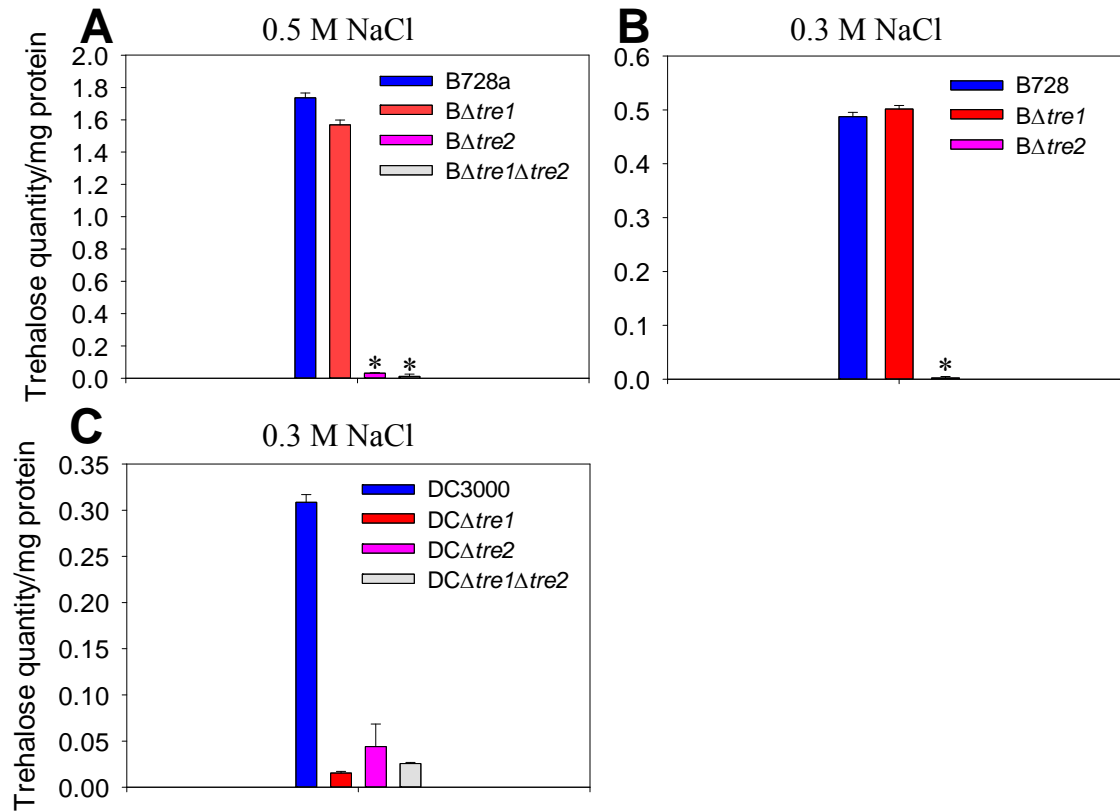


Fig.4. Trehalose accumulated by hyperosmotically-stressed cells of B728a and its mutant derivatives (B $\Delta$ *tre1*, B $\Delta$ *tre2*, and B $\Delta$ *tre1* $\Delta$ *tre2*) in MinAS medium amended with (A) 0.5 M NaCl and (B) 0.3 M NaCl. Trehalose accumulated by hyperosmotically-stressed cells of DC3000 and its mutant derivatives (DC  $\Delta$ *tre1*, DC  $\Delta$ *tre2*, and DC  $\Delta$ *tre1* $\Delta$ *tre2*) in MinAS medium amended with (C) 0.3 M NaCl. Values represent mean  $\pm$  SEM (n =2). \*,  $P < 0.05$  in pairwise Student's *t*-tests comparing the trehalose levels in a mutant to the levels in the wild type.

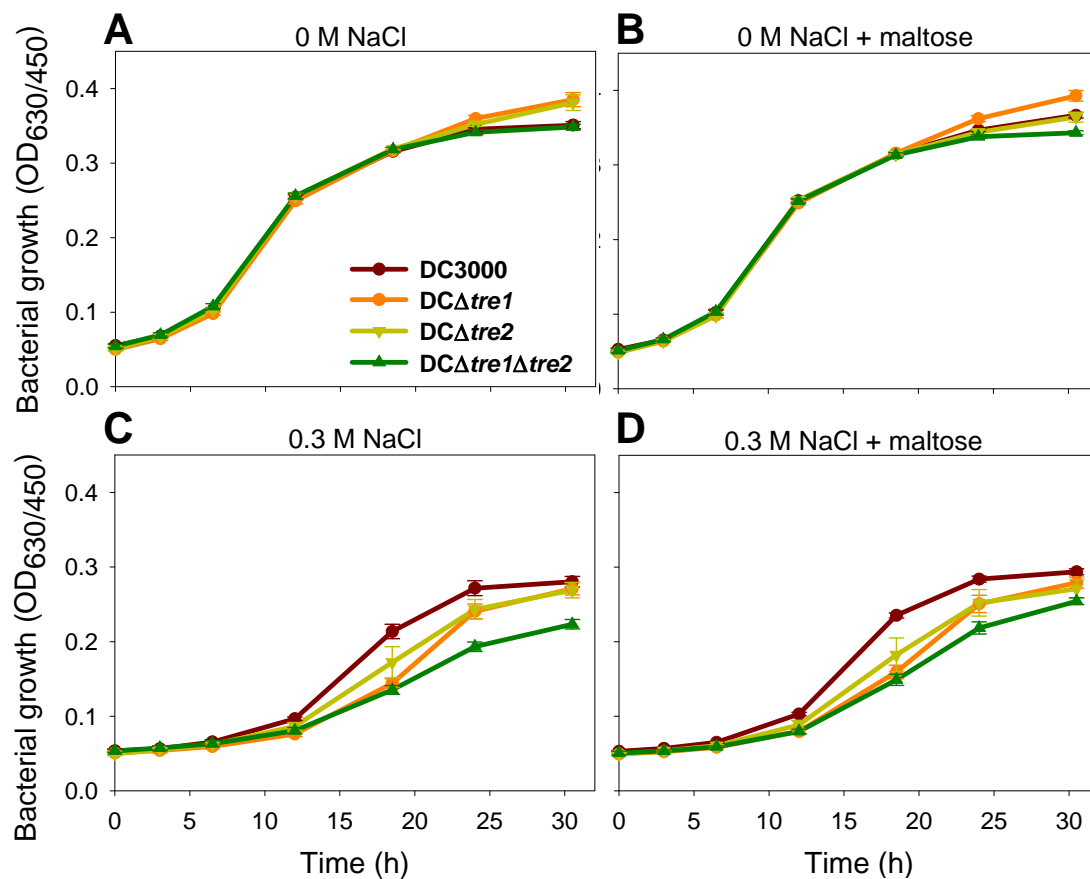


Fig. 5. Growth of DC3000 and its mutant derivatives in unamended MinAS medium (A) without and (B) with maltose, and in MinAS medium amended with 0.3 M NaCl (C) without and (D) with maltose. Values represent mean  $\pm$  SEM (n=3).

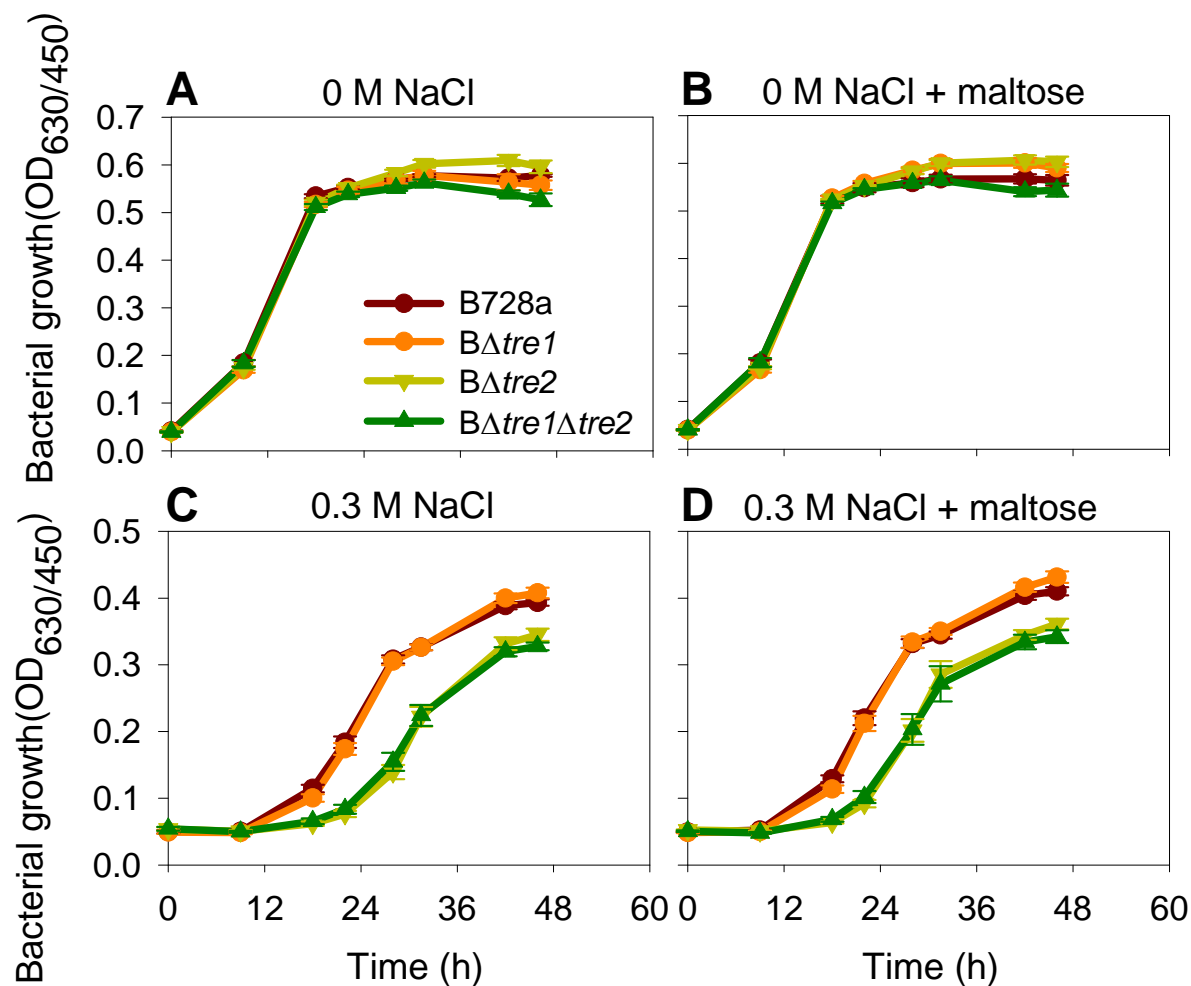


Fig. 6. Growth of B728a and its mutant derivatives in unamended MinAS medium (A) without and (B) with maltose, and in MinAS medium amended with 0.3 M NaCl (C) without and (D) with maltose. Values represent mean  $\pm$  SEM ( $n=3$ ).

## **CHAPTER 4. TRANSCRIPTIONAL ANALYSIS OF THE GLOBAL REGULATORY NETWORKS ACTIVE IN *PSEUDOMONAS SYRINGAE* DURING LEAF COLONIZATION**

Xilan Yu and Gwyn A. Beattie

Department of Plant Pathology & Microbiology,

Iowa State University; Ames, IA, 50010, USA

(To be submitted to *mBio* as a co-authored publication by Xilan Yu, Steven P. Lund,

Jessica W. Greenwald, Angela H. Records, Russell A. Scott, Dan Nettleton, Steven E.

Lindow, Dennis C. Gross, and Gwyn A. Beattie)

### **Abstract**

The plant pathogen *Pseudomonas syringae* pv. *syringae* B728a grows and survives on leaf surfaces and in the leaf apoplast of its host plant, bean. To understand the contribution of distinct regulators to B728a fitness and pathogenicity, we performed a transcriptome analysis of B728a and mutants lacking each of nine regulators, including quorum-sensing regulators, global regulators, and alternative sigma factors, with cells recovered from the surface and interior of bean leaves as well as exposed to various environmental stresses. The quorum-sensing regulators AhlR and AefR had a negligible role during B728a leaf colonization based on the small number of genes showing altered expression in the mutants. In contrast, GacS and a downstream regulator SalA formed a large regulatory network that included a plant signal-independent

branch, which regulated a diversity of traits, and a plant signal-dependent branch, which positively regulated genes for secondary metabolites and negatively regulated the type III secretion system. A third regulator, RetS, affected only a small subset of the GacS regulon and functioned almost exclusively to repress secondary metabolite genes when B728a cells were not in the leaf environment. SalA also functioned as a central regulator of both iron status, based on its reciprocal regulation of pyoverdine and achromobactin genes, and sulfur uptake, which suggests a role in maintaining an iron-sulfur balance. Among the alternative sigma factors AlgU, RpoS and RpoN, RpoN influenced the majority of the genome, AlgU influenced a much greater number of genes than RpoS, and many AlgU regulated genes were dependent on RpoN. RpoN activation of AlgU-activated genes was attenuated in cells recovered from epiphytic sites, and was strongly attenuated in cells recovered from the leaf interior, both of which implicated signals associated with the leaf habitat in altering regulation by these sigma factors. Gene activation by the sigma factor HrpL was suppressed by GacS and SalA in most cells recovered from plants; however, RpoN-dependent activation in nitrogen-limited conditions in culture suggests the possibility that RpoN-mediated activation may occur in subpopulations located in environmentally favorable sites. The influence of signals in the leaf environment on many branches of these global regulatory networks of *P. syringae* demonstrates the power of this multifactorial approach of network characterization using multiple regulatory mutants in multiple environmental conditions.

## Introduction

*Pseudomonas syringae* is a bacterial foliar pathogen with a complex interaction with the host plant. *P. syringae* pv. *syringae* B728a is one of the most thoroughly studied *P. syringae* strains.

As an epiphyte and a pathogen, B728a has evolved to survive and exploit two distinct habitats, the leaf surface and the leaf apoplast. Our previous global transcriptome profiling in B728a investigated the environmental conditions that *P. syringae* encounters in leaf habitats during their association with plants (Chapter 2). The results indicated that *P. syringae* encounters distinct nutritional and abiotic environments during the growth on leaf surfaces versus in the leaf interior. The study also identified the genes and traits that likely contribute to the *P. syringae* adaptations for growth and survival in these leaf habitats.

The extensive body of research on *P. syringae* includes the identification and characterization of a large number of regulators, consistent with the adaptation of this species to a diversity of habitats during its lifecycle. Although the majority of these regulators influence only a small number of genes involved in a single cellular process, such as catabolism of a nutrient or resistance to a toxic compound, others are known or predicted to function as global regulators based on regulation of many genes that collectively are involved in a wide array of functions.

The global activator GacS/A is among the most widely studied of these global regulators in *P. syringae*. GacS/GacA is a two-component system that was first discovered in *P. syringae* B728a based on the dramatic loss of virulence when it was inactivated (Willis et al., 1990). Although first named LemA based on the loss of lesion manifestation, it was later discovered as a regulator of antibiotic production in *P. fluorescens* and was renamed GacS for its ability to function in global antibiotic and cyanide control (Laville et al., 1992). In B728a, GacS/GacA is involved not only in necrotic lesion formation on bean, but also the production of the phytotoxins syringomycin and syringopeptin (Kitten et al., 1998), as well as the synthesis of secondary metabolite syringolin (Reimann et al., 1995), the exopolysaccharide alginate, and other

extracellular products (Heeb and Haas, 2001; Willis et al., 2001). Although GacS/A has been extensively studied in *P. fluorescens* due to its role in regulating properties that are relevant to biocontrol on roots (Laville et al., 1992; Maurhofer et al., 1994), and it is known to play a critical role in regulating pathogenesis traits in foliar *P. syringae* pathogens (Chatterjee et al., 2003), the profile of genes that GacS/A regulates in cells during colonization and pathogenesis of leaves, or even during colonization of roots, has not been identified; such characterizations have been performed only in laboratory media.

SalA was identified as a regulator that functions downstream of GacS/GacA in *P. syringae* B728a and activates genes involved in both syringomycin production and lesion formation (Kitten et al., 1998). It has since been shown to be a component of the GacS/GacA regulatory hierarchy in other *P. syringae* strains, including *P. syringae* pv. *syringae* B301D (Wang et al., 2006a) and *P. syringae* pv. *tomato* DC3000 (Chatterjee et al., 2003), indicating that, like GacA/GacS, SalA is a common component of the regulatory networks in *P. syringae*. Like the GacA/S-regulated genes, the SalA-regulated genes have been examined in culture but not yet *in planta*, despite that plant factors are known to influence some of the genes that are regulated by SalA, including the genes encoding syringomycin and syringopeptin (Lu et al., 2002; Lu et al., 2005).

GacA/GacS regulates the alternative sigma factor RpoS (Chatterjee et al., 2003; Kinscherf and Willis, 1999) in addition to SalA and many genes involved in pathogenicity. RpoS is a stationary phase sigma factor that is widely recognized for its role in stress tolerance in bacteria, including in pseudomonads such as *P. fluorescens* (Stockwell and Loper, 2005). In *P. syringae* RpoS has been shown to contribute to protection from near-UV irradiation (Miller et al., 2001),



but not to other stresses; thus, whether RpoS serves as a regulator of environmental stress tolerance in *P. syringae* cells *in planta* is not yet known.

In contrast to RpoS, AlgU (also known as AlgT) has been found to be important to *P. syringae* fitness on leaves (Yu et al., 1999). AlgU is an alternative sigma factor belonging to the extracytoplasmic function (ECF) family of sigma factors (Missiakas and Raina, 1998). In *P. syringae*, AlgU controls production of the acidic polysaccharide alginate as well as contributes to tolerance to several environmental stresses, including osmotic stress and oxidative stress (Keith and Bender, 1999).

Another ECF family sigma factor, HrpL, is required for the expression of genes for the type III secretion system and effector proteins in *P. syringae*. The HrpL-regulated genes have been well-studied in *P. syringae* (Lindeberg et al., 2006; Studholme et al., 2009), including *P. syringae* strain B728a, and are known to be induced primarily *in planta*; therefore, HrpL could provide a useful point of comparison when evaluating the contribution of other regulators to *P. syringae* fitness and pathogenicity on plants.

Several genes involved in *P. syringae*- host plant interactions are known to require the sigma factor RpoN. RpoN was first identified as a sigma factor that is active during nitrogen starvation, and continues to be widely recognized for its contribution to the use of alternative nitrogen sources, including in *P. syringae* (Alarcon-Chaidez et al., 2003). RpoN-regulated genes include *hrpL* and biosynthetic genes for the phytotoxin coronatine in *P. syringae* pvs. tomato and maculicola (Alarcon-Chaidez et al., 2003; Hendrickson et al., 2000a; Hendrickson et al., 2000b; Hutcheson et al., 2001).

Three other regulators are predicted to function as global regulators in *P. syringae* based on their activities in other bacteria, but the extent to which they regulate other genes has not been

examined in culture, much less plants. AhlR and AefR are the regulators that control the quorum sensing signaling system in *P. syringae*. Many bacteria and particularly those associated with eukaryotic hosts, produce signals that function in sensing population density in diffusion-limited environments. B728a has been found to produce a quorum-sensing signal, 3-oxo-hexanoyl-homoserine lactone (C6-HSL), and loss of the production of this signal was found to reduce epiphytic fitness in *P. syringae* pv. *syringae* B728a (Quinones et al., 2005; Quinones et al., 2004); in particular, C6-HSL was found to induce EPS production and suppresses motility. Although regulators of the quorum sensing signaling system are known in B728a, as is the fact that the gene for one of these regulators, *ahlR*, is positively regulated by GacA (Chatterjee et al., 2003; Quinones et al., 2004), we do not yet have a comprehensive picture of the breadth of genes and traits that are influenced by quorum sensing in *P. syringae*.

The last regulator of interest to the present report is RetS, which is a sensor kinase first identified in *P. aeruginosa* as a regulator of virulence gene expression (Ventre et al., 2006). RetS positively regulates the expression of T3SS and motility genes but negatively regulates the genes for T6SS and biofilm-associated exopolysaccharide production (Moscoso et al., 2011; Ventre et al., 2006). RetS controls these virulence factors by directly inhibiting GacS (Goodman et al., 2009). In *P. syringae* B728a, RetS also positively regulates the expression of T3SS genes and negatively regulates the expression of genes involved in T6SS as well as in alginate production (Records and Gross, 2010). In addition, RetS contributes to B728a surface colonization of bean leaves under controlled conditions (Records and Gross, 2010). The extent to which RetS has a role in switching between secretion systems and regulating other virulence-related phenotypes *in planta* is not yet known.

To understand the interaction between these regulators and host environments, we utilized transcriptome analysis of *P. syringae* B728a wild type and regulatory mutants lacking the quorum sensing regulators AhlR and AefR, the global regulators GacS, SalA, and RetS, and the alternative sigma factors AlgU, RpoS, HrpL, and RpoN. We examined the global gene expression profile of all of the strains on leaf surfaces and in the leaf apoplast, as well as in a basal medium and four environmentally stressful conditions proposed to occur on or in plant leaves. This chapter addresses the regulatory networks of these regulators with a particular focus on their importance to *P. syringae* during leaf colonization.

## Results and Discussion

### A few replicate treatments showed high variability

To understand the interaction between these regulators and host environments, we examined the global gene expression profile of B728a and  $\Delta ahlR$ ,  $\Delta aefR$ ,  $\Delta gacS$ ,  $\Delta salA$ ,  $\Delta retS$ ,  $\Delta algU$ ,  $\Delta rpoS$ ,  $\Delta hrpL$ , and  $\Delta rpoN$  single-gene deletion mutants on bean leaf surfaces after a 24-h moist and 48-h dry incubation period, and in the leaf apoplast after a 48-h incubation, as well as in five conditions *in vitro*, including exposure to 15-min of osmotic or oxidative stress, 2-h of starvation for nitrogen or iron, and a basal medium, as described in Chapter 2. Each treatment was performed using two biological replicates in each of three laboratories. Transcriptome data were generated based on hybridization of cDNA derived from total RNA to a B728a microarray, with subsequent calculation of robust estimated mean values for the fluorescence intensity measures for each ORF on the array, and these values were then subject to linear models for microarray data analysis (Limma), as described in Chapter 2.

First of all, we evaluated the variability among replicates of all of the strains based on the median absolute residuals estimated from the Limma analysis model (Figure 1). The low Fe treatment showed particularly high variability among the replicates in the Gross dataset, which may reflect experimental variation in the addition of the chelating agent in this dataset based on the consistent level of variability observed among the samples starved of iron in the other datasets. The apoplastic treatment showed an exceptionally high level of variability among the replicates in two of the three datasets. Unlike the epiphytic cells, which were collected from leaves that had been grown and inoculated in a single chamber, the apoplastic cells were recovered from leaves that had been grown and inoculated in each of the three laboratories, which are located in distinct climatic zones. Moreover, within a laboratory, the replicate samples for the apoplastic treatment were collected in potentially distinct seasons. Thus, we speculate that the high variability among the apoplastic samples was due to environmental variability during sample preparation, despite efforts to employ uniform plant incubation conditions. Furthermore, we speculate that this was coupled with a high sensitivity of these samples to the environment, and particularly to the moisture in the environment, which changes dramatically with seasons even within a given laboratory.

### **The regulons differed greatly in size, gene content, and responsiveness to distinct environmental conditions**

Here, we use the term regulon to indicate a collection of genes directly or indirectly affected by a single regulator. We first identified the number of genes that significantly differed in transcript levels between the regulatory mutant and the wild type under each of the seven environmental conditions tested, and then added up the number of distinct genes among these

seven gene sets (Table 1). The criterion used for differential expression (DE) was a false discovery rate of 1% (i.e.,  $q\text{-value} < 0.01$ ). These regulons, shown as the Total Unique Genes in Table 1, ranged from only 9 genes for AhlR to 3635 genes, or 71% of the B728a ORFs examined, for RpoN. The magnitude of the differences in the size of these regulons was not expected, with the greatest surprise being the small sizes of the regulons influenced by AhlR, AefR, and HrpL; these findings will be discussed below. The Minimal Regulon, i.e. the genes that were differentially expressed under every condition, was very small for each regulator, suggesting a major impact of environmental conditions on the composition of most of the regulons.

We further investigated the subset of each regulon that is differentially regulated by the environmental conditions by considering the genes that differed in transcript levels between the mutant and the wild type in the basal medium as the primary regulon, and then identifying additional genes for which the difference in transcript levels between the mutant and the wild type in a given environmental condition was distinct from that same difference in the basal medium. This is a more conservative approach in that it minimizes the inclusion of genes that may be differentially expressed in a given environmental condition due to random variation in gene expression by either the mutant or the wild type. We performed a contrast analysis on the differences in transcript levels between each mutant and the wild type in each of the six stressful environmental conditions versus in the basal medium (Table 2). The contrast analysis reflected how these regulons were impacted by each environmental condition. Among the regulons comprised of at least 15 genes, the RpoN, GacS and SalA regulons were especially impacted by environmental condition, as no more than about half (53%) of the genes in the total regulon were differentially expressed in any single condition, as compared to RpoS and AlgU for which over

90% of the regulon exhibited differential expression in a single condition, namely limited nitrogen and low water availability, respectively.

Furthermore, we performed hierarchical clustering and generated dendograms to evaluate the similarity in global transcript profiles among the samples, including each replicate of each strain under all seven treatments in each lab (Figure 2). In the data from all three labs, the treatment effects among all the wild type strains were the same as the one among all the wild types from all the three labs (Chapter 2, Figure 1). In our previous study with the wild-type B728a strain we found that the low N treatment had the largest effect on the transcript profiles, the *in planta* treatments had the next largest effect, with the two *in planta* treatments distinct, and the NaCl treatment had the third greatest effect. The results shown for the wild type and the  $\DeltaahlR$  and  $\DeltaaefR$  mutants (Figure 2A) illustrate these results, which reflect the negligible impact of these two regulators on the B728a transcriptomes under the conditions tested. Whereas the  $\DeltaretS$  mutant was also similar to the wild type, the other two mutants in the Gross dataset,  $\DeltagacS$  and  $\DeltasalaA$ , were highly distinct from the wild type in the impact of the environmental conditions on their transcript profiles (Figure 2B). For the  $\DeltagacS$  and  $\DeltasalaA$  mutants, however, the *in planta* treatments diverged from the other treatments, with clear differences between the epiphytic and apoplastic treatments. In the Beattie dataset, the transcriptomes of the  $\DeltarpoN$  mutant diverged from those of the other mutants in all of the treatments (Figure 2C), demonstrating the extent to which this regulatory factor is involved globally in sensing the environment. In contrast, the  $\DeltaalgU$  mutant diverged from the other mutants only in response to the NaCl treatment and the *in planta* treatments, confirming the specificity of the AlgU response to hyperosmotic stress, as indicated in Tables 1 and 2.

### **AefR and AhlR form a regulatory network comprised of surprisingly few genes**

AhlR appears to be a positive regulator of only nine genes (P<sub>syr</sub>\_1616- P<sub>syr</sub>\_1625) (Table 3), all of which are located at the same locus as *ahlR*. The relative transcript levels of the genes within the AhlR regulon varied substantially in the five *in vitro* treatments, with particularly striking differences between the two *in planta* treatments (Table 3). The basal medium in these experiments was amended with the quorum-sensing signal from B728a, C6-HSL (N-( $\beta$ -ketocaproyl)-L-homoserine lactone from Sigma-Aldrich) (10  $\mu$ M), to maximize the detection of differences between the wild type and the  $\Delta$ *ahlR* mutant. The consistent decrease in the expression of the AhlR regulon genes in the  $\Delta$ *ahlR* mutant compared to B728a (Table 3) supports a role for AhlR as a positive regulator of the genes at the *ahlR* locus. The attenuated decrease in the transcript levels of the  $\Delta$ *ahlR* mutant in epiphytic sites could be due to the presence of lower concentrations of quorum sensing signals on the leaf surface than were present in the basal medium. Similarly, the larger decreases in transcript levels for the mutant in the apoplastic sites could be associated with active and strong signaling from the abundant cell growth in the apoplast.

AefR appears to positively regulate the expression of the genes in the AhlR regulon in cells in the *in planta* treatments. This augmentation by AefR of AhlR-mediated activation was reported previously, as was a contribution of AefR to epiphytic fitness (Quinones et al., 2004); this contribution is consistent with AefR regulation of AhlR regulon loci in the plant environment, although the basis for the specificity to the plant habitat is not clear (Table 3).

AefR regulation of P<sub>syr</sub>\_1616-1623 was distinct from AhlR regulation of these genes in that the AhlR-dependent activation, but not AefR-dependent activation, was influenced by iron limitation (Table 3). In contrast to its activation of the AhlR regulon genes, AefR predominantly

suppressed genes encoding several efflux systems, and this suppression was evident in cells under all of the environmental conditions tested, although the differences were not significant for the MexAB-OprM efflux pump except in the apoplastic cells (Table 3). Both of the efflux pumps under AefR control (encoded by Psyr\_2967-2969 and Psyr\_4007-4009) are predicted to be involved in the transport of hydrophobic molecules. The RND family multidrug efflux pump MexAB-OprM was characterized in B728a and found to contribute to tolerance to antibacterial compounds, consistent with an efflux function, and reduced fitness on leaves (Stoitsova et al., 2008). This pump appeared to be most effective in exporting hydrophobic molecules such as various phenolic antimicrobial compounds associated with host plant defenses, and thus suggesting a role in evasion of the host immune response to enhance *in planta* survival and growth. However, AefR appears to function in the repression of these efflux pump genes, which contrasts with the reduced epiphytic fitness of both AefR (Quinones et al., 2004) and MexAB-OprM mutants (Stoitsova et al., 2008). This repression is independent of AhlR based on that the loss of AhlR did not affect the expression of the AefR-regulated efflux pump genes.

### **GacS and SalA are global regulators of diverse functions, including traits influencing virulence and environmental adaptation**

*GacS and SalA exhibit primarily positive regulation.*

We identified the functional categories in which the representation of differentially expressed genes was greater than their representation among all of the B728a genes (Figure 3); genes were designated as differentially expressed based on  $q\text{-value} < 0.01$ . The majority of differentially-expressed genes in the  $\Delta gacS$  and  $\Delta salA$  mutants showed decreased rather than increased expression, indicating GacS and SalA are primarily positive regulators under all of the conditions tested (Figure 3). For instance, in  $\Delta gacS$ , 237 of the 320 genes that were differentially



expressed in the basal medium (Table 1) showed decreased expression whereas 83 showed increased expression; moreover, a majority of the differentially-expressed genes generally showed decreased expression under each of the environmental conditions tested. The role of the GacS/GacA as primarily an activator of gene expression is consistent with a mechanism of regulation in which this two-component system induces the transcription of several small RNAs RsmX/Y/Z that bind to translational repressor proteins in the RsmA family and relieve translational repression (Kay et al., 2005). This was shown to be the exclusive mechanism of GacS/GacA signal transduction in *P. aeruginosa* (Brencic et al., 2009), GacS/GacA also bind directly to the promoters of many genes in *P. syringae* (Cha et al., 2012).

SalA was similar to GacS in exhibiting a bias toward positive regulation, which was expected based on the fact that SalA, a transcriptional regulator, is regulated at the transcriptional level by GacS/GacA (Kitten et al., 1998). In the basal medium (Table 1), 207 of the 243 genes that were differentially expressed in  $\Delta salA$  showed decreased expression whereas 36 showed increased expression. Moreover, 50% to almost 90% of the differentially-expressed genes showed decreased expression in  $\Delta salA$  under other environmental conditions. A previous study evaluating the SalA regulon in *P. syringae* pv. *syringae* B301D using an oligonucleotide microarray found that SalA exclusively mediated positive regulation of genes (Lu et al., 2005).

To identify the B728a sRNAs that are involved in GacS/GacA signal transduction we first used the bioinformatic tool SIPHT (Livny et al., 2008) to predict the identity of all of the sRNAs and then included these in the microarray design (Chapter 2). Out of 45 candidate sRNAs, we identified only two that exhibited significantly reduced expression in  $\Delta gacS$  under most of the conditions examined (Table 4); these also showed reduced expression in  $\Delta salA$ . The two

GacS/SalA-regulated genes include one that was predicted to be RsmY, and one that was identified as a plant-inducible gene in a promoter-trapping assay applied to B728a on bean leaves (Marco et al., 2005).

*GacS- and SalA-mediated changes in gene expression are consistent with known phenotypic effects of inactivating gacS and salA in B728a.*

Despite the fact that *gacS* was originally identified in B728a, the GacS/GacA regulon has not yet been characterized in this strain. The phenotypic effects resulting from the inactivation of *gacS* or *gacA* in B728a, however, were found to include the loss of swarming but not swimming motility (Kinscherf and Willis, 1999), reduced expression of acyl-homoserine lactone genes (Kitten et al., 1998) and reductions in the production of alginate (Willis et al., 2001), one or more secreted proteases, and the phytotoxin syringomycin (Hrabak and Willis, 1993). The GacS transcriptome identified in this study provides insights into the genetic mechanisms underlying these phenotypic changes. For example, the reduced swarming but not swimming motility of a *gacS* mutant (Kinscherf and Willis, 1999) suggested GacS/GacA-mediated regulation of surfactant production (Burch et al., 2012; Patrick and Kearns, 2012), and here we found that, of the two surfactants made by *P. syringae*, syringafactin and 3-(3-hydroxyalkanoyloxy)alkanoic acid (HAA) (Burch et al., 2012), the genes for HAA synthesis (*rhIA*) but not for syringafactin synthesis (*syfAB*) were positively regulated by GacS in the basal medium, whereas both were regulated *in planta* (Figure 4, Table 5). Thus the loss of swarming motility in culture media is likely attributable to the loss of HAA production. The  $\Delta salA$  mutant was similar to the  $\Delta gacS$  mutant in the transcript levels of *syfAB* and *rhIA* (Table 5), suggesting that these surfactants were regulated by SalA despite the fact that inactivation of *salA* did not influence swarming motility in a previous study (Kinscherf and Willis, 1999). Although the syringafactin regulatory gene

*syfR* was expressed at a level >10-fold higher than the biosynthetic genes in B728a in the basal medium (Chapter 2) and appeared to be subject to regulation by GacS and SalA under most of the environmental conditions tested, this regulation did not affect the transcription of the *syfAB* genes; in fact, these genes were influenced by GacS and SalA only *in planta* (Table 5), suggesting that GacS/SalA activation of syringafactin synthesis requires a plant signal. We found a similar regulatory pattern for some phytotoxin genes, discussed below.

Two genes involved in quorum sensing, *ahlI* and *ahlR*, showed reduced expression in  $\Delta gacS$  and  $\Delta salA$  across all of the environmental conditions tested (Table 6). This is consistent with previous observations that GacS is required for both the production of the C6-AHL signal (Kitten et al., 1998) and the transcriptional induction of the C6-AHL biosynthetic gene *ahlI* (Quinones et al., 2004). Our data, however, were not consistent with reports that C6-AHL production was independent of SalA (Kitten et al., 1998), rather *ahlI* regulation appeared to be due to the GacA/SalA regulatory cascade. Quiñones et al. (2004) reported that *ahlR* expression was independent of GacA (Quinones et al., 2004). Our data demonstrating a reduction in *ahlR* transcripts upon loss of GacS or SalA was, in fact, due to the loss of GacS/SalA-mediated activation of *ahlI* and concurrent loss of a read-through transcript containing an antisense *ahlR* gene and three additional downstream genes; this is due to transcriptional readthrough from the *ahlI* promoter through the downstream, but divergently oriented, *ahlR* gene (Chapter 2). Thus, although the AhIR regulon was small, our data support the previous finding that this regulon, and thus quorum sensing, is under the control of GacS/GacA in B728a.

The B728a genome encodes enzymes for synthesizing three extracellular polysaccharides (EPS): alginate, Psl, and levan. The reduced transcripts of the genes encoding the synthases for all three of these EPS in both the  $\Delta gacS$  and  $\Delta salA$  mutants (Table 7) indicate that GacS and

SalA positively regulate EPS biosynthesis (Figure 4). This is consistent with the demonstration of reduced alginate production by inactivation of *gacS* (Willis et al., 2001), and although SalA regulation occurred, the impact of the loss of *gacS* was much greater than the loss of *salA* (Table 7) consistent with some direct regulation of alginate production by GacS/GacA. Interestingly, although transcripts for the alginate biosynthetic genes were increased in B728a in epiphytic and apoplastic sites (Chapter 2), this increase was not associated with GacS activation (Table 7).

Other than loss of pathogenicity, the first *gacS* mutant phenotype reported in B728a was reduction in the production of secreted proteases and syringomycin (Hrabak and Willis, 1993). Out of 17 identified proteases, the B728a transcriptome data identified only one that was regulated by GacA, Psyr\_3041 (Table 8); this was an ortholog of LasB, which is a secreted protease from *P. aeruginosa* involved in virulence. We found evidence for *lasB* activation by GacA and SalA under all conditions except the low Fe treatment (Table 8), which may be related to its status as a zinc metalloprotease. As predicted based on the reduced phytotoxin production in  $\Delta gacA$  (Hrabak and Willis, 1992) and  $\Delta salA$  (Kitten et al., 1998) mutants, the genes for the synthesis and secretion of the phytotoxins syringomycin and syringopeptin were greatly repressed in epiphytic and apoplastic sites in both  $\Delta gacS$  and  $\Delta salA$  (Table 8), and as observed previously (Chapter 2), these genes were altered more in the apoplast than on leaf surfaces. The expression of the phytotoxin genes was not generally impacted by the loss of these regulators under other environmental conditions, which supports the previous finding that, like with syringafactin synthesis, positive regulation of syringomycin and syringopeptin synthesis by the GacS/SalA cascade involves a plant signal (Wang et al., 2006b).

The GacS/GacA regulatory system is considered to be a master regulator of secondary metabolism genes in pseudomonads (Lapouge et al., 2007). We have seen this in its regulation of

syringafactin, HAA and phytotoxin synthesis. We also found that it regulates two operons encoding non-ribosomal peptide synthases (NRPSs) based on the reduced expression of these genes in both  $\Delta gacS$  and  $\Delta salA$  (Table 8). Expression of the operon Psyr\_5009-5012, which includes genes originally misidentified as mangotoxin synthase genes (Arrebola et al., 2012), was more strongly altered by loss of the regulators in the *in vitro* than the *in planta* conditions (Table 8) and was not induced *in planta* (Chapter 2). In contrast, the operon Psyr\_4312-4314 was strongly induced *in planta*, was induced more in the apoplast than in the epiphytic sites (Chapter 2), and appeared to be subject to plant signal-dependent GacS- and SalA-dependent activation (Table 8), similar to the phytotoxin genes (Figure 4). These results thus identified an additional secondary metabolite in the GacS regulon that is potentially relevant to B728a-host interactions.

*GacS/SalA reciprocally regulates genes for the type III and type VI secretion systems.*

Changes in gene expression upon loss of the *gacA* gene from *P. syringae* pv. tomato DC3000 identified not only *rsmB*, *rsmZ*, *salA*, *ahII*, and *ahlR* as members of the GacA regulon, but also positive regulation by GacA of *rpoS*, *hrpL* and *hrpL*-regulated genes (Chatterjee et al., 2003). Whereas our data indicate strong positive regulation of *rpoS* by GacS, as well as SalA, in B728a, they indicate negative regulation of *hrpL*, genes for components of the type III secretion pilus and several type III secreted effector proteins during the association of B728a with bean leaves (Table 9). The lack of an effect of a  $\Delta gacS$  mutation on the expression of *hrpL* and other T3SS-associated genes in culture (Table 9) is consistent with previous findings (Records and Gross, 2010) and supports the involvement of a plant signal in GacS- and SalA-mediated regulation of the T3SS genes. The involvement of GacS/GacA and SalA in positive regulation of phytotoxins but negative regulation of the T3SS, despite that each of these traits contributes to *P.*

*syringae* virulence on plants, illustrates the complexity of factors involved in the regulation of these virulence traits on plants.

The genes encoding the recently identified type VI secretion system (T6SS) in B728a (Records and Gross, 2010) were positively regulated by GacS and SalA (Table 10). Positive regulation by GacS was shown previously when the *icmF* and *hcp* genes were used as indicators of the T6SS (Records and Gross, 2010); *icmF* and *hcp* showed reduced expression in  $\Delta gacS$  in culture both in that study (Records and Gross, 2010) and, along with many other T6SS genes, in ours (Table 10). The T3SS and T6SS are reciprocally regulated by GacS/GacA in *P. aeruginosa* (Gooderham and Hancock, 2009), but this regulation was found to be distinct in B728a based on the absence of GacS regulation of the T3SS genes (Records and Gross, 2010); however, the latter study examined gene expression only in culture. Our results demonstrate that B728a shows GacS/SalA-mediated repression of many T3SS genes *in planta* (Table 9), consistent with the established role of T3SS in plant-pathogen interactions, and GacS/SalA-mediated induction of many T6SS genes independent of the plant (Table 10), consistent with the recent demonstration that the T6SS secretion contributes to interactions with other microbes, namely yeasts, rather than with the plant (Haapalainen et al., 2012).

*SalA reciprocally regulates genes for the synthesis and transport of two siderophores.*

B728a produces two siderophores, pyoverdine, which is common to all fluorescent pseudomonads, and achromobactin, which is found in various plant pathogens, including some *P. syringae* strains. As expected, these genes were induced in B728a by iron limitation (Chapter 2). The transcriptome data indicate that SalA reciprocally regulates the genes encoding these siderophores, showing positive regulation of pyoverdine and negative regulation of achromobactin (Figure 4). In particular, the expression of genes for pyoverdine synthesis and

transport in  $\Delta salA$  was dramatically decreased in the low Fe treatment but not in the other treatments (Table 11), indicating a major role for SalA in the induction of the pyoverdine genes by iron limitation. In contrast, the expression of genes for achromobactin synthesis and transport in  $\Delta salA$  was generally increased in the many treatments that involved iron-replete conditions, but was not affected or was slightly decreased in the low Fe treatment (Table 11), indicating that SalA functions to repress the achromobactin genes when iron is replete. The large decrease in the expression of the achromobactin genes in the  $\Delta gacS$  mutant suggest that GacS also contributes to the positive regulation of the pyoverdine genes, although its contribution was smaller than that of SalA, but these decreases were not significant. This lack of significance may be due to the high variability among the two replicate samples of the  $\Delta gacS$  mutant that were subjected to the low Fe treatment (Figure 1).

The *gacS* and *salA* mutations generally did not result in altered expression of the siderophore biosynthesis and transport genes *in planta*. This is consistent with a lack of evidence for iron limitation by most B728a cells *in planta*, as determined using pyoverdine gene-based biosensors (Joyner and Lindow, 2000). This finding suggests not only the absence of GacS- or SalA-mediated pyoverdine induction, but also that SalA is not a major contributor to the suppression of the achromobactin genes *in planta*. That said, the achromobactin genes showed up to 5-fold induction in B728a cells in both epiphytic and apoplastic sites relative to in the basal medium, whereas the pyoverdine genes did not (Chapter 2). Thus, achromobactin genes were not actually suppressed on leaves, which supports the possibility that the leaf habitat has a moderate level of iron, i.e., one that is too high to allow SalA-mediated activation of pyoverdine, but too low to promote SalA-mediated repression of the achromobactin genes. Consequently, the cells produce this low affinity siderophore (Owen and Ackerley, 2011) for iron uptake *in planta*.

Interestingly, our results are in sharp contrast to those of Hassan et al. (2010), who showed that GacA suppresses the pyoverdine biosynthetic genes in *P. fluorescens* (Hassan et al., 2010), and these results together indicate that global control of siderophore synthesis differs among the pseudomonads.

*GacS and SalA independently regulate processes involved in oxidative stress tolerance and iron-sulfur chemistry, respectively*

A global transcriptome analysis of a *P. fluorescens gacA* mutant discovered that GacA negatively regulated 18 of 20 extracytoplasmic function sigma (ECF- $\sigma$ ) factors and positively regulated genes involved in oxidative stress (Hassan et al., 2010). In B728a, we found evidence that GacS negatively regulated four of its 10 ECF- $\sigma$  factors, which include five recently identified ECF- $\sigma$  factors (Thakur et al., 2013), and that this regulation was specific to the oxidative stress conditions (Table 12). In particular, all of the ECF- $\sigma$  factors that showed greater expression levels in the  $\Delta gacS$  mutant were related to iron homeostasis, namely two FecI-type regulators, Ecf5 (P syr\_1040) and Ecf6 (P syr\_4731), the pyoverdine regulator PvdS, and the achromobactin regulator AcsS. Furthermore, we found that 10 of 17 antioxidant enzymes in B728a also exhibited increased expression levels in the  $\Delta gacS$  mutant, and did so only in the oxidative stress conditions (Table 12). Despite their GacS-mediated suppression, five of these 10 antioxidant enzymes were induced in B728a upon exposure to the oxidative stress conditions (Chapter 2). Importantly, none of the GacS-regulated ECFs or antioxidant enzymes was influenced by the loss of *salA* (Table 12). Collectively, these expression results support a model in which GacS/GacA function to modulate the levels of antioxidant enzymes, and also processes related to iron homeostasis, in response to oxidative stress, with this regulation occurring via gene repression and in a SalA-independent manner.



About half of the sulfur metabolism and transport genes were increased in expression in the  $\Delta gacS$  and  $\Delta salA$  mutants, with these increases particularly pronounced in the  $\Delta salA$  mutant under iron- and N-limited conditions (Table 13). These genes included many involved in the transport and metabolism of sulfur, sulfate and sulfonate. A major use for sulfur in cells is as a component of iron-sulfur proteins. The dramatic increase in the expression of genes for sulfur transporters caused by the loss of *salA* in the iron-limited conditions (an average of 28-fold for the genes shown in Table 13), combined with the central role of SalA in balancing the expression of the pyoverdinin and achromobactin biosynthetic genes in response to iron, strongly indicates that SalA serves as a central regulator to coordinate the stoichiometric uptake of iron and sulfur compounds for iron-sulfur cluster synthesis. This suppression includes not only inorganic sulfur compounds, but also organic sulfur sources such as methionine, cysteine and sulfonates (Table 14). A putative ribose transporter, Psyr\_2874-2877, also showed a dramatic increase in expression in the  $\Delta salA$  mutant under low Fe conditions, although the mechanistic association with iron limitation was not clear. The transcriptome of a *P. fluorescens gacA* mutant identified regulation of iron homeostasis as one of the dominant roles of GacA (Hassan et al., 2010), demonstrating a similarity in the cellular processes impacted by the GacA/SalA regulatory network across pseudomonads, although the details of the regulation differ as reflected in the GacA-mediated positive regulation of sulfate and sulfonate transporters in *P. fluorescens* as compared to SalA-mediated negative regulation in *P. syringae*.

### **RetS negatively regulates a subset of the GacS regulon, including biosynthesis genes for phytotoxins and other secondary metabolites**

Loss of the RetS regulator altered the expression of 43 genes under at least one environmental condition (q-value < 0.01) (Tables 1 and 14). Among these genes, 41 showed increased expression in at least one condition, whereas only 3 showed decreased expression, indicating that RetS functions primarily as a negative regulator. Furthermore, the majority of genes that were differentially expressed in  $\Delta retS$  were also differentially expressed in  $\Delta gacS$  (Table 14, lines 2 and 3), and these genes all showed decreased expression in  $\Delta gacS$  (Table 14, line 4). Since the RetS regulon is much smaller than the GacS regulon, these findings indicate that RetS functions in the reciprocal regulation of a subset of the GacS regulon genes (Figure 4). This phenomenon was previously recognized in *P. aeruginosa* (Goodman et al., 2009) and more recently in studies focused on a few target genes in B728a (Records and Gross, 2010).

The genes that were regulated by RetS are mainly involved in phytotoxin synthesis and transport and secondary metabolite production (Figure 5). In  $\Delta retS$ , 7 out of 24 genes involved in phytotoxin synthesis and transport, as well as the Psyr\_4312-4314 genes encoding a secondary metabolite, showed increased expression in the basal medium and other *in vitro* environmental conditions but no change or decreased expression *in planta* (Figure 4 and Table 15). We previously showed that these genes were induced in B728a cells *in planta* (Chapter 2), and that this results, in part, from activation involving both GacS and one or more plant signals (Tables 8), as shown previously for the syringomycin and syringopeptin genes (Wang et al., 2006b). A similar pattern of regulation was observed for an operon with genes for organic and fatty acid metabolism, Psyr\_0748-0750, including their induction *in planta* (Chapter 2), their increased expression in the basal medium but not *in planta* (Figure 4), and their decreased expression in the  $\Delta gacS$  mutant

(Table 15). If RetS were actively repressing these genes *in planta*, then the  $\Delta retS$  mutant should have shown further induction of these genes; therefore, their lack of induction indicates that RetS was not active in repression *in planta*. This regulation could result from one or more plant signals acting upstream of RetS to suppress its activity, either directly or via GacS/GacA following GacS perception of the plant signals.

The genes for the type III and VI secretion systems and for alginate production were not differentially expressed in  $\Delta retS$  under any condition, although they were regulated by RetS in B728a under the conditions used in a previous study (Records and Gross, 2010). In particular, using the expression of the *icmF* and *hcp* genes as indicators of the T6SS genes, Records and Gross (2010) showed RetS repression in cells in a rich culture medium (potato dextrose agar). Similarly, they demonstrated increased alginate production in a  $\Delta retS$  mutant grown on a mannitol-glutamate-yeast extract-sorbitol medium, suggesting RetS repression of alginate genes. The absence of evidence for RetS repression of either the T6SS or alginate genes in our study may be due to a requirement of additional factors for RetS repression, although such factors were not provided *in planta*. Records and Gross (2010) also found evidence that RetS induces the T3SS genes; this increase, as measured with qRT-PCR, was quite small, and thus may have been missed in our study due to a lower sensitivity of the microarray analysis than the qRT-PCR analysis to differences in transcript abundance.

**RpoS regulates genes for Psl polysaccharide synthesis and chemosensing and chemotaxis, but few involved in stress tolerance.**

RpoS regulation was detected primarily under conditions of low iron or nitrogen or in cells recovered from leaf surfaces (Table 1). The majority of genes that were altered in epiphytic cells

were also altered in apoplastic cells, but the expression differences in apoplastic cells generally were not statistically significant due to the high variability between the replicate samples (Figure 1). RpoS positively regulated almost all of the genes involved in Psl polysaccharide synthesis and 25% of the genes involved in chemosensing and chemotaxis (Figure 3 and Table 16). RpoS regulated several genes involved in trehalose synthesis, although only under iron limited conditions where trehalose is not known to provide a benefit (Figure 3). The RpoS-regulated genes were also positively regulated by GacS (Figure 6, Table 16), as expected based on GacS regulation of *rpoS* in B728a. A previous study found that RpoS contributed to the tolerance of B728a to UV irradiation (Miller et al., 2001), but we did not identify RpoS regulated genes that may explain this. Overall, the cellular role of RpoS in B728a was relatively limited, particular with regard to genes involved in environmental stress tolerance. Although RpoS contributes to the tolerance of two *P. fluorescens* strains to stresses including osmotic and oxidative stresses, desiccation, UV irradiation, freezing and starvation (Stockwell et al., 2009; Stockwell and Loper, 2005), it has little to no influence on the stress tolerance of *P. fluorescens* strain A506 (Hagen et al., 2009). This illustrates both the potential for differences among pseudomonad strains in the role of RpoS and that there is precedence for a lack of a central role for RpoS in stress tolerance in this genus, in which RpoS had little influence on, in comparison to its significant role in environmental stress tolerance in other bacteria, including in oxidative stress tolerance in *P. fluorescens* (Hagen et al., 2009; Whistler et al., 1998) and UV tolerance in *P. syringae* (Miller et al., 2001).

### **The HrpL regulon may be subject to repression by a negative regulatory element**

We selected a basal medium for this study based, in part, on its potential to enable expression of the T3SS genes, as first demonstrated in *P. syringae* pv. *glycinea* (Huynh et al., 1989); however, the transcriptome data indicate that the T3SS genes were not detectably expressed in this medium. In fact, when the genes were ranked by their expression levels in the basal medium, the *hrpL* gene was in the bottom 15%, explaining why the deletion of the *hrpL* gene had a relatively small impact on the *hrpL* transcript levels in  $\Delta hrpL$  (Table 17) and few genes were influenced by its loss (Table 1). Yet, three genes were differentially expressed under all of the conditions except in the apoplastic cells (Table 1), which again was attributable to the high variability in the replicates (Figure 1) rather than to the lack of a detectable change in gene expression (Table 17). These three genes, Psyr\_1218-1220, were dramatically increased in expression in  $\Delta hrpL$  under all of the conditions (Table 17). They also were immediately downstream of *hrpL* (Figure 6). A correlation analysis of the transcript levels of these genes across the 168 transcriptomes included in this study indicated that Psyr\_1218-1220 is probably co-transcribed ( $R^2 \geq 0.94$ ). Assuming that they are also co-transcribed with *hrpL*, as predicted by the Pseudomonas database (Winsor et al., 2011), the most direct explanation for the dramatically increased expression of Psyr\_1218-1220 in  $\Delta hrpL$  is the presence of a negative regulatory element (Vinatzer et al., 2006) that is internal to *hrpL* (Figure 6). We propose that this NRE helps silence *hrpL* under non-inducing conditions, as supported by the high transcript levels of the downstream genes under all of the conditions examined. To the best of our knowledge, this is the first report of a possible NRE functioning in a regulatory network controlling the T3SS.

Approximately 50 genes are associated with the T3SS in B728a, including genes for the structural components of the T3SS, helper proteins, and at least 22 confirmed effectors (Vinatzer

et al., 2006). Whereas many of these are predicted or known to be in the HrpL regulon (Lindeberg et al., 2006; Vinatzer et al., 2006), only 13 genes in addition to Psyr\_1218-1220 were altered in expression upon the deletion of *hrpL*, with alterations occurring only in cells recovered from plants or exposed to nitrogen limitation (Table 1). The change in the transcript levels of these genes reflected positive control by HrpL, and parallel positive regulation by RpoN (Table 17), as expected since the expression of T3SS-related genes requires RpoN (Tang et al., 2006). Lee et al. (2012) showed that *hrcC* and *avrPto*, as indicators of the T3SS genes, were expressed on leaf surfaces, thus complementing previous evidence of their expression in the apoplast (Boureau et al., 2002) and supporting our evidence for at least some HrpL-regulated gene expression in cells recovered from the epiphytic sites. Using microscopy to visualize cells expressing the T3SS-related genes, Lee et al. (2012) also found that only a fraction of the leaf-associated B728a cells expressed T3SS-related genes. This could explain our finding that only a subset of the expected HrpL regulon genes exhibited differential expression on leaves (presumably those with the greatest changes, thus allowing their detection). Interestingly, the genes that exhibited the largest change in expression in the nitrogen-limited conditions, which provided inducing conditions for the T3SS genes in the wild type (Chapter 2), were genes encoding the extracellular components of the T3SS system. These included the pilus protein HrpA2 and the harpins HrpW1 and HrpZ1, which are extracellular helper proteins. These extracellular components were previously shown to be the most rapidly activated HrpL regulon genes (Ferreira et al., 2006). Thus, although our results provide novel information in the form of a putative NRE involved in T3SS regulation, they also provide evidence in support of the expression of the T3SS genes on the leaf surface, which is a trait that may be unique to B728a and contribute to its uniquely robust epiphytic fitness.

### **AlgU and RpoN form a regulatory network for stress tolerance that is strongly influenced by signals on and in leaves**

The vast majority of the differentially-expressed genes in  $\Delta algU$  under each environmental condition showed decreased rather than increased expression, indicating that AlgU functions primarily as a positive regulator. For example, 253 of the 272 genes that were differentially expressed in the epiphytic sites in  $\Delta algU$  (Table 1) showed decreased expression whereas only 19 showed increased expression. A bias also occurred in the NaCl treatment, where 59% of the 810 genes that were differentially expressed in  $\Delta algU$  (Table 1) showed decreased expression. As an ECF sigma factor, AlgU (also called AlgT) responds to stresses sensed in the periplasm or extracellular environment. It is functionally equivalent to RpoE in many gram-negative bacteria and to AlgU in *P. aeruginosa*; RpoE contributes to oxidative stress tolerance and AlgU additionally regulates alginate synthesis (Kazmierczak et al., 2005). Our data with B728a indicate that AlgU influenced the largest number of genes in response to osmotic stress, and influenced a large number of genes *in planta* (Table 1).

The alginate synthesis and regulation genes generally showed reduced expression in the  $\Delta algU$  mutant in the basal medium, but this reduction was much larger under the osmotic stress conditions (Table 18), consistent with the finding that *P. syringae* requires AlgU for osmoregulation of alginate gene expression (Keith and Bender, 1999). The B728a alginate biosynthetic genes were induced *in planta* (Chapter 2) and showed greatly decreased expression upon loss of *algU* (Table 18). As shown in Figure 7, AlgU regulated genes for the synthesis of the compatible solutes trehalose and NAGGN, based on their decreased transcript levels in  $\Delta algU$  in the NaCl and *in planta* treatments compared with the wild type (Table 18). Similarly, AlgU regulated genes encoding several of the B728a transporters for osmoprotective quaternary

ammonium compounds (QAC) (Chen and Beattie, 2007; Xu et al., 2010), as shown by the decreased expression of the CbcXWV and OpuC transporter genes in the osmotic stress and, at least for the OpuC transporter genes, *in planta* treatments (Table 18). This is the first report of the involvement of AlgU in the regulation of QAC transporters in response to osmotic stress. AlgU also regulated genes for the OsmC and OsmE proteins, which are orthologs of proteins known to be osmoresponsive, and an operon encoding an outer-membrane protein (P syr\_1316-1317) (Table 18), consistent with its general role in responding to osmotic stress. Like RpoE, AlgU in B728a induced genes likely involved in oxidative stress tolerance, including *katE*, *sodC*, *cpoF* and two glutathione S-transferases (Table 18). Lastly, we observed that the majority of the genes for the T6SS, the LasB protease and a small RNA, sRNA\_42, were positively regulated by AlgU in the osmotic stress and *in planta* conditions.

Our data indicate that RpoN is involved in the AlgU-mediated induction of hyperosmotic tolerance genes, as was recently reported in *P. aeruginosa* (Damron et al., 2012). The osmotic stress treatment increased transcript levels of *algU* in B728a (Chapter 2), but these transcript levels were decreased in  $\Delta rpoN$  in this treatment; in contrast, *rpoN* did not show differential expression in  $\Delta algU$  in any of the seven environmental conditions (Table 18). This suggests that RpoN contributes to *algU* induction in response to osmotic stress (Figure 7). Interestingly, the *algU* transcripts were increased in  $\Delta rpoN$  cells recovered from epiphytic sites as compared to in wild-type cells, and were even further increased in  $\Delta rpoN$  cells recovered from apoplastic sites. These changes are consistent with a physical or chemical signal in these *in planta* environments suppressing the RpoN-mediated induction of *algU*, with the apoplastic factor having a greater suppressive effect than the epiphytic factor; this attenuation of the RpoN regulation of *algU* is shown in Figure 7. The decreased expression of almost all of the AlgU-regulated genes



highlighted in Table 18 also occurred in  $\Delta rpoN$  in the NaCl treatment as well as in the basal medium, for those that showed decreased expression in  $\Delta algU$  in the basal medium (Table 18), supporting a general role for RpoN in AlgU-mediated gene activation in response to osmotic stress. Furthermore, the attenuation or reversal of these gene expression changes in the cells recovered from the plant habitats as compared to the cells in the osmotic stress treatments was observed for almost all of these genes, suggesting the general phenomenon of plant factor-mediated suppression of RpoN-mediated induction of AlgU activity, with a consistently greater suppressive effect of the apoplastic signal than the epiphytic signal (Table 18, Figure 7). Lastly, we found that RpoN represses the genes for Psl polysaccharide synthesis and did so specifically in the osmotic stress treatment (Table 18).

## Conclusions

This is the first global transcriptome study investigating the complex regulatory network of putative quorum sensing regulators (AhlR and AefR), global regulators (GacS, SalA and RetS), and alternative sigma factors (RpoS, HrpL, AlgU, and RpoN) in *P. syringae*, and particularly in the context of stressful environmental and *in planta* conditions. One of our first surprises was that loss of the only known quorum regulator in B728a, AhlR, or an associated regulator AefR, influenced the expression of only a small number of genes. Quorum regulation in most pathogens, including *P. aeruginosa*, generally impacts large gene sets. In subsequent experiments carried out by a collaborator on this project, the small size of the AhlR regulon was found to result from antisense repression of *ahlR* expression. This antisense transcript was generated by *ahlI* expression through the divergently-oriented *ahlR* gene. Thus, at least for B728a, quorum

regulation plays a relatively minor role in gene regulation on leaves and under each of the environmental conditions examined.

The two-component regulator GacS/GacA and its associated downstream regulator SalA are known to be global regulators. We showed that their regulatory network includes distinct branches that are separable based on their dependence on co-activation by plant signals (Figure 4). In this work, we expanded the inventory of plant signal-dependent traits from primarily phytotoxins to other secondary metabolites, including the surfactant syringafactin and an as-yet uncharacterized secondary metabolite. We also discovered unexpected negative regulation of the T3SS by GacS, which in the context of previous studies indicates that *P. syringae* pathovars differ in how they regulate this dominant virulence trait. Our results support the emerging model in *P. aeruginosa* and *P. syringae* that RetS regulation is reciprocal to that of GacS, but only for a small number of genes. Importantly, our findings strongly indicate that the primary function of RetS is to prevent the expression of genes for secondary metabolite synthesis in the absence of the plant (Figure 4). The need for such tight regulation may reflect a benefit of these metabolites primarily in plants, as well as a centrality of these secondary metabolites to B728a-plant interactions, as evidenced in the proposal that production of syringomycin and syringopeptin, in particular, may decrease the dependence of this pathovar of *P. syringae* on its effector genes for virulence (Lindeberg et al. 2012). Collectively, our data highlight the global nature of GacS/GacA regulation by also confirming its major role in oxidative stress tolerance, as suggested in *P. fluorescens*, but go further by showing a role for SalA as an independent regulator of both iron homeostasis and sulfur transport, presumably to ensure an iron-sulfur balance for iron-sulfur cluster synthesis (Figure 4).

With the exception of HrpL, the magnitude of the size of the gene sets altered by the loss of the sigma factor genes was paralleled by the change in population sizes during leaf colonization (Figures 8 and 9). In particular, RpoS influenced a surprisingly small number of genes, consistent with its similarity to the wild type in growth. As observed with *P. fluorescens* A506 (Hagen 2009), RpoS is not a major regulator of environmental stress tolerance. In contrast, AlgU regulated a wide inventory of genes involved in mediating tolerance to water limitation and oxidative stress. The major role of this regulator to *P. syringae in planta* is reflected in its establishment of populations that are approximately 10-fold lower than the wild type on leaves (Figure 8) as well as in leaves (Figure 9).

Much of the AlgU network appears to be subject to co-regulation by RpoN. Although deleting *rpoN* dramatically influenced growth *in planta* and influenced the expression of a majority of the genes in B728a in at least one environmental condition, the regulatory pattern of the genes affected by *algU* and *rpoN* indicated that the plant environment attenuates the impact of RpoN on AlgU-regulated genes (Figure 7). Furthermore, this attenuation was markedly greater in the apoplast than on leaf surfaces. If AlgU and RpoN additively influence the expression of AlgU-regulated genes, then one possible explanation is that RpoN is titrated away as it is directed to other genes due to the environmental conditions *in planta*, and this reduces its availability as a co-activator for AlgU.

Lastly, although the number of genes that were differentially expressed in the  $\Delta hrpL$  mutant in these studies was low, HrpL has a large impact on B728a growth *in planta* (Figures 8 and 9), as predicted based on its known role in regulating the T3SS. The findings of Lee et al. (2012) showed that only a fraction of B728a cells actually express *hrpL*-regulated genes *in planta*. Thus, it is tempting to speculate that the two major regulatory systems in B728a, GacS/GacA-SalA

(Figure 4) and RpoN (Figure 7), influence distinct subpopulations of B728a cells by reciprocally influencing their expression of HrpL. We propose that the T3SS is suppressed in many cells due to the GacS response to particular plant signals, but that it is activated in a subpopulation of cells due to the RpoN response to particular environmental signals.

Collectively, these data demonstrate the activity of multiple regulatory networks in B728a *in planta*. The major impact of physical or chemical signals in the leaf environment on the activity of both the GacS/GacA- and RpoN-driven regulatory networks illustrates the importance of evaluating these networks *in planta*. Although we have yet to identify these signals, this multifactorial approach of examining regulatory mutants in multiple environments including leaf habitats provided strong evidence that such signals exist, and interestingly, that at least some of these signals differ in epiphytic versus apoplastic sites, thus allowing *P. syringae* to fine-tune its expression of traits to best exploit each habitat.

## Materials and Methods

### Bacterial strains, plasmids, and growth conditions

The complete genome sequence is available for *P. syringae* pv. *syringae* strain B728a, a foliar pathogen originally isolated from bean leaf (*Phaseolus vulgaris* L.) in Wisconsin. Bacteria were grown as described previously (Chapter 2), using the same HMM medium with the same amendments (glutamine, FeCl<sub>3</sub>, and AHL) at 25°C.

### Construction of unmarked deletion mutations

Unmarked deletions of the following open reading frames of *Pss* B728a were prepared: *ahlR* (Psyr\_1622), *aefR* (Psyr\_3324), *retS* (Psyr\_4408), *gacS* (Psyr\_3698), *salA* (Psyr\_2601), *rpoS* (Psyr\_1374), *algU* (Psyr\_3958), *hrpL* (Psyr\_1217), and *rpoN* (Psyr\_4147). Unmarked deletion mutants of B728a were generated as described previously (Chen et al., 2010). Briefly, two 1-kb fragments flanking the target locus were PCR-amplified from B728a genomic DNA and a kanamycin (*kan*) cassette containing flanking FRT sites was PCR-amplified from pKD13 (Datsenko and Wanner, 2000) using the primer pairs 5'GTGTAGGCTGGAGCTGCTTC (Kan-F) and 5'ATTCCGGGGATCCGTCGACC (Kan-R). The three fragments were ligated together by splice-overlap-extension PCR using the original F1 and R2 primers to produce a single 3.5-kb fusion product consisting of the *kan* cassette and the flanking sequences. This product was cloned into *Sma*I-digested pTOK2T, which was then introduced into B728a cells by a triparental mating with pRK2013. The deletion mutants were identified as Rif<sup>r</sup> Km<sup>r</sup> Tet<sup>s</sup> and confirmed by PCR. The *kan* cassette was excised by introducing pFlp2Ω, which was later cured using sucrose (20%) counter-selection, and excision was confirmed by PCR and DNA sequencing.

### Evaluation of bacterial growth in planta of bean leaves

Cells were grown in HMM-basal medium, washed 2X in HMM-basal medium lacking FeCl<sub>3</sub>, NH<sub>3</sub>, glutamine and AHL, and diluted in water containing 0.01% Silwet L-77. Plants were grown

at a high density (10 plants per 4-inch pot) until their primary leaves were fully expanded. For epiphytic growth, plants were inoculated with bacterial cells by submerging the leaves in 1L of the inoculum for 20 sec, enclosing each pot in a plastic bag to create a tent, and incubating the pots on a laboratory bench at 25°C for 24 h. The bags were removed and the plants were incubated at 25°C for 48 h at the ambient relative humidity. The cells were recovered by sonication and enumerated by plating on King's B agar containing rifampin (50 µg/ml) and cycloheximide (100 µg/ml). For apoplastic growth, bacterial cells were inoculated by submerging the plants in 500 ml of the inoculum and subjecting the submerged plants to a vacuum for approximately 2 min, and then gently releasing the vacuum and leaving the plants submerged until they were infiltrated with the bacterial suspension. The plants were then removed from the inoculum and allowed to dry on a laboratory bench. The plants were incubated for 48 h under plant growth lights with a 12-h photoperiod for 48 h. The cells were recovered by homogenization and enumerated by plating as described before.

### **Exposure of bacteria to environmental stress conditions *in vitro* for RNA extraction**

B728a cells of wild type and nine mutant strains were grown on solid King's B medium, transferred to liquid HMM medium and subcultured twice in this medium. The cell collection, subsequent exposure to *in vitro* treatments, and RNA stabilization in harvest cells were performed as described previously (Chapter 2).

### **Growth of bacteria in planta for RNA extraction**

The beans and inoculum cells were grown as described previously (Chapter 2). To establish *in planta* populations, bean leaves were inoculated with bacteria cells at a density of  $1 \times 10^6$  CFU/ml for B728a wild type and eight mutants except  $\Delta rpoN$ , which was  $1 \times 10^8$  CFU/ml. Bean leaves were collected and immediately treated with RNA stabilization solution for subsequent bacterial cell collection.

### **RNA extraction, microarray design and hybridization**

RNA was extracted and purified as described previously (Chapter 2), and RNA samples were sent to Roche NimbleGen Inc. The same microarray experiment was performed including one B728a wild-type strain from each lab and a total of nine B728a mutant strains, and the data for all 12 strains were included in the analysis, described below.

### **Microarray data analysis**

The data analysis was performed as described previously (Chapter 2). Briefly, the fluorescence intensity was measured and subjected to background adjustment,  $\log_2$  transformation, quantile normalization and median polishing (Irizarry et al., 2003). An estimated mean was determined and used in the linear model analysis. Each linear model included fixed effects, fixed intercept parameter and one random error. Limma analysis (Smyth, 2004) was applied and done separately for distinct groups of treatments that had similar absolute median residuals. The

resulting variance estimates were used to calculate Welch  $t$ -statistics and corresponding  $P$ -values among all pairwise treatment comparisons of interest, for each of which,  $q$ -values were estimated from the corresponding distribution of  $P$ -values. Genes exhibiting an estimated False Discovery Rate less than 1% (a  $q$ -value  $< 0.01$ ), were identified as differentially expressed. Median absolute residuals for each strain-by-treatment sample were compared in each laboratory dataset to illustrate the variability between two replicates for each sample.

### **Hierarchical clustering**

A dendrogram was generated using the fluorescent intensities for each of the biological replicates of B728a wild-type strain and mutant strains from each laboratory datasets. The same ANOVA, F-test and `hclust` function in R were used to perform hierarchical clustering among all the samples, as described previously (Chapter 2).

### **Assignment and analysis of gene representation in functional categories**

The B728a genes were assigned to 63 functional categories. The same Fisher's exact test was used as described previously (Chapter 2), to perform overrepresentation test for B728a wild-type strain and mutant strains in each laboratory datasets, separately.



## References

- Alarcon-Chaidez, F.J., Keith, L., Zhao, Y.F., and Bender, C.L. (2003). RpoN (sigma(54)) is required for plasmid-encoded coronatine biosynthesis in *Pseudomonas syringae*. *Plasmid* 49, 106-117.
- Arrebola, E., Carrion, V.J., Cazorla, F.M., Perez-Garcia, A., Murillo, J., and de Vicente, A. (2012). Characterisation of the *mgo* operon in *Pseudomonas syringae* pv. *syringae* UMAF0158 that is required for mangotoxin production. *BMC Microbiol* 12, 10.
- Boureau, T., Routtu, J., Roine, E., Taira, S., and Romantschuk, M. (2002). Localization of *hrpA*-induced *Pseudomonas syringae* pv. *tomato* DC3000 in infected tomato leaves. *Mol Plant Pathol* 3, 451-460.
- Brencic, A., McFarland, K.A., McManus, H.R., Castang, S., Mogno, I., Dove, S.L., and Lory, S. (2009). The GacS/GacA signal transduction system of *Pseudomonas aeruginosa* acts exclusively through its control over the transcription of the RsmY and RsmZ regulatory small RNAs. *Mol Microbiol* 73, 434-445.
- Burch, A.Y., Shimada, B.K., Mullin, S.W.A., Dunlap, C.A., Bowman, M.J., and Lindow, S.E. (2012). *Pseudomonas syringae* coordinates production of a motility-enabling surfactant with flagellar assembly. *J Bacteriol* 194, 1287-1298.
- Cha, J.Y., Lee, D.G., Lee, J.S., Oh, J.I., and Baik, H.S. (2012). GacA directly regulates expression of several virulence genes in *Pseudomonas syringae* pv. *tabaci* 11528. *Biochem Biophys Res Commun* 417, 665-672.
- Chatterjee, A., Cui, Y.Y., Yang, H.L., Collmer, A., Alfano, J.R., and Chatterjee, A.K. (2003). GacA, the response regulator of a two-component system, acts as a master regulator in *Pseudomonas syringae* pv. *tomato* DC3000 by controlling regulatory RNA, transcriptional activators, and alternate sigma factors. *Mol Plant-Microbe Interact* 16, 1106-1117.
- Chen, C., Malek, A.A., Wargo, M.J., Hogan, D.A., and Beattie, G.A. (2010). The ATP-binding cassette transporter Cbc (choline/betaine/carnitine) recruits multiple substrate-binding proteins with strong specificity for distinct quaternary ammonium compounds. *Mol Microbiol* 75, 29-45.
- Chen, C.L., and Beattie, G.A. (2007). Characterization of the osmoprotectant transporter OpuC from *Pseudomonas syringae* and demonstration that cystathionine-beta-synthase domains are required for its osmoregulatory function. *J Bacteriol* 189, 6901-6912.
- Damron, F.H., Owings, J.P., Okkotsu, Y., Varga, J.J., Schurr, J.R., Goldberg, J.B., Schurr, M.J., and Yu, H.W.D. (2012). Analysis of the *Pseudomonas aeruginosa* regulon controlled by the sensor kinase KinB and sigma factor RpoN. *J Bacteriol* 194, 1317-1330.
- Datsenko, K.A., and Wanner, B.L. (2000). One-step inactivation of chromosomal genes in *Escherichia coli* K-12 using PCR products. *Proc Natl Acad Sci U S A* 97, 6640-6645.
- Ferreira, A.O., Myers, C.R., Gordon, J.S., Martin, G.B., Vencato, M., Collmer, A., Wehling, M.D., Alfano, J.R., Moreno-Hagelsieb, G., Lamboy, W.F., *et al.* (2006). Whole-genome

- expression profiling defines the HrpL regulon of *Pseudomonas syringae* pv. *tomato* DC3000, allows de novo reconstruction of the Hrp *cis* element, and identifies novel coregulated genes. *Mol Plant-Microbe Interact* 19, 1167-1179.
- Gooderham, W.J., and Hancock, R.E.W. (2009). Regulation of virulence and antibiotic resistance by two-component regulatory systems in *Pseudomonas aeruginosa*. *FEMS Microbiol Rev* 33, 279-294.
- Goodman, A.L., Merighi, M., Hyodo, M., Ventre, I., Filloux, A., and Lory, S. (2009). Direct interaction between sensor kinase proteins mediates acute and chronic disease phenotypes in a bacterial pathogen. *Genes Dev* 23, 249-259.
- Haapalainen, M., Mosorin, H., Dorati, F., Wu, R.F., Roine, E., Taira, S., Nissinen, R., Mattinen, L., Jackson, R., Pirhonen, M., *et al.* (2012). Hcp2, a secreted protein of the phytopathogen *Pseudomonas syringae* pv. *tomato* DC3000, is required for fitness for competition against bacteria and yeasts. *J Bacteriol* 194, 4810-4822.
- Hagen, M.J., Stockwell, V.O., Whistler, C.A., Johnson, K.B., and Loper, J.E. (2009). Stress tolerance and environmental fitness of *Pseudomonas fluorescens* A506, which has a mutation in RpoS. *Phytopathology* 99, 679-688.
- Hassan, K.A., Johnson, A., Shaffer, B.T., Ren, Q.H., Kidarsa, T.A., Elbourne, L.D.H., Hartney, S., Duboy, R., Goebel, N.C., Zabriskie, T.M., *et al.* (2010). Inactivation of the GacA response regulator in *Pseudomonas fluorescens* Pf-5 has far-reaching transcriptomic consequences. *Environ Microbiol* 12, 899-915.
- Heeb, S., and Haas, D. (2001). Regulatory roles of the GacS/GacA two-component system in plant-associated and other Gram-negative bacteria. *Mol Plant-Microbe Interact* 14, 1351-1363.
- Hendrickson, E.L., Guevera, P., and Ausubel, F.M. (2000a). The alternative sigma factor RpoN is required for hrp activity in *Pseudomonas syringae* pv. *maculicola* and acts at the level of *hrpL* transcription. *J Bacteriol* 182, 3508-3516.
- Hendrickson, E.L., Guevera, P., Penaloza-Vazquez, A., Shao, J., Bender, C., and Ausubel, F.M. (2000b). Virulence of the phytopathogen *Pseudomonas syringae* pv. *maculicola* is *rpoN* dependent. *J Bacteriol* 182, 3498-3507.
- Hrabak, E.M., and Willis, D.K. (1992). The *lemA* gene required for pathogenicity of *Pseudomonas syringae* pv. *syringae* on bean is a member of a family of two-component regulators. *J Bacteriol* 174, 3011-3020.
- Hrabak, E.M., and Willis, D.K. (1993). Involvement of the *lemA* gene in production of syringomycin and protease by *Pseudomonas syringae* pv. *syringae*. *Mol Plant-Microbe Interact* 6, 368-375.
- Hutcheson, S.W., Bretz, J., Sussan, T., Jin, S.M., and Pak, K. (2001). Enhancer-binding proteins HrpR and HrpS interact to regulate hrp-encoded type III protein secretion in *Pseudomonas syringae* strains. *J Bacteriol* 183, 5589-5598.

- Huynh, T.V., Dahlbeck, D., and Staskawicz, B.J. (1989). Bacterial blight of soybean: regulation of a pathogen gene determining host cultivar specificity. *Science* 245, 1374-1377.
- Irizarry, R.A., Hobbs, B., Collin, F., Beazer-Barclay, Y.D., Antonellis, K.J., Scherf, U., and Speed, T.P. (2003). Exploration, normalization, and summaries of high density oligonucleotide array probe level data. *Biostatistics* 4, 249-264.
- Joyner, D.C., and Lindow, S.E. (2000). Heterogeneity of iron bioavailability on plants assessed with a whole-cell GFP-based bacterial biosensor. *Microbiology* 146, 2435-2445.
- Kay, R.A., Ellis, I.R., Jones, S.J., Perrier, S., Florence, M.M., Schor, A.M., and Schor, S.L. (2005). The expression of migration stimulating factor, a potent oncofetal cytokine, is uniquely controlled by 3'-untranslated region-dependent nuclear sequestration of its precursor messenger RNA. *Cancer Res* 65, 10742-10749.
- Kazmierczak, M.J., Wiedmann, M., and Boor, K.J. (2005). Alternative sigma factors and their roles in bacterial virulence. *Microbiol Mol Biol Rev* 69, 527-543.
- Keith, L.M.W., and Bender, C.L. (1999). AlgT (sigma(22)) controls alginate production and tolerance to environmental stress in *Pseudomonas syringae*. *J Bacteriol* 181, 7176-7184.
- Kinscherf, T.G., and Willis, D.K. (1999). Swarming by *Pseudomonas syringae* B728a requires *gacS* (*lemA*) and *gacA* but not the acyl-homoserine lactone biosynthetic gene *ahII*. *J Bacteriol* 181, 4133-4136.
- Kitten, T., Kinscherf, T.G., McEvoy, J.L., and Willis, D.K. (1998). A newly identified regulator is required for virulence and toxin production in *Pseudomonas syringae*. *Mol Microbiol* 28, 917-929.
- Lapouge, K., Sineva, E., Lindell, M., Starke, K., Baker, C.S., Babitzke, P., and Haas, D. (2007). Mechanism of *hcnA* mRNA recognition in the Gac/Rsm signal transduction pathway of *Pseudomonas fluorescens*. *Mol Microbiol* 66, 341-356.
- Laville, J., Voisard, C., Keel, C., Maurhofer, M., Defago, G., and Haas, D. (1992). Global control in *Pseudomonas fluorescens* mediating antibiotic-synthesis and suppression of black root rot of tobacco. *Proc Natl Acad Sci U S A* 89, 1562-1566.
- Lee, J., Teitzel, G.M., Munkvold, K., del Pozo, O., Martin, G.B., Micheltore, R.W., and Greenberg, J.T. (2012). Type III secretion and effectors shape the survival and growth pattern of *Pseudomonas syringae* on leaf surfaces. *Plant Physiol* 158, 1803-1818.
- Lindeberg, M., Cartinhour, S., Myers, C.R., Schechter, L.M., Schneider, D.J., and Collmer, A. (2006). Closing the circle on the discovery of genes encoding Hrp regulon members and type III secretion system effectors in the genomes of three model *Pseudomonas syringae* strains. *Mol Plant-Microbe Interact* 19, 1151-1158.
- Livny, J., Teonadi, H., Livny, M., and Waldor, M.K. (2008). High-throughput, kingdom-wide prediction and annotation of bacterial non-coding RNAs. *PLoS One* 3, e3197.
- Lu, S.E., Scholz-Schroeder, B.K., and Gross, D.C. (2002). Characterization of the *sala*, *syrF*, and *syrG* regulatory genes located at the right border of the syringomycin gene cluster of *Pseudomonas syringae* pv. *syringae*. *Mol Plant-Microbe Interact* 15, 43-53.

- Lu, S.E., Wang, N., Wang, J.L., Chen, Z.J., and Gross, D.C. (2005). Oligonucleotide microarray analysis of the SalA regulon controlling phytotoxin production by *Pseudomonas syringae* pv. *syringae*. *Mol Plant-Microbe Interact* 18, 324-333.
- Marco, M.L., Legac, J., and Lindow, S.E. (2005). *Pseudomonas syringae* genes induced during colonization of leaf surfaces. *Environ Microbiol* 7, 1379-1391.
- Maurhofer, M., Hase, C., Meuwly, P., Metraux, J.P., and Defago, G. (1994). Induction of systemic resistance of tobacco to tobacco necrosis virus by the root-colonizing *Pseudomonas fluorescens* strain CHA0 - influence of the *gacA* gene and of pyoverdine production. *Phytopathology* 84, 139-146.
- Miller, C.D., Mortensen, W.S., Braga, G.U.L., and Anderson, A.J. (2001). The *rpoS* gene in *Pseudomonas syringae* is important in surviving exposure to the near-UV in sunlight. *Curr Microbiol* 43, 374-377.
- Missiakas, D., and Raina, S. (1998). The extracytoplasmic function sigma factors: role and regulation. *Mol Microbiol* 28, 1059-1066.
- Moscoso, J.A., Mikkelsen, H., Heeb, S., Williams, P., and Filloux, A. (2011). The *Pseudomonas aeruginosa* sensor RetS switches Type III and Type VI secretion via c-di-GMP signalling. *Environ Microbiol* 13, 3128-3138.
- Owen, J.G., and Ackerley, D.F. (2011). Characterization of pyoverdine and achromobactin in *Pseudomonas syringae* pv. *phaseolicola* 1448a. *BMC Microbiol* 11, 218.
- Patrick, J.E., and Kearns, D.B. (2012). Swarming motility and the control of master regulators of flagellar biosynthesis. *Mol Microbiol* 83, 14-23.
- Quinones, B., Dulla, G., and Lindow, S.E. (2005). Quorum sensing regulates exopolysaccharide production, motility, and virulence in *Pseudomonas syringae*. *Mol Plant-Microbe Interact* 18, 682-693.
- Quinones, B., Pujol, C.J., and Lindow, S.E. (2004). Regulation of AHL production and its contribution to epiphytic fitness in *Pseudomonas syringae*. *Mol Plant-Microbe Interact* 17, 521-531.
- Records, A.R., and Gross, D.C. (2010). Sensor kinases RetS and LadS regulate *Pseudomonas syringae* type VI secretion and virulence factors. *J Bacteriol* 192, 3584-3596.
- Reimann, C., Hofmann, C., Mauch, F., and Dudler, R. (1995). Characterization of a rice gene induced by *Pseudomonas syringae* pv. *syringae*: requirement for the bacterial *lemA* gene function. *Physiol Mol Plant P* 46, 71-81.
- Smyth, G.K. (2004). Linear models and empirical bayes methods for assessing differential expression in microarray experiments. *Stat Appl Genet Mol Biol* 3, Art 3.
- Stockwell, V.O., Hockett, K., and Loper, J.E. (2009). Role of RpoS in stress tolerance and environmental fitness of the phyllosphere bacterium *Pseudomonas fluorescens* strain 122. *Phytopathology* 99, 689-695.
- Stockwell, V.O., and Loper, J.E. (2005). The sigma factor RpoS is required for stress tolerance and environmental fitness of *Pseudomonas fluorescens* Pf-5. *Microbiology* 151, 3001-3009.

- Stoitsova, S.O., Braun, Y., Ullrich, M.S., and Weingart, H. (2008). Characterization of the RND-type multidrug efflux pump MexAB-OprM of the plant pathogen *Pseudomonas syringae*. *Appl Environ Microb* 74, 3387-3393.
- Studholme, D.J., Ibanez, S.G., MacLean, D., Dangl, J.L., Chang, J.H., and Rathjen, J.P. (2009). A draft genome sequence and functional screen reveals the repertoire of type III secreted proteins of *Pseudomonas syringae* pathovar *tabaci* 11528. *BMC Genomics* 10, 569.
- Tang, X.Y., Xiao, Y.M., and Zhou, J.M. (2006). Regulation of the type III secretion system in phytopathogenic bacteria. *Mol Plant-Microbe Interact* 19, 1159-1166.
- Thakur, P.B., Vaughn-Diaz, V.L., Greenwald, J.W., and Gross, D.C. (2013). Characterization of five ECF sigma factors in the genome of *Pseudomonas syringae* pv. *syringae* B728a. *PLoS One* 8, e58846.
- Ventre, I., Goodman, A.L., Vallet-Gely, I., Vasseur, P., Soscia, C., Molin, S., Bleves, S., Lazdunski, A., Lory, S., and Filloux, A. (2006). Multiple sensors control reciprocal expression of *Pseudomonas aeruginosa* regulatory RNA and virulence genes. *Proc Natl Acad Sci U S A* 103, 171-176.
- Vinatzer, B.A., Teitzel, G.M., Lee, M.-W., Jelenska, J., Hotton, S., Fairfax, K., Jenrette, J., and Greenberg, J.T. (2006). The type III effector repertoire of *Pseudomonas syringae* pv. *syringae* B728a and its role in survival and disease on host and non-host plants. *Mol Microbiol* 62, 26-44.
- Wang, N., Lu, S.E., Records, A.R., and Gross, D.C. (2006a). Characterization of the transcriptional activators Sala and SyrF, which are required for syringomycin and syringopeptin production by *Pseudomonas syringae* pv. *syringae*. *J Bacteriol* 188, 3290-3298.
- Wang, N., Lu, S.E., Wang, J.L., Chen, Z.J., and Gross, D.C. (2006b). The expression of genes encoding lipodepsipeptide phytotoxins by *Pseudomonas syringae* pv. *syringae* is coordinated in response to plant signal molecules. *Mol Plant-Microbe Interact* 19, 257-269.
- Whistler, C.A., Corbell, N.A., Sarniguet, A., Ream, W., and Loper, J.E. (1998). The two-component regulators GacS and GacA influence accumulation of the stationary-phase sigma factor sigma(S) and the stress response in *Pseudomonas fluorescens* Pf-5. *J Bacteriol* 180, 6635-6641.
- Willis, D.K., Holmstadt, J.J., and Kinscherf, T.G. (2001). Genetic evidence that loss of virulence associated with *gacS* or *gacA* mutations in *Pseudomonas syringae* B728a does not result from effects on alginate production. *Appl Environ Microb* 67, 1400-1403.
- Willis, D.K., Hrabak, E.M., Rich, J.J., Barta, T.M., Lindow, S.E., and Panopoulos, N.J. (1990). Isolation and characterization of a *Pseudomonas syringae* pv. *syringae* mutant deficient in lesion formation on bean. *Mol Plant-Microbe Interact* 3, 149-156.
- Winsor, G.L., Lam, D.K.W., Fleming, L., Lo, R., Whiteside, M.D., Yu, N.Y., Hancock, R.E.W., and Brinkman, F.S.L. (2011). *Pseudomonas* Genome Database: improved comparative

analysis and population genomics capability for *Pseudomonas* genomes. Nucleic Acids Res 39, D596-D600.

Xu, S., Zhou, J.W., Liu, L.M., and Chen, J. (2010). Proline enhances *torulopsis glabrata* growth during hyperosmotic stress. Biotechnol Bioprocess Eng 15, 285-292.

Yu, J., Penaloza-Vazquez, A., Chakrabarty, A.M., and Bender, C.L. (1999). Involvement of the exopolysaccharide alginate in the virulence and epiphytic fitness of *Pseudomonas syringae* pv. *syringae*. Mol Microbiol 33, 712-720.

Table 1. Numbers of genes that significantly differed in transcript levels between the regulatory mutants and the wild type under seven environmental conditions (q-value<0.01) <sup>1</sup>.

Regulon	Basal	NaCl	H <sub>2</sub> O <sub>2</sub>	low Fe	low N	Epi	Apo	Total Unique Genes <sup>2</sup>	Minimal Regulon <sup>3</sup>
AhlR	1	3	3	7	0	5	9	9	0
AefR	5	9	7	9	6	8	20	29	3
GacS	320	311	920	9	1643	360	28	2305	3
SalA	243	273	307	134	633	234	22	990	4
RetS	33	12	12	0	1	14	0	43	0
RpoS	1	3	3	44	162	104	2	213	0
HrpL	3	3	3	5	14	8	0	16	0
AlgU	63	810	19	12	29	272	34	866	6
RpoN	1344	2171	900	1248	801	733	22	3635	9

<sup>1</sup> The regulatory genes that were deleted in the mutants were excluded from these genes counts.

<sup>2</sup> The total number of genes influenced by at least one environmental condition.

<sup>3</sup> The total number of genes that significantly differed in every one of the seven environmental conditions.

Table 2. Numbers of genes in which the transcript abundance between the mutant and the wild type in a given environmental condition significantly differed from that same abundance in the basal medium (q-value<0.01) <sup>1</sup>.

Regulon	NaCl	H <sub>2</sub> O <sub>2</sub>	low Fe	low N	Epi	Apo	Total Unique Genes <sup>2</sup>	Total Regulon <sup>3</sup>
AhlR	0	0	0	0	0	0	1	2
AefR	0	0	0	0	0	7	7	12
GacS	0	93	0	307	52	0	422	657
SalA	0	1	34	63	36	0	113	324
RetS	0	0	0	1	13	0	13	33
RpoS	0	0	0	60	5	0	60	61
HrpL	1	0	0	10	1	0	12	14
AlgU	490	0	0	0	176	1	502	527
RpoN	848	181	324	883	539	117	2013	2538

<sup>1</sup> The regulatory genes that were deleted in the mutants were excluded from these genes counts.

<sup>2</sup> The total number of genes influenced by at least one of the six environmental conditions.

<sup>3</sup> The total number of genes influenced by at least one of the seven environmental conditions including the basal medium.

Table 3. Selected quorum sensing locus and efflux genes showing differential expression in  $\Delta ahlR$  and  $\Delta aefR$  mutants.

ID	Gene	Function	Basal <sup>a</sup>		NaCl <sup>a</sup>		H <sub>2</sub> O <sub>2</sub> <sup>a</sup>		Low Fe <sup>a</sup>		Low N <sup>a</sup>		Epi <sup>a</sup>		Apo <sup>a</sup>	
			AhlR	AefR	AhlR	AefR	AhlR	AefR	AhlR	AefR	AhlR	AefR	AhlR	AefR	AhlR	AefR
Quorum sensing locus genes																
Psyr_1616		Iron-sulfur proteins	-3.77	-1.21	-1.89	-1.29	<b>-4.45</b>	1.09	<b>-12.47</b>	-1.13	-3.09	1.41	-1.74	-1.28	<b>-12.00</b>	<b>-12.71</b>
Psyr_1617		Hypothetical	-8.70	-1.21	-2.57	1.12	<b>-6.25</b>	1.17	<b>-18.62</b>	1.07	-4.95	1.38	<b>-2.71</b>	-2.38	<b>-27.03</b>	<b>-26.67</b>
Psyr_1618	dapA-2	Amino acid metabolism and transport	-7.21	-1.12	-2.29	1.09	-5.39	1.10	<b>-17.09</b>	1.01	-5.38	1.37	-2.06	-1.64	<b>-20.12</b>	<b>-24.15</b>
Psyr_1619		Hypothetical	-9.27	1.05	-3.45	1.07	-8.00	1.40	<b>-23.87</b>	1.19	-4.98	1.41	<b>-2.77</b>	<b>-2.68</b>	<b>-29.94</b>	<b>-41.84</b>
Psyr_1620		Hypothetical	-10.43	-1.04	-4.00	1.15	-13.30	1.27	<b>-40.00</b>	1.08	-6.25	1.43	<b>-3.47</b>	<b>-3.75</b>	<b>-42.55</b>	<b>-58.48</b>
Psyr_1621	ahlI	Quorum regulation	<b>-43.67</b>	1.03	<b>-47.62</b>	-1.32	<b>-29.41</b>	-1.04	<b>-61.73</b>	-1.35	-9.22	1.99	<b>-3.80</b>	<b>-2.86</b>	<b>-70.92</b>	<b>-50.51</b>
Psyr_1622	ahlR	Quorum regulation	<b>-416.67</b>	-1.01	<b>-833.33</b>	-1.17	<b>-416.67</b>	1.17	<b>-370.37</b>	-1.17	<b>-416.67</b>	-1.07	<b>-56.82</b>	-2.05	<b>-434.78</b>	<b>-12.64</b>
Psyr_1623			-14.25	1.30	<b>-15.38</b>	-1.95	-5.60	1.01	<b>-14.95</b>	-1.37	-2.35	1.53	-1.41	-1.29	<b>-10.70</b>	<b>-12.92</b>
Psyr_1624		Transcriptional regulation	-3.25	1.47	<b>-5.61</b>	-1.80	-1.96	1.13	-5.61	-1.41	-1.41	1.31	-1.39	-1.39	<b>-4.31</b>	<b>-5.09</b>
Psyr_1625	aceE-1		-21.01	1.13	-12.99	-1.87	-6.90	1.07	-16.18	-1.14	-3.48	1.56	<b>-4.71</b>	<b>-5.08</b>	<b>-60.98</b>	<b>-67.11</b>
Efflux genes																
Psyr_3322		Transport	1.04	<b>16.53</b>	-1.04	<b>17.50</b>	-1.14	<b>10.67</b>	1.08	<b>14.02</b>	-1.01	<b>14.72</b>	1.18	<b>22.62</b>	-2.31	<b>7.66</b>
Psyr_3323		Hypothetical	1.28	<b>23.63</b>	-1.08	<b>21.88</b>	1.30	<b>18.26</b>	1.02	<b>32.80</b>	-1.03	<b>52.33</b>	1.11	<b>37.85</b>	-1.47	<b>13.99</b>
Psyr_3324	aefR	Quorum regulation	1.51	-2.35	-1.21	<b>-3.23</b>	1.03	<b>-4.27</b>	1.00	<b>-3.14</b>	-1.06	<b>-3.52</b>	1.07	<b>-2.72</b>	1.05	<b>-4.62</b>
Psyr_2967		Secretion/Efflux/Export	-1.21	<b>27.83</b>	1.16	3.15	-1.02	<b>18.46</b>	1.07	<b>77.79</b>	1.08	<b>58.74</b>	1.16	<b>4.97</b>	-1.42	<b>12.94</b>
Psyr_2968		Secretion/Efflux/Export	-1.06	<b>35.36</b>	-1.05	<b>3.96</b>	-1.16	<b>15.76</b>	-1.09	<b>69.64</b>	-1.10	<b>30.61</b>	1.13	<b>7.38</b>	-1.19	<b>18.73</b>
Psyr_2969		Secretion/Efflux/Export	1.15	<b>9.25</b>	1.06	1.70	1.13	3.23	-1.12	<b>11.97</b>	1.07	<b>6.26</b>	-1.28	1.95	1.15	<b>5.16</b>
Psyr_4006		Transcriptional regulation	-1.04	3.30	-1.02	1.50	-1.01	3.20	-1.03	4.88	1.12	3.23	-1.11	1.94	1.34	<b>3.29</b>
Psyr_4007	mexA	Secretion/Efflux/Export	1.13	4.36	-1.01	2.61	-1.35	3.10	1.11	6.46	1.03	3.29	1.11	1.99	1.34	3.46
Psyr_4008	mexB	Secretion/Efflux/Export	-1.03	3.69	1.01	1.88	-1.19	2.70	-1.20	4.68	-1.10	2.87	1.11	2.18	1.18	<b>3.72</b>
Psyr_4009	oprM	Secretion/Efflux/Export	1.21	4.26	-1.08	1.46	-1.27	1.98	-1.12	4.14	1.06	1.63	1.01	1.80	1.35	<b>4.19</b>



Table 3. Continued.

<sup>a</sup> Values shown are the fold-changes of transcript levels of selected genes in the mutant relative to transcript levels in the wild type, with positive numbers reflecting an increase in gene expression in the mutant as compared to the wild type, and negative numbers reflecting a decrease in gene expression in the mutant as compared to the wild type. The bolded values are the fold-changes of differentially expressed genes (q-value<0.01).

Table 4. Selected small RNAs genes showing differential expression in  $\Delta gacS$  and  $\Delta salA$  mutants.

ID	Gene	Function	Basal <sup>a</sup>		NaCl <sup>a</sup>		H <sub>2</sub> O <sub>2</sub> <sup>a</sup>		Low Fe <sup>a</sup>		Low N <sup>a</sup>		Epi <sup>a</sup>		Apo <sup>a</sup>	
			GacS	SalA	GacS	SalA	GacS	SalA	GacS	SalA	GacS	SalA	GacS	SalA	GacS	SalA
sRNA_RsmY		Regulation	<b>-6.27</b>	<b>-4.34</b>	<b>-8.05</b>	<b>-6.39</b>	<b>-5.16</b>	<b>-6.19</b>	-10.54	-2.38	<b>-2.71</b>	-1.33	<b>-6.03</b>	<b>-4.73</b>	-19.49	-12.06
PIG-a29_21		Regulation	<b>-3.27</b>	<b>-3.64</b>	<b>-3.87</b>	<b>-4.44</b>	<b>-2.35</b>	<b>-5.41</b>	-4.55	-4.45	<b>-3.26</b>	<b>-3.34</b>	<b>-5.51</b>	<b>-4.02</b>	-2.38	-1.59

<sup>a</sup> Values are the same as in Table 3.

Table 5. Surfactants (syringafactin and HAA) genes showing differential expression in  $\Delta gacS$  and  $\Delta salA$  mutants.

ID	Gene	Function	Basal <sup>a</sup>		NaCl <sup>a</sup>		H <sub>2</sub> O <sub>2</sub> <sup>a</sup>		Low Fe <sup>a</sup>		Low N <sup>a</sup>		Epi <sup>a</sup>		Apo <sup>a</sup>	
			GacS	SalA	GacS	SalA	GacS	SalA	GacS	SalA	GacS	SalA	GacS	SalA	GacS	SalA
Psyr_2575	<i>syfR</i>	Syringafactin regulation	<b>-3.24</b>	<b>-3.27</b>	<b>-2.39</b>	-2.07	-1.84	<b>-3.74</b>	-3.72	-2.58	-1.15	-1.23	<b>-3.04</b>	<b>-3.62</b>	-4.09	-2.92
Psyr_2576	<i>syfA</i>	Syringafactin synthesis	1.02	-1.11	1.07	1.03	-1.12	-1.21	-1.39	-1.12	1.07	1.09	-2.03	<b>-2.55</b>	-2.51	-2.25
Psyr_2577	<i>syfB</i>	Syringafactin synthesis	1.07	-1.20	-1.13	-1.08	-1.20	-1.08	-1.20	1.01	1.07	-1.02	<b>-2.47</b>	<b>-2.89</b>	-5.00	-3.41
Psyr_3129	<i>rhlA</i>	HAA synthesis	<b>-2.92</b>	<b>-2.52</b>	-1.29	1.01	<b>1.67</b>	<b>-4.70</b>	-2.25	-1.42	-1.25	<b>-1.99</b>	<b>-4.27</b>	<b>-3.64</b>	-6.88	-3.29

<sup>a</sup> Values are the same as in Table 3.

Table 6. Quorum sensing genes and three additional downstream genes showing differential expression in  $\Delta gacS$  and  $\Delta salA$  mutants.

ID	Gene	Function	Basal <sup>a</sup>		NaCl <sup>a</sup>		H <sub>2</sub> O <sub>2</sub> <sup>a</sup>		Low Fe <sup>a</sup>		Low N <sup>a</sup>		Epi <sup>a</sup>		Apo <sup>a</sup>	
			GacS	SalA	GacS	SalA	GacS	SalA	GacS	SalA	GacS	SalA	GacS	SalA	GacS	SalA
Psysr_1621	<i>ahlI</i>	Quorum regulation	<b>-6.17</b>	<b>-6.54</b>	<b>-7.33</b>	<b>-10.10</b>	<b>-7.70</b>	<b>-6.00</b>	-9.77	<b>-7.34</b>	<b>-4.98</b>	<b>-6.12</b>	<b>-2.92</b>	<b>-2.45</b>	-5.60	-4.27
Psysr_1622	<i>ahlR</i>	Quorum regulation	<b>-4.09</b>	<b>-4.21</b>	<b>-4.22</b>	<b>-5.07</b>	<b>-5.77</b>	<b>-4.00</b>	-4.26	-4.13	<b>-4.18</b>	<b>-3.28</b>	<b>-4.26</b>	<b>-2.70</b>	-4.13	-2.74
Psysr_1623			<b>-7.11</b>	<b>-6.86</b>	-1.01	-1.37	-1.33	-1.07	-1.32	1.10	2.31	1.58	6.37	<b>4.90</b>	4.30	5.13
Psysr_1624		Transcriptional regulation	<b>-3.95</b>	<b>-4.00</b>	-1.35	-1.67	1.09	1.07	1.10	1.65	<b>4.16</b>	3.11	<b>4.43</b>	3.40	3.40	4.17
Psysr_1625	<i>aceE-1</i>		<b>-19.84</b>	<b>-16.64</b>	1.09	-1.20	-1.60	1.08	-1.20	-1.72	2.92	3.85	5.75	4.29	1.69	2.07

<sup>a</sup> Values are the same as in Table 3.Table 7. Selected EPS biosynthetic genes showing differential expression in  $\Delta gacS$  and  $\Delta salA$  mutants.

ID	Gene	Function	Basal <sup>a</sup>		NaCl <sup>a</sup>		H <sub>2</sub> O <sub>2</sub> <sup>a</sup>		Low Fe <sup>a</sup>		Low N <sup>a</sup>		Epi <sup>a</sup>		Apo <sup>a</sup>	
			GacS	SalA	GacS	SalA	GacS	SalA	GacS	SalA	GacS	SalA	GacS	SalA	GacS	SalA
Alginate synthesis genes																
Psysr_1052	<i>algA-2</i>	Alginate synthesis	-4.85	-2.16	-5.07	-1.66	-9.14	-2.46	-2.15	1.28	-8.55	-3.56	1.19	1.18	-1.99	-4.42
Psysr_1053	<i>algF</i>	Alginate synthesis	-4.19	-1.92	-3.77	-1.65	-10.40	-2.01	1.03	1.50	-2.31	1.03	1.29	1.15	-1.62	-2.74
Psysr_1054	<i>algJ</i>	Alginate synthesis	-3.48	-2.18	-3.89	-2.43	-10.68	-2.36	1.24	1.70	-1.70	-1.23	1.33	1.01	-1.31	-2.30
Psysr_1055	<i>algI</i>	Alginate synthesis	-3.91	-1.96	-3.88	-2.64	-12.06	-2.67	1.03	1.13	-2.27	1.06	1.38	1.19	-1.77	-2.16
Psysr_1056	<i>algL</i>	Alginate synthesis	-3.12	-1.73	-2.51	-2.10	-6.59	-2.74	1.12	2.26	-1.51	1.10	1.73	1.40	-1.48	-2.08
Psysr_1057	<i>algX</i>	Alginate synthesis	-3.31	-1.83	-4.14	-4.55	-13.44	-4.12	1.16	2.86	-2.26	1.08	1.30	1.28	-1.41	-1.75
Psysr_1058	<i>algG</i>	Alginate synthesis	-3.06	-1.93	-4.42	-5.25	-20.88	-5.97	1.06	1.51	-1.64	-1.22	1.35	1.12	-1.49	-1.95
Psysr_1059	<i>algE</i>	Alginate synthesis	-3.68	-1.78	-3.86	-4.02	-22.88	-7.36	1.22	1.77	-1.95	-1.34	1.29	1.02	-1.78	-2.69
Psysr_1060	<i>algK</i>	Alginate synthesis	-2.94	-1.47	-3.45	-3.38	-15.92	-6.79	1.17	1.95	-2.15	-1.46	1.33	-1.03	-1.72	-2.03
Psysr_1061	<i>alg44</i>	Alginate synthesis	-4.10	-1.97	-3.30	-3.06	-16.75	-7.71	-1.04	1.72	-2.74	-1.65	1.24	-1.02	-2.02	-3.93
Psysr_1062	<i>alg8</i>	Alginate synthesis	-4.20	-1.72	-3.57	-3.34	-18.25	-5.83	-1.38	1.11	-3.23	-1.46	1.14	-1.01	-2.20	-3.12

Table 7. Continued.

ID	Gene	Function	Basal <sup>a</sup>		NaCl <sup>a</sup>		H <sub>2</sub> O <sub>2</sub> <sup>a</sup>		Low Fe <sup>a</sup>		Low N <sup>a</sup>		Epi <sup>a</sup>		Apo <sup>a</sup>	
			GacS	SalA	GacS	SalA	GacS	SalA	GacS	SalA	GacS	SalA	GacS	SalA	GacS	SalA
Alginate synthesis genes																
Psyr_1063	<i>algD</i>	Alginate synthesis	-3.60	-1.51	-3.58	-2.61	<b>-14.84</b>	-3.54	-2.75	1.60	<b>-10.44</b>	-2.23	1.31	1.21	-1.90	-4.27
Psl polysaccharide synthesis genes																
Psyr_3301	<i>pslA</i>	Psl synthase	-1.56	-2.32	<b>-2.79</b>	<b>-2.66</b>	<b>-3.45</b>	<b>-4.50</b>	-3.08	-2.51	<b>-6.12</b>	<b>-7.84</b>	<b>-3.29</b>	<b>-3.06</b>	-3.60	-2.40
Psyr_3302	<i>pslB</i>	Psl synthase	-1.78	<b>-2.57</b>	<b>-2.75</b>	<b>-2.43</b>	<b>-2.44</b>	<b>-5.15</b>	-3.62	-3.15	<b>-8.16</b>	<b>-11.12</b>	<b>-4.18</b>	<b>-4.28</b>	<b>-6.16</b>	-3.37
Psyr_3303	<i>pslD</i>	Psl synthase	-2.76	<b>-4.37</b>	<b>-2.93</b>	-2.03	<b>-4.04</b>	<b>-7.40</b>	-5.31	<b>-5.43</b>	<b>-12.38</b>	<b>-11.96</b>	<b>-5.26</b>	<b>-5.17</b>	-5.46	-3.14
Psyr_3305	<i>pslF</i>	Psl synthase	-2.24	<b>-3.28</b>	-2.19	-1.91	<b>-3.69</b>	<b>-4.31</b>	-3.31	-2.59	<b>-5.45</b>	<b>-6.44</b>	-2.15	-3.11	-2.91	-2.25
Psyr_3306	<i>pslG</i>	Psl synthase	-2.11	<b>-3.39</b>	-2.31	-2.23	<b>-4.86</b>	<b>-6.09</b>	-3.58	-3.73	<b>-7.94</b>	<b>-7.48</b>	<b>-4.77</b>	<b>-4.58</b>	-4.32	-2.00
Psyr_3307	<i>pslH-1</i>	Psl synthase	-2.34	-3.23	-2.32	-2.58	<b>-6.23</b>	<b>-6.24</b>	-3.88	-3.86	<b>-7.62</b>	<b>-9.18</b>	-3.46	<b>-4.03</b>	-5.04	-2.93
Psyr_3308	<i>psiI</i>	Psl synthase	<b>-3.84</b>	<b>-5.71</b>	-3.28	<b>-3.86</b>	<b>-9.28</b>	<b>-10.49</b>	<b>-8.06</b>	<b>-6.62</b>	<b>-9.09</b>	<b>-15.50</b>	<b>-3.64</b>	<b>-5.11</b>	<b>-8.33</b>	-4.63
Psyr_3309	<i>psiJ</i>	Psl synthase	<b>-4.04</b>	<b>-5.21</b>	<b>-4.05</b>	<b>-5.55</b>	<b>-12.71</b>	<b>-11.40</b>	-5.09	-4.74	<b>-6.66</b>	<b>-5.16</b>	<b>-3.87</b>	<b>-4.41</b>	-3.70	-1.67
Psyr_3310		Psl synthase	<b>-2.64</b>	<b>-3.38</b>	<b>-2.88</b>	<b>-3.34</b>	<b>-5.91</b>	<b>-6.42</b>	-2.73	-3.62	<b>-6.54</b>	<b>-6.31</b>	<b>-4.36</b>	<b>-3.37</b>	-3.30	-1.69
Psyr_3311	<i>psiK</i>	Psl synthase	-1.02	-1.28	-1.34	-1.58	<b>-2.57</b>	<b>-3.03</b>	-1.09	1.21	-1.37	-1.61	-1.16	-1.27	-1.37	1.06
Levan synthesis genes																
Psyr_0754	<i>lsc-1</i>	Levansucrase	-2.72	<b>-3.44</b>	-1.46	<b>-3.27</b>	-1.89	-1.57	-2.71	<b>-10.09</b>	-1.29	<b>-3.62</b>	1.76	-1.18	-1.39	-5.11
Psyr_2103	<i>lsc-2</i>	Levansucrase	-1.11	-1.21	-1.33	-1.27	-1.03	1.13	1.09	-1.09	-1.72	-1.17	1.26	-1.14	-1.37	-2.05

<sup>a</sup> Values are the same as in Table 3.

Table 8. Selected protease, phytotoxin, and secondary metabolism genes showing differential expression in  $\Delta gacS$  and  $\Delta salA$  mutants.

ID	Gene	Function	Basal <sup>a</sup>		NaCl <sup>a</sup>		H <sub>2</sub> O <sub>2</sub> <sup>a</sup>		Low Fe <sup>a</sup>		Low N <sup>a</sup>		Epi <sup>a</sup>		Apo <sup>a</sup>	
			GacS	SalA	GacS	SalA	GacS	SalA	GacS	SalA	GacS	SalA	GacS	SalA	GacS	SalA
<i>Protease gene</i>																
Psyr_3041	<i>lasB</i>	Protease	<b>-2.95</b>	<b>-3.09</b>	<b>-3.54</b>	<b>-2.82</b>	<b>-2.56</b>	<b>-6.31</b>	-1.26	3.05	<b>-2.47</b>	-1.52	<b>-4.65</b>	<b>-5.68</b>	-5.46	-10.00
<i>Phytotoxin-related genes</i>																
Psyr_2601	<i>salA</i>	Syringomycin regulation	-2.21	<b>-19.49</b>	-1.16	<b>-24.10</b>	<b>-2.72</b>	<b>-20.70</b>	-2.00	<b>-15.02</b>	<b>-2.25</b>	<b>-24.81</b>	<b>-8.96</b>	<b>-47.39</b>	-7.60	<b>-57.14</b>
Psyr_2602	<i>syrG</i>	Syringomycin regulation	-3.42	<b>-4.43</b>	-3.55	-3.44	-3.00	-3.78	-1.25	-1.50	<b>-3.73</b>	-2.80	<b>-10.22</b>	<b>-10.15</b>	<b>-14.88</b>	<b>-8.22</b>
Psyr_2606		Syringomycin efflux	1.21	-1.11	-1.26	-1.26	-1.36	-1.24	-1.11	1.30	1.10	-1.10	-1.92	<b>-3.28</b>	-3.99	-2.97
Psyr_2607	<i>syrF</i>	Syringomycin regulation	<b>-2.43</b>	<b>-2.34</b>	<b>-2.77</b>	<b>-2.72</b>	<b>-2.06</b>	-1.90	-1.35	-2.11	<b>-3.04</b>	-1.56	<b>-8.47</b>	<b>-6.70</b>	-15.24	-6.83
Psyr_2608	<i>syrE</i>	Syringomycin synthesis	-1.04	-1.14	-1.19	-1.14	-1.20	-1.15	-1.09	1.11	1.04	1.02	<b>-3.94</b>	<b>-4.44</b>	<b>-9.75</b>	<b>-7.36</b>
Psyr_2609	<i>syrC</i>	Syringomycin synthesis	1.03	-1.05	-1.11	-1.04	-1.22	-1.04	1.09	1.12	-1.10	1.12	<b>-2.95</b>	<b>-2.84</b>	<b>-7.02</b>	-5.05
Psyr_2610	<i>syrB2</i>	Syringomycin synthesis	<b>-2.00</b>	<b>-2.03</b>	-1.51	-1.58	<b>-1.98</b>	-1.52	-1.69	-1.83	<b>-1.63</b>	-1.30	<b>-13.46</b>	<b>-9.78</b>	<b>-34.72</b>	<b>-21.60</b>
Psyr_2611	<i>syrB1</i>	Syringomycin synthesis	-1.47	-1.62	-1.33	-1.30	-1.51	-1.46	-1.32	-1.26	-1.22	1.06	<b>-12.48</b>	<b>-10.53</b>	<b>-34.48</b>	<b>-21.65</b>
Psyr_2612	<i>syrP</i>	Syringomycin synthesis	-1.54	-1.83	-1.67	-1.53	-1.64	-1.86	-2.24	-2.06	-1.05	-1.01	<b>-7.90</b>	<b>-9.18</b>	<b>-47.17</b>	<b>-26.32</b>
Psyr_2613	<i>syrD</i>	Syringomycin synthesis	-1.55	-1.54	-1.59	-1.46	-1.59	-1.50	-1.25	-1.45	-1.56	1.01	<b>-7.58</b>	<b>-7.65</b>	<b>-27.93</b>	-8.70
Psyr_2614	<i>sypA</i>	Syringopeptin synthesis	1.42	1.18	1.07	1.18	-1.22	1.04	1.14	1.65	1.22	-1.12	-1.56	<b>-2.56</b>	-3.36	-2.09
Psyr_2615	<i>sypB</i>	Syringopeptin synthesis	1.10	-1.01	1.03	1.01	-1.21	-1.05	1.12	1.36	1.02	-1.04	-1.92	<b>-2.72</b>	<b>-6.83</b>	-3.53
Psyr_2616	<i>sypC</i>	Syringopeptin synthesis	1.33	1.06	1.07	1.07	1.03	-1.01	1.09	1.42	1.11	1.28	-1.57	<b>-2.06</b>	-2.74	-1.93
Psyr_2617	<i>pseE</i>	Secretion	1.16	-1.18	-1.13	-1.07	-1.41	-1.26	1.62	1.26	-1.46	-1.10	<b>-2.41</b>	<b>-3.19</b>	-4.00	-1.77
Psyr_2618	<i>pseF</i>	Secretion	1.14	-1.14	-1.04	-1.11	-1.32	-1.09	1.17	1.14	-1.27	1.06	<b>-2.42</b>	<b>-2.35</b>	-3.58	-1.66
Psyr_2619	<i>dat-2</i>	Secretion	-1.01	-1.11	-1.06	1.12	-1.10	-1.32	1.02	1.23	-1.15	-1.32	<b>-3.23</b>	<b>-3.05</b>	<b>-9.17</b>	<b>-5.27</b>
Psyr_2620	<i>pseA</i>	Secretion	1.25	1.11	-1.10	1.03	-1.08	-1.18	1.19	1.60	-1.02	-1.04	-1.03	-1.14	-1.91	-1.17
Psyr_2621	<i>pseB</i>	Secretion	1.33	1.11	1.12	1.12	1.05	1.06	1.24	1.69	1.03	-1.07	1.16	1.02	-1.16	1.02
Psyr_2622	<i>pseC</i>	Secretion	1.19	1.07	1.06	1.12	-1.23	-1.15	1.09	1.40	1.03	1.06	1.06	-1.16	-1.35	1.43

Table 8. Continued.

ID	Gene	Function	Basal <sup>a</sup>		NaCl <sup>a</sup>		H <sub>2</sub> O <sub>2</sub> <sup>a</sup>		Low Fe <sup>a</sup>		Low N <sup>a</sup>		Epi <sup>a</sup>		Apo <sup>a</sup>	
			GacS	SalA	GacS	SalA	GacS	SalA	GacS	SalA	GacS	SalA	GacS	SalA	GacS	SalA
Secondary metabolism genes																
Psysr_5009		Secondary metabolism	-5.27	-4.17	-5.84	-4.22	-5.25	-4.46	-5.00	-5.24	-8.45	-5.71	-3.86	-3.40	-4.36	-2.06
Psysr_5010		Secondary metabolism	-3.19	-3.20	-3.49	-3.04	-3.86	-3.25	-3.55	-2.98	-3.99	-3.48	-2.00	-2.34	-1.97	-1.47
Psysr_5011		Secondary metabolism	-2.84	-3.35	-3.81	-3.51	-5.01	-3.78	-4.24	-4.57	-4.53	-3.01	-1.93	-2.27	-2.52	-1.56
Psysr_5012		Secondary metabolism	-1.17	-1.40	1.15	-1.28	-2.50	-1.27	-1.36	-2.42	-3.72	-2.27	1.06	1.01	-1.51	-1.09
Psysr_4312		Secondary metabolism	1.08	-1.15	-1.01	-1.03	-1.71	1.12	1.54	-1.57	-2.41	-1.30	-4.71	-3.67	-15.29	-7.25
Psysr_4313		Secondary metabolism	1.04	1.02	-1.01	1.00	-1.07	1.30	1.84	1.35	-1.98	-1.00	-4.50	-3.33	-10.38	-6.38
Psysr_4314		Secondary metabolism	-1.35	-1.31	-1.47	-1.31	-1.09	1.29	1.94	-1.01	-2.31	-1.15	-4.80	-3.73	-17.61	-8.70

<sup>a</sup> Values are the same as in Table 3.Table 9. Selected type III secretion system (T3SS) genes showing differential expression in  $\Delta gacS$  and  $\Delta salA$  mutants.

ID	Gene	Function	Basal <sup>a</sup>		NaCl <sup>a</sup>		H <sub>2</sub> O <sub>2</sub> <sup>a</sup>		Low Fe <sup>a</sup>		Low N <sup>a</sup>		Epi <sup>a</sup>		Apo <sup>a</sup>	
			GacS	SalA	GacS	SalA	GacS	SalA	GacS	SalA	GacS	SalA	GacS	SalA	GacS	SalA
Psysr_1217	<i>hrpL</i>	Type III regulation	-1.55	-1.82	-1.24	-1.01	-1.96	-1.48	1.84	2.22	1.01	1.06	2.42	1.99	2.93	4.22
Psysr_1192	<i>hrpA2</i>	Type III pilus	-1.57	-1.88	1.38	1.12	1.30	-1.70	1.39	3.16	1.26	2.20	<b>4.15</b>	<b>2.93</b>	12.71	4.48
Psysr_1193	<i>hrpZ1</i>	Type III pilus	-2.27	<b>-2.80</b>	-1.06	-1.45	1.02	-1.68	1.18	1.79	-1.09	1.67	<b>4.16</b>	<b>3.18</b>	10.20	5.06
Psysr_1194	<i>hrpB</i>	Type III pilus	-1.85	-2.44	1.13	-1.17	-1.01	-1.39	1.30	2.72	1.29	1.61	<b>4.34</b>	<b>3.10</b>	5.75	4.99
Psysr_1195	<i>hrcJ</i>	Type III pilus	-1.79	-1.81	1.31	1.05	-1.00	-1.22	1.02	2.09	1.20	1.28	<b>3.34</b>	2.57	4.69	2.91
Psysr_1219	<i>avrB3</i>	Type III effector protein	-1.32	-1.70	1.21	1.22	1.62	1.05	3.50	2.60	2.20	<b>2.67</b>	<b>6.23</b>	<b>4.22</b>	9.42	8.20
Psysr_4919	<i>avrPto1</i>	Type III effector protein	-1.14	-2.05	1.83	1.16	2.65	-1.13	2.82	1.11	1.10	1.68	<b>10.36</b>	<b>5.19</b>	28.14	8.63

<sup>a</sup> Values are the same as in Table 3.

Table 10. Selected type VI secretion system (T6SS) genes showing differential expression in  $\Delta gacS$  and  $\Delta salA$  mutants.

ID	Gene	Function	Basal <sup>a</sup>		NaCl <sup>a</sup>		H <sub>2</sub> O <sub>2</sub> <sup>a</sup>		Low Fe <sup>a</sup>		Low N <sup>a</sup>		Epi <sup>a</sup>		Apo <sup>a</sup>	
			GacS	SalA	GacS	SalA	GacS	SalA	GacS	SalA	GacS	SalA	GacS	SalA	GacS	SalA
Psyr_2626		T6SS	<b>-7.34</b>	<b>-8.66</b>	<b>-7.84</b>	<b>-12.84</b>	<b>-14.04</b>	<b>-7.92</b>	-8.42	<b>-10.49</b>	<b>-4.73</b>	<b>-3.47</b>	-2.49	-2.20	-2.16	-1.20
Psyr_2627	<i>tagSI</i>	T6SS protein	<b>-4.67</b>	<b>-5.20</b>	<b>-5.21</b>	<b>-7.12</b>	<b>-6.99</b>	<b>-4.48</b>	-3.01	-3.67	<b>-2.88</b>	-1.39	-1.58	-1.36	1.17	2.02
Psyr_2628		T6SS	<b>-6.63</b>	<b>-9.07</b>	<b>-6.22</b>	<b>-15.60</b>	<b>-15.34</b>	<b>-6.66</b>	-7.50	-10.42	<b>-6.24</b>	<b>-3.57</b>	<b>-3.08</b>	-2.13	-1.90	1.06
Psyr_2629		T6SS	<b>-6.30</b>	<b>-8.18</b>	<b>-7.10</b>	<b>-14.33</b>	<b>-17.64</b>	<b>-6.75</b>	-8.67	<b>-13.00</b>	<b>-6.42</b>	<b>-4.29</b>	<b>-5.03</b>	<b>-3.62</b>	-2.27	-1.36
Psyr_4953	<i>tssB</i>	T6SS protein	<b>-1.64</b>	-1.32	1.09	-1.21	-1.40	<b>-1.62</b>	-1.30	2.20	-1.06	1.11	-1.33	-1.48	-1.44	-2.23
Psyr_4954	<i>tssC</i>	T6SS protein	<b>-1.93</b>	-1.70	-1.28	-1.53	<b>-1.77</b>	<b>-2.28</b>	-2.16	1.78	-1.53	-1.20	-1.59	-1.78	-1.97	-4.11
Psyr_4955	<i>tssE</i>	T6SS protein	<b>-2.69</b>	<b>-2.69</b>	-1.18	-1.90	<b>-4.35</b>	<b>-3.23</b>	-3.19	-2.42	<b>-5.14</b>	<b>-3.48</b>	<b>-2.29</b>	-2.07	-2.48	-3.98
Psyr_4956	<i>tssF</i>	T6SS protein	-2.30	-2.34	-1.14	-1.92	<b>-4.69</b>	<b>-2.95</b>	-2.31	-1.88	<b>-2.35</b>	-2.14	-1.74	-2.00	-1.69	-1.61
Psyr_4957	<i>tssG</i>	T6SS protein	-1.94	-1.77	1.02	<b>-2.17</b>	<b>-2.81</b>	-1.85	-1.34	-1.02	-1.44	-1.39	-1.52	-1.44	-1.45	-1.25
Psyr_4958	<i>clpV</i> / <i>tssH</i>	T6SS protein	-2.13	-1.68	-1.26	<b>-2.83</b>	<b>-9.65</b>	<b>-3.57</b>	-1.65	-1.49	<b>-2.22</b>	-2.14	-1.44	-1.53	-1.87	-1.89
Psyr_4959	<i>tssJ</i>	T6SS protein	-1.68	-1.56	-1.30	<b>-3.09</b>	<b>-9.98</b>	<b>-2.50</b>	-1.34	-2.00	<b>-2.51</b>	-1.69	-1.51	-1.54	-1.58	-1.95
Psyr_4960	<i>tssK</i>	T6SS protein	-1.89	-2.01	-1.62	<b>-3.45</b>	<b>-10.38</b>	<b>-2.69</b>	-1.43	-2.02	-1.90	-1.63	-1.34	-1.56	-1.50	-1.61
Psyr_4961	<i>tssLa</i>	T6SS protein	-2.02	-2.34	-2.30	<b>-4.80</b>	<b>-13.32</b>	-2.61	-1.33	-2.74	<b>-2.41</b>	-1.81	-1.57	-1.96	-1.78	-1.93
Psyr_4962	<i>icmF</i> / <i>tssM</i>	T6SS protein	-2.41	-2.63	<b>-3.30</b>	<b>-4.54</b>	<b>-8.53</b>	-2.47	-1.45	-1.66	-1.47	-1.84	-1.41	-1.75	-1.74	-1.36
Psyr_4963	<i>tagF</i>	T6SS protein	-2.02	-1.94	<b>-4.53</b>	<b>-3.25</b>	<b>-5.28</b>	-2.27	-1.26	-1.32	-1.21	-1.29	-1.41	-1.70	-1.61	-1.36
Psyr_4964	<i>tssLb</i>	T6SS	-2.38	-2.14	-3.16	-2.68	<b>-4.86</b>	-1.72	-1.46	-1.38	-1.26	-1.17	-1.57	-1.50	-1.56	-1.49
Psyr_4965	<i>hcp</i> / <i>tssD</i>	T6SS	<b>-2.32</b>	-1.89	<b>-3.30</b>	-1.71	<b>-2.78</b>	-2.00	-3.14	-1.71	<b>-3.58</b>	-1.77	-1.93	<b>-2.34</b>	-1.99	-5.56
Psyr_4966	<i>tssA</i>	T6SS	-1.92	-1.76	-2.56	-2.02	<b>-5.31</b>	-1.20	-1.54	-2.63	-2.47	-1.68	-1.66	-2.01	-1.42	-1.89
Psyr_4967		T6SS	-3.64	<b>-4.78</b>	-2.71	-3.33	<b>-9.65</b>	-2.67	-1.28	-3.85	-9.91	-1.86	-3.56	-2.02	-1.36	-1.73
Psyr_4968		T6SS	<b>-3.87</b>	<b>-4.23</b>	-2.76	-3.09	<b>-11.36</b>	-2.87	-1.37	-4.83	-9.18	-2.09	<b>-4.04</b>	-2.41	-4.04	-1.64

Table 10. Continued.

ID	Gene	Function	Basal <sup>a</sup>		NaCl <sup>a</sup>		H <sub>2</sub> O <sub>2</sub> <sup>a</sup>		Low Fe <sup>a</sup>		Low N <sup>a</sup>		Epi <sup>a</sup>		Apo <sup>a</sup>	
			GacS	SalA	GacS	SalA	GacS	SalA	GacS	SalA	GacS	SalA	GacS	SalA	GacS	SalA
Psyr_4969		T6SS	<b>-4.57</b>	<b>-5.05</b>	-3.19	<b>-3.77</b>	<b>-13.04</b>	<b>-3.24</b>	-1.69	-4.83	-8.01	<b>-3.06</b>	<b>-4.46</b>	<b>-3.39</b>	-2.74	-1.73
Psyr_4971		T6SS	<b>-5.78</b>	<b>-7.13</b>	<b>-3.63</b>	<b>-4.66</b>	<b>-9.25</b>	<b>-3.74</b>	-1.51	-5.63	-9.07	<b>-2.50</b>	<b>-3.33</b>	<b>-3.16</b>	-2.65	-1.53
Psyr_4972		T6SS	<b>-11.24</b>	<b>-9.90</b>	<b>-4.07</b>	<b>-6.51</b>	<b>-11.38</b>	<b>-5.07</b>	-1.71	-5.00	-7.59	-2.75	<b>-4.19</b>	-2.33	-3.57	-1.76
Psyr_4973		T6SS	<b>-5.20</b>	<b>-5.79</b>	<b>-2.98</b>	<b>-3.99</b>	<b>-4.42</b>	<b>-3.35</b>	-1.61	-2.55	-2.39	-1.51	-1.64	-1.53	-1.33	1.46
Psyr_4974	<i>vgrG</i>	T6SS	<b>-5.26</b>	<b>-5.18</b>	<b>-3.41</b>	<b>-3.71</b>	<b>-3.37</b>	<b>-2.96</b>	-1.73	-2.60	-3.46	<b>-2.22</b>	<b>-2.12</b>	-1.66	-1.63	1.25

<sup>a</sup> Values are the same as in Table 3.Table 11. Selected siderophore synthesis and transport genes showing differential expression in  $\Delta$ *gacS* and  $\Delta$ *salA* mutants.

ID	Gene	Function	Basal <sup>a</sup>		NaCl <sup>a</sup>		H <sub>2</sub> O <sub>2</sub> <sup>a</sup>		Low Fe <sup>a</sup>		Low N <sup>a</sup>		Epi <sup>a</sup>		Apo <sup>a</sup>	
			GacS	SalA	GacS	SalA	GacS	SalA	GacS	SalA	GacS	SalA	GacS	SalA	GacS	SalA
Psyr_2580	<i>acsS</i>	Achromobactin regulation	1.27	1.18	1.26	-1.13	<b>2.83</b>	-1.56	-1.74	1.53	-1.01	-1.03	-1.15	1.00	1.33	1.37
Psyr_2581		Achromobactin regulation	1.54	1.18	1.14	-1.07	1.65	-1.23	-1.37	-1.04	1.01	1.01	-1.00	-1.19	1.10	1.25
Psyr_2582		Achromobactin transport	2.33	<b>7.09</b>	1.63	4.29	1.78	4.80	-1.39	-1.36	-1.32	2.14	1.94	2.01	1.69	1.45
Psyr_2583	<i>acsF</i>	Achromobactin synthesis	1.98	<b>8.50</b>	1.91	<b>9.04</b>	<b>5.42</b>	3.69	-1.74	1.80	-1.21	<b>4.44</b>	3.51	3.08	4.11	3.62
Psyr_2584	<i>acsD</i>	Achromobactin transport	2.27	4.46	1.63	4.38	1.91	2.68	-1.83	1.05	1.44	2.64	3.27	1.90	3.86	2.56
Psyr_2585	<i>acsE</i>	Achromobactin transport	1.95	4.15	1.59	3.58	1.33	3.34	-2.56	-1.67	1.02	2.22	2.70	2.15	5.24	3.22
Psyr_2586	<i>yhcA</i>	Achromobactin synthesis	1.58	2.37	1.17	1.62	-1.18	1.69	-1.46	-1.36	1.33	1.32	1.50	1.05	1.67	1.57
Psyr_2587	<i>acsC</i>	Achromobactin synthesis	2.34	<b>5.92</b>	1.58	<b>7.23</b>	-1.83	<b>4.40</b>	-2.10	-1.89	1.30	2.48	2.73	1.99	3.73	2.45
Psyr_2588	<i>acsB</i>	Achromobactin synthesis	1.75	<b>3.89</b>	1.22	<b>3.92</b>	-1.03	<b>4.46</b>	-1.72	-2.12	1.09	1.64	2.36	1.58	2.95	2.12
Psyr_2589	<i>acsA</i>	Achromobactin synthesis	2.31	<b>7.00</b>	1.73	<b>8.02</b>	1.03	<b>6.29</b>	-2.28	-2.16	-1.01	<b>3.68</b>	3.33	2.61	3.53	2.40
Psyr_2590	<i>cbrA</i>	Achromobactin transport	1.13	1.48	1.56	1.76	1.28	<b>2.01</b>	-1.45	-1.67	1.38	1.08	1.24	-1.10	1.29	-1.01
Psyr_2591	<i>cbrB</i>	Achromobactin transport	1.81	1.75	1.69	1.65	-1.11	1.75	-1.05	-1.07	1.12	-1.36	1.76	1.07	1.44	2.11

Table 11. Continued.

ID	Gene	Function	Basal <sup>a</sup>		NaCl <sup>a</sup>		H <sub>2</sub> O <sub>2</sub> <sup>a</sup>		Low Fe <sup>a</sup>		Low N <sup>a</sup>		Epi <sup>a</sup>		Apo <sup>a</sup>	
			GacS	SalA	GacS	SalA	GacS	SalA	GacS	SalA	GacS	SalA	GacS	SalA	GacS	SalA
Psyr_2592	<i>cbrC</i>	Achromobactin transport	1.70	1.60	1.72	1.70	-1.21	2.06	-1.00	-1.01	1.14	-1.04	1.71	-1.06	-1.00	1.60
Psyr_2593	<i>cbrD</i>	Achromobactin transport	1.47	1.52	1.29	1.40	1.03	1.92	-1.12	1.02	1.22	-1.03	1.06	1.00	1.26	1.22
Psyr_1943	<i>pvdS</i>	Pyoverdine regulation	-1.08	-1.12	1.27	-1.13	<b>4.78</b>	-2.73	-1.57	-2.46	-1.46	-1.08	-1.90	-2.08	1.24	-1.48
Psyr_1943	<i>pvdS</i>	Pyoverdine regulation	-1.08	-1.12	1.27	-1.13	<b>4.78</b>	-2.73	-1.57	-2.46	-1.46	-1.08	-1.90	-2.08	1.24	-1.48
Psyr_1944	<i>pvdG</i>	Pyoverdine synthesis	1.29	1.37	2.35	1.63	4.05	-2.15	-7.39	<b>-27.25</b>	1.14	1.24	-1.24	-1.63	1.70	1.16
Psyr_1945	<i>pvdL</i>	Pyoverdine synthesis	1.43	1.46	2.50	2.33	1.54	-1.11	-8.78	<b>-16.69</b>	1.26	1.04	1.05	-1.23	1.19	1.31
Psyr_1946	<i>pvdH</i>	Pyoverdine synthesis	1.66	2.19	1.79	1.68	3.66	-1.69	-6.69	<b>-28.99</b>	1.43	1.24	-1.10	-1.76	1.73	1.37
Psyr_1947		Pyoverdine synthesis	-1.11	1.52	1.26	1.77	3.00	-1.67	-4.32	<b>-7.56</b>	-1.20	-1.29	-1.34	-1.60	-1.12	-1.17
Psyr_1956		Pyoverdine regulation	1.71	3.54	1.97	2.73	5.11	-2.58	-5.97	<b>-33.11</b>	-1.27	1.57	-1.77	-2.76	2.14	1.31
Psyr_1957	<i>pvdI</i>	Pyoverdine synthesis	1.75	1.73	2.76	2.24	2.96	-1.19	-4.81	<b>-12.05</b>	1.25	1.25	-1.09	-1.70	1.48	1.37
Psyr_1958	<i>pvdJ</i>	Pyoverdine synthesis	2.22	1.87	2.47	1.99	-1.05	-1.18	-6.35	<b>-11.66</b>	1.23	1.07	1.13	-1.28	1.15	1.29
Psyr_1959	<i>pvdK</i>	Pyoverdine synthesis	2.81	2.83	2.02	2.28	1.76	-1.13	-5.31	<b>-18.59</b>	1.36	1.41	-1.43	-1.83	1.29	1.41
Psyr_1960	<i>pvdD</i>	Pyoverdine synthesis	2.89	2.48	1.61	2.24	1.14	-1.05	-6.36	<b>-11.34</b>	1.34	1.10	1.02	-1.20	1.00	1.13
Psyr_1963	<i>pvdE</i>	Pyoverdine synthesis	1.55	1.46	2.47	1.73	-1.10	1.16	-3.79	-7.21	1.41	1.25	1.36	-1.16	1.37	1.57
Psyr_1964	<i>pvdO</i>	Pyoverdine synthesis	1.89	3.13	2.53	3.04	1.70	1.13	-3.84	<b>-18.76</b>	-1.09	1.58	-1.26	-1.72	1.95	1.88
Psyr_1965	<i>pvdN</i>	Pyoverdine synthesis	1.46	1.66	2.76	2.63	2.17	-1.11	-4.16	<b>-14.25</b>	1.22	1.30	1.05	-1.48	1.47	1.56
Psyr_1966	<i>pvdM</i>	Pyoverdine synthesis	1.56	1.64	2.61	2.19	2.95	-1.60	-5.17	<b>-19.38</b>	1.01	1.44	-1.38	-1.56	1.26	1.35
Psyr_1967	<i>pvdO</i>	Pyoverdine synthesis	1.40	1.32	2.85	2.07	2.68	-1.28	-4.00	<b>-11.51</b>	-1.01	1.14	-1.28	-1.53	1.85	2.10
Psyr_1968	<i>opmQ</i>	Pyoverdine efflux	1.57	1.29	2.08	1.35	1.59	1.11	-2.28	-2.79	1.31	1.14	-1.00	-1.25	-1.02	1.13
Psyr_1969	<i>pvdT</i>	Pyoverdine efflux	1.49	1.31	2.99	1.76	1.86	-1.10	-2.93	<b>-7.71</b>	-1.14	1.01	-1.26	-1.48	1.24	1.85
Psyr_1970	<i>pvdR</i>	Pyoverdine efflux	1.68	1.56	3.67	2.02	2.78	-1.65	-3.49	-6.01	1.74	1.18	1.06	-1.57	1.23	1.42

<sup>a</sup> Values are the same as in Table 3.



Table 12. Extracytoplasmic function (ECF) sigma factor genes and antioxidant enzyme genes showing differential expression in  $\Delta gacS$  and  $\Delta salA$  mutants.

ID	Gene	Function	Basal <sup>a</sup>		NaCl <sup>a</sup>		H2O2 <sup>a</sup>		Low Fe <sup>a</sup>		Low N <sup>a</sup>		Epi <sup>a</sup>		Apo <sup>a</sup>	
			GacS	SalA	GacS	SalA	GacS	SalA	GacS	SalA	GacS	SalA	GacS	SalA	GacS	SalA
Extracytoplasmic function (ECF) sigma factor genes																
Psyr_1040	<i>fecI</i>	ECF Sigma factor	1.84	1.08	1.38	1.11	<b>6.41</b>	-1.22	-1.25	-3.32	1.32	1.17	1.01	-1.16	1.15	1.09
Psyr_4731		ECF Sigma factor	1.38	1.22	1.37	1.02	<b>4.18</b>	-1.15	-1.55	-1.92	1.10	1.12	-1.23	-1.47	1.05	-1.14
Psyr_1943	<i>pvdS</i>	ECF Sigma factor	-1.08	-1.12	1.27	-1.13	<b>4.78</b>	-2.73	-1.57	-2.46	-1.46	-1.08	-1.90	-2.08	1.24	-1.48
Psyr_2580	<i>acsS</i>	ECF Sigma factor	1.27	1.18	1.26	-1.13	<b>2.83</b>	-1.56	-1.74	1.53	-1.01	-1.03	-1.15	1.00	1.33	1.37
Antioxidant enzyme genes																
Psyr_2975	<i>ahpC</i>	Alkyl hydroperoxide reductase subunit C	1.37	1.22	1.35	1.50	<b>2.13</b>	-1.10	-1.58	1.28	<b>1.97</b>	1.50	1.60	1.30	-1.53	-2.44
Psyr_2974	<i>ahpF</i>	Alkyl hydroperoxide reductase subunit F	-1.01	1.00	-1.21	1.04	<b>8.97</b>	-1.44	1.09	2.05	2.43	-1.00	1.52	1.58	-1.46	-1.91
Psyr_4522	<i>katA</i>	Catalase	1.08	1.06	1.27	1.00	<b>5.01</b>	-1.17	1.24	1.28	-1.22	-1.02	1.60	1.45	1.33	1.52
Psyr_3353	<i>katB</i>	Catalase	1.61	1.32	1.26	-1.15	<b>4.05</b>	-1.77	-1.02	1.72	1.24	1.48	1.58	1.28	-1.29	-2.52
Psyr_4208	<i>katG</i>	Peroxidase	<b>-3.01</b>	-2.97	-5.70	<b>-4.40</b>	<b>2.21</b>	-1.88	-3.26	-1.03	<b>-2.63</b>	<b>-3.39</b>	-2.24	<b>-2.69</b>	-5.38	-10.10
Psyr_3627	<i>ohr</i>	Organic hydroperoxide resistance protein	2.11	1.46	2.06	2.00	<b>4.37</b>	1.04	2.59	4.10	<b>5.69</b>	1.53	1.97	-1.19	1.33	1.58
Psyr_4152	<i>sodA</i>	Superoxide dismutase	1.19	2.71	2.10	3.35	<b>8.45</b>	-3.49	-1.76	-3.95	-1.59	2.08	1.47	1.33	1.79	2.10
Psyr_1016	<i>trxB</i>	Thioredoxin reductase	1.31	1.20	1.16	1.31	<b>1.98</b>	1.33	1.19	2.83	<b>3.65</b>	1.55	1.10	1.01	-1.48	-2.14
Psyr_3369		Peroxidase	2.28	1.58	1.43	2.23	<b>5.67</b>	-1.44	-1.64	-1.53	1.27	1.47	1.35	-1.02	1.13	1.32
Psyr_4877		Peroxidase	1.10	1.08	-1.18	1.52	<b>2.31</b>	-1.21	-1.24	<b>7.45</b>	1.05	<b>7.18</b>	-1.16	-1.10	1.15	1.79

<sup>a</sup> Values are the same as in Table 3.

Table 13. Selected sulfur metabolism and transport genes showing differential expression in  $\Delta gacS$  and  $\Delta salA$  mutants.

ID	Gene	Function	Basal <sup>a</sup>		NaCl <sup>a</sup>		H <sub>2</sub> O <sub>2</sub> <sup>a</sup>		Low Fe <sup>a</sup>		Low N <sup>a</sup>		Epi <sup>a</sup>		Apo <sup>a</sup>	
			GacS	SalA	GacS	SalA	GacS	SalA	GacS	SalA	GacS	SalA	GacS	SalA	GacS	SalA
Psyr_0081	<i>cysA</i>	Sulfate transport	<b>5.45</b>	<b>2.96</b>	<b>3.56</b>	2.12	<b>3.21</b>	1.00	1.11	<b>6.75</b>	1.36	<b>3.55</b>	1.22	1.19	1.53	1.39
Psyr_0082	<i>cysW1</i>	Sulfate transport	<b>6.45</b>	3.30	<b>4.21</b>	2.37	2.52	1.21	1.23	<b>4.93</b>	1.39	2.27	1.43	1.04	1.47	1.36
Psyr_0083	<i>cysW2</i>	Sulfate transport	<b>5.84</b>	<b>3.44</b>	<b>4.32</b>	2.62	2.10	-1.14	1.17	4.46	1.45	<b>6.44</b>	1.09	1.15	2.71	2.38
Psyr_0084	<i>cysP</i>	Sulfate transport	<b>7.61</b>	<b>3.63</b>	<b>3.45</b>	2.41	<b>2.88</b>	-1.46	-1.89	<b>17.48</b>	1.11	<b>46.32</b>	1.12	1.24	4.99	3.95
Psyr_0337	<i>tauD-1</i>	Sulfur metabolism and transport	<b>6.60</b>	3.24	<b>3.38</b>	2.64	2.88	-1.97	-2.00	<b>18.99</b>	-1.20	<b>31.72</b>	1.24	1.68	1.96	2.61
Psyr_0352		Sulfonate metabolism	2.29	1.17	1.14	-1.29	1.18	-1.46	-1.22	<b>19.44</b>	-1.08	<b>15.93</b>	1.71	1.70	1.45	2.37
Psyr_2280		Sulfonate metabolism	1.32	1.15	1.01	1.19	1.38	1.05	1.11	<b>179.91</b>	1.25	<b>155.48</b>	<b>5.80</b>	<b>6.39</b>	11.72	9.41
Psyr_2514		Sulfonate transport	1.33	1.06	-1.02	1.11	1.01	-1.01	1.47	<b>27.60</b>	1.23	<b>3.34</b>	1.67	1.89	2.23	2.56
Psyr_2515		Sulfonate transport	1.50	1.17	1.03	1.04	-1.07	1.07	1.27	<b>13.09</b>	-1.25	2.87	1.50	1.35	2.88	4.29
Psyr_2516		Sulfonate transport	1.65	1.39	1.10	1.51	-1.07	1.05	1.49	<b>52.96</b>	1.03	<b>7.42</b>	2.16	1.60	2.51	4.20
Psyr_3220		Sulfur relay system	3.42	1.68	2.17	1.85	2.63	-1.38	-2.39	<b>108.29</b>	1.21	<b>50.01</b>	1.59	1.55	1.94	1.91
Psyr_3233	<i>ssuE</i>	Sulfonate metabolism	1.22	1.13	1.04	1.15	1.16	-1.09	-1.40	<b>34.84</b>	1.54	<b>19.34</b>	1.75	1.77	1.97	1.49
Psyr_3247	<i>msuD</i>	Sulfonate metabolism	<b>8.85</b>	<b>4.33</b>	2.59	2.05	<b>3.45</b>	-2.78	-2.98	<b>65.94</b>	1.34	<b>100.07</b>	1.42	1.61	4.02	2.65
Psyr_3248	<i>sfhR</i>	Sulfonate metabolism regulation	<b>7.60</b>	3.45	2.06	1.85	2.95	-2.65	-3.14	<b>38.80</b>	1.01	<b>75.29</b>	1.15	1.24	3.68	3.86
Psyr_3597		Sulfonate transport	1.32	1.17	1.07	-1.00	-1.01	-1.02	1.06	<b>4.95</b>	1.27	<b>2.29</b>	1.26	1.05	1.10	1.37
Psyr_3598		Sulfonate transport	1.45	1.11	1.01	-1.13	-1.20	-1.28	-1.06	<b>10.24</b>	-1.32	<b>3.19</b>	1.16	1.26	1.56	2.68
Psyr_3599		Sulfonate transport	1.66	1.06	-1.40	-1.12	<b>3.25</b>	-1.61	-2.93	<b>48.23</b>	-1.14	<b>30.28</b>	1.48	1.39	1.83	2.01
Psyr_3601		Sulfur metabolism and transport	1.85	1.21	1.10	1.21	1.28	-1.20	1.06	<b>22.36</b>	1.04	<b>15.62</b>	1.90	1.51	1.66	2.14
Psyr_3603		Sulfonate transport	1.92	1.36	1.13	1.28	<b>3.37</b>	-1.54	-1.32	<b>16.37</b>	1.16	<b>9.63</b>	1.72	2.11	2.07	3.29
Psyr_4873	<i>ssuF</i>	Sulfonate transport	3.44	1.79	2.49	1.67	3.41	-2.15	-1.61	10.20	-1.02	<b>14.72</b>	1.25	1.15	1.39	1.86
Psyr_4874	<i>ssuB</i>	Sulfonate transport	<b>4.68</b>	2.23	2.85	1.85	2.14	-1.74	-1.45	<b>20.11</b>	1.15	<b>9.52</b>	1.43	1.21	1.26	1.23
Psyr_4875	<i>ssuC</i>	Sulfonate transport	<b>6.02</b>	2.46	2.92	1.92	1.73	-1.88	-1.21	12.35	-1.09	<b>10.68</b>	1.25	1.56	2.63	3.27
Psyr_4876	<i>ssuA</i>	Sulfonate transport	<b>5.47</b>	2.43	3.09	2.31	1.49	-1.91	-1.64	<b>20.90</b>	1.22	<b>19.84</b>	1.17	1.25	1.61	2.04

Table 13. Continued.

ID	Gene	Function	Basal <sup>a</sup>		NaCl <sup>a</sup>		H <sub>2</sub> O <sub>2</sub> <sup>a</sup>		Low Fe <sup>a</sup>		Low N <sup>a</sup>		Epi <sup>a</sup>		Apo <sup>a</sup>	
			GacS	SalA	GacS	SalA	GacS	SalA	GacS	SalA	GacS	SalA	GacS	SalA	GacS	SalA
Psyr_0349	<i>metI-1</i>	Methionine transport	1.72	-1.18	1.10	-1.32	-1.08	-1.42	1.11	<b>17.23</b>	-1.09	<b>5.32</b>	1.82	1.78	1.90	2.71
Psyr_0350	<i>metN-1</i>	Methionine transport	1.69	1.02	1.16	1.02	1.12	-1.20	1.25	<b>17.06</b>	1.23	<b>6.46</b>	1.88	1.64	1.37	2.35
Psyr_0351	<i>metQ-1</i>	Methionine transport	1.64	-1.11	-1.10	-1.32	2.29	-1.67	1.07	<b>16.40</b>	1.21	<b>14.52</b>	1.63	2.07	1.84	2.79
Psyr_2962		Cysteine transport	<b>9.50</b>	<b>5.01</b>	<b>4.30</b>	3.05	1.59	-1.21	-1.00	<b>33.23</b>	1.06	<b>32.10</b>	1.91	2.34	4.15	4.82
Psyr_2963		Cysteine transport	<b>3.03</b>	1.68	<b>3.87</b>	2.12	1.14	-1.13	1.26	3.31	-1.50	1.86	1.55	1.70	1.88	2.58
Psyr_2964		Cysteine transport	<b>4.05</b>	2.50	<b>4.74</b>	2.84	1.30	1.14	1.27	2.31	-1.35	1.84	1.81	1.82	1.53	2.63
Psyr_2965		Cysteine transport	<b>4.28</b>	2.11	<b>4.41</b>	2.33	1.46	-1.19	-1.02	3.65	-1.26	<b>3.81</b>	1.25	1.39	1.27	1.59
Psyr_2874		Ribose transport	1.15	1.01	1.13	1.02	1.06	-1.16	1.33	<b>31.65</b>	-1.11	<b>5.93</b>	2.68	2.86	2.70	4.11
Psyr_2875		Ribose transport	1.62	1.27	1.10	-1.07	1.03	-1.18	1.55	<b>60.32</b>	1.03	<b>9.87</b>	<b>3.82</b>	3.39	3.89	5.10
Psyr_2876		Ribose transport	1.34	1.13	-1.00	-1.02	1.08	1.10	1.32	<b>65.59</b>	1.39	<b>18.49</b>	2.77	2.86	2.70	2.83
Psyr_2877		Ribose transport	1.81	1.20	1.10	1.07	1.03	-1.07	1.65	<b>91.88</b>	1.23	<b>14.50</b>	<b>2.65</b>	2.07	5.59	3.50

<sup>a</sup> Values are the same as in Table 3.

Table 14. Transcriptome profiles of  $\Delta retS$  mutant (q-value <0.01). Genes that showed a decreased expression in any conditions were excluded.

	Basal	NaCl	H <sub>2</sub> O <sub>2</sub>	Low Fe	Low N	Epi	Apo	Total unique genes
# of differentially-expressed (DE) genes in $\Delta retS$	33	12	12	0	1	14	0	43
# of DE genes in $\Delta retS$ with increased transcripts <sup>a</sup>	33	11	11	0	1	13	0	41
# of DE genes in $\Delta retS$ also differentially expressed in $\Delta gacS$	13	6	10	0	1	8	0	25
# of DE genes in $\Delta retS$ with decreased transcripts in $\Delta gacS$	13	6	10	0	1	8	0	25

Table 15. Selected phytotoxin, secondary metabolism, and organic and fatty acid metabolism genes showing reciprocal regulation between RetS and GacS.

ID	Gene	Function	Basal <sup>a</sup>		NaCl <sup>a</sup>		H <sub>2</sub> O <sub>2</sub> <sup>a</sup>		Low Fe <sup>a</sup>		Low N <sup>a</sup>		Epi <sup>a</sup>		Apo <sup>a</sup>	
			RetS	GacS	RetS	GacS	RetS	GacS	RetS	GacS	RetS	GacS	RetS	GacS	RetS	GacS
Phytotoxin-related genes																
Psyr_2602	<i>syrG</i>	Syringomycin regulation	5.99	-3.42	4.33	-3.55	4.27	-3.00	2.95	-1.25	2.48	-3.73	1.15	-10.22	-2.43	-14.88
Psyr_2603		Secretion/Efflux/Export	4.23	-1.37	2.39	-1.71	2.24	-1.82	1.58	-1.02	1.14	-1.72	-1.14	-2.56	-1.62	-3.77
Psyr_2607	<i>syrF</i>	Syringomycin regulation	5.26	-2.43	2.96	-2.77	3.48	-2.06	2.70	-1.35	1.16	-3.04	-1.30	-8.47	-2.58	-15.24
Psyr_2610	<i>syrB2</i>	Syringomycin synthesis	3.76	-2.00	1.54	-1.51	2.37	-1.98	3.52	-1.69	-1.04	-1.63	-1.24	-13.46	-2.46	-34.72
Psyr_2611	<i>syrB1</i>	Syringomycin synthesis	4.18	-1.47	1.73	-1.33	2.53	-1.51	4.70	-1.32	1.13	-1.22	-1.50	-12.48	-2.94	-34.48
Psyr_2612	<i>syrP</i>	Syringomycin synthesis	7.07	-1.54	2.86	-1.67	4.17	-1.64	4.25	-2.24	1.16	-1.05	-1.45	-7.90	-3.16	-47.17
Psyr_2613	<i>syrD</i>	Syringomycin synthesis	5.47	-1.55	2.14	-1.59	2.97	-1.59	2.66	-1.25	1.07	-1.56	-1.30	-7.58	-2.13	-27.93
Secondary metabolism genes																
Psyr_4313		Secondary metabolism	2.07	1.04	1.35	-1.01	1.54	-1.07	-1.12	1.84	1.17	-1.98	-2.08	-4.50	-2.26	-10.38
Psyr_4314		Secondary metabolism	3.16	-1.35	2.13	-1.47	2.65	-1.09	-1.15	1.94	-1.08	-2.31	-1.57	-4.80	-2.25	-17.61
Psyr_4316		Hypothetical	7.54	-3.59	5.25	-2.72	7.99	-3.50	1.14	1.23	1.17	-4.32	-2.17	-41.67	-2.05	-119.05
Psyr_4317			6.78	-2.33	5.21	-2.23	5.76	-3.18	1.24	1.62	1.11	-5.47	-2.26	-30.12	-2.07	-64.94
Organic and fatty acid metabolism genes																
Psyr_0748		Organic acid metabolism and transport	3.68	-1.09	2.02	-1.28	2.25	-1.71	1.67	1.22	-1.17	-2.67	-1.10	-4.70	-2.09	-11.45
Psyr_0749	<i>fadD</i>	Fatty acid metabolism	5.40	-7.08	3.02	-7.45	3.25	-4.69	3.39	-2.71	1.84	-4.93	-1.35	-45.05	-1.65	-57.14
Psyr_0750		Hypothetical	6.99	-18.35	3.90	-14.37	3.85	-13.59	4.28	-4.20	1.96	-12.33	-1.33	-98.04	-1.58	-82.64

<sup>a</sup> Values are the same as in Table 3.

Table 16. Selected Psl polysaccharide synthesis, chemosensing and chemotaxis genes showing differential expression in  $\Delta rpoS$  and  $\Delta gacS$  mutants.

ID	Gene	Function	Basal <sup>a</sup>		NaCl <sup>a</sup>		H <sub>2</sub> O <sub>2</sub> <sup>a</sup>		Low Fe <sup>a</sup>		Low N <sup>a</sup>		Epi <sup>a</sup>		Apo <sup>a</sup>	
			RpoS	GacS	RpoS	GacS	RpoS	GacS	RpoS	GacS	RpoS	GacS	RpoS	GacS	RpoS	GacS
Psyr_3301	<i>pslA</i>	Putative Psl synthase	-1.15	-1.56	-1.32	<b>-2.79</b>	-1.26	<b>-3.45</b>	-1.96	-3.08	<b>-7.18</b>	<b>-6.12</b>	<b>-3.57</b>	<b>-3.29</b>	-2.43	-3.60
Psyr_3302	<i>pslB</i>	Putative Psl synthase	-1.22	-1.78	-1.14	<b>-2.75</b>	-1.21	<b>-2.44</b>	-1.89	-3.62	<b>-7.57</b>	<b>-8.16</b>	<b>-2.94</b>	<b>-4.18</b>	-2.81	<b>-6.16</b>
Psyr_3303	<i>pslD</i>	Putative Psl synthase	-1.34	-2.76	-1.23	<b>-2.93</b>	-1.34	<b>-4.04</b>	-1.83	-5.31	<b>-8.45</b>	<b>-12.38</b>	<b>-3.53</b>	<b>-5.26</b>	-3.76	-5.46
Psyr_3305	<i>pslF</i>	Putative Psl synthase	-1.22	-2.24	-1.13	-2.19	-1.55	<b>-3.69</b>	-2.15	-3.31	<b>-5.13</b>	<b>-5.45</b>	-3.30	-2.15	-1.65	-2.91
Psyr_3306	<i>pslG</i>	Putative Psl synthase	-1.44	-2.11	-1.08	-2.31	-1.47	<b>-4.86</b>	-1.80	-3.58	<b>-5.40</b>	<b>-7.94</b>	<b>-3.36</b>	<b>-4.77</b>	-2.45	-4.32
Psyr_3307	<i>pslH-1</i>	Putative Psl synthase	-1.35	-2.34	-1.23	-2.32	-1.36	<b>-6.23</b>	-2.04	-3.88	<b>-6.46</b>	<b>-7.62</b>	-4.18	-3.46	-2.21	-5.04
Psyr_3308	<i>pslI</i>	Putative Psl synthase	-1.33	<b>-3.84</b>	-1.00	-3.28	-1.20	<b>-9.28</b>	-1.86	<b>-8.06</b>	<b>-8.83</b>	<b>-9.09</b>	<b>-4.25</b>	<b>-3.64</b>	-3.44	<b>-8.33</b>
Psyr_3309	<i>pslJ</i>	Putative Psl synthase	-1.25	<b>-4.04</b>	-1.27	<b>-4.05</b>	-1.35	<b>-12.71</b>	-1.65	-5.09	<b>-3.53</b>	<b>-6.66</b>	<b>-3.23</b>	<b>-3.87</b>	-2.09	-3.70
Psyr_3310		Putative Psl synthase	-1.26	<b>-2.64</b>	-1.25	<b>-2.88</b>	-1.35	<b>-5.91</b>	-1.58	-2.73	<b>-3.86</b>	<b>-6.54</b>	<b>-2.49</b>	<b>-4.36</b>	-3.49	-3.30
Psyr_0783	<i>cheR-1</i>	Chemosensing & chemotaxis	-1.29	<b>-3.06</b>	-1.88	<b>-5.53</b>	-1.33	<b>-2.87</b>	<b>-2.92</b>	-3.73	<b>-5.56</b>	-6.84	<b>-3.90</b>	<b>-4.34</b>	-2.91	<b>-5.48</b>
Psyr_0784	<i>cheW-1</i>	Chemosensing & chemotaxis	-1.24	-1.50	-1.41	<b>-3.77</b>	-1.67	<b>-3.22</b>	<b>-4.08</b>	-3.56	<b>-11.20</b>	-5.78	<b>-4.27</b>	-2.38	-2.34	<b>-6.08</b>
Psyr_0785		Chemosensing & chemotaxis	-2.04	<b>-3.19</b>	-2.36	<b>-9.33</b>	-1.71	<b>-5.54</b>	<b>-3.40</b>	-5.18	<b>-11.99</b>	-18.66	<b>-4.72</b>	<b>-8.76</b>	-6.37	-9.74
Psyr_0786	<i>cheA1</i>	Chemosensing & chemotaxis	-1.38	-2.39	-1.93	<b>-6.33</b>	-1.72	<b>-3.60</b>	<b>-4.28</b>	<b>-5.83</b>	<b>-9.87</b>	-9.66	<b>-4.98</b>	<b>-4.87</b>	-2.90	<b>-7.17</b>
Psyr_0788	<i>cheY1</i>	Chemosensing & chemotaxis	-1.50	-4.64	-2.96	<b>-12.45</b>	-1.53	<b>-4.16</b>	-3.69	-9.13	<b>-15.46</b>	-16.47	<b>-6.10</b>	<b>-15.41</b>	-12.25	<b>-20.88</b>
Psyr_0789		Chemosensing & chemotaxis	-1.50	-2.81	-2.10	<b>-4.85</b>	-1.24	<b>-4.31</b>	-2.47	-6.58	<b>-11.30</b>	-15.50	<b>-4.42</b>	<b>-9.71</b>	-4.13	-6.54
Psyr_1303	<i>wspA</i>	Chemosensing & chemotaxis	1.07	-1.33	-1.22	-1.83	-1.33	-1.48	-1.80	-2.91	<b>-5.41</b>	<b>-3.19</b>	<b>-3.68</b>	<b>-3.39</b>	-2.53	-2.86
Psyr_1304	<i>wspB</i>	Chemosensing & chemotaxis	-1.10	-1.32	-1.03	-1.24	-1.02	-1.69	-1.62	-2.35	<b>-3.55</b>	<b>-2.21</b>	<b>-3.18</b>	<b>-2.24</b>	-1.63	-1.77
Psyr_1305	<i>wspC</i>	Chemosensing & chemotaxis	1.11	-1.40	-1.02	-1.12	-1.19	-1.86	-1.56	-2.16	-2.84	<b>-2.32</b>	-2.01	<b>-2.28</b>	-1.39	-2.12

<sup>a</sup> Values are the same as in Table 3.

Table 17. Selected T3SS genes showing differential expression in  $\Delta hrpL$  and  $\Delta rpoN$  mutants.

ID	Gene	Function	Basal <sup>a</sup>		NaCl <sup>a</sup>		H <sub>2</sub> O <sub>2</sub> <sup>a</sup>		Low Fe <sup>a</sup>		Low N <sup>a</sup>		Epi <sup>a</sup>		Apo <sup>a</sup>	
			HrpL	RpoN	HrpL	RpoN	HrpL	RpoN	HrpL	RpoN	HrpL	RpoN	HrpL	RpoN	HrpL	RpoN
Psyr_1217	<i>hrpL</i>	T3SS regulation	-1.68	1.01	-1.57	-1.17	-1.37	1.11	-1.23	1.22	-4.29	<b>-3.94</b>	-2.05	-1.23	-5.14	-3.72
Psyr_1218	<i>hrpK1</i>	Type III pilus	<b>95.08</b>	-1.00	<b>160.76</b>	-1.49	<b>176.53</b>	1.04	<b>165.87</b>	1.23	<b>21.98</b>	<b>-13.12</b>	<b>39.05</b>	-1.50	41.43	-3.81
Psyr_1219	<i>avrB3</i>	Type III secreted proteins	<b>73.31</b>	-1.51	<b>142.63</b>	<b>-1.73</b>	<b>112.00</b>	-1.57	<b>136.46</b>	1.34	<b>27.05</b>	<b>-4.61</b>	<b>44.15</b>	-1.65	47.41	-5.89
Psyr_1220	<i>hopX1</i>	Type III secreted proteins	<b>29.83</b>	-1.19	<b>97.10</b>	-1.26	<b>46.72</b>	-1.00	<b>68.38</b>	<b>1.48</b>	<b>19.76</b>	<b>-2.42</b>	<b>29.76</b>	1.02	31.63	-2.62
Psyr_1183	<i>hopAAl</i>	Type III secreted proteins	-1.32	1.14	-1.30	-1.26	-1.07	1.02	-1.32	1.06	<b>-9.71</b>	<b>-10.78</b>	-1.96	-1.37	-2.85	-2.88
Psyr_1184	<i>hrpW1</i>	Type III secreted proteins	-1.14	1.04	-1.20	<b>-1.50</b>	-1.19	1.00	-1.44	-1.43	<b>-14.16</b>	<b>-14.88</b>	-2.14	-2.19	-4.69	-4.60
Psyr_1188	<i>avrE1</i>	Type III secreted proteins	-1.12	1.02	1.06	-1.33	1.03	1.10	-1.30	1.03	<b>-9.83</b>	<b>-10.33</b>	-1.14	1.01	-3.41	-3.85
Psyr_1192	<i>hrpA2</i>	Type III pilus	-2.38	-1.07	-1.33	-1.41	-1.56	1.10	<b>-2.85</b>	-1.19	<b>-26.95</b>	<b>-19.76</b>	<b>-4.47</b>	<b>-2.55</b>	-3.55	-1.99
Psyr_1193	<i>hrpZ1</i>	Type III pilus	-2.47	-1.03	-1.02	1.06	-2.31	-1.04	<b>-3.15</b>	<b>-1.98</b>	<b>-24.69</b>	<b>-14.29</b>	<b>-7.81</b>	<b>-6.59</b>	-3.69	-3.77
Psyr_1194	<i>hrpB</i>	Type III pilus	-1.53	1.15	-1.18	-1.06	-1.27	1.23	-1.56	-1.04	<b>-11.24</b>	<b>-6.96</b>	-2.74	-2.02	-2.23	-1.72
Psyr_1195	<i>hrcJ</i>	Type III pilus	-1.02	<b>1.40</b>	-1.07	<b>-1.47</b>	-1.20	-1.00	-1.40	-1.04	<b>-5.62</b>	<b>-3.94</b>	-1.62	-1.28	-1.84	-1.45
Psyr_1199	<i>hrpG</i>	Type III pilus	-1.21	-1.25	-1.19	-1.30	-1.06	1.07	-1.06	-1.02	<b>-7.78</b>	<b>-8.90</b>	-1.48	1.06	-1.34	1.00
Psyr_1200	<i>hrcC</i>	Type III pilus	-1.12	-1.01	-1.05	<b>-1.70</b>	-1.17	-1.04	-1.08	-1.01	<b>-3.92</b>	<b>-4.81</b>	-1.69	-1.07	-2.08	-2.25
Psyr_4326	<i>hopI1</i>	Type III secreted proteins	-1.04	1.05	1.02	-1.27	-1.10	1.06	1.12	1.26	<b>-5.03</b>	<b>-3.88</b>	-1.12	1.09	-2.55	-2.46
Psyr_4919	<i>avrPto1</i>	Type III secreted proteins	-2.27	<b>-3.00</b>	-1.29	<b>-5.33</b>	-1.79	-1.47	-2.41	-1.43	<b>-17.67</b>	<b>-21.41</b>	<b>-6.22</b>	<b>-8.71</b>	-3.42	-9.62

<sup>a</sup> Values are the same as in Table 3.

Table 18. Selected stress tolerance genes showing differential expression in  $\Delta algU$  and  $\Delta rpoN$  mutants.

ID	Gene	Function	Basal <sup>a</sup>		NaCl <sup>a</sup>		H <sub>2</sub> O <sub>2</sub> <sup>a</sup>		Low Fe <sup>a</sup>		Low N <sup>a</sup>		Epi <sup>a</sup>		Apo <sup>a</sup>	
			AlgU	RpoN	AlgU	RpoN	AlgU	RpoN	AlgU	RpoN	AlgU	RpoN	AlgU	RpoN	AlgU	RpoN
Psyr_4147	<i>rpoN</i>	Sigma factor	-1.08	<b>-69.93</b>	1.25	<b>-36.76</b>	1.02	<b>-81.97</b>	1.06	<b>-39.84</b>	-1.09	<b>-39.06</b>	1.41	<b>-7.54</b>	1.54	-6.12
Psyr_3958	<i>algU</i>	ECF sigma factor	<b>-192.31</b>	-1.96	<b>-588.24</b>	<b>-3.25</b>	<b>-188.68</b>	-1.50	<b>-104.17</b>	-1.28	<b>-256.41</b>	-2.36	<b>-88.50</b>	1.55	<b>-166.67</b>	3.00
<i>Alginate-related genes</i>																
Psyr_3955	<i>mucD</i>	AlgU antagonist complex	1.30	<b>1.81</b>	-1.32	-1.15	-1.02	1.73	-1.10	-1.10	1.30	1.37	-1.38	-1.25	2.66	1.72
Psyr_3956	<i>mucB</i>	AlgU antagonist complex	<b>-2.88</b>	<b>-1.86</b>	<b>-15.27</b>	<b>-3.89</b>	<b>-4.24</b>	<b>-2.10</b>	<b>-3.90</b>	<b>-1.70</b>	-2.07	-1.11	<b>-28.57</b>	-1.31	-12.50	1.73
Psyr_3957	<i>mucA</i>	AlgU antagonist	<b>-4.17</b>	-1.54	<b>-22.78</b>	<b>-2.59</b>	<b>-3.67</b>	-1.39	<b>-4.56</b>	-1.62	<b>-8.50</b>	-1.91	<b>-31.35</b>	1.30	<b>-47.62</b>	1.51
Psyr_0263	<i>algB</i>	Alginate regulator	-1.08	-1.21	<b>-1.56</b>	-1.36	-1.14	-1.08	-1.11	-1.38	1.06	-1.20	-1.49	1.01	1.19	1.40
Psyr_0264	<i>kinB</i>	Alginate regulator	1.08	-1.22	<b>-2.10</b>	<b>-2.38</b>	1.10	-1.25	1.09	-1.08	-1.16	-1.32	-1.55	-1.15	-1.06	-1.01
Psyr_1052	<i>algA-2</i>	Alginate synthesis	<b>-11.39</b>	-1.88	<b>-26.53</b>	<b>-4.55</b>	-3.46	1.59	-1.43	-1.01	-2.05	1.19	<b>-9.63</b>	-1.52	<b>-29.24</b>	3.69
Psyr_1053	<i>algF</i>	Alginate synthesis	<b>-15.27</b>	<b>-4.52</b>	<b>-49.75</b>	<b>-11.78</b>	-3.90	-1.26	-1.66	-1.28	-1.58	1.86	<b>-17.79</b>	-1.80	<b>-33.22</b>	2.03
Psyr_1054	<i>algJ</i>	Alginate synthesis	-6.08	<b>-4.21</b>	<b>-53.19</b>	<b>-15.22</b>	-4.40	-1.51	-1.99	-1.51	-1.51	1.24	<b>-8.16</b>	-1.61	-7.08	3.49
Psyr_1055	<i>algI</i>	Alginate synthesis	-6.34	<b>-4.77</b>	<b>-74.63</b>	<b>-22.22</b>	-5.35	-1.98	-1.81	-1.36	-1.18	1.60	<b>-26.32</b>	<b>-2.48</b>	<b>-14.39</b>	4.05
Psyr_1056	<i>algL</i>	Alginate synthesis	<b>-7.30</b>	<b>-3.74</b>	<b>-81.30</b>	<b>-13.61</b>	-4.41	-2.00	-2.15	-1.39	-1.28	1.06	<b>-25.51</b>	<b>-2.13</b>	<b>-13.83</b>	3.03
Psyr_1057	<i>algX</i>	Alginate synthesis	-3.94	<b>-3.47</b>	<b>-70.42</b>	<b>-14.49</b>	-5.36	-2.34	-2.54	-1.56	-1.56	-1.12	<b>-25.97</b>	<b>-2.99</b>	-8.36	3.12
Psyr_1058	<i>algG</i>	Alginate synthesis	-3.62	<b>-2.95</b>	<b>-55.25</b>	<b>-15.06</b>	-3.12	-2.03	-1.75	-1.18	-1.18	-1.01	<b>-10.55</b>	<b>-3.52</b>	-6.16	3.39
Psyr_1059	<i>algE</i>	Alginate synthesis	-3.31	<b>-3.01</b>	<b>-71.43</b>	<b>-17.04</b>	-3.34	-1.81	-2.18	-1.76	-1.82	-1.03	<b>-16.39</b>	<b>-3.55</b>	-5.75	4.45
Psyr_1060	<i>algK</i>	Alginate synthesis	-3.26	<b>-3.02</b>	<b>-67.11</b>	<b>-16.31</b>	-2.69	-1.49	-1.52	-1.27	-2.08	-1.23	<b>-13.12</b>	<b>-3.62</b>	-4.23	5.52
Psyr_1061	<i>alg44</i>	Alginate synthesis	-3.44	<b>-3.02</b>	<b>-74.07</b>	<b>-17.12</b>	-3.27	-1.55	-2.68	-1.97	-3.20	-1.37	<b>-28.17</b>	<b>-3.56</b>	-6.97	5.39
Psyr_1062	<i>alg8</i>	Alginate synthesis	-3.43	-2.51	<b>-114.94</b>	<b>-16.89</b>	<b>-4.66</b>	-1.86	-3.79	-2.01	-2.03	-1.14	<b>-30.12</b>	<b>-3.06</b>	<b>-8.50</b>	5.42
Psyr_1063	<i>algD</i>	Alginate synthesis	<b>-11.19</b>	<b>-6.05</b>	<b>-172.41</b>	<b>-13.70</b>	<b>-11.05</b>	-2.90	-7.04	-2.53	<b>-9.86</b>	<b>-3.00</b>	<b>-42.02</b>	<b>-2.14</b>	<b>-30.49</b>	3.98
<i>Compatible solute synthesis genes</i>																
Psyr_2489	<i>glgE</i>	Trehalose synthesis	-1.49	1.37	<b>-40.49</b>	<b>-6.45</b>	-1.51	1.23	-1.81	1.04	<b>-3.21</b>	-1.66	<b>-19.96</b>	<b>-3.77</b>	-17.42	-1.49
Psyr_2490	<i>treS</i>	Trehalose synthesis	-1.16	1.33	<b>-22.27</b>	<b>-6.67</b>	-1.32	1.05	-1.19	1.18	-2.07	-1.04	<b>-14.18</b>	<b>-4.59</b>	-8.93	-1.09



Table 18. Continued.

ID	Gene	Function	Basal <sup>a</sup>		NaCl <sup>a</sup>		H <sub>2</sub> O <sub>2</sub> <sup>a</sup>		Low Fe <sup>a</sup>		Low N <sup>a</sup>		Epi <sup>a</sup>		Apo <sup>a</sup>	
			AlgU	RpoN	AlgU	RpoN	AlgU	RpoN	AlgU	RpoN	AlgU	RpoN	AlgU	RpoN	AlgU	RpoN
Psyr_2491	<i>glgB</i>	Trehalose synthesis	-1.38	1.17	<b>-17.01</b>	<b>-4.62</b>	-1.64	-1.32	-1.15	1.08	-1.20	-1.08	<b>-8.95</b>	<b>-3.96</b>	-8.08	-1.34
Psyr_2992	<i>glgA</i>	Trehalose synthesis	-1.73	1.57	<b>-19.92</b>	<b>-4.91</b>	-1.44	1.21	-1.23	-1.10	-1.12	<b>-2.76</b>	<b>-3.64</b>	-1.70	-4.96	1.54
Psyr_2993	<i>treZ</i>	Trehalose synthesis	-1.42	1.43	<b>-19.34</b>	<b>-4.50</b>	-1.41	1.03	-1.18	-1.13	-1.02	<b>-2.25</b>	<b>-4.18</b>	<b>-2.43</b>	-3.86	2.05
Psyr_2994	<i>malQ</i>	Trehalose synthesis	-1.55	1.13	<b>-22.37</b>	<b>-3.55</b>	-1.73	-1.19	-1.33	-1.10	-1.21	<b>-2.09</b>	<b>-6.06</b>	<b>-2.59</b>	-4.35	1.46
Psyr_2995	<i>treY</i>	Trehalose synthesis	-2.14	1.27	<b>-18.66</b>	<b>-3.98</b>	-1.97	-1.39	-1.29	1.00	-1.40	<b>-2.01</b>	<b>-5.34</b>	<b>-3.48</b>	-3.23	1.82
Psyr_2996		Trehalose synthesis	<b>-2.49</b>	1.06	<b>-20.66</b>	<b>-3.14</b>	-1.76	-1.09	-1.34	1.08	-1.21	<b>-4.99</b>	<b>-5.35</b>	<b>-3.70</b>	-8.28	-1.45
Psyr_2997	<i>treX</i>	Trehalose synthesis	-2.26	-1.53	<b>-37.59</b>	<b>-8.71</b>	<b>-2.82</b>	-1.94	-1.95	-1.79	-1.69	<b>-2.52</b>	<b>-18.59</b>	<b>-5.87</b>	-10.43	-1.51
Psyr_2998		Trehalose synthesis	-1.16	-1.19	<b>-11.71</b>	<b>-7.64</b>	-1.11	-1.12	-1.02	1.01	-1.88	-1.90	<b>-4.18</b>	<b>-2.51</b>	-1.67	1.16
Psyr_2999		Trehalose synthesis	1.13	-1.02	<b>-16.75</b>	<b>-9.26</b>	-1.69	-1.27	-1.19	-1.11	-1.24	-1.39	<b>-4.94</b>	<b>-2.60</b>	-2.68	-1.38
Psyr_3000		Trehalose synthesis	1.03	-1.06	<b>-16.53</b>	<b>-12.05</b>	-1.34	-1.18	-1.10	1.03	-1.31	-1.39	<b>-6.54</b>	<b>-4.89</b>	-3.49	-2.62
Psyr_3001		Trehalose synthesis	-1.01	1.06	<b>-10.18</b>	<b>-5.73</b>	-1.31	-1.05	-1.07	1.17	-1.48	-1.51	<b>-5.58</b>	<b>-4.32</b>	-4.08	-2.05
Psyr_3747	<i>ggnA</i>	NAGGN synthesis	-1.99	-2.09	<b>-222.22</b>	<b>-15.11</b>	-1.88	-1.73	-2.81	-2.09	<b>-5.00</b>	<b>-4.08</b>	<b>-12.55</b>	-1.71	-19.42	1.81
Psyr_3748	<i>ggnB</i>	NAGGN synthesis	-1.46	-1.50	<b>-166.67</b>	<b>-11.70</b>	-1.52	-1.39	-1.64	-1.62	-2.43	-1.98	<b>-7.67</b>	-2.10	-10.48	2.09
Psyr_3749	<i>ggnC</i>	NAGGN synthesis	-1.26	-1.31	<b>-100.00</b>	<b>-7.73</b>	-1.41	-1.38	-1.43	-1.45	<b>-2.91</b>	-2.08	<b>-7.62</b>	-1.80	-13.74	1.28
Psyr_3750	<i>ggnD</i>	NAGGN synthesis	-1.03	1.13	<b>-14.03</b>	<b>-7.59</b>	1.18	-1.04	-1.05	1.44	-1.05	-1.01	-1.65	1.20	-2.89	-1.19
<b>Osmoprotectant transporter genes</b>																
Psyr_4709	<i>cbcX</i>	QAC transport	<b>-2.00</b>	<b>-1.96</b>	<b>-31.35</b>	<b>-11.89</b>	-1.38	-1.09	-1.44	-1.14	-1.12	<b>-9.01</b>	1.04	<b>-2.89</b>	-1.71	-3.47
Psyr_4710	<i>cbcW</i>	QAC transport	-1.19	-1.43	<b>-28.65</b>	<b>-12.09</b>	-1.10	-1.20	-1.20	-1.01	1.37	<b>-3.47</b>	-1.42	<b>-2.50</b>	-2.34	-4.27
Psyr_4711	<i>cbcV</i>	QAC transport	1.14	-1.12	<b>-24.10</b>	<b>-10.91</b>	-1.12	1.14	-1.38	-1.45	-1.09	<b>-5.90</b>	1.11	<b>-2.87</b>	-1.29	-2.81
Psyr_4249	<i>opuCA</i>	QAC transport	-1.43	-1.45	<b>-8.69</b>	<b>-14.99</b>	-1.19	-1.26	-1.31	-1.49	-1.29	-1.28	<b>-3.16</b>	<b>-2.09</b>	-1.88	-1.09
Psyr_4250	<i>opuCB</i>	QAC transport	-1.85	<b>-2.35</b>	<b>-6.27</b>	<b>-9.33</b>	-1.60	-1.46	-1.68	-2.38	-1.53	-1.35	<b>-5.59</b>	<b>-3.80</b>	-1.43	1.10
Psyr_4251	<i>opuCC</i>	QAC transport	-2.12	<b>-2.29</b>	<b>-7.63</b>	<b>-11.74</b>	-1.47	-1.61	-1.86	-1.88	-1.27	-1.24	<b>-4.16</b>	<b>-2.93</b>	-1.81	-1.03
Psyr_4252	<i>opuCD</i>	QAC transport	<b>-2.66</b>	<b>-3.32</b>	<b>-6.52</b>	<b>-11.24</b>	-1.61	-1.78	-1.97	-1.17	-1.06	-1.24	<b>-6.72</b>	<b>-3.52</b>	-2.15	-1.12

Table 18. Continued.

ID	Gene	Function	Basal <sup>a</sup>		NaCl <sup>a</sup>		H <sub>2</sub> O <sub>2</sub> <sup>a</sup>		Low Fe <sup>a</sup>		Low N <sup>a</sup>		Epi <sup>a</sup>		Apo <sup>a</sup>	
			AlgU	RpoN	AlgU	RpoN	AlgU	RpoN	AlgU	RpoN	AlgU	RpoN	AlgU	RpoN	AlgU	RpoN
<i>Additional osmotic stress-related genes and Oxidative stress-related genes</i>																
Psyr_0040	<i>osmC</i>	Osmoresponsive protein	-1.47	<b>2.61</b>	<b>-8.06</b>	-1.76	-1.45	1.58	-1.06	-1.01	-1.15	1.23	<b>-1.94</b>	-1.10	-2.93	-1.17
Psyr_4446	<i>osmE</i>	Transcriptional activator	<b>-3.79</b>	<b>-3.56</b>	<b>-32.05</b>	<b>-6.23</b>	<b>-4.51</b>	<b>-2.85</b>	-3.20	-1.60	<b>-5.51</b>	<b>-2.80</b>	<b>-33.11</b>	-1.39	<b>-15.48</b>	-2.27
Psyr_1317		Hypothetical	<b>-28.90</b>	<b>-4.38</b>	<b>-322.58</b>	<b>-4.21</b>	<b>-31.45</b>	-2.55	<b>-15.20</b>	<b>-4.55</b>	<b>-46.51</b>	<b>-4.60</b>	<b>-217.39</b>	<b>-2.65</b>	<b>-238.10</b>	-1.68
Psyr_1316		Outer-membrane protein	<b>-13.83</b>	<b>-3.90</b>	<b>-204.08</b>	<b>-5.58</b>	<b>-11.20</b>	-2.49	<b>-8.54</b>	<b>-3.21</b>	<b>-19.34</b>	<b>-2.86</b>	<b>-55.25</b>	<b>-3.58</b>	<b>-129.87</b>	-2.87
Psyr_0280	<i>katE</i>	Hydroperoxidase II	-1.09	-1.44	<b>-12.48</b>	<b>-11.81</b>	-1.28	-1.30	-1.39	-1.20	-2.27	-1.78	<b>-16.67</b>	<b>-10.15</b>	-22.27	-21.79
Psyr_1154	<i>sodC</i>	Superoxide dismutase	1.01	-1.05	<b>-5.35</b>	<b>-3.11</b>	-1.20	-1.17	-1.13	1.04	-1.46	-1.23	<b>-6.91</b>	<b>-1.99</b>	-4.23	-1.41
Psyr_4478	<i>cpoF</i>	Chloroperoxidase	1.07	1.33	<b>-14.12</b>	<b>-5.67</b>	-1.31	-1.07	-1.29	1.06	-1.51	-1.51	<b>-15.24</b>	<b>-5.61</b>	<b>-23.31</b>	-6.74
Psyr_1175	<i>gstA</i>	Glutathione S-transferase	1.05	1.00	<b>-3.93</b>	<b>-3.42</b>	-1.27	-1.27	-1.17	-1.02	-1.58	<b>-1.83</b>	<b>-7.76</b>	<b>-3.56</b>	-6.29	-2.08
Psyr_3173		Glutathione S-transferase	1.22	-1.15	<b>-6.46</b>	<b>-6.61</b>	-1.00	-1.08	-1.19	-1.04	-1.50	-1.50	<b>-9.34</b>	<b>-4.32</b>	-9.03	-4.52
<i>Type VI secretion system genes</i>																
Psyr_4953	<i>tssB</i>	T6SS protein	<b>-2.71</b>	1.23	<b>-10.65</b>	<b>-2.56</b>	-2.01	1.71	-1.96	<b>2.32</b>	-1.41	1.63	<b>-2.77</b>	-1.49	-1.08	1.64
Psyr_4954	<i>tssC</i>	T6SS protein	<b>-3.02</b>	1.39	<b>-14.16</b>	<b>-2.42</b>	-2.15	<b>2.19</b>	-2.35	<b>2.04</b>	-1.82	1.72	<b>-3.84</b>	<b>-2.18</b>	1.06	2.94
Psyr_4955	<i>tssE</i>	T6SS protein	<b>-2.89</b>	1.44	<b>-14.79</b>	<b>-2.86</b>	<b>-2.41</b>	<b>1.82</b>	<b>-2.24</b>	<b>1.99</b>	-1.76	2.08	<b>-4.32</b>	<b>-3.41</b>	-1.28	4.51
Psyr_4956	<i>tssF</i>	T6SS protein	<b>-2.23</b>	1.34	<b>-14.79</b>	<b>-3.30</b>	-2.03	1.51	-1.98	<b>2.09</b>	-1.82	2.03	<b>-4.08</b>	<b>-2.89</b>	-1.23	2.80
Psyr_4957	<i>tssG</i>	T6SS protein	-1.78	1.49	<b>-11.05</b>	<b>-3.29</b>	-1.74	<b>1.78</b>	-1.43	<b>2.17</b>	-1.31	2.01	<b>-3.08</b>	-1.73	-1.08	2.14
Psyr_4958	<i>tssH</i>	T6SS protein	<b>-2.63</b>	1.34	<b>-15.95</b>	<b>-3.38</b>	<b>-2.73</b>	<b>1.96</b>	-1.86	<b>2.15</b>	-1.88	2.46	<b>-3.58</b>	<b>-3.47</b>	1.10	3.99
Psyr_4959	<i>tssJ</i>	T6SS protein	<b>-2.99</b>	1.02	<b>-13.00</b>	<b>-5.46</b>	<b>-2.61</b>	1.56	-1.65	<b>2.26</b>	-1.05	<b>3.54</b>	<b>-3.91</b>	<b>-4.43</b>	-1.29	2.23
Psyr_4960	<i>tssK</i>	T6SS protein	<b>-2.44</b>	1.13	<b>-10.65</b>	<b>-3.80</b>	<b>-2.57</b>	1.35	-1.66	<b>1.91</b>	-1.47	2.44	<b>-3.48</b>	<b>-3.25</b>	1.02	2.47
Psyr_4961	<i>tssLa</i>	T6SS protein	<b>-2.30</b>	-1.02	<b>-11.53</b>	<b>-5.45</b>	<b>-3.05</b>	-1.02	-1.80	1.60	-1.15	<b>3.36</b>	-3.03	<b>-2.99</b>	-1.19	2.36
Psyr_4962	<i>icmF</i>	T6SS protein	<b>-2.69</b>	1.02	<b>-10.65</b>	<b>-7.91</b>	-2.19	1.28	-1.67	1.45	-1.20	<b>2.81</b>	-2.19	<b>-2.35</b>	1.22	2.24
Psyr_4963	<i>tagF</i>	T6SS protein	<b>-3.41</b>	-1.17	<b>-9.48</b>	<b>-5.73</b>	-2.18	1.68	-1.55	1.77	-1.94	1.91	-2.47	-2.40	-1.04	2.40
Psyr_4964	<i>tssLb</i>	T6SS	<b>-3.50</b>	-1.52	<b>-6.74</b>	<b>-5.70</b>	-2.00	1.41	-1.46	1.49	-1.23	1.96	-2.47	<b>-3.14</b>	-1.08	2.19

Table 18. Continued.

ID	Gene	Function	Basal <sup>a</sup>		NaCl <sup>a</sup>		H <sub>2</sub> O <sub>2</sub> <sup>a</sup>		Low Fe <sup>a</sup>		Low N <sup>a</sup>		Epi <sup>a</sup>		Apo <sup>a</sup>	
			AlgU	RpoN	AlgU	RpoN	AlgU	RpoN	AlgU	RpoN	AlgU	RpoN	AlgU	RpoN	AlgU	RpoN
Type VI secretion system genes																
Psyr_4965	<i>hcp</i>	T6SS	-2.50	1.31	-2.31	1.59	-1.61	2.48	-1.50	1.89	-1.73	1.26	-1.54	-1.85	-1.19	1.43
Psyr_4966	<i>tssA</i>	T6SS	-3.42	-1.11	-4.93	-2.91	-2.07	3.42	-1.50	2.25	-1.13	5.12	-2.44	-2.14	-1.34	2.54
Psyr_4967		T6SS	-2.05	-1.03	-4.33	-4.76	-1.68	1.59	-1.20	2.15	1.90	3.39	-2.02	-2.19	-3.17	1.08
Psyr_4968		T6SS	-4.42	-1.64	-5.74	-6.27	-1.46	1.75	-1.23	3.29	1.37	2.88	-2.73	-2.30	-4.64	1.54
Psyr_4969		T6SS	-3.42	-1.39	-5.34	-4.69	-1.92	1.84	-1.23	2.06	1.19	2.60	-1.97	-2.28	-3.11	1.84
Psyr_4971		T6SS	-3.84	-1.46	-3.47	-4.30	-1.01	1.59	-1.05	2.22	1.52	3.17	-1.65	-1.48	-3.30	-1.12
Other regulated genes																
Psyr_3041	<i>lasB</i>	LasB protease	-2.09	1.20	-11.89	-1.67	-2.73	1.08	-1.77	1.03	-2.82	-1.25	-25.19	-2.73	-21.14	-1.84
sRNA_42			-1.96	-1.68	-28.01	-13.97	-1.21	-1.15	-1.43	1.05	-1.10	-1.56	-3.48	-2.75	-3.79	-2.72
Psl polysaccharide synthesis genes																
Psyr_3301	<i>pslA</i>	Psl synthase	1.01	1.08	1.45	2.40	1.11	1.45	1.10	-1.15	-1.12	1.25	-1.03	-1.66	-1.30	3.73
Psyr_3302	<i>pslB</i>	Psl synthase	-1.12	-1.07	1.52	2.74	1.02	1.19	-1.04	-1.13	-1.18	1.09	1.08	-1.88	-1.56	4.07
Psyr_3305	<i>pslF</i>	Psl synthase	1.09	-1.47	1.34	3.19	-1.19	-1.37	-1.02	-2.39	-1.48	1.86	-1.11	-1.43	-1.05	4.92
Psyr_3306	<i>pslG</i>	Psl synthase	1.01	-1.81	1.54	3.19	-1.17	-1.68	-1.04	-1.82	1.00	2.41	1.15	-1.70	-1.83	2.94
Psyr_3307	<i>pslH-1</i>	Psl synthase	-1.20	-1.48	1.22	3.79	-1.05	-1.48	-1.10	-1.74	-1.54	1.93	-1.21	-1.97	-1.60	4.47
Psyr_3308	<i>pslI</i>	Psl synthase	1.17	-1.23	1.63	6.17	-1.06	-2.38	1.02	-2.30	-1.29	1.89	-1.01	-1.95	-2.02	4.82
Psyr_3309	<i>pslJ</i>	Psl synthase	1.22	-1.52	1.27	3.13	-1.11	-2.60	1.01	-1.83	-1.07	2.25	1.06	-2.07	-1.48	3.77
Psyr_3310		Psl synthase	1.11	-1.34	1.16	2.57	1.15	-2.17	-1.01	-1.47	-1.25	1.93	1.18	-1.67	-2.76	2.20
Psyr_3311	<i>pslK</i>	Psl synthase	1.20	-1.05	-1.10	1.52	-1.05	-1.31	1.02	-1.68	-1.13	1.65	1.21	1.04	1.32	2.50

<sup>a</sup> Values are the same as in Table 3.

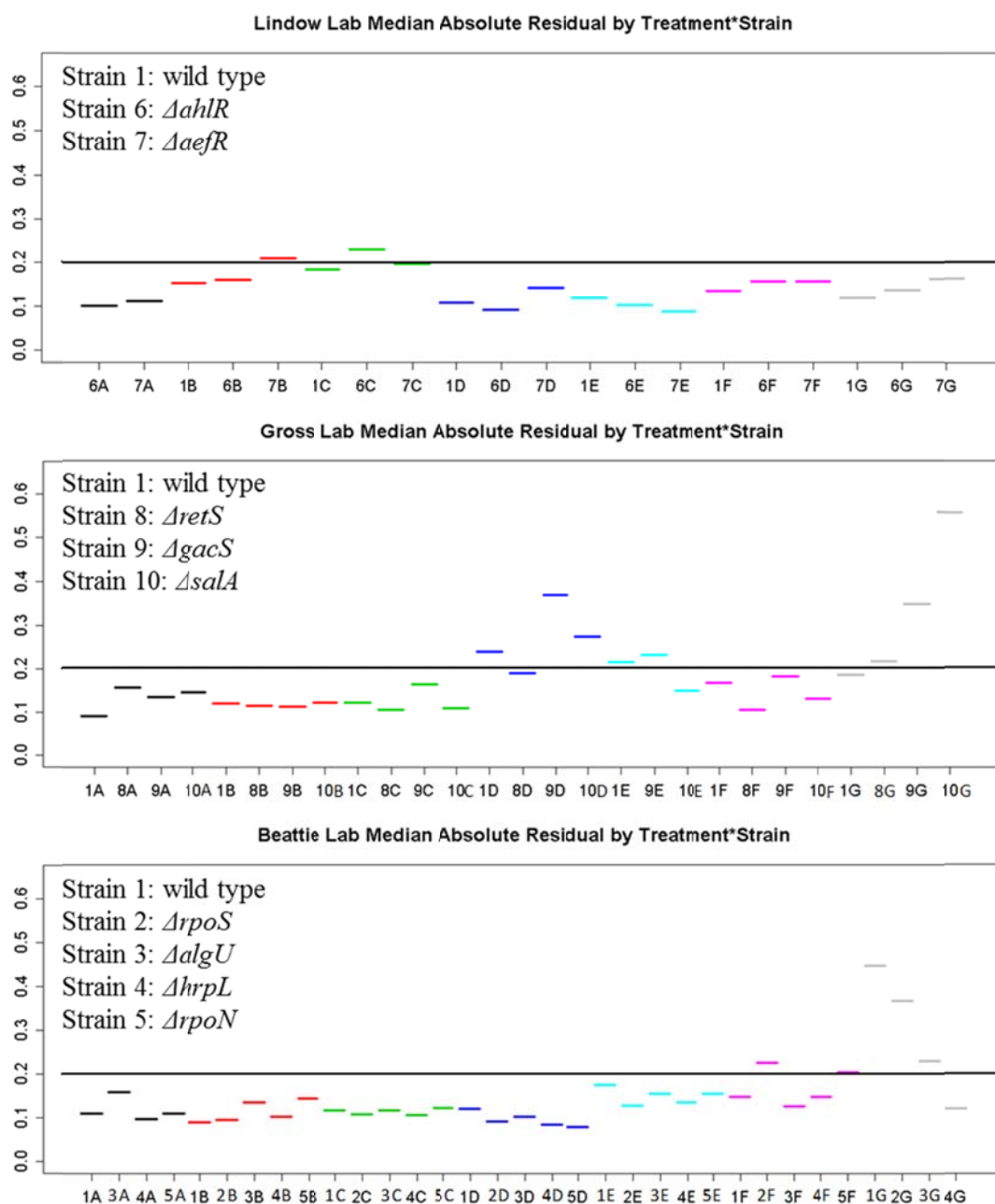


Figure 1. Median Absolute Residual by Treatment\*Strain in the three labs (Colors indicate treatments, which include Trt A: Basal; Trt B: NaCl; Trt C: H<sub>2</sub>O<sub>2</sub>; Trt D: Low Fe; Trt E: Low N; Trt F: Epiphytic; Trt G: Apoplastic).

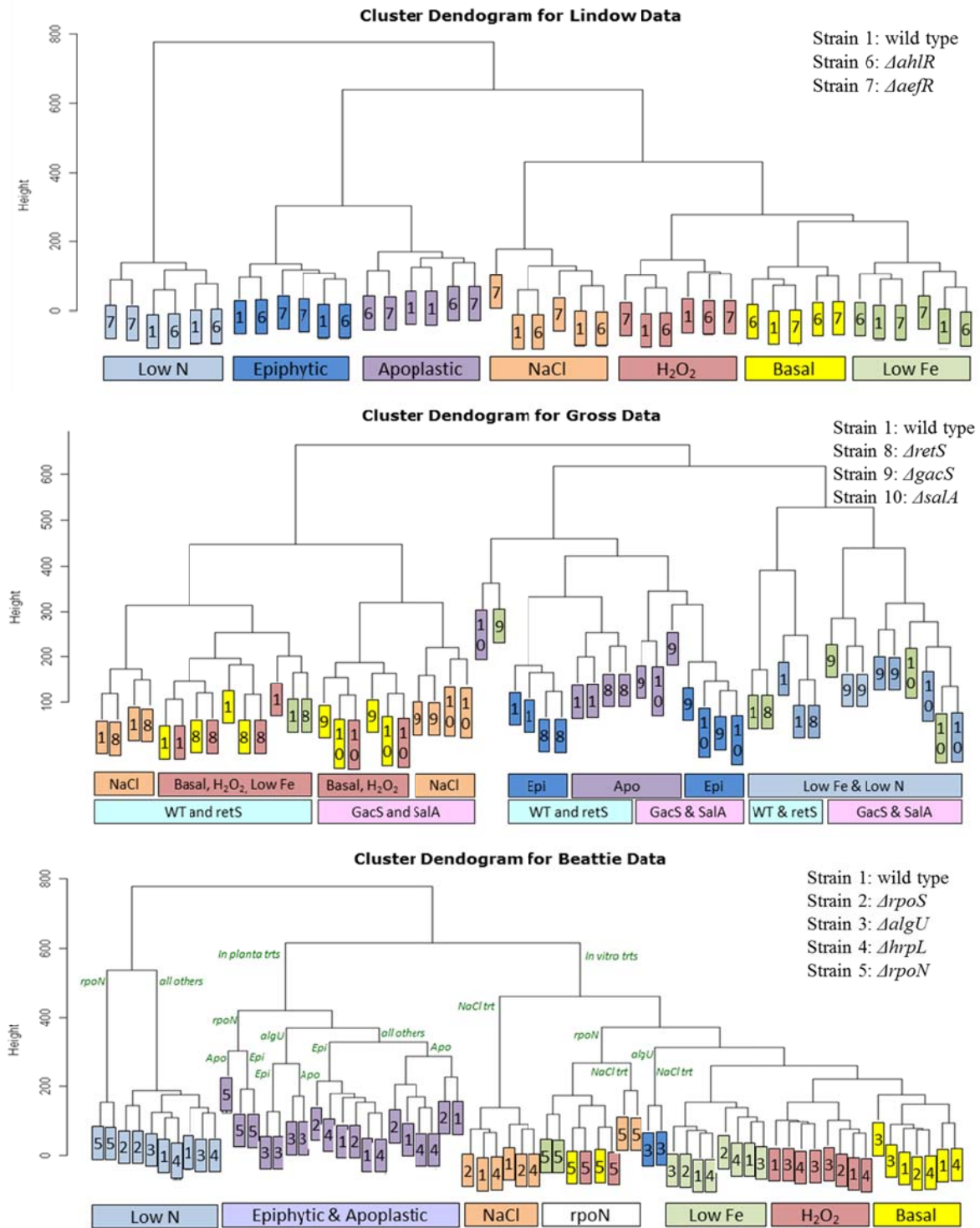


Figure 2. Hierarchical clustering for transcript similarity (Colors indicate treatments, which include Trt A: Basal; Trt B: NaCl; Trt C: H<sub>2</sub>O<sub>2</sub>; Trt D: Low Fe; Trt E: Low N; Trt F: Epiphytic; Trt G: Apoplastic).



162

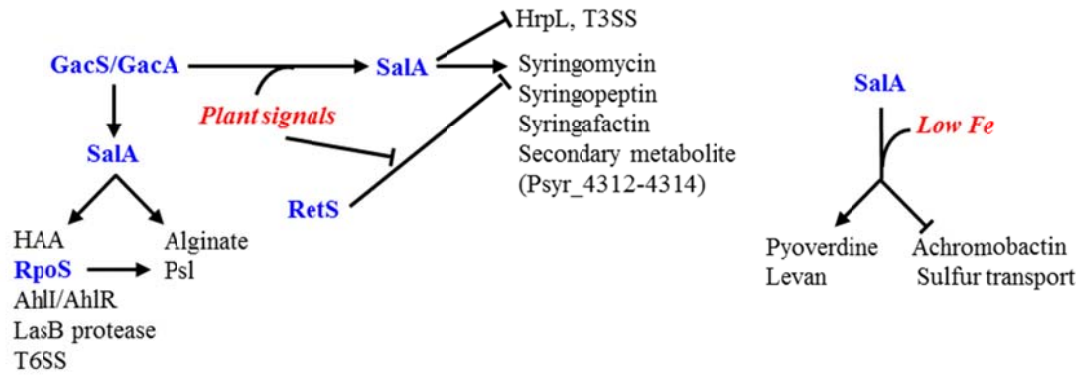


Figure 4. GacS, SalA and RetS regulatory networks in B728a. The regulators are in bold blue, regulated genes or traits are in black, and involved signals are in red. Not all traits identified in these networks are shown.



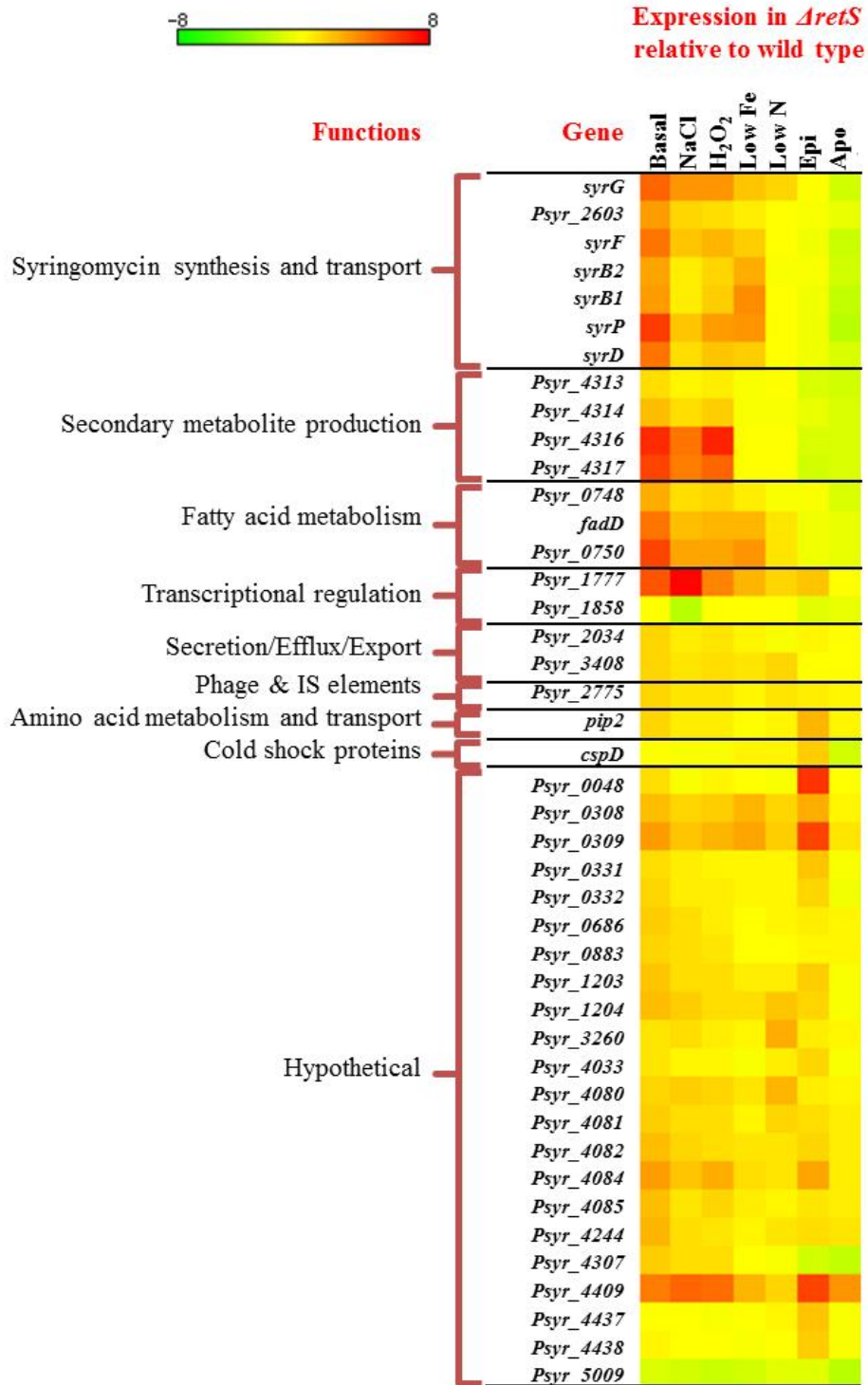


Figure 5. Heatmap for expression of differentially-expressed (DE) genes (q-value <0.01) in  $\Delta retS$ . Genes were grouped by functional category and the relative expression were color coded.

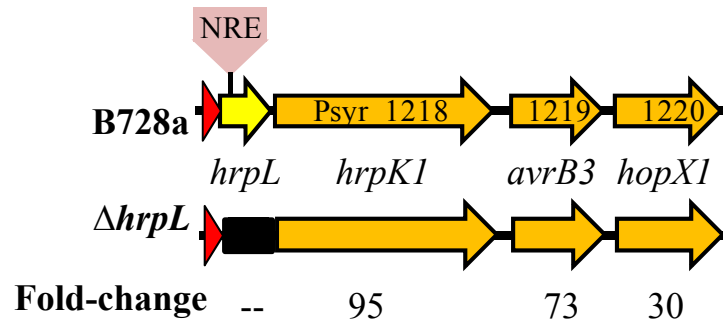


Figure 6. Map of the *hrpL* locus. The predicted site of a negative regulatory element (Vinatzer et al., 2006) is shown. The numbers at the bottom indicate the fold-change in gene expression of each of the genes downstream of *hrpL* in the  $\Delta hrpL$  mutant in the basal medium.

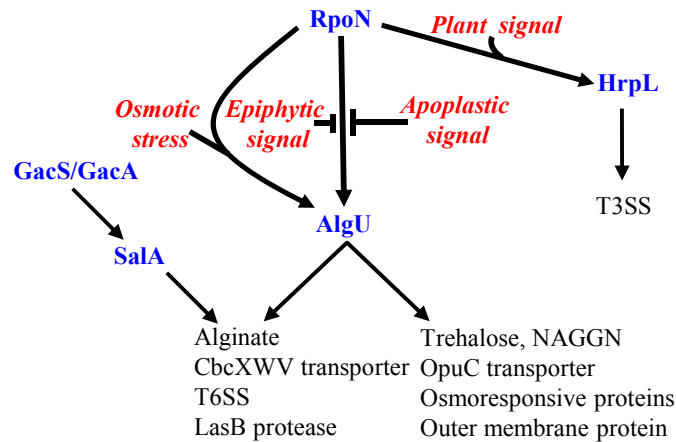


Figure 7. RpoN, AlgU and HrpL regulatory networks in B728a. The regulators are in bold blue, regulated genes or traits are in black, and involved signals are in red. Not all traits identified in these networks are shown.

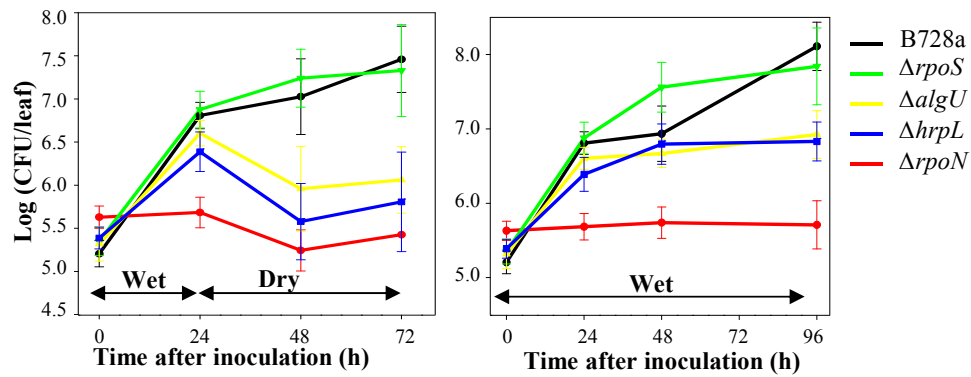


Figure 8. Growth of B728a and four sigma factor mutants on leaf surfaces of bean plants. Plants were inoculated with bacterial cells by submersion of the leaves in bacterial suspensions that contained  $1 \times 10^6$  CFU/ml for B728a and the mutants  $\Delta rpoS$ ,  $\Delta algU$ , and  $\Delta hrpL$  and  $1 \times 10^8$  CFU/ml for  $\Delta rpoN$ .

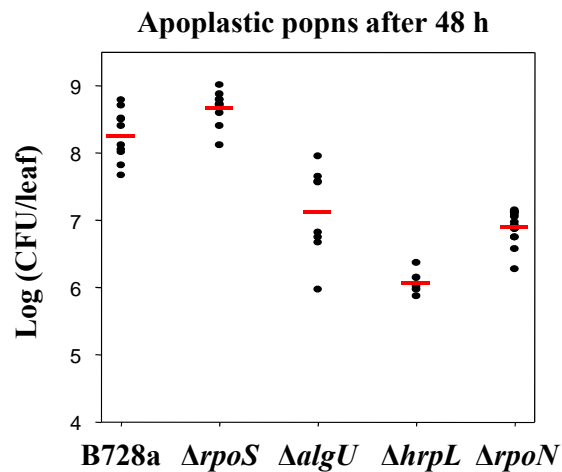


Figure 9. Population sizes of B728a and four sigma factor mutants at 48 h after inoculation by infiltration into the apoplast of bean leaves. Plants were inoculated with bacterial suspensions that contained  $1 \times 10^6$  CFU/ml for B728a and the mutants  $\Delta rpoS$ ,  $\Delta algU$ , and  $\Delta hrpL$  and  $1 \times 10^8$  CFU/ml for  $\Delta rpoN$ .

## CHAPTER 5. GENERAL CONCLUSIONS

### General Discussions

*Pseudomonas syringae* is a gram-negative bacterial foliar pathogen that causes diseases on a broad range of plant species. As a foliar pathogen, *P. syringae* is well-adapted for colonizing leaf surfaces and the leaf apoplast, where it is likely exposed to stressful conditions. *P. syringae* cells modify the plant environment to favor surface growth and survival, and establish and maintain large epiphytic populations that serve as inocula for subsequent infection. As a pathogen, *P. syringae* invades plant leaves through natural openings such as open stomata, hydathodes or wounds, and multiplies in the intercellular spaces. In the apoplast, *P. syringae* initiates the onset of disease on susceptible plants and elicits a localized necrosis, or hypersensitive response, on resistant and non-host plants.

We performed global transcriptome profiling of B728a to understand the environmental conditions that B728a experiences and the cellular traits that it uses to grow and survive during these stages of its lifecycle. The data indicates that the leaf surface and leaf interior offer distinct environments for the bacteria and thus likely present distinct driving forces for *P. syringae* adaptation. We found that the leaf environment is water limited in general; the leaf surface offers a nutritional environment that requires scavenging of phosphate but not iron, active uptake of exogenous sulfur compounds, and utilization of plant-derived indole as a source of tryptophan, while the apoplast space offers some low levels of oxidative stress and surprisingly high levels of water stress. The results support a model in which the epiphytic environment specifically favors flagellar motility, swarming motility, chemosensing and chemotaxis, altogether indicating active relocation primarily on the leaf surface. It also favors phenylalanine degradation, which may be a mechanism to counteract phenylpropanoid-based plant defenses before entry into the apoplast. In contrast, the apoplastic environment favors the degradation of the alternative amino acid GABA, which would attenuate GABA repression of virulence, and synthesis of phytotoxins, two novel

secondary metabolites, and syringolin A, which supports roles for these compounds in virulence, expanding a role for syringolin A in suppressing host defenses beyond stomatal closure.

One important finding of above study is that water limitation is a major stress influencing *P. syringae* growth and survival both on and in plant leaves. *P. syringae* can adapt to water stress by accumulating compatible solutes, such as trehalose, the production of which could influence the water stress tolerance in *P. syringae* strains. We characterized trehalose production in B728a and specifically investigated the relative contribution of distinct trehalose biosynthetic pathways (TreXYZ and TreS) to trehalose production and water stress tolerance in B728a and DC3000, a *P. syringae* strain that is less tolerant to water stress than B728a and a poor epiphytic colonist. We found that B728a utilizes primarily TreXYZ pathway to synthesize trehalose, different from DC3000 that requires both pathways for trehalose production. The data also suggests that B728a did not exhibit the interdependency between the *treXYZ* and *treS* loci for trehalose production, as observed in DC3000. We further found that the dependence of the *treS* locus on a functional *treXYZ* locus in DC3000 was not due to the maltose provided by TreXYZ pathway.

In order to develop a comprehensive understanding of the contribution of distinct regulators to fitness and virulence of *P. syringae*, we performed global transcriptome profiling of B728a and mutants lacking each of nine regulators, including quorum-sensing regulators (AhlR and AefR), global regulators (GacS, SalA and RetS), and alternative sigma factors (RpoN, AlgU, RpoS, and HrpL). We found that AhlR and AefR had negligible roles during B728a leaf colonization, whereas GacS and SalA had major roles. GacS/SalA formed a large regulatory network with both plant signal-dependent and plant signal-independent branches to regulate a diversity of traits. The data also showed that RetS functioned almost exclusively to repress secondary metabolite genes when B728a cells were not in the leaf environment. Among the alternative sigma factors, RpoN influenced the majority of the genome whereas AlgU influenced a large number and RpoS a small number of genes. Many AlgU regulated genes were dependent on RpoN, and the RpoN activation

of the AlgU-regulated genes was attenuated by plant signals. Lastly, HrpL influenced very few genes *in planta*, due primarily to suppression by GacS and SalA.

### **Recommendations for Future Research**

This is the first global transcriptome study using a multifactorial approach to systematically investigate the complex regulatory networks in *P. syringae* in multiple environments including leaf habitats. The plant signals in the leaf environment may influence many branches of these global regulatory networks, and our data provided strong evidence that such signals exist. Although we have yet to identify these signals, some good candidate signals have been discovered, some of which were reviewed in Chapter 1, and would be worthy of further investigation. In addition, functional studies could be performed to further evaluate the contribution of these gene networks to *P. syringae* behavior during bacterial-plant associations.

One interesting finding in Chapter 1 was that the genes for phenylalanine degradation were induced more on leaf surfaces than in the apoplast. The role of phenylalanine in plant-pathogen interactions has not yet been characterized, although the presence of phenylalanine as an important defense compound precursor in plants has been established. The gene expression study of phenylalanine degradation genes in *P. syringae* as well as metabolomics analyses of phenylalanine metabolism during the *P. syringae*-plant interaction would provide key information in investigating the possible virulence role of phenylalanine degradation. Further detailed analysis of phenylalanine metabolism on leaf surfaces versus the leaf interior could be particularly valuable for dissecting the functional sites of phenylalanine during the plant defense response.

The exact mechanistic basis for the interdependency of the two trehalose biosynthetic pathways in DC3000 has not been characterized, although we have excluded one possible explanation. The mechanisms underlying the greater osmotolerance of B728a over DC3000 remain unclear. At least two mechanisms could explain why loss of the *treS* locus decreased the osmotolerance of DC3000 but not B728a. Greater trehalose levels or higher production of another compatible solute could explain this difference between B728a and DC3000 under hyperosmolarity. Alternatively, from the perspective of trehalose as an intermediate in the glycogen biosynthetic pathway, a biochemical study could be utilized to evaluate the involvement and contribution of trehalose in glycogen biosynthesis and therefore better understand the interdependency of the pathways in DC3000.

## **ACKNOWLEDGEMENTS**

First and foremost, I would like to thank my major advisor Gwyn A. Beattie for her wisdom, positive attitude, patience and problem-solving skills. She has not only taught me how to do science, but also guided me to being mature and independent, for which I am very grateful.

I would like to thank all of my labmates for their helpful comments and technique support. Thanks to my husband Shanshan for his encouragement and support, and to my parents for their encouragement over many years of graduate school.



## APPENDIX: SUPPLEMENTAL INFORMATION TO CHAPTER 2.

**Table S1.** The results of an over-representation analysis that shows the functional categories that contained significantly more differentially expressed genes than were present in the transcriptome of the indicated treatment.

**Table S2.** B728a genes that were assigned to each functional category (numbers shown are Psyr#).

**Table S3.** Expression levels of selected B728a genes using data from the meta-analysis of the datasets from the three laboratories.

**Table S4.** Expression levels of genes that were specific to nitrogen versus carbon starvation stress in two previous studies with *Sinorhizobium meliloti* (Sm) and *Bacillus licheniformis* (Bl).

**Table S5.** Genes involved in nutrient transport or metabolism that were induced *in planta*.

**Fig S1.** Evaluation of conditions used to impose osmotic stress on B728a cells.

**Fig S2.** Evaluation of conditions used to impose oxidative stress on B728a cells.





**Fig S3.** Evaluation of conditions used to impose iron starvation on B728a cells.

**Fig S4.** Evaluation of conditions used to impose nitrogen starvation on B728a cells.

**Fig S5.** Evaluation of conditions used to generate epiphytic populations of B728a cells on bean leaves.

**Fig S6.** Evaluation of conditions used to generate apoplastic populations of B728a cells in bean leaves.

**Fig S7.** Effect of phenylalanine on the transcript levels of *phhA* and *phhB*.

**Table S1. The results of an over-representation analysis that shows the functional categories that contained significantly more differentially expressed genes than were present in the transcriptome of the indicated treatment.** The data is shown for analyses performed separately for each laboratory, indicated as A, B, and C, and for the combined dataset. Functional categories in which the transcripts that were *increased* were significantly over-represented are indicated by  if the  $q$ -value  $< 0.05$  or by  if the  $q$ -value  $< 0.1$ . Functional categories in which the transcripts that were *decreased* were significantly over-represented are indicated by  if the  $q$ -value  $< 0.05$  or by  if the  $q$ -value  $< 0.1$ .

	NaCl		H <sub>2</sub> O <sub>2</sub>		LowFe		LowN		Epi		Apo		NaCl	H <sub>2</sub> O <sub>2</sub>	LowFe	LowN	Epi	Apo
Functional category	A	B	A	B	A	B	A	B	A	B	A	B	Combined dataset					
Amino acid metabolism and transport																		
Amino acid metabolism and transport (GABA)																		
Carbohydrate metabolism and transport																		
Cell division																		
Chaperones/Heat shock proteins																		
Chemotaxis & chemotaxis																		
Cofactor metabolism																		
Compatible solute synthesis																		
Cyclic di-GMP cyclase proteins																		
Degradation of xenobiotics																		
Energy generation																		
Fatty acid metabolism																		
Flagellar synthesis and motility																		
Iron metabolism and transport																		
Iron-sulfur proteins																		
Light and oxygen sensing																		
LPS synthesis and transport																		
Mechanosensitive ion channel																		
Nitrogen metabolism																		
Nucleotide metabolism and transport																		
Organic acid metabolism and transport																		
Outer membrane proteins																		
Oxidative stress tolerance																		
Oxidative stress tolerance (Antioxidant enzymes)																		
Peptidoglycan/cell wall polymers																		
Phage & IS elements																		
Phosphate metabolism and transport																		
Phospholipid metabolism																		
Phytotoxin synthesis and transport																		
Pili synthesis and regulation																		
Polyamine metabolism and transport																		
Polysaccharide synthesis and regulation																		
Post-translational modification																		
Proteases																		
QAC metabolism and transport																		
Replication and DNA repair																		

**Table S1 (continued)**

The genes were each assigned to a single functional category and were identified as differentially expressed by the treatment if the False discovery rate was  $<1\%$  in the LIMMA analysis. Over-representation was evaluated using a Fisher's exact test, as described in the Methods.

	NaCl	H <sub>2</sub> O <sub>2</sub>	LowFe	LowN	Epi	Apo
Functional category	A B C	A B C	A B C	A B C	A B C	A B C
RNA degradation						
Secondary metabolism						
Secretion/Efflux/Export						
Siderophore synthesis and transport						
Special						
Stress resistance						
Sulfur metabolism and transport						
TAT secretion system						
Terpenoid backbone synthesis						
Toxin-Antitoxin system						
Transcription						
Transcription - Sigma factor						
Transcriptional regulation						
Translation						
Transport						
Transport (peptides)						
Type III secretion system						
Type VI secretion system						

**Table S2. B728a genes that were assigned to each functional category (numbers shown are Psyr#).**

Amino acid metabolism and transport	0025 0033 0034 0035 0065 0147 0150 0158 0165 0174 0182 0183 0218 0227 0237 0247 0253 0254 0272 0281 0282 0283 0295 0296 0297 0298 0349 0350 0351 0356 0357 0358 0366 0367 0375 0385 0386 0408 0409 0455 0460 0466 0473 0474 0476 0506 0507 0557 0576 0597 0598 0599 0600 0601 0678 0690 0696 0697 0704 0756 0771 0888 0952 0973 0974 0975 1072 1073 1074 1075 1095 1096 1097 1151 1235 1257 1290 1331 1336 1433 1548 1583 1618 1660 1663 1669 1672 1853 1855 1856 1857 1915 1925 1973 1983 1984 1985 1986 2015 2073 2079 2130 2132 2201 2202 2203 2204 2205 2261 2262 2330 2358 2418 2427 2464 2467 2468 2469 2470 2471 2504 2505 2506 2638 2683 2684 2685 2855 2888 2889 2890 2891 2900 2941 2942 2943 2944 2962 2963 2964 2965 3237 3238 3241 3280 3325 3326 3330 3522 3523 3525 3555 3557 3559 3561 3562 3563 3564 3565 3566 3567 3568 3569 3570 3571 3574 3575 3576 3615 3622 3633 3644 3645 3648 3778 3845 3846 3847 3848 3849 3874 3875 3876 3878 3892 3901 3908 3909 3910 3911 3916 3962 3977 3978 3987 4093 4132 4133 4134 4193 4217 4270 4369 4381 4399 4426 4427 4428 4429 4430 4569 4579 4580 4581 4609 4712 4766 4794 4812 4818 4828 4829 4830 4831 4832 4833 4835 4836 4846 4852 4893 4894 4896 4897 4898 4911 4912 4913 4914 4932 4933 5042 5052
Amino acid metabolism and transport (GABA)	0090 0091 0146 0149 2413 3515 4909
Carbohydrate metabolism and transport	0370 0374 0603 0758 0759 0760 0761 0762 0775 0820 0821 0822 0823 0826 0839 0916 0944 1043 1109 1110 1111 1113 1114 1115 1116 1174 1737 1738 1739 1740 1781 1788 1898 1914 1987 1988 1989 2129 2151 2152 2153 2154 2155 2156 2179 2181 2297 2306 2371 2372 2373 2421 2434 2435 2436 2437 2438 2439 2440 2510 2530 2557 2569 2570 2571 2572 2574 2696 2704 2715 2874 2875 2876 2877 2883 2884 2885 2886 2908 2923 2926 2980 2988 2989 3063 3134 3138 3153 3263 3264 3265 3267 3268 3269 3270 3271 3272 3273 3274 3337 3767 3768 3769 3930 3993 4142 4487 4488 4491 4611 4787 4791 4792 4813 4842 4847 5117
Cell division	1364 1555 1611 1612 1613 1818 3179 3284 3587 4097 4098 4099 4103 4109 4111 4161 4162 4163 4364 4749 4750
Chaperones/Heat shock proteins	0058 0169 0170 0268 0394 0395 1140 1240 1241 1440 1751 1980 2017 3616 3657 3785 3914 3997 3998 4072 4073 4194 4195 4196 4440 4441 4621 4917
Chemosensing & chemotaxis	0071 0143 0379 0380 0578 0781 0782 0783 0784 0785 0786 0788 0789 0860 0868 0905 0906 0913 1139 1150 1303 1304 1305 1306 1307 1308 1491 1539 1776 1789 1798 2059 2109 2188 2214 2215 2220 2237 2240 2241 2246 2315 2356 2446 2447 2634 2682 2878 2966 3114 3261 3297 3348 3351 3406 3428 3429 3433 3434 3435 3436 3485 3486 3534 3589 3735 4209 4218 4706 4907 5004 5092 5093
Cofactor metabolism	0024 0059 0060 0061 0062 0221 0292 0302 0303 0317 0322 0323 0387 0389 0414 0440 0454 0459 0469 0471 0544 0594 0595 0631 0709 0721 0795 0815 0827 0828 0829 0846 0847 0848 0948 0951 0967 1019 1020 1021 1067 1068 1069 1104 1148 1291 1411 1542 1650 1665 1685 1708 1743 1828 1845 1901 2074 2075 2080 2098 2135 2136 2137 2157 2225 2226 2327 2402 2442 2453 2595 3013 3014 3015 3016 3019 3020 3070 3125 3174 3215 3423 3430 3558 3650 3672 3673 3674 3675 3676 3677 3678 3680 3681 3853 3932 3948 3959 4088 4090 4186 4271 4340 4341 4342 4368 4414 4415 4416 4417 4418 4419 4420 4456 4457 4459 4460 4461 4462 4563 4564 4574 4626 4635 4636 4661 4670 4671 4672 4673 4674 4675 4683 4684 4685 4686 4687 4737 4740 4741 4758 4816 5016 5017 5018 5030 5031 5070 5072 5075 5130
Cold shock proteins	1094 1403 2160 3185 3884
Compatible solute synthesis	0334 2489 2490 2491 2992 2993 2994 2995 2996 2997 2998 2999 3000 3001 3002 3747 3748 3749 3750
Cyclic di-GMP cyclase proteins	0074 0086 0266 0509 0870 1125 1157 1159 1309 1598 1684 1981 2110 2281 2432 2486 2535 2597 2711 2939 3328 3329 3653 3655 3763 3843 3942 4060 4206 4265 4377 4642 4678 4770
Degradation of xenobiotics	0159 0669 1170 1769 1791 2534 2734 2869 2934 2946 2956 4677 4681 4718 4825

Energy generation	0049 0168 0239 0284 0285 0293 0456 0517 0518 0624 0790 1024 1108 1120 1121 1122 1141 1142 1143 1144 1145 1280 1481 1726 1880 1897 1994 1995 1996 2004 2005 2006 2007 2008 2009 2010 2012 2013 2087 2173 2174 2862 3186 3196 3197 3198 3199 3200 3201 3202 3203 3204 3205 3206 3207 3208 3209 3279 3386 3388 3389 3404 3413 3414 3415 3416 3509 3887 4031 4184 4779 4780 4790 4885 5060 5061 5120 5121 5122 5123 5124 5125 5126 5127 5128
Fatty acid metabolism	0087 0120 0123 0422 0423 0425 0436 0437 0442 0443 0444 0445 0446 0447 0448 0644 0645 0742 0749 0990 1025 1354 1359 1628 1646 1647 1649 1664 1754 1770 1875 1892 2019 2020 2068 2452 2487 2728 3030 3239 3289 3290 3467 3514 3524 3542 3830 4075 4293 4311 4400 4401 5028 5043 5069
Flagellar synthesis and motility	0314 0561 0562 1098 3431 3432 3438 3439 3440 3441 3442 3443 3444 3445 3446 3447 3448 3449 3453 3454 3455 3456 3457 3458 3459 3460 3461 3462 3463 3464 3465 3466 3470 3471 3472 3473 3474 3475 3476 3477 3478 3479 3480 3481 3487 3488 3489 4493
Glutathione metabolism	0255 0487 1010 1091 1175 1629 1690 1842 2499 2526 2979 3173 3548 3613 3670 4092 4118 4727
Iron metabolism and transport	0244 0245 0664 0665 0666 0667 1038 1039 1040 1105 1106 1107 1124 1242 1404 2501 3367 3714 3897 3902 4198 4448 4521 4730 4731 5102 5103 5104
Iron-sulfur proteins	0566 0838 1236 1239 1334 1335 1375 1616 2388 3387 3419 3896 4568 4759
Light and oxygen sensing	2384 2385 2451 2700 3425 3504 3505 4230 4231 4281 4282
LPS synthesis and transport	0010 0014 0520 0521 0522 0523 0524 0525 0537 0542 0610 0611 0619 0917 0918 1032 1092 1093 1353 1355 1356 1362 1614 1635 1636 1732 2496 2689 2690 2691 3304 4067 4096 4115 4143 4146 4185 5108
Mechanosensitive ion channel	1822 3549 3803 4086 4276 4477 5003
Nitrogen metabolism	0189 0190 0235 0246 0288 0411 0412 0519 0607 0859 1166 1341 1576 1724 2099 2100 2195 2196 2197 2198 2199 2200 2273 2274 2275 2276 2277 2292 2686 2706 2755 3068 3099 3100 3112 3483 3492 3969 4149 4315 4431 4432 4435 4436 4451 4452 4453 4454 4817 4821 4822 4867 4868 5051 5053
Nucleotide metabolism and transport	0076 0177 0209 0210 0211 0216 0220 0294 0472 0481 0482 0483 0545 0547 0577 0661 0676 0968 0969 0970 1244 1261 1262 1269 1277 1319 1345 1361 1551 1610 1639 1652 1668 1806 1807 1810 1812 1814 1815 1836 2106 2116 2133 2389 2390 2391 2555 2556 2922 3009 3192 3426 3531 3581 3617 3643 3689 3690 3694 3717 3721 3776 3883 3894 3981 4018 4176 4191 4192 4283 4284 4285 4286 4336 4337 4406 4407 4629 4717 4840 4941 5047 5048
Organic acid metabolism and transport	0015 0198 0338 0339 0340 0401 0417 0449 0450 0462 0463 0679 0689 0692 0693 0694 0695 0748 0764 0863 0898 0899 0900 0908 0976 1007 1158 1278 1318 1367 1368 1479 1561 1640 1676 1709 1761 1801 1839 1899 1990 2085 2086 2090 2122 2123 2124 2125 2126 2143 2184 2209 2247 2248 2249 2250 2251 2252 2253 2254 2255 2256 2257 2258 2259 2314 2387 2396 2672 2708 2709 2710 2716 2973 3119 3120 3167 3313 3331 3332 3333 3338 3500 3501 3651 3707 3756 3964 3965 3966 3967 3968 4010 4011 4012 4013 4029 4169 4225 4226 4227 4610 4700 4945 4946
Osmosensing & regulation	0040 0258 0259 4446 4576
Outer membrane proteins	0368 0763 0903 0946 1005 1117 1316 1352 1400 1416 1999 2071 2097 2127 2730 3178 3669 3854 3893 4237 4473 4807 4878 4930
Oxidative stress tolerance	0202 0300 1082 1289 3043 3044 3661 3701 3898 4466 4883
Oxidative stress tolerance (Antioxidant enzyme)	0280 1016 1154 2544 2974 2975 3353 3369 3626 3627 4059 4152 4208 4478 4522 4877 5095
Peptidoglycan/cell wall polymers	0265 0402 0569 0630 0708 0842 1637 2111 2313 2414 3008 3281 3919 4100 4101 4102 4104 4105 4106 4107 4108 4110 4135 4361 4365 4387 4743 5077 5119
Phage & IS elements	0095 0096 0105 0106 0273 0274 0651 0652 0751 1030 1421 1475 1492 1508 1975 1976

	2605 2653 2654 2667 2699 2751 2762 2763 2764 2765 2766 2767 2768 2769 2770 2771 2772 2773 2774 2775 2776 2777 2778 2779 2780 2781 2782 2783 2784 2785 2786 2787 2788 2789 2790 2791 2792 2793 2794 2795 2796 2797 2798 2799 2800 2801 2802 2803 2804 2805 2806 2807 2808 2809 2810 2811 2812 2813 2814 2815 2816 2817 2818 2819 2820 2821 2822 2823 2824 2825 2826 2827 2828 2829 2830 2831 2832 2834 2835 2836 2837 2838 2839 2840 2841 2842 2843 2844 2845 2846 2847 2848 2850 2851 2852 2854 2976 4512 4586 4587 4588 4589 4590 4591 4592 4595 4646 4859 4860
Phosphate metabolism and transport	0872 1034 1233 1773 2475 3103 3104 3105 3106 4016 4494 4500 4507 5032 5033 5037 5038 5039 5040 5041
Phospholipid metabolism	0009 0229 0438 0559 0627 0628 0849 0866 0878 0956 0980 1328 1348 1385 1586 1645 1823 1902 2022 2566 2895 2954 3140 3242 3244 3277 3905 3906 3907 4044 4049 4506 4637 4970 5079 5080
Phytotoxin synthesis and transport	1702 1703 1704 1705 1706 2601 2602 2606 2607 2608 2609 2610 2611 2612 2613 2614 2615 2616 2617 2618 2619 2620 2621 2622
Pili synthesis and regulation	0249 0403 0404 0405 0406 0407 0478 0488 0489 0490 0491 0492 0493 0714 0715 0716 0717 0718 0719 0720 0722 0723 0796 0797 0798 0799 1131 1132 1133 1134 1246 1509 1510 1511 1512 1513 1514 1515 1516 1517 1518 1654 2036 2037 2038 2039 2906 3418 4389 4390 4392
Plant-associated proteins	0852 1536 1882 2208 3985 4158 4170 4268 4508 4667
Polyamine metabolism and transport	1602 1864 2398 2399 2400 2401 2547 4247 4575 4612 4613 4614 4615 4861 4862 4863 4864 4865 4866
Polysaccharide synthesis and regulation	0054 0056 0063 0064 0219 0263 0264 0377 0378 0754 0937 1052 1053 1054 1055 1056 1057 1058 1059 1060 1061 1062 1063 1065 1350 1809 2103 2443 2528 2692 3222 3232 3301 3302 3303 3305 3306 3307 3308 3309 3310 3311 3551 3636 3937 3955 3956 3957 5085
Post-translational modification	0019 0055 1594 1733 2146 2340 2907 3097 3780 3826 4255 4887
Proteases	0574 0575 0728 1580 1746 1747 1748 1749 2460 3041 3183 3184 3191 3944 4117 4187 4259
QAC metabolism and transport	0028 0029 0824 1590 2175 2221 2222 2223 2224 2546 2915 2916 2917 2918 2919 3054 3236 3758 4249 4250 4251 4252 4708 4709 4710 4711 4713 4714 4715 4716 4732 4733 4734 4738 4775 4776 4781 4782 4827 5013
Quorum regulation	1621 1622 1712 1971 3324 3871 4858
Replication and DNA repair	0001 0002 0003 0004 0013 0075 0185 0201 0215 0222 0270 0398 0516 0551 0554 0570 0585 0606 0680 0681 0682 0733 0819 0919 1090 1259 1286 1298 1357 1358 1376 1378 1397 1408 1409 1410 1424 1425 1459 1473 1522 1531 1534 1653 1655 1750 1763 1764 1819 1825 1832 1896 1974 2060 2244 2361 2476 2520 2523 2759 2761 2896 2977 3245 3246 3283 3287 3366 3396 3647 3686 3831 3842 3856 3873 3888 3895 3949 3970 4020 4057 4091 4197 4275 4300 4320 4354 4370 4518 4520 4640 4703 4761 4796 4927 5065 5129
RNA degradation	0453 0458 0572 0579 0830 1070 1363 1482 1638 2914 3619 3738 3804 4843 4948
Secondary metabolism	0924 0925 0926 1792 1793 1794 1795 2363 2575 2576 2577 2665 3129 3359 3722 4312 4313 4314 4662 4935 4936 5009 5010 5011 5012
Secretion/Efflux/Export	0073 0336 0344 0345 0346 0541 0543 0620 0711 0865 0933 0934 0935 1045 1048 1126 1127 1129 1229 1230 1231 1281 1497 1498 1730 1731 1772 2034 2191 2193 2282 2283 2316 2482 2483 2484 2485 2492 2603 2864 2865 2866 2867 2868 2931 2967 2968 2969 3075 3076 3077 3081 3083 3130 3131 3141 3142 3143 3144 3145 3146 3147 3148 3149 3150 3151 3159 3160 3161 3380 3381 3390 3391 3392 3393 3408 3733 3734 3870 3953 4004 4007 4008 4009 4094 4183 4391 4393 4394 4395 4528 4561 4606 4643 4751 4801 4802 4803 4882 5134
Siderophore synthesis and transport	0135 0136 0137 0138 0203 0204 0205 0306 0486 0874 0875 0876 0877 1412 1413 1414 1633 1634 1784 1943 1944 1945 1946 1947 1956 1957 1958 1959 1960 1961 1962 1963 1964 1965 1966 1967 1968 1969 1970 2229 2287 2288 2289 2290 2580 2581 2582 2583

	2584 2585 2586 2587 2588 2589 2590 2591 2592 2593 2859 2892 3094 3095 3096 3124 3243 3345 3864 3927 4480 4481 4482 4483 4496 4497 4498 4499 4826
Signal transduction mechanisms	0089 0831 0832 0886 1099 1112 1585 1912 1918 1938 1941 2021 2031 2104 2115 2374 2444 2445 2448 2449 3085 3128 3211 3451 3495 3512 3591 3612 3715 3792 3912 3994 4069 4339 4388 4439 4701 4937 5036 5089
Special	2698 2856 3417 3832 3989 3990 4035 4036 4205 4233 4645 4777
Stress resistance	0262 0535 0656 0808 0809 0810 0811 0812 0813 1128 1371 1493 1494 1495 1496 1502 1503 1504 1570 1571 1667 1681 1682 1729 2194 2481 3132 3176 3374 3375 3695 3702 3708 3709 4138 4273 4624 4799 4800 4837 5081
Sulfur metabolism and transport	0026 0081 0082 0083 0084 0134 0287 0337 0352 0359 0360 0850 0851 1015 1237 1562 1827 1865 2077 2078 2177 2280 2354 2462 2514 2515 2516 3086 3168 3169 3190 3220 3233 3247 3248 3363 3372 3383 3506 3597 3598 3599 3601 3603 3605 3606 3614 3697 4126 4128 4243 4324 4358 4359 4630 4756 4824 4873 4874 4875 4876
TAT secretion system	0157 0382 0383 0384 1169 1266 2235 2285 4171 4690
Terpenoid backbone synthesis	0604 0605 0700 0713 0945 1248 1347 1349 1365 2725 3031
Toxin-Antitoxin system	0889 0890 0894 0895 4651 4652
Transcription	0301 2065 3193 4190 4263 4458 4524 4554 4555 4560
Transcription - Sigma factors	0327 0362 0787 0891 0892 1374 1913 2096 3437 3452 3958 4137 4147 4148 4593 4641 4748
Transcriptional regulation	0030 0072 0121 0144 0193 0230 0234 0251 0299 0421 0451 0495 0571 0596 0653 0659 0660 0675 0677 0688 0741 0757 0767 0777 0909 0962 0993 1000 1044 1119 1152 1161 1172 1294 1366 1384 1386 1435 1437 1478 1547 1558 1607 1624 1657 1707 1777 1780 1800 1802 1811 1816 1840 1858 1928 1940 1982 1991 1993 2000 2032 2045 2084 2114 2121 2131 2142 2169 2180 2183 2189 2192 2219 2268 2284 2336 2357 2375 2378 2395 2397 2405 2422 2441 2472 2473 2480 2508 2531 2532 2536 2564 2578 2671 2675 2707 2713 2719 2723 2729 2738 2740 2754 2882 2897 2910 2913 2920 2927 2929 2933 2938 2945 2951 3004 3022 3036 3051 3057 3062 3073 3084 3087 3091 3102 3111 3118 3127 3135 3154 3156 3165 3188 3212 3226 3282 3299 3312 3327 3336 3347 3357 3377 3484 3511 3521 3526 3530 3538 3543 3546 3547 3600 3607 3624 3634 3698 3716 3737 3793 3796 3801 3825 3890 3917 3926 3939 4006 4014 4051 4070 4216 4228 4266 4278 4318 4325 4335 4376 4408 4450 4463 4490 4605 4618 4757 4793 4814 4838 4869 4923 4944 5008 5015 5050 5056 5057 5062 5088 5118
Translation	Candidate_sRNA_1 Candidate_sRNA_10 Candidate_sRNA_11 Candidate_sRNA_13 Candidate_sRNA_14 Candidate_sRNA_15 Candidate_sRNA_16 Candidate_sRNA_17 Candidate_sRNA_18 Candidate_sRNA_2 Candidate_sRNA_20 Candidate_sRNA_21 Candidate_sRNA_22 Candidate_sRNA_23 Candidate_sRNA_25 Candidate_sRNA_26 Candidate_sRNA_27 Candidate_sRNA_3 Candidate_sRNA_30 Candidate_sRNA_32 Candidate_sRNA_34 Candidate_sRNA_35 Candidate_sRNA_36 Candidate_sRNA_37 Candidate_sRNA_38 Candidate_sRNA_4 Candidate_sRNA_41 Candidate_sRNA_42 Candidate_sRNA_43 Candidate_sRNA_44 Candidate_sRNA_45 Candidate_sRNA_46 Candidate_sRNA_6 Candidate_sRNA_7 Candidate_sRNA_8 PIG-a19_30 PIG-a19_30A PIG-a19_30B PIG-a19_30C PIG-a19_30D PIG-a19_30E PIG-a22_5 PIG-a26_17 PIG-a28_7 PIG-a29_21 PIG-a34_1 PIG-a39_13 PIG-a40_4 PIG-a42_1 PIG-AnaS_227 PIG-AnaS_412 sRNA_g150 sRNA_P11 sRNA_P15 sRNA_P16 sRNA_P24 sRNA_P26 sRNA_PrrB_RsmZ_long sRNA_PrrF_minus sRNA_PrrF_plus sRNA_RsmY 0011 0012 0017 0018 0213 0224 0225 0269 0376 0381 0397 0399 0581 0582 0584 0701 0702 0707 0710 0834 0857 0942 0943 0949 1086 1227 1249 1282 1283 1284 1285 1310 1311 1342 1343 1344 1346 1370 1399 1406 1644 1662 1734 1735 1936 1977 2107 2108 2162 2163 2164 2165 2166 2167 2351 2749 3058 3175 3181 3182 3339 3554 3556 3579 3628 3642 3696 3751 3886 3920 4119 4120 4123 4164 4165 4166 4177 4178 4180 4253 4287 4345 4352 4380 4523 4525 4526 4527 4529 4530 4531 4532 4533 4534 4535 4536 4537 4538 4539 4540 4541 4542 4543 4544 4545 4546 4547 4548 4549 4550 4551 4552 4553 4556 4557 4558 4559 4565 4639 4739 4771 5133 5137
Transport	0052 0108 0139 0140 0141 0142 0223 0228 0325 0328 0420 0513 0536 0648 0671 0672

	0673 0774 1002 1003 1004 1164 1167 1168 1268 1488 1587 1603 1604 1606 1677 1742 1771 1830 1854 1948 2067 2170 2187 2232 2295 2304 2329 2333 2334 2335 2366 2368 2493 2495 2503 2513 2902 2903 2904 2905 2928 2958 2959 2960 2961 3025 3052 3126 3166 3294 3322 3360 3491 3578 3656 3671 3743 3762 3800 3827 3936 3972 3973 3974 3999 4052 4116 4141 4175 4202 4211 4229 4470 4519 4660 4692 4693 4694 4695 4696 4769 4899 5066 5090 5091
Transport (inorganic ions)	0016 0069 0275 0276 0277 0278 0364 0501 0502 0654 0668 1394 1774 1862 1874 1949 1950 1951 2046 2047 2048 2049 2050 2051 2093 2102 2139 2228 2230 2305 2328 2525 2756 2757 2758 3252 3253 3254 3255 3256 3257 3382 3552 3593 4210 4333 4810 5068
Transport (organic compounds)	0305 1630 1631 1904 1905 1906 3904 4502 4503 4504 4505
Transport (peptides)	0154 0155 0156 1179 1755 1756 1757 1758 1759 2263 2264 2265 2266 2267 2538 2539 2540 2541 2542 2676 2677 2678 2679 2680 4212 4213 4214 4215 4234 4235 4236 4238 4239 4240 4241 4242
Type III secretion system	0738 0778 0779 1017 1183 1184 1185 1186 1187 1188 1189 1190 1191 1192 1193 1194 1195 1196 1197 1198 1199 1200 1201 1202 1205 1206 1207 1208 1209 1210 1211 1212 1213 1214 1215 1216 1217 1218 1219 1220 1224 1889 3123 3813 3839 4269 4326 4659 4919
Type VI secretion system	0101 1935 2626 2627 2628 2629 4039 4953 4954 4955 4956 4957 4958 4959 4960 4961 4962 4963 4964 4965 4966 4967 4968 4969 4971 4972 4973 4974



**Table S3. Expression levels of selected B728a genes using data from the meta-analysis of the datasets from the three laboratories.**

Note that the fluorescence intensity is the average fluorescence intensity in the basal medium, which reflects the relative expression level of each gene. The values ranged from 42 to 55,935. The highlighted values were differentially expressed compared to in the basal medium ( $P$ -value < 0.05 and  $q$ -value < 0.01), with pink indicating induced genes and green indicating repressed genes. The treatments were osmotic stress (NaCl), oxidative stress ( $H_2O_2$ ), iron limitation (low Fe), nitrogen limitation (low N), epiphytic cells (Epi), and apoplastic cells (Apo).

Psysr#	Gene	Product Name	Fluorescence Intensity	Fold-induction compared to basal medium					
			Basal medium	NaCl	H <sub>2</sub> O <sub>2</sub>	Low Fe	Low N	Epi	Apo
Flagellar synthesis and motility (all genes in category are shown)									
Psysr_0314		flagellar basal body-associated protein FliL-like protein	1,059	-2.1	1.1	1.1	1.4	1.8	-2.1
Psysr_0561	motA	flagellar motor protein MotA	917	-2.4	-1.2	-1.1	-1.4	2.3	-2.4
Psysr_0562	motB	flagellar motor protein MotB	427	-2.6	-1.6	-1.6	-1.9	2.0	-2.6
Psysr_1098	morA-1	PAS:GGDEF	248	-1.3	1.4	1.2	2.0	1.5	-1.1
Psysr_3431	motD	flagellar motor protein MotD	442	-1.5	-1.6	-1.2	-2.6	1.1	-2.1
Psysr_3432	motC	flagellar motor protein MotC	353	-1.8	-1.8	-1.2	-3.4	1.0	-2.6
Psysr_3438	fleN	Flagellar synthesis regulator	1,162	1.1	1.8	3.9	5.6	10.9	2.0
Psysr_3439	flhF	flagellar biosynthesis regulator FlhF	1,007	1.3	1.8	3.1	6.5	10.9	2.7
Psysr_3440	flhA	flagellar biosynthesis protein FlhA	349	1.2	1.5	3.3	5.1	15.5	3.3
Psysr_3441	flhB	flagellar biosynthesis protein FlhB	600	1.3	1.3	2.6	4.4	8.5	3.0
Psysr_3442	fliR	Flagellar biosynthesis protein FliR	212	1.4	1.2	2.5	2.9	8.9	2.4
Psysr_3443	fliQ	Flagellar biosynthesis protein FliQ	195	1.2	1.2	3.1	2.8	7.4	1.7
Psysr_3444	fliP	flagellar biosynthesis protein FliP	643	-1.1	1.2	5.1	2.8	11.9	1.9
Psysr_3445	fliO	Flagellar biosynthesis protein, FliO	1,060	-1.4	1.5	7.1	5.0	15.3	2.8
Psysr_3446	fliN	flagellar motor switch protein	3,184	-1.3	1.7	6.6	5.8	13.3	4.0
Psysr_3447	fliM	Flagellar motor switch protein FliM	867	-1.2	1.8	7.0	7.1	16.9	3.1
Psysr_3448	fliL	Flagellar basal body-associated protein FliL	2,364	-1.7	1.8	7.3	7.7	19.2	4.4
Psysr_3449	fliK	Flagellar hook-length control protein	1,919	-1.5	1.0	1.6	3.1	4.8	-1.1
Psysr_3453	fliJ	flagellar biosynthesis chaperone	328	1.7	1.3	2.0	1.7	5.0	1.9
Psysr_3454	fliI	flagellum-specific ATP synthase	339	1.4	1.4	2.1	1.8	4.8	1.6
Psysr_3455	fliH	flagellar assembly protein H	479	1.3	1.4	2.3	2.0	4.8	1.4
Psysr_3456	fliG	flagellar motor switch protein G	1,909	1.1	1.6	3.7	3.9	12.6	2.5
Psysr_3457	fliF	flagellar MS-ring protein	654	1.0	1.4	4.3	4.6	18.8	3.2
Psysr_3458	fliE	flagellar hook-basal body protein FliE	1,644	-1.2	1.7	5.9	11.0	28.4	4.7
Psysr_3459	fleR	flagellar response regulator	535	-1.2	1.5	2.8	5.3	17.1	3.1
Psysr_3460	fleS	flagellar sensor histidine kinase FleS	451	-1.4	1.2	2.2	5.5	13.7	2.9
Psysr_3461	fleQ	Central regulator of flagellar biosynthesis	1,318	-2.1	-1.1	-1.1	1.1	1.3	-2.0
Psysr_3462	fleP	hypothetical protein	11,128	-4.0	-1.1	-1.2	1.5	2.0	-2.4
Psysr_3463	fliS	Flagellar protein FliS	5,922	-4.1	-1.0	-1.1	1.8	2.6	-2.2
Psysr_3464	fliD	Flagellar hook-associated protein 2	18,176	-3.2	1.0	1.1	2.6	2.1	-1.6
Psysr_3465	flaG	Flagellar protein FlaG protein	31,026	-3.0	-1.1	-1.0	1.4	1.4	-2.1
Psysr_3466	fliC	flagellin	29,368	-3.2	1.3	1.2	2.1	2.2	-1.7
Psysr_3470	flgL	flagellar hook-associated protein FlgL	2,120	-3.1	-1.0	1.4	2.8	4.3	-1.4
Psysr_3471	flgK	flagellar hook-associated protein FlgK	2,510	-3.1	-1.2	1.3	2.0	3.5	-2.0
Psysr_3472	flgJ	flagellar rod assembly protein/muramidase FlgJ	1,308	-1.3	1.9	4.5	9.3	23.5	3.1
Psysr_3473	flgI	flagellar basal body P-ring protein	472	-1.3	1.6	3.9	6.5	19.3	2.0
Psysr_3474	flgH	flagellar basal body L-ring protein	4,386	-1.8	1.8	5.5	11.0	23.5	3.6
Psysr_3475	flgG	flagellar basal body rod protein FlgG	6,187	-2.3	1.9	5.7	12.8	21.3	4.4
Psysr_3476	flgF	flagellar basal body rod protein FlgF	2,895	-2.3	2.2	6.1	14.2	25.3	4.1
Psysr_3477	flaE	Flagellar basal body rod protein	82	-1.1	1.1	-1.1	1.4	2.1	1.2

Psysr#	Gene	Product Name	Fluorescence Intensity	Fold-induction compared to basal medium					
			Basal medium	NaCl	H <sub>2</sub> O <sub>2</sub>	Low Fe	Low N	Epi	Apo
Psysr_3478	flgE	flagellar hook protein FlgE	5,189	-4.1	1.5	2.3	6.3	10.2	1.5
Psysr_3479	flgD	flagellar basal body rod modification protein	2,353	-4.4	1.2	2.1	4.6	8.5	-1.0
Psysr_3480	flgC	flagellar basal body rod protein FlgC	3,924	-4.1	1.2	2.0	4.2	8.0	1.1
Psysr_3481	flgB	flagellar basal body rod protein FlgB	4,865	-3.5	1.2	2.1	4.2	8.6	1.6
Psysr_3487	flgA	flagellar basal body P-ring biosynthesis protein FlgA	593	-1.3	1.4	2.6	4.8	8.3	2.3
Psysr_3488	flgM	Anti-sigma-28 factor, FlgM	9,359	-2.2	-1.0	1.0	1.8	2.3	-1.7
Psysr_3489	flgN	FlgN	4,256	-2.1	-1.2	-1.1	-1.2	1.9	-2.7
Psysr_4493	morA-2	Motility regulator MorA; PAS:GGDEF	626	-1.9	-1.1	-1.1	1.3	1.1	-1.9
<b>Surfactant production</b>									
Psysr_3129	rhlA	HAA surfactant synthase; 3-hydroxyacyl-CoA-acyl carrier protein transferase	13,878	-1.2	4.7	4.5	49.5	9.1	6.7
Psysr_2575	syfR	regulatory protein, LuxR	1,315	-1.6	1.7	5.3	1.8	1.5	2.2
Psysr_2576	syfA	Syringafactin synthase; non-ribosomal peptide synthetase	168	-1.0	-1.0	2.6	1.2	3.4	4.7
Psysr_2577	syfB	Syringafactin synthase; non-ribosomal peptide synthetase	142	1.1	-1.1	1.8	1.2	3.5	5.6
<b>Chemotaxis and chemotaxis (all genes in category are shown)</b>									
Psysr_0071		chemotaxis sensory transducer	210	-1.9	-1.8	-2.4	-2.3	1.6	-2.6
Psysr_0143		chemotaxis sensory transducer	286	-1.2	1.6	1.4	8.2	1.1	-1.2
Psysr_0379		chemotaxis sensory transducer	112	1.1	1.0	-1.0	1.7	1.4	1.6
Psysr_0380		chemotaxis sensory transducer	1,081	-1.8	1.1	2.1	3.3	1.9	1.1
Psysr_0578		chemotaxis sensory transducer	742	-1.2	1.8	1.7	6.9	-1.0	-1.9
Psysr_0781	cheB1	chemotaxis-specific methylesterase	892	2.4	1.2	1.8	2.8	2.1	1.8
Psysr_0782	cheD	chemoreceptor glutamine deamidase CheD	1,258	3.2	1.1	1.5	2.5	2.8	1.9
Psysr_0783	cheR-1	Protein-glutamate O-methyltransferase	702	1.2	-1.1	1.7	2.8	1.9	1.7
Psysr_0784	cheW-1	CheW-like protein	270	-1.2	1.1	1.8	4.6	2.0	1.6
Psysr_0785		chemotaxis sensory transducer	2,453	-1.3	1.1	2.5	8.0	3.7	3.9
Psysr_0786	cheA1	CheW-like protein;Signal transducing histidine kinase	459	-1.1	1.1	2.2	5.1	2.2	2.1
Psysr_0788	cheY1	Response regulator receiver	2,565	-1.5	1.2	2.3	7.5	3.4	3.2
Psysr_0789		chemotaxis sensory transducer	996	-1.3	1.1	2.2	6.5	4.8	2.6
Psysr_0860		chemotaxis sensory transducer	86	-1.1	-1.1	-1.1	-1.0	1.2	1.1
Psysr_0868		chemotaxis sensory transducer	845	-2.1	2.0	1.6	7.8	1.3	-2.4
Psysr_0905		chemotaxis sensory transducer	1,613	-7.0	-1.4	-1.4	-1.1	1.3	-4.3
Psysr_0906		chemotaxis sensory transducer	488	-5.7	-1.1	-1.1	-2.5	1.1	-3.5
Psysr_0913		chemotaxis sensory transducer	609	-1.2	1.5	1.7	5.3	3.3	-1.1
Psysr_1139	cheV-1	Response regulator receiver:CheW-like protein	3,236	-2.6	-1.0	1.0	1.2	1.8	-2.0
Psysr_1150		chemotaxis sensory transducer	1,776	-4.6	-1.4	1.0	-1.0	1.9	-3.6
Psysr_1303	wspA	chemotaxis sensory transducer	1,117	-1.1	-1.1	1.1	1.7	1.6	-1.4
Psysr_1304	wspB	CheW-like protein	494	1.2	-1.2	-1.2	-1.3	-1.2	-2.1
Psysr_1305	wspC	Chemotaxis protein methyltransferase CheR, putative	451	1.3	-1.2	-1.2	-1.3	-1.2	-1.7
Psysr_1306	wspD	CheW-like protein	523	1.1	-1.2	-1.0	-1.0	-1.4	-1.8
Psysr_1307	wspE	Response regulator receiver:CheW-like protein	359	1.0	-1.1	-1.0	-1.2	-1.8	-2.0
Psysr_1308	cheB2	chemotaxis-specific methylesterase	179	1.0	-1.1	-1.1	-1.1	-1.7	-1.6
Psysr_1491		chemotaxis sensory transducer	358	-1.7	-1.1	-1.0	1.1	6.2	-1.2
Psysr_1539		chemotaxis sensory transducer	871	-2.9	-1.5	-2.3	-1.3	5.0	-2.3
Psysr_1776		chemotaxis sensory transducer	196	-1.6	-1.0	1.1	2.2	5.4	1.1
Psysr_1789		chemotaxis sensory transducer	197	1.3	1.9	1.5	2.1	1.5	1.2
Psysr_1798		chemotaxis sensory transducer	256	-4.4	-1.6	-1.6	-1.5	1.4	-3.5
Psysr_2059		chemotaxis sensory transducer	105	-1.3	-1.2	-2.8	-1.7	-2.0	-1.9

Psysr#	Gene	Product Name	Fluorescence Intensity	Fold-induction compared to basal medium					
			Basal medium	NaCl	H <sub>2</sub> O <sub>2</sub>	Low Fe	Low N	Epi	Apo
Psysr_2109		chemotaxis sensory transducer	98	-1.2	-1.2	-1.2	1.5	-1.0	1.2
Psysr_2188		histidine kinase	215	-3.1	-1.1	1.0	1.2	1.5	-2.2
Psysr_2214	bdlA	Methyl-accepting chemotaxis protein	1,775	-2.9	1.0	-1.2	1.3	2.7	-2.4
Psysr_2215		CheW-like protein	500	-2.6	-1.4	-1.2	-1.4	1.9	-1.9
Psysr_2220		chemotaxis sensory transducer	1,185	-2.1	1.9	4.8	5.0	5.9	1.2
Psysr_2237		chemotaxis sensory transducer	740	-2.9	-2.5	-1.7	-1.9	2.5	-1.6
Psysr_2240		chemotaxis sensory transducer	456	-1.4	1.2	1.0	3.8	3.8	1.4
Psysr_2241		chemotaxis sensory transducer	1,167	-3.2	-1.1	1.5	1.1	1.2	-2.5
Psysr_2246		chemotaxis sensory transducer	339	-6.9	-1.5	-1.7	-1.3	-1.3	-7.2
Psysr_2315		chemotaxis sensory transducer	376	-2.4	-1.2	-2.1	-2.1	6.3	-1.7
Psysr_2356		chemotaxis sensory transducer	952	-3.1	-1.2	1.1	1.0	5.1	-2.0
Psysr_2446		MCP methyltransferase, CheR-type	980	-1.4	-1.4	-1.5	-4.4	-3.1	-3.2
Psysr_2447		Protein-glutamate methylesterase	727	-1.2	-1.6	-2.0	-4.9	-4.3	-3.3
Psysr_2634		chemotaxis sensory transducer	1,611	-2.7	1.8	1.4	9.5	7.8	2.0
Psysr_2682	tlpQ	chemotaxis sensory transducer	87	-1.1	1.1	1.0	1.8	-1.1	1.3
Psysr_2878		chemotaxis sensory transducer	385	-4.2	-1.2	1.1	-1.7	2.2	-3.1
Psysr_2966		chemotaxis sensory transducer	243	-1.6	3.2	-1.2	1.3	2.5	1.2
Psysr_3114		chemotaxis sensory transducer	124	-1.8	-1.4	-1.2	-1.3	2.6	-1.3
Psysr_3261		chemotaxis sensory transducer	180	-1.3	-1.3	-1.3	2.6	1.6	-1.1
Psysr_3297	cheV-2	Response regulator receiver: CheW-like protein	896	-3.3	1.0	1.2	1.4	2.6	-3.3
Psysr_3348		chemotaxis sensory transducer	915	1.1	-1.3	1.1	-1.1	8.7	1.2
Psysr_3351		chemotaxis sensory transducer	331	3.9	1.2	-1.2	1.7	2.8	1.2
Psysr_3406	aer-2	Aerotaxis receptor; PAS	836	-3.8	-1.1	1.2	1.0	1.6	-2.5
Psysr_3428	cheW-2	CheW-like protein	6,865	-2.4	1.1	1.3	1.9	3.0	-1.3
Psysr_3429		CheW-like protein	2,319	-2.0	-1.1	-1.1	1.1	2.9	-2.1
Psysr_3433	cheB3	chemotaxis-specific methylesterase	576	-2.2	-1.3	1.0	-1.4	1.8	-2.1
Psysr_3434	cheA2	CheW-like protein; Signal transducing histidine kinase	1,766	-3.0	-1.2	1.2	-1.2	2.3	-3.5
Psysr_3435	cheZ	Chemotaxis phosphatase, CheZ	12,046	-2.3	-1.1	1.3	-1.2	1.9	-1.8
Psysr_3436	cheY2	Chemotaxis response regulator receiver	10,993	-2.6	-1.0	1.3	1.1	2.0	-1.8
Psysr_3485	cheR-2	Chemotaxis protein methyltransferase CheR, putative	2,359	-2.5	1.1	1.1	2.0	1.8	-1.2
Psysr_3486	cheV-3	Response regulator receiver: CheW-like protein	7,263	-3.2	1.4	1.2	3.2	2.3	-1.5
Psysr_3534		chemotaxis sensory transducer	460	-9.7	-3.1	-2.1	-8.8	1.2	-6.6
Psysr_3589		Response regulator receiver	1,023	-1.2	-1.1	-1.1	-2.1	-2.5	-2.7
Psysr_3735	aer-1	Aerotaxis receptor; PAS	417	-1.5	1.7	2.0	4.5	1.4	1.4
Psysr_4209		chemotaxis sensory transducer	648	-3.4	-1.2	-2.1	-2.0	2.0	-2.4
Psysr_4218		chemotaxis sensory transducer	265	-3.5	1.0	-1.8	2.5	1.3	-2.4
Psysr_4706		Methyl-accepting chemotaxis protein	258	-1.8	-1.9	-1.7	-1.4	2.3	-1.2
Psysr_4907		PAS	915	-1.3	1.8	1.4	6.1	2.4	1.1
Psysr_5004		chemotaxis sensory transducer	100	-1.4	1.0	-1.1	1.3	2.1	-1.1
Psysr_5092		chemotaxis sensory transducer	254	-3.7	1.0	-1.1	-1.2	-2.1	-4.6
Psysr_5093		chemotaxis sensory transducer	237	1.9	1.1	-1.3	1.2	4.5	1.2
<b>Phenylalanine catabolism</b>									
Psysr_3575	phhA	phenylalanine 4-monooxygenase	759	1.1	1.1	1.4	1.9	37.9	9.6
Psysr_3576	phhB	pterin-4-alpha-carbinolamine dehydratase	1,142	-1.7	1.5	1.8	1.9	8.0	2.8
Psysr_3325	hmgB	Fumarylacetoacetase	315	1.5	1.2	1.5	6.3	7.0	5.3
Psysr_3326	hmgA	Homogentisate 1,2-dioxygenase	360	1.6	1.1	1.4	8.3	10.0	5.9
Psysr_3330	hpd	4-hydroxyphenylpyruvate dioxygenase	647	-1.0	1.2	1.1	9.9	8.2	8.4

Psysr#	Gene	Product Name	Fluorescence Intensity	Fold-induction compared to basal medium					
			Basal medium	NaCl	H <sub>2</sub> O <sub>2</sub>	Low Fe	Low N	Epi	Apo
Psysr_3237	dhcA	3-oxoacid-CoA transferase	762	-1.6	-1.4	1.2	2.1	16.4	5.5
Psysr_3238	dhcB	3-oxoacid-CoA transferase	868	-1.7	-1.6	1.3	1.5	13.8	6.7
<b>Tryptophan and indole acetic acid metabolism</b>									
Psysr_0033	trpA	tryptophan synthase subunit alpha	723	1.6	1.7	1.7	2.2	4.1	1.4
Psysr_0034	trpB	tryptophan synthase subunit beta	1,803	1.7	1.6	2.0	2.3	4.2	1.8
Psysr_0035	trpI	Transcriptional regulator of the trpAB operon	316	7.8	1.1	-1.0	1.1	1.3	5.9
Psysr_4579	trpC	Indole-3-glycerol-phosphate synthase	2,474	-1.3	1.7	1.2	-1.2	-2.1	-1.5
Psysr_4580	trpD	anthranilate phosphoribosyltransferase	1,873	-1.3	2.0	1.1	-2.2	-2.4	-1.8
Psysr_4581	trpG	anthranilate synthase component II	5,777	-1.2	1.9	1.0	-1.8	-1.9	-1.5
Psysr_4609	trpE	Anthranilate synthase component I	1,341	-1.4	1.2	-1.5	-2.1	-2.3	-2.1
Psysr_4667	iaaM-1	Tryptophan 2-monooxygenase	947	1.4	4.9	1.5	7.2	6.9	5.3
Psysr_1536	iaaM-2	Tryptophan-2-monooxygenase	4,631	-1.6	2.2	1.3	4.8	-2.2	-1.1
Psysr_4268	iaaH-1	Indole acetamide hydrolase	93	-1.0	1.2	1.1	2.4	1.1	-1.0
Psysr_2208	iaaH-2	Indole acetamide hydrolase	48	1.0	1.0	-1.0	1.3	1.2	1.2
Psysr_0006		putative phenylacetaldoxime dehydratase	66	1.1	1.0	1.1	1.9	1.2	1.5
Psysr_0007	nit	Aliphatic nitrilase	100	1.1	-1.0	1.1	2.5	1.1	1.7
<b><math>\gamma</math>-amino butyric acid (GABA) metabolism (all genes in category are shown)</b>									
Psysr_4909	gabP	GABA permease	546	1.3	1.1	1.2	1.9	1.0	1.9
Psysr_0090	gabT	4-aminobutyrate aminotransferase	564	4.4	2.4	1.9	2.1	3.8	4.5
Psysr_0091	gabD	Succinate-semialdehyde dehydrogenase I	733	8.9	2.3	2.3	2.2	3.2	8.3
Psysr_0146	gabT-1	4-aminobutyrate aminotransferase	252	1.4	1.2	1.1	1.6	3.1	11.4
Psysr_0149	gabD-1	Succinic semialdehyde dehydrogenase	156	1.2	1.2	1.2	3.4	2.3	8.0
Psysr_2413	gabD-2	Succinate-semialdehyde dehydrogenase	544	-1.2	1.4	1.9	2.4	1.2	1.1
Psysr_3515	gabT-2	4-aminobutyrate aminotransferase	112	1.3	1.1	-1.0	1.7	2.0	2.7
<b>Syringomycin and syringopeptin synthesis and transport</b>									
Psysr_2601	salA	regulatory protein, LuxR	2,082	1.8	1.1	1.2	1.8	4.2	5.4
Psysr_2602	syrG	regulatory protein, LuxR	5,096	-2.3	-1.2	2.1	3.2	11.2	16.1
Psysr_2607	syrF	regulatory protein, LuxR	1,530	1.2	-1.1	2.1	1.7	7.2	23.2
Psysr_2608	syrE	Syringomycin synthesis, Amino acid adenylation	322	-1.1	-1.1	1.0	1.2	5.6	15.2
Psysr_2609	syrC	Syringomycin synthesis, Alpha/beta hydrolase fold	227	1.1	1.0	1.1	1.2	3.9	10.1
Psysr_2610	syrB2	Syringomycin synthesis, chlorinating enzyme	4,198	1.1	-1.0	1.7	1.0	12.5	37.5
Psysr_2611	syrB1	Syringomycin synthesis, Amino acid adenylation	1,266	1.1	1.1	1.9	1.3	19.1	49.1
Psysr_2612	syrP	Syringomycin regulation, syrP protein, putative	1,432	1.0	1.0	3.1	1.1	13.5	63.3
Psysr_2613	syrD	Syringomycin synthesis, Cyclic peptide transporter	981	1.0	1.0	2.2	1.3	12.3	38.8
Psysr_2614	sypA	Syringopeptin synthesis, Amino acid adenylation	193	1.1	-1.0	-1.0	1.3	3.0	7.2
Psysr_2615	sypB	Syringopeptin synthesis, Amino acid adenylation	255	1.2	1.1	1.1	1.4	3.2	9.8
Psysr_2616	sypC	Syringopeptin synthesis, Amino acid adenylation	200	-1.0	-1.1	1.0	1.3	2.7	5.8
Psysr_2617	pseE	Secretion protein HlyD	937	1.1	-1.1	1.1	1.3	6.2	14.7
Psysr_2618	pseF	ABC transporter	323	1.3	-1.0	1.1	1.3	4.6	8.2
Psysr_2620	pseA	Syringomycin and syringopeptin secretion; RND efflux system, outer membrane lipoprotein, NodT	109	1.0	1.0	1.1	1.3	1.5	4.4
Psysr_2621	pseB	Syringomycin and syringopeptin secretion; Secretion protein HlyD	74	-1.0	-1.1	-1.0	1.5	1.3	1.6
Psysr_2622	pseC	Syringomycin and syringopeptin secretion; Acriflavin resistance protein	72	1.0	-1.0	1.0	1.2	1.3	1.9
<b>Syringolin synthesis and transport</b>									
Psysr_1702	sylA	Syringolin A regulator, regulatory protein, LuxR	619	-1.2	1.1	1.3	1.6	1.8	5.7
Psysr_1703	sylB	Syringolin A synthesis, Fatty acid desaturase	595	-1.4	-1.2	1.4	2.2	2.0	8.7
Psysr_1704	sylC	Syringolin A synthesis, Amino acid adenylation	931	-1.1	1.4	1.7	4.9	1.6	9.9

Psysr#	Gene	Product Name	Fluorescence Intensity	Fold-induction compared to basal medium					
			Basal medium	NaCl	H <sub>2</sub> O <sub>2</sub>	Low Fe	Low N	Epi	Apo
Psysr_1705	syID	Syringolin A synthesis, Amino acid adenylation	426	1.6	1.1	1.2	1.2	1.4	6.1
Psysr_1706	syIE	Syringolin A exporter, major facilitator transporter	119	1.1	-1.1	-1.0	1.2	1.1	2.2
<b>Selected nonribosomal peptide synthases (and co-transcribed genes)</b>									
Psysr_4311	fabD-2	Malonyl CoA-acyl carrier protein transacylase	1,130	-1.4	-1.3	1.0	1.4	1.6	4.1
Psysr_4312		Erythronolide synthase	2,968	-1.6	-1.2	-1.0	1.3	2.3	6.0
Psysr_4313		beta-ketoacyl synthase	1,428	-1.0	-1.1	-1.2	1.8	3.1	9.4
Psysr_4314		beta-ketoacyl synthase	818	-1.1	-1.1	-1.1	2.3	4.5	15.4
Psysr_4315		Asparagine synthase, glutamine-hydrolyzing	1,826	-1.3	-1.3	-1.2	1.1	11.3	35.6
Psysr_3722		Amino acid adenylation	160	1.5	1.1	1.1	1.3	1.1	2.5
Psysr_1792		Amino acid adenylation	151	-1.2	1.3	1.0	1.0	1.0	1.1
Psysr_1793		Amino acid adenylation	104	1.2	1.3	1.3	1.0	-1.1	1.2
Psysr_1794		Amino acid adenylation	86	1.2	1.1	1.2	1.1	-1.1	1.2
Psysr_1795		Taurine dioxygenase	99	-1.1	-1.2	1.3	-1.3	-1.6	-1.3
Psysr_4662		Amino acid adenylation	104	1.1	-1.1	-1.2	-1.2	-1.5	-1.2
Psysr_5009		Signal metabolite synthesis <sup>1</sup>	597	-1.4	1.4	1.8	2.7	1.1	1.2
Psysr_5010		Signal metabolite synthesis <sup>1</sup>	168	-1.3	1.3	1.7	2.0	-1.2	1.0
Psysr_5011		Signal metabolite synthesis <sup>1</sup> ; Amino acid adenylation	217	-1.2	1.1	1.8	1.5	-1.3	1.3
Psysr_5012		Signal metabolite synthesis <sup>1</sup>	306	-1.0	-1.3	1.2	1.3	-1.2	1.7
<b>Polysaccharide synthesis (selected genes in category are shown)</b>									
Psysr_0054	algR3	Alginate regulatory protein AlgR3	20,871	-1.4	1.4	1.5	1.9	1.7	1.7
Psysr_0056	algQ	Anti-RNA polymerase sigma 70 factor	2,481	-1.5	1.3	1.3	2.3	-1.1	1.0
Psysr_0063	algR	Alginate regulatory protein; Response regulator receiver	1,190	8.1	1.7	2.0	7.8	4.9	5.9
Psysr_0064	algZ	Histidine kinase internal region	1,039	3.2	1.7	1.8	6.5	3.4	4.9
Psysr_0219	algC	Phosphomannomutase	3,731	2.6	-1.0	1.1	-1.4	1.2	-1.1
Psysr_0263	algB	Alginate regulator; Two-component response regulator	1,604	1.6	1.2	1.1	1.4	-1.5	-1.4
Psysr_0264	kinB	Putative two-component sensor kinase for AlgB	422	2.3	1.0	-1.2	-1.0	-1.3	-1.1
Psysr_0937	algA-1	Mannose-1-phosphate guanylyltransferase/mannose-6-phosphate isomerase	4,816	-1.7	-1.1	-1.3	-2.5	-1.4	-3.0
Psysr_1052	algA-2	phosphate isomerase	4,071	1.2	-2.8	-5.2	-1.5	-1.7	1.2
Psysr_1053	algF	Alginate biosynthesis protein AlgF	6,158	1.5	-2.9	-8.4	-7.4	-1.7	1.3
Psysr_1054	algJ	Alginate biosynthesis protein AlgJ	2,019	3.6	-1.8	-5.3	-3.9	1.1	1.5
Psysr_1055	algI	Alginate biosynthesis; Membrane bound O-acyl transferase, MBOAT	2,465	5.0	-1.6	-5.2	-5.4	1.4	1.9
Psysr_1056	algL	Alginate lyase; Poly(beta-D-mannuronate) lyase	2,184	8.7	1.1	-2.7	-2.1	2.3	3.3
Psysr_1057	algX	Alginate biosynthesis protein AlgX	1,388	9.8	1.2	-3.2	-1.9	3.1	2.9
Psysr_1058	algG	Alginate biosynthesis; parallel beta-helix repeat-containing protein	1,524	11.0	1.2	-2.5	-1.5	4.0	3.1
Psysr_1059	algE	Alginate biosynthesis protein AlgE	737	13.8	1.2	-2.6	-1.5	5.2	3.0
Psysr_1060	algK	Alginate biosynthesis; Sel1 repeat-containing protein	681	13.2	1.2	-2.5	-1.1	6.1	3.0
Psysr_1061	alg44	Alginate biosynthesis protein Alg44	828	14.5	1.1	-2.4	-1.1	7.7	4.3
Psysr_1062	alg8	Alginate biosynthesis protein Alg8	1,704	19.9	1.1	-2.1	-1.2	8.1	5.1
Psysr_1063	algD	Alginate biosynthesis; GDP-mannose 6-dehydrogenase	2,975	8.8	-1.2	-3.5	1.2	4.1	3.1
Psysr_3955	mucD	Negative regulator of alginate biosynthesis	2,034	1.2	-1.1	1.6	-1.2	1.1	1.1
Psysr_3956	mucB	Negative regulator of alginate biosynthesis	6,867	4.7	1.0	-1.6	-2.4	3.1	2.4
Psysr_3957	mucA	Anti-sigma factor for AlgU	8,317	4.8	1.5	-1.2	1.8	4.7	4.1
Psysr_3958	algU	RNA polymerase sigma factor	10,460	3.7	1.1	-1.5	1.1	2.2	1.9
Psysr_0754	lsc-1	Levan synthesis; Levansucrase	2,419	-2.0	-1.6	2.5	-1.5	-1.0	3.6
Psysr_2103	lsc-2	Levan synthesis; Levansucrase	545	-1.1	-1.2	1.7	1.8	1.6	5.4

Psysr#	Gene	Product Name	Fluorescence Intensity	Fold-induction compared to basal medium					
			Basal medium	NaCl	H <sub>2</sub> O <sub>2</sub>	Low Fe	Low N	Epi	Apo
Psysr_0377	mdoG	Glucan biosynthesis protein G	9,273	1.8	1.1	-1.2	-1.7	-1.1	-1.3
Psysr_0378	mdoH	Glucan biosynthesis; Glucosyltransferase MdoH	1,142	1.9	-1.3	-1.4	-2.6	-1.5	-2.0
Psysr_5085	mdoD	Glucan biosynthesis protein D	1,209	3.9	1.6	-1.1	1.1	2.0	3.1
<b>Compatible solute synthesis (selected genes in category are shown)</b>									
Psysr_2489		Trehalose synthesis, Alpha amylase, catalytic region	1,789	22.2	1.9	1.3	4.1	14.9	31.3
Psysr_2490	treS	Trehalose synthesis, Alpha amylase, catalytic region	637	16.2	1.7	1.0	1.9	8.5	13.7
Psysr_2491	glgB	Trehalose synthesis, glycogen branching enzyme	1,913	10.4	1.9	-1.1	1.8	5.4	10.3
Psysr_2992	glgA	Trehalose synthesis, glycogen synthase	3,952	11.2	2.2	2.3	25.3	10.2	13.5
Psysr_2993	treZ	Trehalose synthesis, Alpha amylase, catalytic region	1,392	14.0	2.5	2.1	11.5	5.5	8.9
Psysr_2994	malQ	Trehalose synthesis, glycoside hydrolase family protein	1,897	13.1	2.1	1.6	5.9	6.2	8.7
Psysr_2995	treY	Trehalose synthesis, Alpha amylase, catalytic region	940	10.3	1.8	1.2	4.1	5.1	5.6
Psysr_2996		Trehalose synthesis (putative), hypothetical protein	5,167	10.2	2.1	1.7	22.9	11.2	14.3
Psysr_2997	glgX	Trehalose synthesis (putative), glycoside hydrolase	2,197	13.2	2.3	1.0	3.9	14.5	12.3
Psysr_2998		Trehalose synthesis operon, hypothetical protein	137	6.9	1.1	-1.3	1.4	3.4	2.9
Psysr_2999		Trehalose synthesis operon, LmbE-like protein	286	11.8	1.3	-1.2	1.5	4.9	5.4
Psysr_3000		Trehalose synthesis operon, methyltransferase, putative	187	12.4	1.2	-1.2	1.3	4.5	5.2
Psysr_3001		Trehalose synthesis operon, glycosyl transferase protein	221	8.8	1.4	-1.0	1.8	5.9	6.1
Psysr_3002		Trehalose synthesis operon, hypothetical protein	321	3.7	1.1	1.2	10.1	4.8	2.8
Psysr_3747	ggnA	NAGGN synthase, Asparagine synthase	2,458	81.3	1.6	1.0	1.6	6.1	21.0
Psysr_3748	ggnB	NAGGN synthase, GCN5-related N-acetyltransferase	1,440	77.5	1.4	-1.1	1.5	5.1	16.6
Psysr_3749	ggnC	NAGGN synthase, Peptidase M42	1,110	52.3	1.5	-1.2	1.7	5.2	19.6
Psysr_3750	ggnD	Putative NAGGN synthase, hypothetical protein	977	9.9	1.1	-1.1	1.3	1.6	4.4
<b>Quaternary ammonium compound (QAC) transporters</b>									
Psysr_4249	opuCA	Glycine betaine, choline, carnitine (BCC) ABC transporter, ATP-binding subunit	523	25.7	1.0	-1.3	-1.5	1.7	3.0
Psysr_4250	opuCB	BCC transporter, permease	1,888	31.9	-1.0	-1.6	-2.7	1.7	4.0
Psysr_4251	opuCC	BCC transporter, substrate binding protein	1,886	37.4	-1.1	-1.7	-2.6	1.5	3.8
Psysr_4252	opuCD	BCC transporter, permease	3,616	27.0	-1.0	-1.9	-4.3	1.4	4.5
Psysr_4709	cbcX	BCC ABC transporter, substrate binding protein	2,947	19.4	-1.1	-1.2	7.2	3.2	4.5
Psysr_4710	cbcW	BCC ABC transporter, permease	2,136	22.4	-1.1	-1.1	3.9	2.7	5.2
Psysr_4711	cbcV	BCC transporter, ATP-binding subunit	895	20.1	-1.1	1.1	7.6	3.1	4.8
Psysr_4827	betT	Choline transporter transporter family	476	5.3	-1.2	-1.2	-1.7	1.5	3.7
<b>Siderophore synthesis and transport (selected genes in category are shown)</b>									
Psysr_1943	pvdS	Pyoverdin regulator; ECF Sigma-70 factor	640	1.7	3.5	7.6	-2.6	1.5	1.9
Psysr_1944	pvdG	Pyoverdin synthesis; Thioesterase	929	1.0	12.7	53.4	-1.1	1.3	1.1
Psysr_1945	pvdL	Pyoverdin synthesis; peptide synthase	588	-1.0	7.6	48.5	-1.0	1.3	1.2
Psysr_1946	pvdH	Pyoverdin synthesis; Diaminobutyrate-2-oxoglutarate aminotransferase	1,751	1.5	16.0	65.4	-1.2	1.7	1.3
Psysr_1947		Pyoverdin synthesis; MbthH-like protein	5,040	1.6	8.8	27.2	3.5	2.5	2.4
Psysr_1956		Pyoverdin regulator	5,278	1.2	23.3	93.5	-1.4	4.2	2.4
Psysr_1957	pvdI	Pyoverdin synthesis; Amino acid adenylation	702	1.2	10.1	35.6	-1.2	1.2	1.1
Psysr_1958	pvdJ	Pyoverdin synthesis; Non-ribosomal peptide synthase	472	1.0	9.0	30.6	1.1	1.3	1.2
Psysr_1959	pvdK	Pyoverdin synthesis; Amino acid adenylation	928	1.5	18.8	53.8	-1.0	1.6	1.6
Psysr_1960	pvdD	Pyoverdin synthesis; Non-ribosomal peptide synthase	577	1.5	7.3	35.0	-1.0	1.2	1.4
Psysr_1963	pvdE	Pyoverdin transport; Cyclic peptide transporter	397	-1.2	4.7	18.2	1.0	1.3	1.1
Psysr_1964	pvdO	Pyoverdin synthesis; hypothetical protein	2,113	-1.1	11.7	49.4	-1.6	2.1	1.9
Psysr_1965	pvdN	Pyoverdin synthesis; aminotransferase	929	1.1	9.1	30.9	-1.3	1.2	1.4
Psysr_1966	pvdM	Pyoverdin synthesis; Peptidase M19, renal dipeptidase	1,395	1.4	10.1	32.0	-1.8	1.5	1.5



Psysr#	Gene	Product Name	Fluorescence Intensity	Fold-induction compared to basal medium					
			Basal medium	NaCl	H <sub>2</sub> O <sub>2</sub>	Low Fe	Low N	Epi	Apo
Psysr_1967		Pyoverdinin synthesis; TAT pathway signal	518	1.3	6.9	18.2	-1.4	1.1	1.2
Psysr_1968	opMQ	Pyoverdinin efflux; outer membrane lipoprotein	125	1.0	2.9	6.9	1.1	1.3	1.2
Psysr_1969	pvdT	Pyoverdinin efflux; ABC transporter	333	1.4	5.4	13.4	-1.2	1.3	1.4
Psysr_2582		Transporter for Fe-Achromobactin	538	1.2	1.6	2.9	-2.7	1.6	2.5
Psysr_2583	acsF	Diaminobutyrate-2-oxoglutarate aminotransferase	2,426	-1.1	3.8	17.2	-1.3	2.8	4.8
Psysr_2584	acsD	Achromobactin synthesis, lucA/lucC	325	-1.2	2.1	9.4	-1.0	2.0	2.0
Psysr_2585	acsE	Achromobactin synthesis, Orn/DAP/Arg decarboxylase	345	-1.1	2.2	12.1	1.2	2.0	2.4
Psysr_2586	yhcA	Achromobactin synthesis	113	-1.1	1.3	4.1	1.1	1.5	1.3
Psysr_1970	pvdR	Pyoverdinin efflux; Secretion protein HlyD	321	1.2	5.0	13.0	-1.1	1.4	1.2
Psysr_2587	acsC	Achromobactin synthesis, lucA/lucC	351	-1.2	1.9	9.8	-1.2	1.8	2.2
Psysr_2588	acsB	Achromobactin synthesis, HpcH/HpaI aldolase	181	-1.1	1.3	6.2	-1.1	1.3	1.4
Psysr_2589	acsA	Achromobactin synthesis, lucA/lucC	904	-1.1	1.7	11.9	-1.2	1.7	2.8
Psysr_2590	cbrA	Achromobactin ABC transporter, substrate binding protein	124	-1.0	-1.1	1.8	-1.4	-1.4	-1.3
Psysr_2591	cbrB	Achromobactin ABC transporter, permease	221	1.5	-1.0	1.4	-1.5	-1.3	1.1
Psysr_2592	cbrC	Achromobactin ABC transporter, permease	229	1.5	-1.1	1.1	-1.6	-1.3	1.0
Psysr_2593	cbrD	Achromobactin ABC transporter	253	1.2	-1.0	1.2	-1.6	-1.9	-1.4
Psysr_0203	tonB-1	Tripartite ferric-siderophore uptake complex; TonB	1,006	1.2	-1.3	4.1	-7.2	1.1	-1.7
Psysr_0204	exbD-1	Tripartite ferric-siderophore uptake complex; ExbD	3,232	1.1	-1.1	4.2	-12.3	1.2	-1.5
Psysr_0205	exbB-1	Tripartite ferric-siderophore uptake complex; ExbB	1,666	1.1	1.2	4.2	-4.9	1.1	-1.3
<b>Iron metabolism and transport (selected genes in category are shown)</b>									
Psysr_1124		Ferritin-like superfamily protein; hypothetical protein	19,987	17.3	-1.1	1.1	2.0	14.7	20.6
Psysr_1404	dps	Ferritin and Dps	8,650	1.0	1.3	1.2	1.3	-1.2	1.0
Psysr_4521	bfrA	Bacterioferritin	1,607	-1.6	1.1	-2.5	3.6	-1.4	-2.9
Psysr_3897	bfrB	Bacterioferritin	985	-1.9	-1.3	-2.4	4.5	1.2	-1.6
Psysr_4448		Ferritin and Dps family protein	5,990	11.1	-2.3	-6.4	2.5	5.7	8.4
Psysr_1039	fecR	FecR protein; Anti-sigma factor for FecI	96	-1.1	1.2	2.7	-1.3	-1.3	-1.4
Psysr_1040	fecI	FecI protein; RNA polymerase ECF sigma factor	296	-1.2	1.5	4.4	-3.1	-2.1	-2.6
Psysr_1106		FecR-like protein; Anti-sigma factor	77	1.2	1.3	1.4	1.4	1.1	1.3
Psysr_1107		FecI-like protein; RNA polymerase ECF sigma factor	412	5.5	1.2	2.9	2.0	-1.2	3.2
Psysr_4730		FecR-like protein; Anti-sigma factor	163	1.0	1.1	2.5	-1.7	-1.1	-1.2
Psysr_4731		FecI-like protein; RNA polymerase ECF sigma factor	157	1.1	1.3	3.4	-1.9	-1.2	-1.3
<b>Antioxidant enzymes involved in oxidative stress tolerance (all genes in category are shown)</b>									
Psysr_2974	ahpF	Alkyl hydroperoxide reductase subunit F	932	-1.8	4.1	-1.0	1.4	1.3	-1.1
Psysr_2975	ahpC	Alkyl hydroperoxide reductase subunit C	20,975	-1.3	2.2	1.5	1.1	-1.1	1.3
Psysr_3627	ohr	Organic hydroperoxide resistance protein	473	-1.3	3.0	-1.4	2.8	-1.6	-1.9
Psysr_4522	katA	Catalase	278	1.4	2.8	-1.2	1.1	1.1	1.5
Psysr_3353	katB	Catalase	3,174	-1.0	3.2	-9.8	1.7	-1.0	2.1
Psysr_0280	katE	Hydroperoxidase II	1,084	12.9	1.1	-1.3	1.3	11.8	31.0
Psysr_4208	katG	Haem catalase/peroxidase	6,627	-1.0	1.9	-1.8	6.6	1.9	3.4
Psysr_5095	katN	Catalase	340	1.2	1.3	1.0	4.9	7.7	14.9
Psysr_4152	sodA	Superoxide dismutase	5,623	1.6	11.9	40.2	-2.0	3.2	2.7
Psysr_4059	sodB	Superoxide dismutase	13,513	1.1	-1.6	-3.6	1.5	-1.3	1.4
Psysr_1154	sodC	Copper/Zinc superoxide dismutase	250	6.2	1.5	1.1	1.9	5.9	6.6
Psysr_4478	cpoF	chloroperoxidase precursor; Alpha/beta hydrolase fold	2,173	13.2	1.8	1.3	3.4	10.6	49.4
Psysr_1016	trxB	Thioredoxin reductase	1,119	-1.6	1.3	-1.1	-1.0	-1.5	-1.7
Psysr_2544		Alkylhydroperoxidase AhpD core	97	1.3	-1.2	-1.2	1.3	1.1	-1.1
Psysr_3369		Tat-translocated enzyme:Dyp-type peroxidase	1,389	-1.5	1.3	3.4	-7.7	-3.6	-4.9

Psysr#	Gene	Product Name	Fluorescence Intensity	Fold-induction compared to basal medium					
			Basal medium	NaCl	H <sub>2</sub> O <sub>2</sub>	Low Fe	Low N	Epi	Apo
Psysr_3626	ohrR	Organic hydroperoxide resistance regulatory protein	1,325	-1.2	1.3	1.1	2.2	-1.4	-1.0
Psysr_4877		Peroxidase	7,449	-2.2	1.4	1.3	1.8	1.6	-1.1
<b>Nitrogen metabolism (the 15 gene that were most induced by N limitation are shown)</b>									
Psysr_4453	ureG-2	Urease accessory protein UreG	1,257	-1.0	1.5	-1.1	38.2	1.1	1.1
Psysr_0189	amtB-1	Ammonium transporter	6,676	-1.4	1.4	1.2	37.8	1.7	1.5
Psysr_4451	ureE	Urease accessory protein UreE	530	1.1	1.3	-1.0	28.1	1.2	1.3
Psysr_4822	ntrC	Two-component response regulator NtrC	2,065	1.4	1.6	1.2	27.5	2.1	1.3
Psysr_4821	ntrB	Two-component sensor histidine kinase NtrB	1,434	1.4	1.1	1.1	24.7	1.3	1.2
Psysr_1166	amiF	Formamidase	818	-1.0	1.1	1.5	24.4	1.5	1.3
Psysr_3099	nirB	Nitrite/sulfite reductase	347	1.0	1.0	1.0	22.6	2.0	1.9
Psysr_4452	ureF-2	Urease accessory protein UreF	329	-1.1	1.3	-1.1	22.6	1.2	-1.1
Psysr_4454	ureJ-2	HupE/UreJ protein	235	1.0	1.3	-1.1	16.9	1.1	-1.1
Psysr_0190	glnK	Nitrogen regulatory protein P-II	15,714	-1.6	1.4	1.5	10.9	1.4	1.6
Psysr_2099	nasA	Assimilatory nitrate reductase	201	1.1	-1.0	1.0	8.8	1.7	2.0
Psysr_4817	glnA-1	Glutamine synthetase type I	12,515	-1.6	1.6	2.0	8.3	1.5	1.3
Psysr_3100	nirD	Nitrite reductase [NAD(P)H], small subunit	148	1.2	1.1	-1.1	7.7	1.6	1.7
Psysr_2275		Glutamate synthase, alpha subunit, C-terminal	267	-1.0	1.1	1.1	6.7	1.5	1.6
Psysr_2273	glnA-2	Glutamine synthetase, type III	232	1.0	1.0	1.2	6.6	1.5	1.7
<b>Sulfur metabolism and transport (selected genes in category are shown)</b>									
Psysr_2514		Sulfonate ABC transporter	154	-1.1	1.1	1.1	1.8	2	1.9
Psysr_2515		Sulfonate ABC transporter, permease	129	1.1	1	1.2	1.6	3.2	2.8
Psysr_2516		Sulfonate ABC transporter, substrate-binding protein	298	-1.1	1.1	1.2	1.8	4.4	3.1
Psysr_4873	ssuF	Molybdenum-pterin binding protein	355	3	1.2	-1.1	-1.2	2.5	1.1
Psysr_4874	ssuB	Sulfonate ABC transporter, ATP-binding subunit	425	5.3	1.7	1	1.4	2.7	1.3
Psysr_4875	ssuC	Sulfonate ABC transporter, permease	1,318	5.8	1.8	-1.2	1.2	3.8	1.9
Psysr_4876	ssuA	Sulfonate ABC transporter, substrate-binding protein	577	4.2	1.5	-1.1	1.1	3.9	1.2
Psysr_3598		Putative sulfonate ABC transporter, permease	145	1.5	1.1	1	1.4	1.9	2.5
Psysr_3599		Alkanesulfonate monooxygenase	1,083	1.2	2.3	2.1	2.4	8.8	8.4
Psysr_3601		Cysteine dioxygenase type I	200	1	1.6	1	1.4	2.5	2.3
Psysr_3603		Sulfonate ABC transporter, substrate-binding protein	271	-1	1.8	1.2	1.3	2.8	2.6
Psysr_4824		Alkanesulfonate transporter substrate-binding protein	284	1.4	1.3	1	1	1.1	1.7
Psysr_3233	ssuE	Sulfonate metabolism gene; FMN reductase	205	-1.2	1.1	1.3	2	2.7	2.1
Psysr_3247	msuD	Methanesulfonate sulfonase MsuD	1,461	6	2.3	-1.1	-1.3	5.1	1
Psysr_3248	sfnR	Regulator of sulfonate metabolism	1,337	6.4	1.8	-1.1	-1.5	5.2	1.2
Psysr_0352		Putative sulfonate monooxygenase protein	196	1.2	1.1	1	1.3	1.8	2.2
Psysr_2280		Alkanesulfonate monooxygenase	2,189	1.1	1.3	1.6	5.2	17.6	7.7
Psysr_0081	cysA	Sulfate ABC transporter protein, ATPase component	488	2.8	1	-1.1	-1.5	1.9	-2
Psysr_0082	cysW1	Sulfate ABC transport protein, permease	393	2.8	-1.2	-1.4	-2.1	1.9	-1.8
Psysr_0083	cysW2	Sulfate ABC transport protein, permease	1,153	2.5	-1	-1.5	-3.7	2.2	-2.5
Psysr_0084	cysP	Sulfate ABC transport protein, substrate-binding protein	3,844	3.8	1.4	-1.3	-3	4.4	-1.5
Psysr_0287		Sulfate transporter	1,891	2	1.4	1.2	1.9	35.1	13.5
Psysr_3086		Sulfate transporter/antisigma-factor antagonist STAS	217	-1.9	-1.1	1.1	-2.2	1.8	-1.2
Psysr_0850		Putative sulfite oxidase subunit YedY	3,155	-1.1	1.5	1.5	4.5	2.9	2.3
Psysr_0851		Putative sulfite oxidase subunit YedZ	3,471	-1	1.3	1.4	2.6	1.9	2
Psysr_0337	tauD-1	Taurine dioxygenase	725	5.2	2.1	-1.1	-1.1	3.3	1.1
Psysr_2354	tauD-2	Taurine catabolism dioxygenase TauD/TfdA	584	1.6	1.7	1.4	1.4	1.9	2
Psysr_0134		Putative cysteine desulfurase	467	-1.6	1.4	1.2	2.4	5.8	1.7



Psysr#	Gene	Product Name	Fluorescence Intensity	Fold-induction compared to basal medium					
			Basal medium	NaCl	H <sub>2</sub> O <sub>2</sub>	Low Fe	Low N	Epi	Apo
Psysr_3372		Putative thiosulfate reductase cytochrome B subunit	2,911	1.5	1.8	2.8	17.4	3.8	9.4
<b>Phosphate metabolism and transport (selected genes in category are shown)</b>									
Psysr_2354	phoD	Alkaline phosphatase	166	1.0	1.3	1.2	3.1	1.4	1.3
Psysr_3150	gspF	Alkaline phosphatase secretion	216	7.7	-1.0	-1.3	-1.3	2.1	1.8
Psysr_5032	phoB	PhoB regulator of phosphate assimilation	401	-1.4	1.0	1.1	3.7	3.1	1.5
Psysr_5033	phoR	PhoR regulator of phosphate assimilation	118	1.1	1.1	1.0	1.6	1.5	1.4
Psysr_3103	pstB	Phosphate ABC transporter, ATP-binding subunit	544	-1.5	1.1	1.3	3.1	10.1	1.8
Psysr_3104	pstA	Phosphate ABC transporter permease	670	-1.5	-1.3	-1.0	2.0	12.6	2.4
Psysr_3105	pstC	phosphate ABC transporter permease	808	-1.6	-1.2	1.1	1.8	19.0	3.4
Psysr_3106	pstS	phosphate ABC transporter, substrate-binding protein	4,094	-2.5	-1.1	1.3	3.4	32.4	5.2
<b>Amino acid metabolism and transport (selected genes in category are shown)</b>									
Psysr_3878	hisP	Amino acid ABC transporter	374	-1.8	-1.1	-1	2.6	1	-1.5
Psysr_3908	gltI	Glutamate/aspartate ABC transporter, substrate-binding protein	2,017	-5.2	-1.2	1.4	1.4	6	2.4
Psysr_3909	gltJ	Glutamate/aspartate ABC transporter, permease	934	-3.8	-1.5	1.3	-1.1	4.9	2.1
Psysr_3910	gltK	Glutamate/aspartate ABC transporter, permease	874	-3.4	-1.6	1.3	-1.4	4.6	2.2
Psysr_3911	gltL	Glutamate/aspartate ABC transporter, ATP-binding protein	881	-2.5	-1.1	1.2	1.7	3.3	1.7
Psysr_2941	glnH	Glutamine ABC transporter, substrate-binding protein	719	3.4	1.3	-1.1	1.1	4	2.4
Psysr_2942	glnQ	Glutamine ABC transporter, ATP-binding protein	216	3.1	1.1	-1.2	-1	2.4	1.2
Psysr_2943	glnP	Glutamine ABC transporter, permease	1,506	4.4	1.1	-1.3	-1.1	3.4	2.8
Psysr_2944		Glutamine ABC transporter, permease	361	3.7	1.1	-1.1	1.1	2.7	2
Psysr_0349	metI-1	Methionine ABC transporter, permease	164	1.1	1.2	1.1	1.4	1.7	2.3
Psysr_0350	metN-1	Methionine ABC transporter, ATP-binding protein	139	-1	1.1	1.1	1.4	1.5	1.9
Psysr_0351	metQ-1	Methionine ABC transporter, substrate-binding protein	265	1.1	1.3	1.3	2.1	2.1	2.5
Psysr_4828	hutG	urocanate hydratase	436	-1	1.2	-1	7.3	17.0	6.5
Psysr_4829		Histidine ABC transporter, substrate-binding protein	1,131	1.2	1.2	1.1	17.4	13.0	7.0
Psysr_4830		Histidine ABC transporter, permease	452	1.6	1.7	1.3	4.9	4.4	2.5
Psysr_4831		Histidine ABC transporter, ATP-binding protein	412	1.5	1.4	1.2	4.3	4.1	2.4
Psysr_4832	hutH-2	Histidine ammonia-lyase	118	1.3	1.1	1.1	2.0	2.0	1.5
Psysr_4833	hutH	Histidine ammonia-lyase	308	1.5	1.4	1.4	2.2	2.3	2.2
Psysr_0597	livK-1	Amino acid (branched chain) ABC transporter, substrate-binding protein	4,649	-1.5	1.4	3	69.9	9.0	5.9
Psysr_0598	livH-1	Amino acid (branched chain) ABC transporter, permease	818	-1.3	1	2	16	3.5	3.1
Psysr_0599	livM-1	Amino acid (branched chain) ABC transporter, permease	352	-1.3	-1.1	1.7	7.9	2.4	2.6
Psysr_0600	livG-1	Amino acid (branched chain) ABC transporter, permease	335	-1.1	1.1	1.7	11.0	2.5	1.9
Psysr_0601	livF-1	Amino acid (branched chain) ABC transporter, ATP-binding protein	176	-1.1	1.1	1.2	8.7	2.0	1.7
Psysr_2467	liuD	Leucine catabolism; Carbamoyl-phosphate synthase subunit L	97	1	-1.1	-1.1	1.2	4.2	2.8
Psysr_2468	liuC	Leucine catabolism; Gamma-carboxygeranoyl-CoA hydratase	63	-1	-1.1	-1.1	1.2	2.4	2.3
Psysr_2469	liuB	Leucine catabolism; Propionyl-CoA carboxylase	290	-1.1	1	-1.1	1.5	12.3	9.1
Psysr_2470	liuA	Leucine catabolism; Isovaleryl-CoA dehydrogenase	946	-1	-1.1	1.1	1.6	27.7	24.9
Psysr_2471	liuE	Leucine catabolism; Hydroxymethylglutaryl-CoA lyase	583	1	-1.1	-1.1	1.3	1.6	1.5
<b>Xanthine metabolism</b>									
Psysr_1814	xdhB	Xanthine dehydrogenase	430	1.3	1.9	1.5	15.2	1.9	2.5
Psysr_1815	xdhA	Xanthine dehydrogenase	800	1.1	1.5	1.5	19.5	2.1	2.9
Psysr_2390		Aldehyde oxidase and xanthine dehydrogenase	140	3.7	1.0	-1.2	1.4	4.4	4.9
Psysr_2391		Xanthine dehydrogenase accessory factor XdhC	210	4.7	-1.0	-1.2	1.1	4.5	7.4
Psysr_4283		Xanthine dehydrogenase and aldehyde oxidase	683	17.1	1.4	-1.1	2.3	12.0	25.2

Psysr#	Gene	Product Name	Fluorescence Intensity	Fold-induction compared to basal medium					
			Basal medium	NaCl	H <sub>2</sub> O <sub>2</sub>	Low Fe	Low N	Epi	Apo
Psysr_4284		Xanthine degradation; Molybdopterin dehydrogenase	336	11.9	1.1	-1.1	1.6	7.7	17.1
Psysr_4285		Xanthine degradation; Ferredoxin:[2Fe-2S]-binding	384	15.3	1.2	1.0	1.8	11.1	24.4
<b>Potassium transport</b>									
Psysr_2046	kdpF	hypothetical protein	406	1.2	-1.0	1.1	1.9	6.5	3.6
Psysr_2047	kdpA	potassium-transporting ATPase subunit A	152	1.1	1.1	-1.0	1.4	3.8	1.5
Psysr_2048	kdpB	potassium-transporting ATPase subunit B	88	1.1	1.1	1.0	1.4	2.6	1.3
Psysr_2049	kdpC	potassium-transporting ATPase subunit C	90	-1.1	-1.1	-1.1	1.3	2.5	1.4
<b>Choline and glycine betaine catabolism</b>									
Psysr_4732	betA	Choline dehydrogenase	594	3.1	-1.1	-1.1	-1.1	2.8	7.4
Psysr_4733	betB	Betaine aldehyde dehydrogenase	1,580	3.5	-1.1	-1.2	-1.3	3.2	8.7
Psysr_4734	betI	transcriptional repressor BetI	2,095	2.6	-1.1	-1.3	-1.1	4.0	8.3
Psysr_4708	gbdR	GbdR regulator of glycine betaine catabolism	5,676	-1.6	-1.2	1.1	114.1	11.1	4.6
Psysr_4776	gbcA	Glycine betaine catabolism protein	1,624	-1.4	1.4	1.9	19.5	9.6	6.4
Psysr_4775	gbcB	Glycine betaine catabolism protein	170	-1.4	1.0	-1.2	2.4	2.1	1.5
Psysr_4782	dgcA	Dimethylglycine catabolism protein	269	-1.0	1.0	-1.0	5.4	5.3	4.5
Psysr_4781	dgcB	Dimethylglycine catabolism protein	153	1.1	-1.0	-1.1	1.9	2.1	2.0
Psysr_4713	soxB-1	Sarcosine oxidase, beta subunit, heterotetrameric	357	1.3	1.1	1.0	7.8	6.4	4.9
Psysr_4714	soxD-1	Sarcosine oxidase, delta subunit, heterotetrameric	541	1.2	1.4	1.1	8.4	5.4	4.9
Psysr_4715	soxA-1	Sarcosine oxidase, alpha subunit, heterotetrameric	347	1.1	1.3	-1.0	6.9	4.7	3.9
Psysr_4716	soxG-1	Sarcosine oxidase, gamma subunit, heterotetrameric	379	1.1	1.2	1.0	4.6	3.9	3.7
Psysr_2221	soxG-2	sarcosine oxidase, gamma subunit	186	1.1	1.5	1.9	2.6	2.4	2.0
Psysr_2222	soxA-2	Aminomethyltransferase	107	-1.1	1.2	1.6	2.1	1.5	1.2
Psysr_2223	soxD-2	sarcosine oxidase, delta subunit	1,841	-1.1	1.8	3.1	5.5	4.6	4.3
Psysr_2224	soxB-2	FAD dependent oxidoreductase	545	-1.2	1.7	2.6	4.7	3.2	2.5
<b>Polyamine transport</b>									
Psysr_2398		Polyamine ABC transporter, ATP-binding protin	227	-1.2	1.1	1.1	3.7	5.7	3.9
Psysr_2399		Polyamine ABC transporter, permease	292	-1.0	1.1	1.2	4.3	12.4	7.1
Psysr_2400		Polyamine ABC transporter, permease	650	-1.1	-1.1	1.4	10.9	22.6	15.3
Psysr_2401		Polyamine ABC transporter, substrate-binding protein	948	-1.1	1.0	1.4	13.8	20.2	13.7
<b>Type III secretion system</b>									
Psysr_1192	hrpA2	Type III helper protein HrpA2	1,719	-1.1	-1.4	1.1	13.9	2.5	1.6
Psysr_1193	hrpZ1	Type III helper protein HrpZ1	2,791	-1.3	-1.8	1.1	15.5	2.4	1.5
Psysr_1194	hrpB	Type III secretion protein HrpB	408	-1.1	-1.6	-1.2	7.0	1.3	1.1
Psysr_1195	hrcJ	Type III secretion protein HrcJ	178	1.2	-1.1	1.1	4.4	1.2	1.2
Psysr_1196	hrpD	Type III secretion protein HrpD	82	1.1	-1.2	-1.1	1.9	1.2	1.1
Psysr_1197	hrpE	Type III secretion protein HrpE	48	1.1	1.0	-1.0	1.5	1.2	1.1
Psysr_1198	hrpF	Type III secretion protein HrpF	147	-1.0	-1.1	-1.2	4.4	1.3	1.2
Psysr_1199	hrpG	Type III secretion protein HrpG	135	-1.1	-1.1	-1.2	4.5	1.3	1.0
Psysr_1200	hrcC	Outer-membrane type III secretion protein HrcC	237	1.1	-1.3	-1.1	3.8	1.4	1.2
Psysr_1201	hrpT	Type III secretion protein HrpT	280	1.0	-1.2	-1.3	4.5	1.4	1.1
Psysr_1205	hrcU	Type III secretion protein HrcU	65	1.1	1.0	1.1	1.6	1.1	1.8
Psysr_1206	hrcT	Type III secretion protein HrcT	60	1.2	-1.1	-1.1	1.3	1.1	1.4
Psysr_1207	hrcS	Type III secretion protein HrcS	114	1.3	-1.2	-1.1	2.1	1.3	1.9
Psysr_1208	hrcR	Type III secretion system protein	84	1.1	-1.0	-1.1	1.8	1.3	1.4
Psysr_1209	hrcQb	Type III secretion protein HrcQb	85	-1.0	-1.2	-1.1	2.1	1.2	1.1
Psysr_1210	hrcQa	Type III secretion protein HrcQa	54	-1.0	-1.1	-1.1	1.5	1.2	1.1
Psysr_1211	hrpP	Type III secretion protein HrpP	74	-1.1	-1.1	-1.2	2.0	1.2	1.0

Psysr#	Gene	Product Name	Fluorescence Intensity	Fold-induction compared to basal medium					
			Basal medium	NaCl	H <sub>2</sub> O <sub>2</sub>	Low Fe	Low N	Epi	Apo
Psysr_1212	hrpO	Type III secretion protein HrpO	127	1.1	-1.2	-1.1	2.9	1.0	1.2
Psysr_1213	hrcN	Type III secretion cytoplasmic ATPase HrcN	82	1.1	1.0	1.0	1.8	-1.0	1.0
Psysr_1214	hrpQ	Type III secretion protein HrpQ	233	1.1	1.0	1.1	3.3	1.2	1.2
Psysr_1215	hrcV	Type III secretion protein HrcV	60	-1.0	-1.1	-1.1	1.4	1.0	1.1
Psysr_1216	hrpJ	Type III secretion protein HrpJ	85	-1.0	-1.1	-1.1	1.4	1.2	1.2
Psysr_1218	hrpK1	Type III helper protein HrpK1	1,243	-1.5	-1.6	-1.2	6.2	1.5	1.4
Psysr_0738	avrRpm1	Type III effector protein AvrRpm1	1,183	-1.5	-1.3	-1.3	1.9	-1.1	1.2
Psysr_0778	hopAG1	Type III effector HopAG1	256	1.2	-1.3	-1.1	2.9	1.8	3.6
Psysr_0779	hopAH1	Type III effector HopAH1	472	1.0	1.5	1.9	4.4	1.9	1.7
Psysr_1017	hopJ1	Type III effector HopJ1	826	-1.4	1.0	-1.1	-1.0	-2.3	-3.4
Psysr_1183	hopAA1	Type III effector HopAA1	312	-1.0	-1.0	1.1	8.6	1.5	1.7
Psysr_1184	hrpW1	Type III helper protein HrpW1	335	-1.5	-1.6	1.1	6.6	1.6	1.6
Psysr_1185	shcM	Effector locus protein (chaperone)	126	1.3	-1.0	1.1	4.1	1.2	1.9
Psysr_1186	hopM1	Type III effector HopM1	112	1.2	1.1	-1.0	2.2	1.2	1.3
Psysr_1187	shcE	Chaperone ( previously annotated as AvrF)	313	1.4	-1.5	-1.4	-1.0	-2.1	-1.9
Psysr_1188	avrE1	Type III effector protein AvrE1	357	1.0	-1.1	1.2	11.1	1.2	1.7
Psysr_1189	hrpH		82	1.0	1.0	-1.0	1.9	1.3	1.2
Psysr_1219	avrB3	Type III effector protein AvrB3	2,046	-2.1	-1.4	-1.6	3.7	1.2	-1.0
Psysr_1220	hopX1	Type III effector HopX1	470	-1.5	-1.1	-1.3	2.9	1.1	1.0
Psysr_1224	hopZ3	Type III effector HopZ3	407	-1.0	-1.2	1.2	2.4	1.1	1.9
Psysr_1889	hopH1	Type III effector HopH1	419	-2.1	-2.2	-2.0	1.2	1.1	-1.3
Psysr_3123	hopAH2-2	Type III effector HopAH2	721	-2.1	-1.2	-1.6	-1.5	-1.7	-2.3
Psysr_3813	hopAF1	Type III effector HopAF1	439	-1.7	-1.4	-1.3	2.7	-1.9	-1.6
Psysr_3839	hopAK1	Type III helper protein HopAK1	626	-1.5	-1.4	-1.3	1.7	1.3	1.1
Psysr_4269	hopAE1	Type III effector HopAE1	70	1.0	-1.1	-1.2	1.1	1.1	-1.0
Psysr_4326	hopI1	Type III effector HopI1	554	-1.0	-1.2	-1.2	1.9	-1.7	-1.1
Psysr_4659	hopAB1	Type III effector HopAB1	3,169	1.6	1.3	1.6	1.1	-1.1	1.0
Psysr_4919	avrPto1	Type III effector protein AvrPto1	1,728	-1.0	-2.3	-1.8	7.5	1.3	1.2
Psysr_1217	hrpL	Sigma factor	147	-1.4	-1.3	-1.4	2.7	1.2	1.2
Psysr_1190	hrpR	Type III transcriptional regulator HrpR	433	3.1	-1.0	-1.2	2.3	2.0	4.4
Psysr_1191	hrpS	Type III transcriptional regulator HrpS	203	2.3	1.0	-1.1	1.6	1.6	2.6
Psysr_1202	hrpV	Negative regulator of hrp expression HrpV	196	1.2	-1.0	-1.0	4.0	1.1	1.4
<b>Degradation of xenobiotics</b>									
Psysr_2734		Aldehyde dehydrogenase	120	-1.7	-1.1	-1.4	1.3	1.0	1.3
Psysr_0669		Hydroxydechloroatrazine ethylaminohydrolase	121	1.2	-1.1	-1.2	1.5	1.4	1.4
Psysr_1170		Allophanate hydrolase	164	-1.1	1.1	1.0	6.8	1.9	1.3
Psysr_0159	dehII	Haloacid dehalogenase, type II	653	1.2	2.2	3.2	4.6	4.3	13.2
Psysr_1791		HAD family hydrolase	159	1.1	1.4	1.6	8.7	1.8	1.8
Psysr_4718		Zn-containing alcohol dehydrogenase superfamily	660	1.2	1.5	2.2	7.2	4.5	9.1
Psysr_2534		Carboxymethylenebutenolidase	1,215	-1.4	1.8	1.4	3.1	1.7	1.2
Psysr_2956		Zn-containing alcohol dehydrogenase superfamily	96	1.1	1.1	1.1	1.2	1.1	1.5
Psysr_1769	acdA	Acyl-CoA dehydrogenase	1,735	-1.0	2.0	2.7	4.8	1.5	2.8
Psysr_4677		Acyl-CoA dehydrogenase	723	1.1	1.9	1.3	1.9	2.2	-1.3
Psysr_4681		Acyl-CoA dehydrogenase	2,097	1.4	3.1	1.7	2.7	7.5	1.5
Psysr_2934		NADH:flavin oxidoreductase/NADH oxidase	299	-1.4	-1.3	-1.3	-1.2	1.2	1.9
Psysr_2946		4-oxalocrotonate tautomerase	112	1.3	-1.1	-1.1	1.1	-1.1	1.2
Psysr_2869		Xenobiotic compound monooxygenase	624	1.1	1.2	1.2	2.8	4.4	3.8

P syr#	Gene	Product Name	Fluorescence Intensity	Fold-induction compared to basal medium					
			Basal medium	NaCl	H <sub>2</sub> O <sub>2</sub>	Low Fe	Low N	Epi	Apo
P syr_4825		Xenobiotic compound monooxygenase A subunit	231	1.6	1.4	-1.0	1.4	1.6	1.9
<b>Mechanosensitive ion channels</b>									
P syr_1822		MscS Mechanosensitive ion channel	414	11.5	-1.0	-1.1	1.2	1.8	27.6
P syr_3549		MscS Mechanosensitive ion channel	312	-1.9	-1.2	-1.2	-1.9	-2.1	-2.1
P syr_3803	m scM	Putative MscM mechanosensitive channel	384	-1.0	-1.1	-1.1	-1.1	-1.5	-1.3
P syr_4086	m csS	MscS Mechanosensitive ion channel	2,219	1.6	-1.5	-1.2	-4.4	-2.5	-1.7
P syr_4276	m scL	Large-conductance mechanosensitive channel	2,681	3.9	1.3	1.5	4.4	2.6	3.2
P syr_4477		MscS Mechanosensitive ion channel	254	8.9	1.2	-1.0	1.4	2.1	4.2
P syr_5003		MscS Mechanosensitive ion channel	325	1.6	1.1	1.1	1.9	-1.1	2.2

<sup>1</sup> Annotation of these genes is based on similarity to *Pseudomonas entomophila* proteins involved in synthesizing a secondary metabolite that is a signal molecule controlling virulence (Vallet-Gely, I., O. Opota, A. Boniface, A. Novikov and B. Lemaitre. 2010. A secondary metabolite acting as a signaling molecule controls *Pseudomonas entomophila* virulence. Cell. Microbiol. 12:1666-1679.

**Table S4. Expression levels of genes that were specific to nitrogen versus carbon starvation stress in two previous studies with *Sinorhizobium meliloti* (Sm) and *Bacillus licheniformis* (Bl).**

Gene	Gene	Protein function	Functional classification	Low N	Epi	Apo	N-starv <sup>a</sup>	C-starv <sup>a</sup>
Psyr_4828		Urocanate hydratase	Amino acid metabolism and transport	7.3	17	6.5	Sm	
Psyr_0544	thiC	Thiamine biosynthesis protein ThiC	Cofactor metabolism	2.0	-19.2	-26.9	Sm	
Psyr_4670	pqqA	Coenzyme PQQ synthesis protein PqqA	Cofactor metabolism	-2.3	-1.5	1.6	Sm	
Psyr_0790	ndh	NADH dehydrogenase	Energy generation	-1.9	-1.4	-1.5	Sm	
Psyr_3290	fadB	Multifunctional fatty acid oxidation complex	Fatty acid metabolism	1.4	2.2	-1.1	Sm	
Psyr_4276	mscL	Large-conductance mechanosensitive channel	Mechanosensitive ion channel	4.4	2.6	3.2	Sm	
Psyr_0190	glnK	Nitrogen regulatory protein P-II	Nitrogen metabolism	10.9	1.4	1.6	Sm	
Psyr_3099	nirB	Nitrite/sulfite reductase	Nitrogen metabolism	22.6	2.0	1.9	Sm	
Psyr_4817	glnA-1	Glutamine synthetase Type I	Nitrogen metabolism	8.3	1.5	1.3	Sm	
Psyr_2099	nasA	Assimilatory nitrate reductase	Nitrogen metabolism	8.8	1.7	2.0	Bl	
Psyr_3100	nirD	Nitrite reductase, small subunit	Nitrogen metabolism	7.7	1.6	1.7	Bl	
Psyr_1747	clpP	ATP-dependent Clp protease proteolytic subunit	Proteases	-2.1	-1.6	-2.5	Bl	
Psyr_0189	amtB-1	Ammonium transporter	Nitrogen metabolism	37.8	1.7	1.5	Sm,Bl	
Psyr_2273	glnA-2	Glutamine synthetase, Type III	Nitrogen metabolism	6.6	1.5	1.7	Sm,Bl	
Psyr_2277	amtB-2	Ammonium transporter	Nitrogen metabolism	3.6	1.5	1.4	Sm,Bl	
Psyr_4821	ntrB	Two-component sensor histidine kinase NtrB	Nitrogen metabolism	24.7	1.3	1.2	Sm	
Psyr_4822	ntrC	Two-component response regulator NtrC	Nitrogen metabolism	27.5	2.1	1.3	Sm	
Psyr_2104	nasT	Response regulator receiver:ANTAR	Signal transduction mechanisms	5.8	1.2	1.2	Sm	
Psyr_2068		Arylesterase	Fatty acid metabolism	1.1	-1.2	1.3		Sm
Psyr_3289	fadA	3-ketoacyl-CoA thiolase	Fatty acid metabolism	1.4	2.1	-1.1		Sm
Psyr_3277		Cardiolipin synthase 2	Phospholipid metabolism	1.5	5.1	6.5		Sm
Psyr_3906	glpR	Glycerol-3-phosphate regulon repressor	Phospholipid metabolism	-2.1	-1.7	-1.4		Sm
Psyr_4567	anmK	Anhydro-N-acetylmuramic acid kinase		1.3	1.1	1.0		Sm
Psyr_1769	acdA	Acyl-CoA dehydrogenase	Degradation of xenobiotics	4.8	1.5	2.8		Bl
Psyr_4700	glcB	Malate synthase G	Organic acid metabolism and transport	1.3	-1.2	-2.4		Bl
Psyr_3907	glpD	Glycerol-3-phosphate dehydrogenase	Phospholipid metabolism	2.8	34.0	17.3		Bl
Psyr_0305	glpT	sn-Glycerol-3-phosphate transporter	Transport (glycerol-3-phosphate)	-1.6	1.9	2.0		Bl
Psyr_3904	glpF	Glycerol uptake facilitator protein	Transport (glycerol-3-phosphate)	-1.5	5.1	2.0		Bl
Psyr_3196	aceA	Isocitrate lyase	Energy generation (TCA cycle)	-1.5	11.9	2.1		Sm,Bl

<sup>a</sup> The expression of genes indicated by Sm were altered in *S. meliloti* in response to either nitrogen or carbon starvation for 40 minutes in a study by Krol and Becker (2011) ppGpp in *Sinorhizobium meliloti*: biosynthesis in response to sudden nutritional downshifts and modulation of the transcriptome. *Molecular Microbiology* 81:1233-1254. The expression of genes indicated by Bl were altered in *B. licheniformis* in response to either nitrogen or carbon starvation imposed for various times in a study by Voigt et al. (2007) The glucose and nitrogen starvation response of *Bacillus licheniformis*. *Proteomics* 7:413-423. Genes highlighted in pink were significantly induced, while those highlighted in green were significantly repressed ( $q$ -value < 0.01).

**Table S5. Genes involved in nutrient transport or metabolism that were induced *in planta*.**

				Fold increase <sup>c</sup>	
Substrate	Pred <sup>a</sup>	Genes	Function <sup>b</sup>	Epiphytic	Apoplastic
Carbohydrates					
Arabinose	A	Psyr_2306,Psyr_2371-3 ( <i>araFGH</i> )	T	1.8	2.3
Disaccharide	A	Psyr_0759-0762	T	2.8	23.5
Fucose	A	Psyr_4488 ( <i>fucP</i> )	T	3.1	(1.7)
Inositol	D	Psyr_3267-3274	M	6.6	14.8
Ribose	A	Psyr_2569-2571	T	3.4	2.2
Ribose	A	Psyr_2874-2877	T	2.5	2.2
Ribose/xylose/arabinose/galactoside	A	Psyr_3263-3265	T	10.6	17.2
Sucrose	A	Psyr_0758 ( <i>scrB</i> )	M	2.3	20.3
Xylose	A	Psyr_2883 ( <i>xylA</i> )	M	22.3	22.3
Xylose	A	Psyr_2884-2886 ( <i>xylFGH</i> )	T	4.4	4.8
Organic acids					
Acetate	A	Psyr_3756 ( <i>actP</i> )	T	8.2	2.6
Citrate	A	Psyr_0198	T	6.7	3.5
Citrate	A	Psyr_3167 ( <i>citA</i> )	T	1.7	1.9
Dicarboxylate	A	Psyr_0898-0900 ( <i>dctMPQ</i> )	T	6.3	4.9
D-Galactonate	A	Psyr_4426	T	8.4	4.1
D-Galactonate	A	Psyr_1990	T	1.7	5.1
Gluconate	A	Psyr_0463( <i>gntP-2</i> )	T	4.2	1.8
Gluconate	A	Psyr_3338 ( <i>gntP-4</i> )	T	(1.2)	1.8
Glycolate	A	Psyr_3331-3333 ( <i>glcDEF</i> )	T	2.3	4.0
4-Hydroxybenzoate	A	Psyr_2124 ( <i>pcaK</i> )	T	1.4	1.8
4-Hydroxyphenylacetate	D	Psyr_3501	T	2.1	1.8
Malate	A	Psyr_3313 ( <i>maeI</i> )	T	2.2	1.6
Malate	A	Psyr_1479	T	2.4	(1.2)
Malonate	A	Psyr_0449-0450 ( <i>madLM</i> )	T	10.2	21.5
Phosphonate	A	Psyr_2247-2249	T	1.8	1.4
Tricarboxylate	D	Psyr_3966-3968 ( <i>tctABC</i> )	T	5.2	7.3

<sup>a</sup>The source of the prediction for the substrate specificity for the transporters and metabolic enzymes. A, B728a genome annotation; D, DC3000 genome annotation for gene orthologs showing synteny; K, Kegg pathway prediction.

<sup>b</sup> M, metabolism; T, transport

<sup>c</sup> Average induction level relative to in the basal medium, calculated using log-transformed data. Boxes highlighted in grey indicate a greater induction in one leaf habitat over the other.

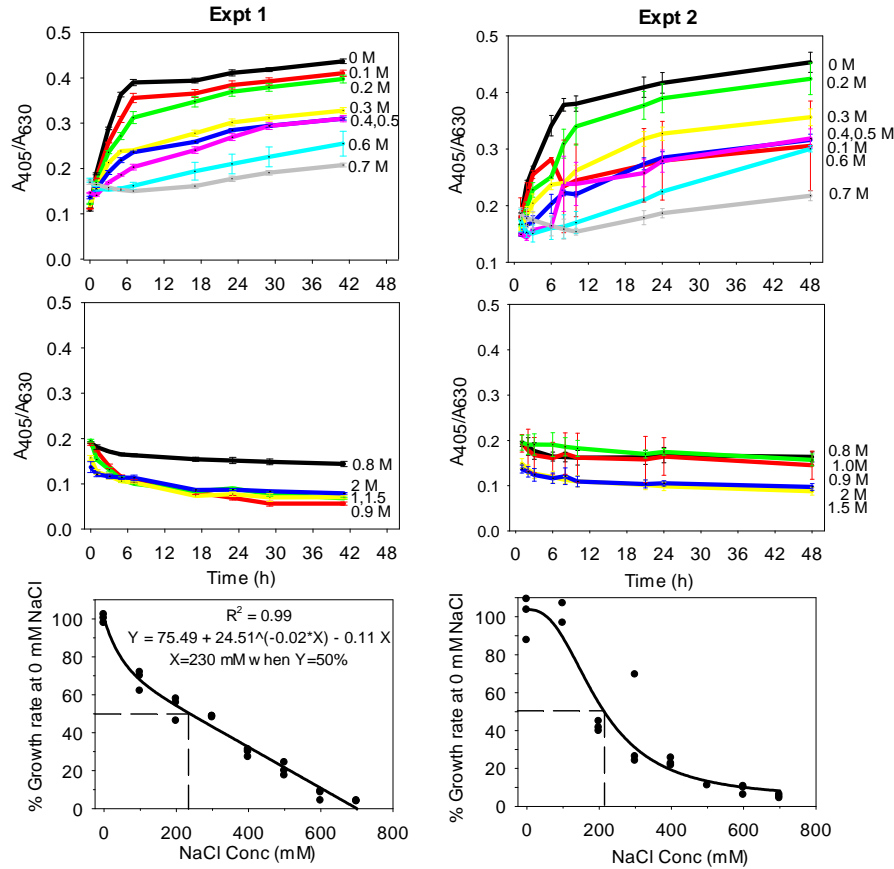


**Fig S1. Evaluation of conditions used to impose osmotic stress on B728a cells.** Data for two replicate experiments are shown. Cells were grown in HMM-basal medium, washed 2X in HMM-basal medium, transferred to the wells of a microtiter plate, and amended with NaCl to final concentrations ranging from 0.1 to 2 M. Cell growth was monitored using a microtiter plate reader based on a ratio of the absorbance values at 405 nm ( $A_{405}$ ) to  $A_{630}$ . The growth of cultures amended with 0 to 0.7 M NaCl (top panels) or 0.8 to 2 M NaCl (middle panels) was plotted. The growth rates during the period of exponential growth were calculated. The percentage growth rate at each NaCl concentration was determined based on the average growth rate of three replicate cultures in the absence of amended NaCl (bottom panels); in both experiments, a NaCl concentration of approximately 230 mM resulted in a 50% reduction in growth rate. Values shown in the top two plots are means  $\pm$  SE ( $n = 3$ ). *The final protocol for imposing osmotic stress was to amend the cells with NaCl to a final concentration of 230 mM and incubate them with shaking for 15 min.*

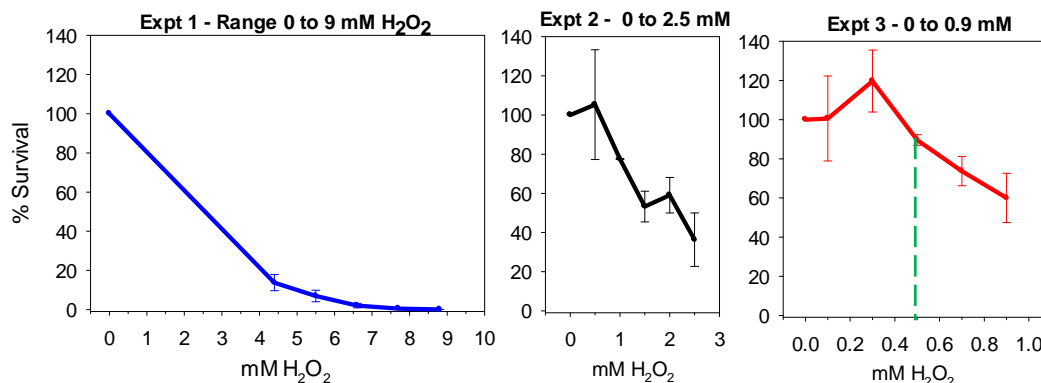


**Fig S2. Evaluation of conditions used to impose oxidative stress on B728a cells.** Data for three experiments attempting to identify a sublethal concentration of H<sub>2</sub>O<sub>2</sub> are shown. Cells were grown in HMM-basal medium, washed 2X in HMM-basal medium, transferred to microfuge tubes, and amended with H<sub>2</sub>O<sub>2</sub> to final concentrations ranging 0 to 9 mM in experiment 1 and to increasingly narrower ranges in the subsequent experiments. The cells were incubated for 15 min with shaking and then serial dilutions were plated on King's B agar to enumerate the surviving cells. The percentage of cells surviving the H<sub>2</sub>O<sub>2</sub> treatment was determined for each replicate based on the number of cells recovered from the 0 mM H<sub>2</sub>O<sub>2</sub> treatment. Values shown are the mean  $\pm$  SE ( $n = 3$ ). Experiment 3 had our target bacterial density,  $5 \times 10^8$  cells /ml, whereas expts 1 and 2 had slightly higher densities, which possibly explains the higher survival rate in the presence of 0.5 mM H<sub>2</sub>O<sub>2</sub> in these two experiments, since higher cell densities allow for greater cross protection from secreted catalases. We selected the H<sub>2</sub>O<sub>2</sub> concentration of 0.5 mM to use in our studies based on the results in expt 3. Although 10% of the cells were killed by this level, so it was not technically sublethal, this concentration represented a good balance between a high enough concentration to induce oxidative regulons and one low enough to minimize lethality. ***The final protocol for imposing oxidative stress was to amend the cells with hydrogen peroxide to a final concentration of 0.5mM and incubate them with shaking for 15 min.***



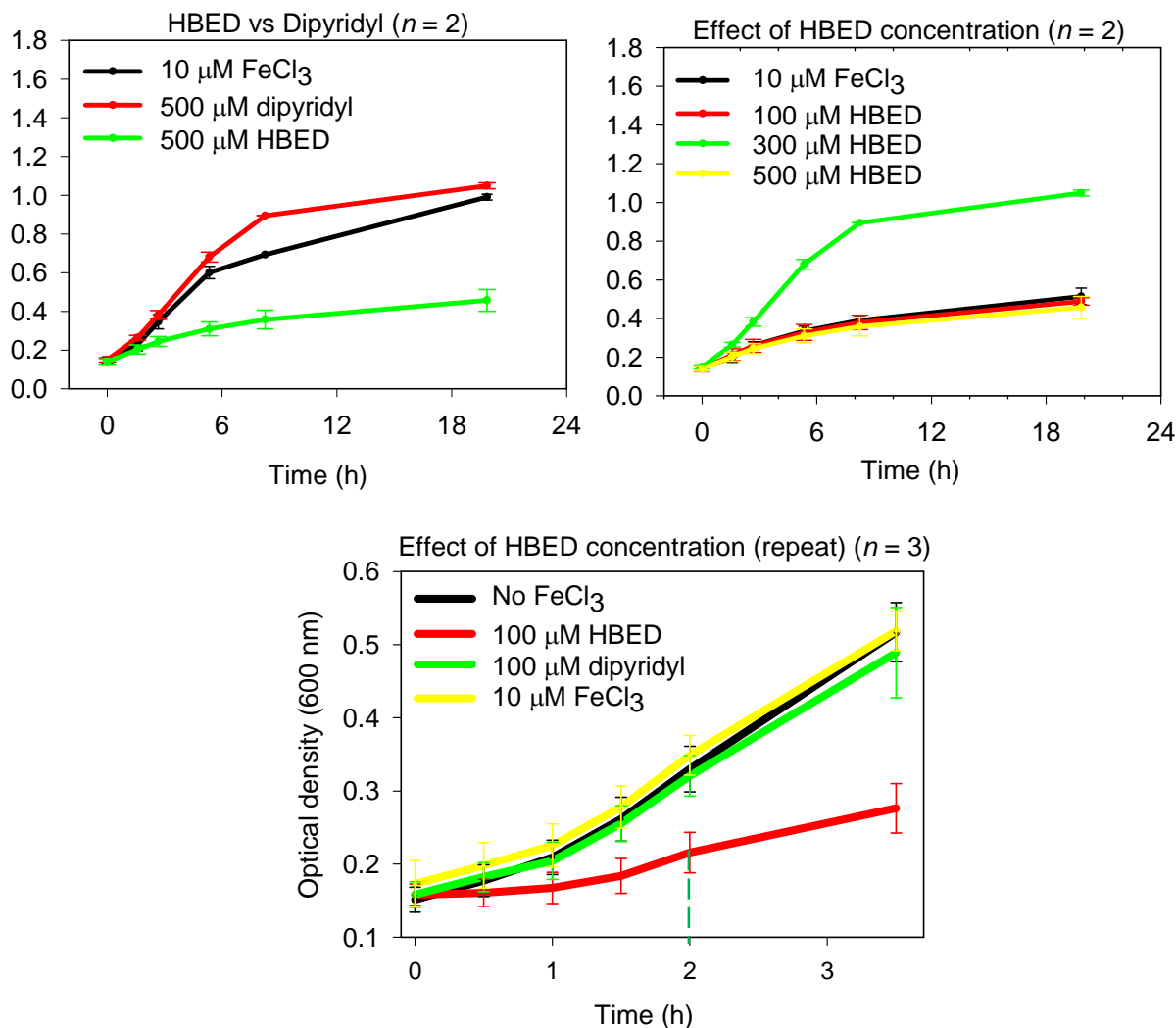


**Fig S3. Evaluation of conditions used to impose iron starvation on B728a cells.** Cells were grown in HMM-basal medium, washed 2X in HMM-basal medium lacking FeCl<sub>3</sub> (HMM-Fe), and then transferred into HMM-Fe in tubes either lacking Fe or containing various concentrations of FeCl<sub>3</sub> or the iron chelators dipyritydyl or N,N'-di(2-hydroxybenzyl)ethylenediamin-N,N'-diacetic acid monohydrochloride hydrate (HBED) (Strem Chemicals). Cell growth was monitored based on optical density at 600 nm (OD<sub>600</sub>). The acyl-homoserine lactone was omitted from the HMM and HMM-Fe media here. Dipyritydyl was not as effective as HBED at limiting iron. A concentration of 100  $\mu\text{M}$  of HBED was sufficient to limit growth. ***The final protocol for imposing iron limitation was to wash the cells twice in HMM medium lacking an iron source, resuspend them in this same medium but containing 100  $\mu\text{M}$  HBED, and incubate them with shaking for 2 h.***

**100 mM HBED:** 0.0425 g HBED was placed in 1 ml of HMM-basal medium, a partial pellet of KOH was added, and 1 M HCl was added in 10  $\mu\text{l}$  aliquots to adjust the pH to  $\sim 8.0$  (using pH paper). The final concentration was calculated based on the final volume. (Note: HBED does not dissolve in an aqueous solution until it has been alkalinized, then the pH must be readjusted to the desired level)

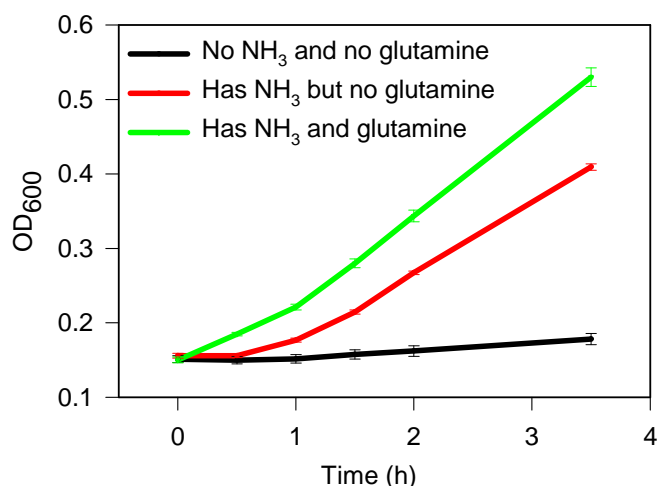


**Fig S4. Evaluation of conditions used to impose nitrogen starvation on B728a cells.** Cells were grown in HMM-basal medium, washed 2X in HMM-basal medium lacking NH<sub>3</sub> and glutamine (HMM-N), and then transferred into HMM-N in tubes either lacking NH<sub>3</sub> and glutamine or containing NH<sub>3</sub> with or without glutamine. Cell growth was monitored based on optical density at 600 nm (OD<sub>600</sub>). Values shown are the mean  $\pm$  SE ( $n = 3$ ). N limitation was detected within 1 h based on a difference in the growth of cells in the absence and presence of an N source. *The final protocol for imposing nitrogen limitation was to wash the cells twice in HMM medium lacking a N source, resuspend them in this same medium, and incubate them with shaking for 2 h.*

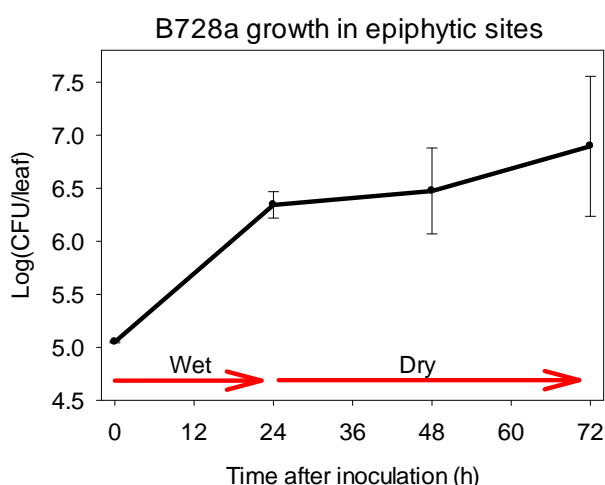


**Fig S5. Evaluation of conditions used to generate epiphytic populations of B728a cells on bean leaves.** Cells were grown in HMM-basal medium, washed 2X in HMM-basal medium lacking FeCl<sub>3</sub>, NH<sub>3</sub>, glutamine and AHL, and diluted in water containing 0.01% Silwet L-77 to a density of  $1 \times 10^6$  cells/ml. Plants were grown at a high density (10 plants per 4-inch pot) until their primary leaves were fully expanded. They were inoculated with B728a cells by submerging the leaves in 1L of the inoculum for 20 sec, enclosing each pot in a plastic bag to create a tent, and incubating the pots on a laboratory bench at 25°C for 24 h. The bags were removed and the plants were incubated at 25°C for 48 h at the ambient relative humidity. The cells were recovered from 4 leaves by sonication and enumerated by plating on King's B agar containing rifampin (50  $\mu$ g/ml) and cycloheximide (100  $\mu$ g/ml). *The final protocol for collecting epiphytic cells varied from this inoculation scheme as described in the Materials and Methods; most importantly, it was performed at a higher relative humidity to enhance the number of cells recovered from the leaves.*

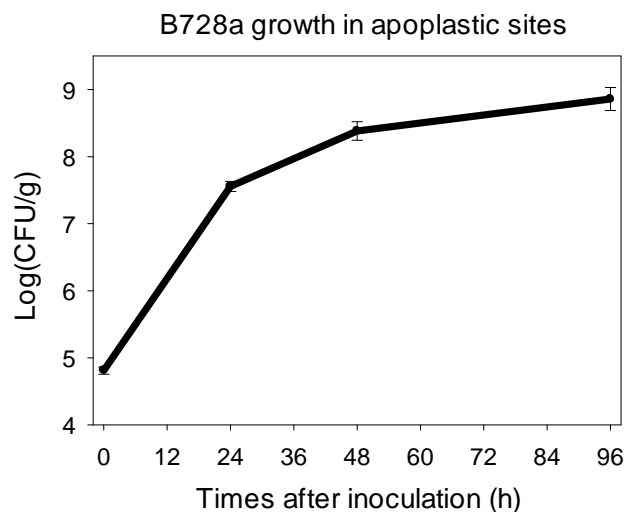


**Fig S6. Evaluation of conditions used to generate apoplastic populations of B728a cells in bean leaves.** Plants were grown and inoculum was prepared as described in Fig S5. B728a cells were inoculated by submerging the plants in 500 ml of the inoculum and subjecting the submerged plants to a vacuum for approximately 2 min, and then gently releasing the vacuum and leaving the plants submerged until they were infiltrated with the bacterial suspension. The plants were then removed from the inoculum and allowed to dry on a laboratory bench. The plants were incubated for 48 h under plant growth lights with a 12-h photoperiod for 48 h. The cells were recovered from 8 leaves by homogenization and enumerated by plating as described in Fig S5. *The final protocol for collecting apoplastic cells involved this inoculation scheme and sampling at the 48-h time point.*

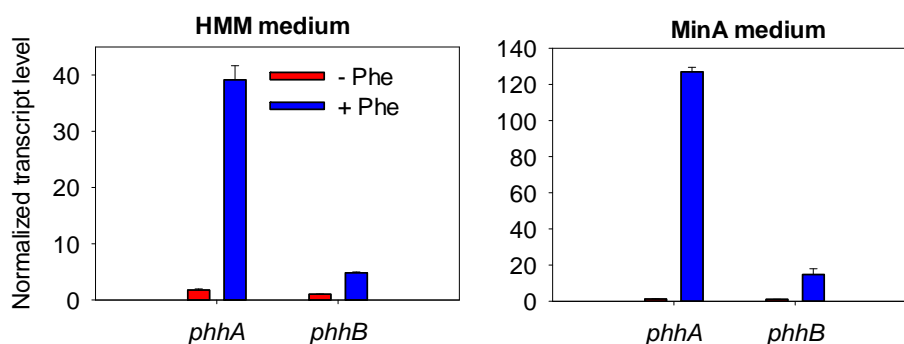


**Fig S7. Effect of phenylalanine on the transcript levels of *phhA* and *phhB*.** Cells that were grown to exponential phase in HMM-basal medium lacking the AHL and in MinA medium were amended with water (- Phe) or 10 mM phenylalanine (+ Phe). Total RNA was extracted after 15 min using the RNeasy mini kit (Qiagen, Valencia, CA), converted to cDNA using qScript One-Step SYBR qRT-PCR Kit (Quanta Biosciences, Gaithersburg, MD), and subjected to qPCR using the primers phhA-F (CGAATTCACCCATACCTACGG), phhA-R (GTAGATTTTCCGCCCTTGTG), phhB-F (AATTGCCGGAAGTCTCA) and phhB-R (CCAGCGCCCATTTGAAATTC). The transcript levels were normalized to the housekeeping gene *hemD* (primers hemD-F (GCACAGCGTTTCGATCATTTTC) and hemD-R (TGCTGAACCCACACTGAAC)).